Qualitative Methods for Inverse Scattering by an Impedant Crack

Yosra Boukari

Université de Tunis El Manar
Ecole Polytechnique de Palaiseau

Doctor of Philosophy Dissertation on
Applied Mathematics

Qualitative Methods for Inverse Scattering by an Impedant Crack

by

Yosra BOUKARI

Advisors:	**Fahmi BEN HASSEN**	Assistant professor, ISI, Tunisia
	Houssem HADDAR	Director of research, INRIA, France
Reviewers:	**Slim CHAABANE**	Professor, FSS, Tunisia
	Michele PIANA	Professor, University of Genova, Italy
Examiners:	**Anne Sophie BONNET-BEN DHIA**	Director of research, CNRS, France
	Marc BONNET	Director of research, CNRS, France

20 January, 2012

INSTITUT NATIONAL
DE RECHERCHE
EN INFORMATIQUE
ET EN AUTOMATIQUE

centre de recherche
SACLAY - ÎLE-DE-FRANCE

Contents

Acknowledgements

It would not have been possible to write this doctoral thesis without the help and support of the kind people around me, to only some of whom it is possible to give particular mention here.

I am deeply indebted to my supervisor at Ecole Polytechnique de Palaiseau, Professor Houssem Haddar, for his encouragement, advice, guidance and patience that stimulated and nourished my intellectual maturity. His never ending enthusiasm for research made this PhD inspiring, challenging and very interesting. The good advice and support of my co-supervisor at Ecole Nationale d'Ingenieurs de Tunis, Dr. Fahmi Ben Hassen, have been invaluable on both an academic and a personal level, for which I am extremely grateful.

I would also like to thank Professor Amel Ben Abda for hosting me within the inverse problems research team at LAMSIN in Ecole Nationale d'Ingenieurs de Tunis and for her support to accomplish this thesis.

I am grateful as well to the reviewers and examiners of my thesis, Professors Slim Chaabane, Michele Piana, Marc Bonnet and Anne Sophie Bonnet-Ben Dhia for their interesting comments on my research work.

I would like to express my sincere gratitude to Wallis, Nasséra, Alexandra and Sandra for their endless help and support during my three years as a PhD student.

I keep a good memory of the discussions and exchanges with my office mates Abdul Wahab, Meisam Sharify, Jean Baptiste Bellet, Georgios Michailidis and with the DEFI team members Anne Cossoniere, Nicolas Chaulet, Armin Lechleiter and Giovanni Giorgi. They were all very nice, friendly and supportive.

Finally, words fail to express my gratitude and appreciation to my parents, my sisters and my husband, whose eternal love, understating, care but most of all confidence in me took this doctoral study towards completion.

Introduction

The inverse scattering problem is gaining nowadays more and more importance in many applications in our real life to detect and identify unknown objects through the use of acoustic, electromagnetic or elastic waves. Examples of applications include the x-ray in medical imaging, the non destructive control in engineering and radar applications.

Different reconstruction methods have been developed in the last decades for the inverse scattering problem. These methods could be classified into two families. The first one includes all the iterative methods and the second one includes the qualitative methods. The latter constitutes the focus of our research work. Note that these methods are known for their attractiveness since they give simple and fast algorithms as compared to other iterative reconstruction methods, they can treat a big class of practically relevant problems where only limited knowledge about the scatterer is available and they avoid to solve any sequence of forward problems. More precisely, our focus is on the detection of cracks with impedance boundary conditions. We recall that the detection of cracks has attracted the attention of many researchers and the relevant literature is getting more and more rich. For the application of the Linear Sampling Method, we can refer to [21, 85, 18], the probe method [48, 68], the reciprocity gap [4, 11, 10], the topological sensitivity [15, 7], etc.

In the present work we propose an application of three qualitative methods, the Linear Sampling Method (LSM), the Factorization method and the Reciprocity Gap Linear Sampling Method (RG-LSM). The LSM has been introduced by A. Kirsh and D. Colton in 1996. The Factorization method has been developed by A. Kirsh in 1998 and compared to the LSM, which is based on an approximated solution, it gives an exact characterization of the scatterer in terms of the range of some measurements operator. The RG-LSM has been proposed by D. Colton and H. Haddar in 2005 as a reformulation of the Linear Sampling Method for near-field measurements in an inhomogeneous domain by using the concept of reciprocity gap.

Overview of the thesis

In this thesis, we focus on the investigation of qualitative methods to retrieve the geometry of cracks from multi-static far field data in the case of impedance boundary conditions on both sides of the crack. This dissertation is structured in six chapters as follows.

In Chapter 1 we propose a study of the forward problem using an integral equation approach in the two cases of a homogeneous and an inhomogeneous domain. The developments in this chapter constitute a basis for the methods developed in the following chapters. In fact, the study of the forward problem in a homogeneous domain will be used in the LSM and the Factorization method, whereas the study in an inhomogeneous domain, will be used for the development of the RG-LSM. The considered direct problem is solved numerically by using a code written in Fortran 90. Furthermore, a variational approach is used to solve the direct problem in the two cases of domain and to validate the results obtained using the integral equation approach. The software Freefem++ is used to solve the problem under the variational approach. We finally present the numerical schemes and the results obtained by using the two approaches.

Chapter 2 constitutes a basis for the study of the inverse scattering problem. We first present some properties of the far field pattern, especially the reciprocity principles, and some other properties of the scattering problem. Then, we present some uniqueness results of the solution of the inverse problem in the case of a crack with impedance boundary conditions from measurements of the far field pattern. We finally present an overview on some reconstruction methods for the inverse problem, that will be classified in three families, the iterative methods, the decomposition schemes and the sampling methods.

In Chapter 3 we focus on the application of the LSM to retrieve the geometry of cracks from multi-static far field data. We consider the case of the impedance boundary conditions on both sides of the crack, which constitutes the originality of this work. After describing in detail our inverse scheme to reconstruct cracks, we present the results of some numerical experiments to test its efficiency in a 2D setting of the problem for different crack shapes and for several ranges of the impedance values. We also propose in this chapter two approaches to find the value of the impedance parameter in both sides of the crack. The first approach, that we call the natural approach, is based on finding the scattered field from the far field pattern and the boundary conditions. The second approach uses the solution of the far field equation founded on the LSM. The numerical results of the two approaches are compared for different geometries and for different ranges of the impedance values. Note that in the study of the LSM, we provide a characterization of the crack using a norme of the Herglotz wave that depends on the geometry of the crack and using the impedance values, which can impact the accuracy of the reconstruction. This leads to an idea of using another method that tackles these issues by giving an explicit indicator function, which motivates our choice of the application of the Factorization method in the

the following chapter.

In Chapter 4 we investigate the application of the Factorization method to reconstruct the shape of cracks with impedance boundary conditions from far field measurements. A factorization of the far field operator is proposed, followed by a theoretical analysis using the so-called the $F_\sharp$ method. In order to study the efficiency of the $F_\sharp$ method, we conduct some experiments in a 2D setting to first test it for different shapes of cracks and different values of the impedance, then we compare it to the LSM developed in Chapter 3. Note that in chapter 3 and Chapter 4 we deal with the case of cracks in a homogeneous domain. Then, it would be interesting to consider the case of cracks with impedance boundary conditions in a non homogenous domain. In this latter case, the use of the LSM is very costly since the Green function of the whole domain should be computed. This motivates our work on the RG-LSM method.

Chapter 5 is devoted to the study of the identification of cracks by applying the RG-LSM. This is performed by considering the case of an impedance boundary condition on the two sides of the crack, that is embedded in an inhomogeneous background domain with piece wise constant index of refraction. We present the theoretical justification of the use of the RG-LSM and we describe our method to solve the inverse problem. The numerical schemes and results are presented. The efficiency of our method is tested for different shapes and different examples of media.

Finally, since the RG-LSM cannot be applied in the case of a crack that is buried in a stratified domain, where there is no access to the Cauchy data on the exterior boundary, we present in Chapter 6 a data completion method to solve the Cauchy problem for the Helmholtz using a non iterative method based on the integral equations approach. The theoretical justification of this method is provided and its efficiency is shown through some numerical results for different shapes of the domain and also for noisy data. We then apply our data completion algorithm to the RG-LSM in order to reconstruct cracks when they are embedded in a stratified domain. A numerical comparison between the crack reconstruction using synthetic data and the completed data is presented for different crack shapes and domain types.

Contributions of the thesis

The contributions of this research work can be summarized in four points:

- An extension of the application of the LSM to retrieve cracks in the case of impedance boundary conditions on both sides of the crack. It should be noted that only cases with an impedance boundary condition on one side of the crack has been developed in the literature. We have also developed a method to reconstruct the impedance values in both sides of the crack using two methods, one that uses the trace of the jump of the scattered field and its normal derivative on the crack and the second

method uses the solution of the far field equation given by the LSM.

- The application of the Factorization method to retrieve cracks in the case of an impedance boundary condition on both sides of the crack. To the best of our knowledge, the Factorization method has only been used in the case of cracks with Dirichlet boundary conditions. Note also that many difficulties arise when applying the Factorization method due to the difficulty to find a good factorization of the far field operator that satisfies some theoretical properties, which was a very challenging task of the research work.

- An efficient solution of the Cauchy problem for the Helmholtz equation using a non-iterative method based on an integral equations approach. The solution applies to different domain shapes.

- An extension of the RG-LSM in the case of impedance boundary conditions and a generalization of its application to more realistic domains such as stratified domains.

CHAPTER 1

The direct scattering problem for cracks

Contents

1.1 Introduction

We are concerned in this chapter by the scattering problem from a crack with an impedance boundary condition. More precisely we propose a study of this forward problem using an integral equation approach and a variational approach in the two cases of a homogeneous and an inhomogeneous background. Then we compare numerically the results obtained by the two approaches to validate the numerical implementation of the forward problem. The integral equation approach is solved using a code written in Fortran 90. This code is used for instance to generate the synthetic data needed for the inverse scheme. The variational approach is solved using the software Freefem++ [45]. The theoretical developments of this first part are inspired by [21]. We also quote the work of [61] for the study of the direct problem using an integral equation approach in Hölder spaces.

1.2 The direct scattering problem for a crack with impedance boundary conditions in a homogeneous medium

1.2.1 The model problem

Let $\sigma \subset \mathbf{R}^m$, $m = 2, 3$, be a smooth nonintersecting open arc. For further considerations, we assume that σ can be extended to an arbitrary smooth, closed curve $\partial\Omega$ enclosing a bounded domain Ω in $\mathbf{R}^m$. The normal vector ν on σ coincides with the outward normal vector to $\partial\Omega$, with simply connected complement.
Impedance type boundary conditions on σ lead to the following problem

$$\Delta u + k^2 u = 0 \quad \text{in } \mathbf{R}^m \setminus \overline{\sigma} \tag{1.1}$$

$$\partial_\nu u_\pm \pm \lambda^\pm u_\pm = 0 \quad \text{on } \sigma \tag{1.2}$$

where the wave number k is positive and $\lambda^\pm \in L^\infty(\sigma)$ are the given (complex-valued) impedance functions with non-negative imaginary part. Notice that

$$u_\pm(x) = \lim_{h \to 0^+} u(x \pm h\nu) \quad \text{and} \quad \partial_\nu u_\pm = \lim_{h \to 0^+} \nu \cdot \nabla u(x \pm h\nu) \quad \text{for} \quad x \in \sigma.$$

The total field $u = u^i + u^s$ is decomposed into a given incident wave and the unknown scattered field u^s which is required to satisfy the Sommerfeld radiation condition

$$\lim_{r=|x| \to +\infty} r^{\frac{m-1}{2}} (\partial_r u^s - iku^s) = 0, \tag{1.3}$$

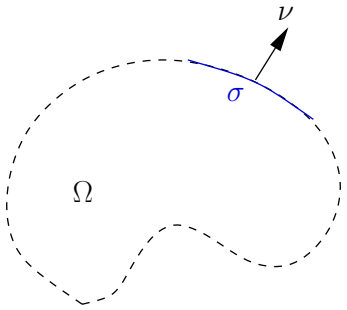

Figure 1.1: Representation of the domain

uniformly in all directions $\hat{x} = \frac{x}{|x|}$.
In order to formulate the scattering problem more precisely we need to define the trace spaces on σ. If $H^1_{loc}(\mathbf{R}^m \setminus \overline{\sigma})$, $H^{1/2}(\partial\Omega)$ and $H^{-1/2}(\partial\Omega)$ denote the usual Sobolev spaces we define the following spaces (see [65]) :

$$\begin{aligned} H^{1/2}(\sigma) &:= \left\{u_{|\sigma} : u \in H^{1/2}(\partial\Omega)\right\} \\ \tilde{H}^{1/2}(\sigma) &:= \left\{u \in H^{1/2}(\sigma) : supp(u) \subset \bar{\sigma}\right\} \\ H^{-1/2}(\sigma) &:= \left\{u_{|\sigma} : u \in H^{-1/2}(\partial\Omega)\right\} \\ \tilde{H}^{-1/2}(\sigma) &:= \left\{u \in H^{-1/2}(\sigma) : supp(u) \subset \bar{\sigma}\right\}. \end{aligned}$$

Note that $H^{-1/2}(\sigma)$ and $\tilde{H}^{-1/2}(\sigma)$ are the dual spaces of $\tilde{H}^{1/2}(\sigma)$ and $H^{1/2}(\sigma)$ respectively. We recall that we have the following inclusions

$$\mathcal{D}(\sigma) \subset \tilde{H}^{1/2}(\sigma) \subset H^{1/2}(\sigma) \subset L^2(\sigma) \subset \tilde{H}^{-1/2}(\sigma) \subset H^{-1/2}(\sigma) \subset \mathcal{D}'(\sigma)$$

where $\mathcal{D}(\sigma) := C_0^\infty(\sigma)$. Using the notation

$$g^\pm = -(\partial_\nu u^i \pm \lambda^\pm u^i), \qquad \text{on} \quad \sigma, \tag{1.4}$$

we define the following (ICP) problem by

Impedance crack problem (ICP) : Given some functions $g^\pm$ defined on σ, find $u^s \in H^1_{loc}(\mathbf{R}^m \setminus \overline{\sigma})$ satisfying the Sommerfeld radiation condition (1.3) and

$$\Delta u^s + k^2 u^s = 0 \quad \text{in } \mathbf{R}^m \setminus \overline{\sigma} \tag{1.5}$$

$$\partial_\nu u^s_\pm \pm \lambda^\pm u^s_\pm = g^\pm \qquad \text{on } \sigma. \tag{1.6}$$

The aim of this section is to prove the existence of the solution of the (ICP) problem. The following uniqueness result can be found in [61] and [38].

Lemma 1.
The (ICP) has at most one solution .

Proof. Let $u \in H^1_{loc}(\mathbf{R}^m \setminus \sigma)$ be a solution of (ICP) with $g^{\pm} = 0$ on σ. Using classical elliptic regularity results, $u \in H^2_{loc}(\mathbf{R}^m \setminus O_\sigma)$ where O_σ is a neighborhood of σ. We also observe that if $g^{\pm} = 0$ then $\frac{\partial u_\pm}{\partial \nu} \in L^2(\sigma)$. Let B_R be a ball with radius $r > 0$ containing the crack σ. Using the Green formula in $B_r \setminus \bar{\sigma}$, we have:

$$\int_{B_R \setminus \bar{\sigma}} |\nabla u|^2 \, dx - k^2 \int_{B_R \setminus \bar{\sigma}} |u|^2 \, dx + \int_\sigma u_+ \frac{\partial \overline{u_+}}{\partial \nu} \, ds - \int_\sigma u_- \frac{\partial \overline{u_-}}{\partial \nu} \, ds = \int_{S_r} u \frac{\partial \bar{u}}{\partial \nu} \, ds.$$

Using the boundary condition we have

$$\int_{B_R \setminus \bar{\sigma}} |\nabla u|^2 \, dx - k^2 \int_{B_R \setminus \bar{\sigma}} |u|^2 \, dx - \int_\sigma (\overline{\lambda^+}|u_+|^2 + \overline{\lambda^-}|u_-|^2) \, ds = \int_{S_r} u \frac{\partial \bar{u}}{\partial \nu} \, ds$$

$$\begin{aligned} \Longrightarrow \quad & -\int_\sigma \left(\Im(\bar{\lambda}^+)|u_+|^2 + \Im(\bar{\lambda}^-)|u_-|^2 \right) \, ds = \Im \left(\int_{S_r} u \frac{\partial \bar{u}}{\partial \nu} \, ds \right) \\ \Longrightarrow \quad & \int_\sigma \left(\Im(\lambda^+)|u_+|^2 + \Im(\lambda^-)|u_-|^2 \right) \, ds = \Im \left(\int_{S_r} u \frac{\partial \bar{u}}{\partial \nu} \, ds \right) \end{aligned}$$

Since $\Im(\lambda^+) \geq 0$ and $\Im(\lambda^-) \geq 0$ then we have:

$$\Im\left(\int_{S_r} u \frac{\partial \bar{u}}{\partial \nu} \, ds \right) \geq 0$$

Using theorem [34, Theorem 2.12, p33] and the unique continuation principle (see Corollary 13) this implies that $u = 0$. □

1.2.2 An approach using integral equations

To prove the existence of the solution of the (ICP), we use a boundary integral equations approach (see [38] for a sound soft crack and a sound hard crack, [21] for a partially coated crack and [61] for a 2D impedance crack when $\lambda^+ = \lambda^-$ is Hölder continuous).
We define $[u^s] := u^s_+ - u^s_-$ and $[\partial_\nu u^s] := \partial_\nu u^s_+ - \partial_\nu u^s_-$, the jump of u^s and $\partial_\nu u^s$ respectively, across the crack σ. Using the Green representation formula, the following relation holds for $z \in \mathbf{R}^m \setminus \overline{\sigma}$ (see [38, theorem 2.24, pp 54])

$$u^s(z) = \int_\sigma \left([u^s(y)] \frac{\partial \Phi(z,y)}{\partial \nu(y)} - \left[\frac{\partial u^s(y)}{\partial \nu(y)} \right] \Phi(z,y) \right) ds(y), \tag{1.7}$$

where Φ is the fundamental solution to the Helmholtz equation defined by

$$\Phi(x,y) := \begin{cases} \dfrac{1}{4\pi} \dfrac{e^{i\kappa|x-y|}}{|x-y|} & m = 3 \\ \dfrac{i}{4} H_0^{(1)}(\kappa|x-y|) & m = 2 \end{cases} \tag{1.8}$$

with $x \neq y$ and $H_0^{(1)}$ being the Hankel function of the first kind of order zero.

Lemma 2. *Assume that* $(\lambda^{\pm})^{-1} \in L^{\infty}(\sigma)$ *and* $g^{\pm} \in H^{-1/2}(\sigma)$ *such that* $(g^{+} - g^{-}) \in \tilde{H}^{-1/2}(\sigma)$. *The scattered field* u^s *is solution of the (ICP) if and only if the vector* $([u^s], [\partial_\nu u^s])^T$ *solves the system of integral equations*

$$A_\sigma \begin{pmatrix} [u^s] \\ \\ [\partial_\nu u^s] \end{pmatrix} = \begin{pmatrix} (\lambda^- g^+ + \lambda^+ g^-) \\ \\ (g^+ - g^-) \end{pmatrix} \tag{1.9}$$

where the matrix operator $A_\sigma : \tilde{H}^{1/2}(\sigma) \times \tilde{H}^{-1/2}(\sigma) \to H^{-1/2}(\sigma) \times \tilde{H}^{-1/2}(\sigma)$ *is given by*

$$A_\sigma := \begin{pmatrix} \lambda^+\lambda^- I + (\lambda^+ + \lambda^-) T_\sigma & -\frac{1}{2}(\lambda^+ - \lambda^-) I - (\lambda^+ + \lambda^-) K'_\sigma \\ \\ \frac{1}{2}(\lambda^+ - \lambda^-) I + (\lambda^+ + \lambda^-) K_\sigma & I - (\lambda^+ + \lambda^-) S_\sigma \end{pmatrix} \tag{1.10}$$

Proof. If u^s is a solution of the (ICP) then $[u^s] \in \tilde{H}^{1/2}(\sigma)$ and $[\partial_\nu u^s] \in \tilde{H}^{-1/2}(\sigma)$ (see Lemma 2.2 in [21]).

Next, by making use of the jump relations of the single and double layer potentials across $\partial\Omega$ (see [65]), we obtain from (1.7)

$$u^s_{\pm} = K_\sigma[u^s] - S_\sigma[\partial_\nu u^s] \pm \frac{1}{2}[u^s] \tag{1.11}$$

$$\partial_\nu u^s_{\pm} = T_\sigma[u^s] - K'_\sigma[\partial_\nu u^s] \pm \frac{1}{2}[\partial_\nu u^s] \tag{1.12}$$

where $S_{\partial\Omega}, K_{\partial\Omega}, K'_{\partial\Omega}, T_{\partial\Omega}$ are the boundary integral operators

$$\begin{aligned} S_{\partial\Omega} &: H^{-1/2}(\partial\Omega) \to H^{1/2}(\partial\Omega) \qquad K_{\partial\Omega} : H^{1/2}(\partial\Omega) \to H^{1/2}(\partial\Omega) \\ K'_{\partial\Omega} &: H^{-1/2}(\partial\Omega) \to H^{-1/2}(\partial\Omega) \qquad T_{\partial\Omega} : H^{1/2}(\partial\Omega) \to H^{-1/2}(\partial\Omega) \end{aligned}$$

defined for regular densities ψ and φ by

$$S_{\partial\Omega}\psi(x) := \int_{\partial\Omega} \psi(y)\Phi(x,y)ds(y), \qquad K_{\partial\Omega}\varphi(x) := \int_{\partial\Omega} \varphi(y)\frac{\partial\Phi(x,y)}{\partial\nu(y)}ds(y),$$

$$K'_{\partial\Omega}\psi(x) := \int_{\partial\Omega} \psi(y)\frac{\partial\Phi(x,y)}{\partial\nu(x)}ds(y), \quad T_{\partial\Omega}\varphi(x) := \lim_{\epsilon \longrightarrow 0} \frac{\partial}{\partial\nu(x)} \int_{\partial\Omega, |x-y|>\epsilon} \varphi(y)\frac{\partial\Phi(x,y)}{\partial\nu(y)}ds(y)$$

and $S_\sigma, K_\sigma, K'_\sigma, T_\sigma$ are the corresponding operators defined on σ. These restricted operators have the following mapping properties (see [65])

$$\begin{aligned} S_\sigma &: \tilde{H}^{-1/2}(\sigma) \to H^{1/2}(\sigma) \qquad K_\sigma : \tilde{H}^{1/2}(\sigma) \to H^{1/2}(\sigma) \\ K'_\sigma &: \tilde{H}^{-1/2}(\sigma) \to H^{-1/2}(\sigma) \qquad T_\sigma : \tilde{H}^{1/2}(\sigma) \to H^{-1/2}(\sigma). \end{aligned}$$

Moreover, from the boundary conditions (1.38) and (1.4), we have

$$\begin{aligned} &[\partial_\nu u^s] + \lambda^+ u^s_+ + \lambda^- u^s_- = g^+ - g^-, \\ &\lambda^+\lambda^-[u^s] + \lambda^- \partial_\nu u^s_+ + \lambda^+ \partial_\nu u^s_- = (\lambda^- g^+ + \lambda^+ g^-). \end{aligned} \tag{1.13}$$

Finally, by combining the relations (1.11), (1.12) and (1.13), we show that $([u^s], [\partial_\nu u^s])^T$ solves the system of equations (1.9). Conversely, assume that $([u^s], [\partial_\nu u^s])^T$ satisfies (1.9)-(1.10), so

$$\lambda^- \left(T_\sigma[u^s] - K'_\sigma[\partial_\nu u^s] + \frac{[\partial_\nu u^s]}{2} \right) + \lambda^+ \left(T_\sigma[u^s] - K'_\sigma[\partial_\nu u^s] - \frac{[\partial_\nu u^s]}{2} \right) + \lambda^+\lambda^-[u^s] = (\lambda^- g^+ + \lambda^+ g^-) \tag{1.14}$$

and

$$\lambda^+ \left(K_\sigma[u^s] - S_\sigma[\partial_\nu u^s] + \frac{[u^s]}{2} \right) + \lambda^- \left(K_\sigma[u^s] - S_\sigma[\partial_\nu u^s] - \frac{[u^s]}{2} \right) + [\partial_\nu u^s] = (g^+ - g^-) \tag{1.15}$$

The potential u^s, defined by (1.7), belongs to $H^1_{loc}(\mathbf{R}^m \setminus \overline{\sigma})$ and satisfies the Helmholtz equation in $\mathbf{R}^m \setminus \bar{\sigma}$ and the Sommerfeld radiation condition. It remains to show that u^s satisfies the boundary condition (1.38). To this end, we first inject (1.12) in (1.14) and (1.11) in (1.15). We obtain

$$\lambda^- \partial_\nu u^s_+ + \lambda^+ \partial_\nu u^s_- + \lambda^+\lambda^- [u^s] = (\lambda^- g^+ + \lambda^+ g^-) \tag{1.16}$$

$$\lambda^+ u^s_+ + \lambda^- u^s_- + [\partial_\nu u^s] = (g^+ + g^-) \tag{1.17}$$

Multiplying (1.17) by $\lambda^\pm$ and adding the results to (1.16), we obtain that

$$\lambda^\pm \left(\partial_\nu u^s_\pm \pm \lambda^\pm u^s_\pm = g^\pm \right) \quad \text{on } \sigma.$$

Therefore, the field u^s given by (1.7) is a solution of the (ICP). □

Lemma 3. *The operator A_σ given by (1.10) has a trivial kernel.*

Proof. Let $\zeta = (\alpha, \beta)^T \in \tilde{H}^{1/2}(\sigma) \times \tilde{H}^{-1/2}(\sigma)$ satisfying $A_\sigma \zeta = 0$. Define the potential

$$v = \int_\sigma \frac{\partial \Phi(x,y)}{\partial n(y)} \alpha(y) ds(y) - \int_\sigma \Phi(x,y)\beta(y) ds(y); \quad x \in \mathbf{R}^m \setminus \overline{\sigma}.$$

This potential belongs to $H^1_{loc}(\mathbf{R}^m \setminus \overline{\sigma})$ and satisfies the Helmholtz equation in $\mathbf{R}^m \setminus \bar{\sigma}$ and the Sommerfeld radiation condition. Moreover, using the jump relations of the single and double layer potentials across σ, we get

$$\begin{aligned} v_\pm &= K_\sigma(\alpha) - S_\sigma(\beta) \pm \frac{\alpha}{2} \\ \partial_\nu v_\pm &= T_\sigma(\alpha) - K'_\sigma(\beta) \pm \frac{\beta}{2} \end{aligned}$$

Hence,

$$[v] = \alpha \text{ and } [\partial_\nu v] = \beta. \tag{1.18}$$

Therefore, as in the proof of Lemma 2, we show that $v \in H^1_{loc}(\mathbf{R}^m \setminus \bar{\sigma})$ satisfies

$$\begin{aligned} \Delta v + k^2 v &= 0 \quad \text{in } \mathbf{R}^m \setminus \bar{\sigma}, \\ \partial_\nu v_\pm \pm \lambda^\pm v_\pm &= 0 \quad \text{on } \sigma \end{aligned}$$

and the Sommerfeld radiation condition. Then, from the uniqueness of the solution of this system, we have $v = 0$ and we conclude, by (1.18), that $\alpha = \beta = 0$. □

Lemma 4. *Assume that* $(\lambda^+ + \lambda^-)^{-1} \in L^\infty(\sigma)$. *The operator* $A_\sigma : \tilde{H}^{1/2}(\sigma) \times \tilde{H}^{-1/2}(\sigma) \to H^{-1/2}(\sigma) \times \tilde{H}^{-1/2}(\sigma)$ *given by (1.10) has a bounded inverse.*

Proof. Let $\tilde{\varphi} \in H^{1/2}(\partial\Omega)$ and $\tilde{\psi} \in H^{-1/2}(\partial\Omega)$ be the extension by zero to $\partial\Omega$ of $\varphi \in \tilde{H}^{1/2}(\sigma)$ and $\psi \in \tilde{H}^{-1/2}(\sigma)$ respectively.

Let $A_{\partial\Omega}$ be the operator defined on $H^{1/2}(\partial\Omega) \times H^{-1/2}(\partial\Omega) \longrightarrow H^{1/2}(\partial\Omega) \times H^{-1/2}(\partial\Omega)$ by

$$A_{\partial\Omega} := \begin{pmatrix} \tilde{\lambda}^+\tilde{\lambda}^- I + (\tilde{\lambda}^+ + \tilde{\lambda}^-)T_{\partial\Omega} & -\frac{1}{2}(\tilde{\lambda}^+ - \tilde{\lambda}^-)I - (\tilde{\lambda}^+ + \tilde{\lambda}^-)K'_{\partial\Omega} \\ \frac{1}{2}(\tilde{\lambda}^+ - \tilde{\lambda}^-)I + (\tilde{\lambda}^+ + \tilde{\lambda}^-)K_{\partial\Omega} & I - (\tilde{\lambda}^+ + \tilde{\lambda}^-)S_{\partial\Omega} \end{pmatrix} \tag{1.19}$$

where $\tilde{\lambda}^\pm \in L^\infty(\partial\Omega)$ such that $\tilde{\lambda}^\pm_{|\sigma} = \lambda^\pm$ and $\tilde{\lambda}^\pm_{|\partial\Omega\setminus\bar{\sigma}} = 0$. A can be decomposed as $A = A_{c,\Omega} + A_{0,\Omega}$, where

$$A_{c,\partial\Omega} = \begin{pmatrix} \tilde{\lambda}^+\tilde{\lambda}^- I + (\tilde{\lambda}^+ + \tilde{\lambda}^-)T_{c,\partial\Omega} & -(\tilde{\lambda}^+ + \tilde{\lambda}^-)K'_{\partial\Omega} \\ \frac{\tilde{\lambda}^+ - \tilde{\lambda}^-}{2} I + (\tilde{\lambda}^+ + \tilde{\lambda}^-)K_{\partial\Omega} & -(\tilde{\lambda}^+ + \tilde{\lambda}^-)S_{\partial\Omega} \end{pmatrix} \tag{1.20}$$

and

$$A_{0,\partial\Omega} = \begin{pmatrix} (\tilde{\lambda}^+ + \tilde{\lambda}^-)T_{0,\partial\Omega} & -\frac{1}{2}(\tilde{\lambda}^+ + \tilde{\lambda}^-)I \\ 0 & I \end{pmatrix}. \tag{1.21}$$

We denote by $T_{0,\partial\Omega}$ the boundary integral operator corresponding to the Laplace operator, defined as $T_{\partial\Omega}$ by replacing the kernel $\Phi(x,y)$ by

$$\Phi_0(x,y) := \begin{cases} \dfrac{1}{4\pi}\dfrac{1}{|x-y|} & m = 3 \\ -\dfrac{1}{2\pi}\ln|x-y| & m = 2 \end{cases} \tag{1.22}$$

The operator $-T_{0,\partial\Omega}$ is coercive on $\partial\Omega$. Consequently, we can deduce directly that $A_{0,\partial\Omega}$ is invertible.
We now prove that the operator $A_{c,\partial\Omega}$ is compact. In fact, $T_{c,\partial\Omega} := T_{\partial\Omega} - T_{0,\partial\Omega}$ is a compact operator since it has a continuous kernel.
Since the injection from $H^{\frac{1}{2}}(\partial\Omega)$ to $H^{-\frac{1}{2}}(\partial\Omega)$ is compact and $\tilde{\lambda}^{\pm} \in L^{\infty}(\partial\Omega)$, the operators $(\tilde{\lambda}^{+} - \tilde{\lambda}^{-})I$ and $\tilde{\lambda}^{+}\tilde{\lambda}^{-}I$ are also compact from $H^{\frac{1}{2}}(\partial\Omega)$ to $H^{-\frac{1}{2}}(\partial\Omega)$.
In the other hand, $K'_{\partial\Omega}$ is a compact operator from $H^{-\frac{1}{2}}(\partial\Omega)$ to $H^{-\frac{1}{2}}(\partial\Omega)$. The operator $S_{\partial\Omega}$ is continuous from $H^{-\frac{1}{2}}(\partial\Omega)$ to $H^{\frac{1}{2}}(\partial\Omega)$. Thus $(\tilde{\lambda}^{+}+\tilde{\lambda}^{-})S_{\partial\Omega}$ is compact from $H^{-\frac{1}{2}}(\partial\Omega)$ to $H^{-\frac{1}{2}}(\partial\Omega)$. The operator $K_{\partial\Omega}$ is continuous from $H^{\frac{1}{2}}(\partial\Omega)$ to $H^{\frac{1}{2}}(\partial\Omega)$, which implies that $(\tilde{\lambda}^{+} + \tilde{\lambda}^{-})K_{\partial\Omega}$ is compact from $H^{\frac{1}{2}}(\partial\Omega)$ to $H^{-\frac{1}{2}}(\partial\Omega)$.
We conclude that $A_{c,\partial\Omega} : H^{1/2}(\partial\Omega) \times H^{-1/2}(\partial\Omega) \to H^{-1/2}(\partial\Omega) \times H^{-1/2}(\partial\Omega)$ is a compact operator.

Let's prove now the same properties for A_{σ}. A decomposition of A_{σ} can be given as $A_{0,\sigma} + A_{c,\sigma}$ where $A_{0,\sigma}$ and $A_{c,\sigma}$ are respectively defined by

$$A_{0,\sigma} = \begin{pmatrix} (\lambda^{+} + \lambda^{-})T_0 & -\frac{1}{2}(\lambda^{+} + \lambda^{-})I \\ \\ 0 & I \end{pmatrix}$$

and

$$A_{c,\sigma} = \begin{pmatrix} \lambda^{+}\lambda^{-}I + (\lambda^{+} + \lambda^{-})T_{c,\sigma} & -(\lambda^{+} + \lambda^{-})K'_{\sigma} \\ \\ \dfrac{\lambda^{+} - \lambda^{-}}{2}I + (\lambda^{+} + \lambda^{-})K_{\sigma} & -(\lambda^{+} + \lambda^{-})S_{\sigma} \end{pmatrix} \tag{1.23}$$

We can observe that $A_{c,\sigma}$ is the restriction of $A_{c,\partial\Omega}$ to $\tilde{H}^{1/2}(\sigma) \times \tilde{H}^{-1/2}(\sigma)$ on σ. Then, we can deduce directly the compactness of this operator. The coercivity of $A_{0,\sigma}$ is deduced from the coercivity of $-T_{0,\sigma}$. In fact, we have for all $\tilde{\varphi} \in H^{1/2}(\partial\Omega)$

$$\Re(\langle -T_{0,\partial\Omega}\tilde{\varphi}, \tilde{\varphi}\rangle_{H^{-1/2}(\partial\Omega),H^{1/2}(\partial\Omega)}) \geq \alpha\|\tilde{\varphi}\|^2_{H^{1/2}(\partial\Omega)},$$

for some $\alpha > 0$. Therefore

$$\Re(\langle -T_{0,\sigma}\varphi, \varphi\rangle_{H^{-1/2}(\sigma),\tilde{H}^{1/2}(\sigma)}) \geq \alpha\|\varphi\|^2_{\tilde{H}^{1/2}(\sigma)},$$

which leads to the coercivity of the operator $-T_{0,\sigma}$ on σ. Consequently, the operator $A_{0,\sigma}$ is invertible. In fact, let $(f, g) \in H^{-1/2}(\sigma) \times \tilde{H}^{-1/2}(\sigma)$ and $(\varphi, \psi) \in \tilde{H}^{1/2}(\sigma) \times \tilde{H}^{-1/2}(\sigma)$ such that

$$A_{\sigma,0}\begin{pmatrix} \varphi \\ \psi \end{pmatrix} = \begin{pmatrix} f \\ g \end{pmatrix}.$$

This is equivalent to

$$\psi = g \qquad \text{and} \qquad T_{0,\sigma}(\varphi) - \frac{\lambda^{+} + \lambda^{-}}{2}\psi = f.$$

Consequently

$$\psi = g \qquad \text{and} \qquad T_{0,\sigma}(\varphi) = f + \frac{\lambda^+ + \lambda^-}{2} g.$$

Therefore the invertibity of $A_{\sigma,0}$ is equivalent to the invertibility of $T_{0,\sigma}$.
Finally A_σ is a Fredholm operator with index zero and since A_σ is injective (see Lemma 3) we conclude that it has a bounded inverse. □

1.2.3 A variational approach

We now prove similar results as in the previous paragraph by using a variational approach.

Lemma 5. *Assume that $g^\pm \in H^{-1/2}(\sigma)$ such that $(g^+ - g^-) \in \tilde{H}^{-1/2}(\sigma)$. Then, The (ICP) has a unique solution that continuously depends on the boundary data g^+ and g^-.*

Proof. Denotes by B_R a sufficiently large ball with radius R containing $\bar{\sigma}$ and by S_R its boundary. The equivalent variational formulation of the (ICP) consists into
$(P2)$: find $u^s \in H^1(B_R \setminus \bar{\sigma})$ satisfying for all $v \in H^1(B_R \setminus \bar{\sigma})$ the following equation

$$\int_{B_R\setminus\bar{\sigma}} \nabla u^s \overline{\nabla v} - k^2 \int_{B_R\setminus\bar{\sigma}} u^s \bar{v} - \int_\sigma \lambda^+ u^s_+ \overline{v_+} - \int_\sigma \lambda^- u^s_- \overline{v_-} - \left\langle T_R(u^s_{|S_R}), v \right\rangle_{S_R}$$
$$= - \left\langle g^+, [v] \right\rangle_{H^{-1/2}(\sigma), \tilde{H}^{1/2}(\sigma)} - \left\langle (g^+ - g^-),\ v_- \right\rangle_{\tilde{H}^{-1/2}(\sigma), H^{1/2}(\sigma)}$$

where $T_R : H^{1/2}(S_R) \to H^{-1/2}(S_R)$ is the Dirichlet to Neuman operator defined by

$$T_R(\varphi) = \partial_r w, \qquad \text{on} \quad S_R, \tag{1.24}$$

with $w \in H^1_{loc}(\mathbf{R}^m \setminus B_R) \cap H^2_{loc}(\mathbf{R}^m \setminus \overline{B_R})$ is the unique solution to

$$\begin{cases} \Delta w + k^2 w & = & 0 & \text{in } \mathbf{R}^m \setminus \overline{B}_R \\ w & = & \varphi & \text{on } S_R \\ \lim_{R\to\infty} \int_{S_R} |\partial_R w - ikw|^2 ds & = & 0 & \end{cases}$$

Let $\langle , \rangle_{S_R}$ denotes the duality product between $H^{-1/2}(S_R)$ and $H^{1/2}(S_R)$ that coincides with $L^2(S_R)$ scalar product for regular functions and let us recall in Theorem 6 (see [75, Theorem 2.6.4, p97]) some properties of this operator.

Theorem 6. *The DtN map T_R is well defined and is continuous map from $H^{1/2}(S_R)$ to $H^{-1/2}(S_R)$. Moreover,*

$$(i) \quad 0 \le \Im \left\langle T_R(\varphi), \varphi \right\rangle_{S_R} \le k \|\varphi\|^2_{L^2(S_R)} \quad \text{and} \quad \|\varphi\|^2_{L^2(S_R)} \le -\Re \left\langle T_R(\varphi), \varphi \right\rangle_{S_R} \le \|\varphi\|^2_{H^{1/2}(S_R)}$$

and

$$(ii) \quad \Im \left\langle T_R(\varphi), \varphi \right\rangle_{S_R} = 0 \implies \varphi = 0.$$

for all $\varphi \in H^{1/2}(S_R)$.

The variational formulation of $(P2)$ can be written in the form

$$A(u^s, v) + B(u^s, v) = l(v) \qquad \text{for all} \qquad v \in H^1(B_R \setminus \sigma) \tag{1.25}$$

where we set

$$\begin{aligned} A(u^s, v) &= \int_{B_R \setminus \bar{\sigma}} \nabla u^s \overline{\nabla v} + k^2 \int_{B_R \setminus \bar{\sigma}} u^s \bar{v} - \left\langle T_R(u^s_{|S_R}), v \right\rangle_{S_R}, \\ B(u^s, v) &= -2k^2 \int_{B_R \setminus \bar{\sigma}} u^s \bar{v} - \int_\sigma \lambda^+ u^s_+ \overline{v_+} - \int_\sigma \lambda^- u^s_- \overline{v_-}, \\ l(v) &= -\left\langle g^+, [v] \right\rangle_{H^{-1/2}(\sigma), \tilde{H}^{1/2}(\sigma)} - \left\langle (g^+ - g^-),\ v_- \right\rangle_{\tilde{H}^{-1/2}(\sigma), H^{1/2}(\sigma)}. \end{aligned}$$

We denote by $\mathcal{A}, \mathcal{B} : H^1(B_R \setminus \bar{\sigma}) \to H^1(B_R \setminus \bar{\sigma})$ the operators satisfying respectively for all $v \in H^1(B_R \setminus \bar{\sigma})$

$$\begin{aligned} (\mathcal{A}(u^s), v)_{H^1(B_R \setminus \bar{\sigma})} &= A(u^s, v) \\ (\mathcal{B}(u^s), v)_{H^1(B_R \setminus \bar{\sigma})} &= B(u^s, v) \\ (\mathcal{L}, v)_{H^1(B_R \setminus \bar{\sigma})} &= l(v) \end{aligned} \tag{1.26}$$

Therefore $(P2)$ is equivalent to the following problem.
$(F1)$: find $u^s \in H^1(B_R \setminus \bar{\sigma})$ such that

$$(\mathcal{A} + \mathcal{B}) u^s = \mathcal{L} \tag{1.27}$$

To prove the existence and the uniqueness of the solution of the equation (1.27) we have to prove that the operator $(\mathcal{A} + \mathcal{B})$ is invertible.
The sesquilinear form A is continuous and coercive on $H^1(B_R \setminus \bar{\sigma}) \times H^1(B_R \setminus \bar{\sigma})$. In fact

$$\begin{aligned} |(Au^s, u^s)| &\geq \left| Re\Big(\int_{B_R \setminus \bar{\sigma}} |\nabla u^s|^2 + k^2 \int_{B_R \setminus \bar{\sigma}} |u^s|^2 - \left\langle T_R(u^s_{|S_r}), u^s \right\rangle_{S_r} \Big) \right| \\ &\geq \int_{B_R \setminus \bar{\sigma}} |\nabla u^s|^2 + k^2 \int_{B_R \setminus \bar{\sigma}} |u^s|^2 - Re \left\langle T_R(u^s_{|S_r}), u^s \right\rangle_{S_r} \\ &\geq c \|u^s\|_{H^1(B_R \setminus \bar{\sigma})} \end{aligned}$$

Therefore, using the Lax-Milgram Theorem the operator $\mathcal{A}$ is an isomorphism.
Let a sequence $(u^s_n)_{n \in \mathbf{N}} \in H^1(B_R \setminus \bar{\sigma})$ and suppose that there exists $u^s \in H^1(B_R \setminus \bar{\sigma})$ such that

$$u^s_n \rightharpoonup u^s \qquad \text{on} \qquad H^1(B_R \setminus \bar{\sigma}).$$

Using the continuity of the trace application then

$$u^s_n \rightharpoonup u^s \qquad \text{on} \qquad H^{1/2}(\sigma).$$

Due to the compact embedding of $H^1(B_R \setminus \bar{\sigma})$ into $L^2(B_R \setminus \bar{\sigma})$ and $H^{1/2}(\sigma)$ into $L^2(\sigma)$, hence we have

$$u^s_n \longrightarrow u^s \qquad \text{on} \qquad L^2(B_R \setminus \bar{\sigma}) \tag{1.28}$$

and

$$u_n^s \longrightarrow u^s \qquad \text{on} \qquad L^2(\sigma) \tag{1.29}$$

On the other hand, we have

$$\|\mathcal{B}u_n^s\|_{H^1(B_R\setminus\bar{\sigma})} \leq C_1 \left(\|u_n^s\|_{L^2(B_R\setminus\bar{\sigma})} + \|u_n^s\|_{L^2(\sigma)}\right) \tag{1.30}$$

Therefore

$$\|\mathcal{B}(u_n^s - u^s)\|_{H^1(B_R\setminus\bar{\sigma})} \leq C_1 \left(\|u_n^s - u^s\|_{L^2(B_R\setminus\bar{\sigma})} + \|u_n^s - u^s\|_{L^2(\sigma)}\right) \tag{1.31}$$

Then the second hand side of the inquality converges to zero and consequently

$$B(u_n^s) \longrightarrow B(u^s) \qquad \text{on} \qquad H^1(B_R \setminus \bar{\sigma}).$$

That proves that the operator $\mathcal{B}$ is compact. It can be clearly seen that the operator $(\mathcal{A}+\mathcal{B})$ is a Fredholm operator of index 0. We should just prove the injectivity of this operator to prove its invertibility. Suppose that we have

$$(\mathcal{A}+\mathcal{B})u^s = 0$$

Due to the equivalence between the problem $(P2)$ and $(F1)$,

$$\int_{B_R\setminus\bar{\sigma}} \nabla u^s \overline{\nabla v} - k^2 \int_{B_R\setminus\bar{\sigma}} u^s \bar{v} - \int_\sigma \lambda^+ u_+^s \overline{v_+} - \int_\sigma \lambda^- u_-^s \overline{v_-} - \left\langle T_R(u_{|S_r}^s), v \right\rangle_{S_r} = 0$$

Consequently, for $v = u^s$

$$Im \left\langle T_R(u_{|S_r}^s), u^s \right\rangle_{S_r} = 0$$

Therefore $(u_{|S_r}^s, \partial_\nu u_{|S_r}^s) = (0,0)$. Hence, using the unique continuation principle (see Corollary 13), u^s vanishes in $\mathbf{R}^m \setminus \bar{\sigma}$. That proves the injectivity of $(\mathcal{A}+\mathcal{B})$ and consequently the invertibility of this operator. Moreover, we have

$$\|\mathcal{L}\| \leq C_2 \left(\|g^+\|_{H^{-1/2}(\sigma)} + \|g^-\|_{H^{-1/2}(\sigma)} + \|g^+ - g^-\|_{H^{-1/2}(\sigma)}\right)$$

Using the invertibily of $(\mathcal{A}+\mathcal{B})$ then

$$\|u^s\|_{H^1(B_R\setminus\bar{\sigma})} \leq C_2 \left(\|g^+\|_{H^{-1/2}(\sigma)} + \|g^-\|_{H^{-1/2}(\sigma)} + \|g^+ - g^-\|_{H^{-1/2}(\sigma)}\right)$$

□

1.3 Case of an inhomogeneous background

In the same way as proposed in Section 1.2.2, we solve the direct problem of scattering of an incident wave by an impedance crack in an inhomogeneous domain containing the crack σ. We assume that the index of refraction n is piecewise-constant complex-valued function with non-negative imaginary part to ensure the uniqueness of the solution of the scattering problem. Moreover we assume that $n = 1$ outside a ball of radius R.
As described in Section 1.2.2, we assume that σ is a smooth non-intersecting open arc which can be extended to an arbitrary smooth, simply connected and closed curve $\partial\Omega_\sigma$. The normal vector ν on σ coincides with the outward normal vector to $\partial\Omega_\sigma$.

The direct scattering problem is to find a scattered field $u^s \in H^1_{loc}(\mathbf{R}^m \setminus \overline{\sigma})$ solution of the Helmholtz equation

$$\Delta u^s + k^2 n u^s = 0 \qquad \text{in } \mathbf{R}^m \setminus \overline{\sigma}, \tag{1.32}$$

which satisfies the Sommerfeld radiation condition

$$\lim_{r=|x|\to+\infty} r^{\frac{m-1}{2}}(\partial_r u^s - ikn u^s) = 0 \tag{1.33}$$

uniformly for all $\hat{x} = \frac{x}{|x|}$ and such that the total field $u = u^i + u^s$ satisfies (1.32) and the impedance boundary condition

$$\partial_\nu u_\pm \pm \lambda^\pm u_\pm = 0 \quad \text{on } \sigma, \tag{1.34}$$

where $\lambda^\pm \in L^\infty(\sigma)$ are the given (complex-valued) impedance functions with non-negative imaginary part. We define

$$g^\pm = -(\partial_\nu u^i \pm \lambda^\pm u^i), \qquad \text{on} \quad \sigma, \tag{1.35}$$

the impedance boundary condition leads to

$$\partial_\nu u^s_\pm \pm \lambda^\pm u^s_\pm = g^\pm \quad \text{on } \sigma. \tag{1.36}$$

Hence, in the case of an inhomogeneous background the (ICP) is defined by

Impedance crack problem (ICP) : Given some functions $g^\pm$ defined on σ, find $u^s \in H^1_{loc}(\mathbf{R}^m \setminus \overline{\sigma})$ satisfying the Sommerfeld radiation condition (1.33) and

$$\Delta u^s + k^2 n u^s = 0 \quad \text{in } \mathbf{R}^m \setminus \overline{\sigma} \tag{1.37}$$

$$\partial_\nu u^s_\pm \pm \lambda^\pm u^s_\pm = g^\pm \qquad \text{on } \sigma. \tag{1.38}$$

1.3.1 The integral equations approach

Here we assume that σ lies in a homogeneous part of the background, i.e $n = n_0 = cte$ in a neighborhood of σ. In the case of an inhomogeneous domain, a representation of u^s is given by

$$u^s(z) = \int_\sigma \left([u^s(y)] \frac{\partial G(z,y)}{\partial \nu(y)} - \left[\frac{\partial u^s(y)}{\partial \nu(y)} \right] G(z,y) \right) ds(y), \qquad \forall z \in \mathbf{R}^m \setminus \overline{\sigma}, \tag{1.39}$$

where G is the fundamental solution of the Helmholtz equation

$$\Delta G(\cdot, x) + k^2 n G(\cdot, x) = -\delta_x \quad \text{in } \mathbf{R}^m,$$

satisfying the Sommerfeld radiation condition

$$\lim_{r=|x|\to+\infty} r^{\frac{m-1}{2}} (\partial_r G(\cdot, x) - ikn G(\cdot, x)) = 0, \qquad \text{uniformly for all } \hat{x} = \frac{x}{|x|}.$$

To prove the existence of (ICP), we use a boundary integral equations approach and the boundary integral operators $K_\sigma^n, K_\sigma^{n'}, T_\sigma^n, S_\sigma^n$ defined in the sub-section 1.2.2 by replacing the Green function Φ by G.

The existence and uniqueness of the scattered field u^s is given by the following result

Lemma 7. *Assume that $(\lambda^+ + \lambda^-)^{-1} \in L^\infty(\sigma)$ and $g^\pm \in H^{-1/2}(\sigma)$ such that $g^+ - g^- \in \tilde{H}^{-1/2}(\sigma)$, then $u^s \in H^1_{loc}(\mathbf{R}^m \setminus \overline{\sigma})$ is the unique solution of the (ICP) if and only if the vector $([u^s], [\partial_\nu u^s])^T$ solves the system of integral equations*

$$A_\sigma^n \begin{pmatrix} [u^s] \\ \\ [\partial_\nu u^s] \end{pmatrix} = \begin{pmatrix} (\lambda^- g^+ + \lambda^+ g^-) \\ \\ (g^+ + g^-) \end{pmatrix} \tag{1.40}$$

where the matrix operator $A_\sigma^n : \tilde{H}^{1/2}(\sigma) \times \tilde{H}^{-1/2}(\sigma) \to H^{-1/2}(\sigma) \times \tilde{H}^{-1/2}(\sigma)$ is given by

$$A_\sigma^n := \begin{pmatrix} \lambda^+\lambda^- I + (\lambda^+ + \lambda^-) T_\sigma^n & -\frac{1}{2}(\lambda^+ - \lambda^-) I - (\lambda^+ + \lambda^-) K_\sigma^{n'} \\ \\ \frac{1}{2}(\lambda^+ - \lambda^-) I + (\lambda^+ + \lambda^-) K_\sigma^n & I - (\lambda^+ + \lambda^-) S_\sigma^n \end{pmatrix} \tag{1.41}$$

Moreover, A_σ^n is invertible with bounded inverse.

Proof. To prove that there is an equivalent relation between finding u^s solution of the (ICP) problem and finding $([u^s], [\partial_\nu u^s])^T$ solution of the integral equations system (1.40), we proceed in the same way as in Lemma 2. The proof that the operator A_σ^n is invertible is similar to that in the case of the homogeneous background domain with a constant index of refraction studied in Section 1.2.2. In fact, since G has the same singularity as the free-space fundamental solution Φ with $k = k\sqrt{n_0}$ then the layer potentials with kernel G or Φ have the same jump properties across σ. □

1.3.2 The variational approach

For the resolution of the scattering problem in the non homogeneous case using the variational approach, we proceed similarly as in the homogeneous case by replacing the variational formulation in $(P2)$ by

$$\int_{B_R\setminus\bar{\sigma}} \nabla u^s \overline{\nabla v} - k^2 \int_{B_R\setminus\bar{\sigma}} n u^s \bar{v} - \int_\sigma \lambda^+ u^s_+ \overline{v_+} - \int_\sigma \lambda^- u^s_- \overline{v_-} - \left\langle T_R(u_{|S_R}), v \right\rangle_{S_R}$$
$$= -\left\langle g^+, [v] \right\rangle_{H^{-1/2}(\sigma),\tilde{H}^{1/2}(\sigma)} - \left\langle (g^+ - g^-),\ v_- \right\rangle_{\tilde{H}^{-1/2}(\sigma),H^{1/2}(\sigma)}$$

where $g^\pm \in H^{-1/2}(\sigma)$ and n is a piecewise-constant complex-valued function with non-negative imaginary part. In this case, we have

$$A(u^s, v) = \int_{B_R\setminus\bar{\sigma}} \nabla u^s \overline{\nabla v} + k^2 \int_{B_R\setminus\bar{\sigma}} u^s \bar{v} - \left\langle T_R(u^s_{|S_R}), v \right\rangle_{S_R}, \tag{1.42}$$

$$B(u^s, v) = -k^2 \int_{B_R\setminus\bar{\sigma}} (n+1)\ u^s \bar{v} - \int_\sigma \lambda^+ u^s_+ \overline{v_+} - \int_\sigma \lambda^- u^s_- \overline{v_-}, \tag{1.43}$$

$$l(v) = -\left\langle g^+, [v] \right\rangle_{H^{-1/2}(\sigma),\tilde{H}^{1/2}(\sigma)} - \left\langle (g^+ - g^-),\ v_- \right\rangle_{\tilde{H}^{-1/2}(\sigma),H^{1/2}(\sigma)} \tag{1.44}$$

We can prove that the operators $\mathcal{A}, \mathcal{B}$ keep the same properties as in the homogeneous case.

1.4 Numerical scheme and results

1.4.1 Numerical discretisation

Let $A_\sigma : \tilde{H}^{1/2}(\sigma) \times \tilde{H}^{-1/2}(\sigma) \to H^{-1/2}(\sigma) \times \tilde{H}^{-1/2}(\sigma)$ be the matrix operator given by (1.10). We use a Galerkin method to solve numerically the system of integral equations

$$A_\sigma \begin{pmatrix} \varphi \\ \psi \end{pmatrix} = \begin{pmatrix} f_1 \\ f_2 \end{pmatrix}. \tag{1.45}$$

We multiply the two equations in (1.45) by test functions α and $\beta \in \tilde{H}^{\frac{1}{2}}(\sigma)$ respectively and we integer over σ (in the sense of the duality pairing between $H^{-1/2}(\sigma)$ and $\tilde{H}^{\frac{1}{2}}(\sigma)$)

$$\int_\sigma \lambda^+\lambda^- \alpha\varphi + \int_\sigma C_1 \alpha T_\sigma \varphi - \int_\sigma C_2 \alpha \psi - \int_\sigma C_1 \alpha K'_\sigma \psi = \int_\sigma \alpha f_1 \tag{1.46}$$

$$\int_\sigma C_1 \beta \varphi + \int_\sigma C_2 \beta K_\sigma \varphi + \int_\sigma \lambda^+\lambda^- \beta\psi - \int_\sigma C_1 \beta S_\sigma \psi = \int_\sigma \beta f_2 \tag{1.47}$$

where we simplify the notations by denoting $C_1 = (\lambda^+ + \lambda^-)$, $C_2 = \frac{1}{2}(\lambda^+ - \lambda^-)$.
Then we discretize the space $H^{-1/2}(\sigma) \times \tilde{H}^{1/2}(\sigma)$ using finite elements $P_1 \times P_1$. To compute

the integral involving the operator T_σ we use the following formula (see [43])

$$\begin{aligned}
&\int_\sigma \alpha(x)\frac{\partial}{\partial\nu(x)}\int_\sigma \varphi(y)\frac{\partial\Phi(x,y)}{\partial\nu(y)}\,ds(y)\,ds(x)\\
&= \kappa^2\int_\sigma\int_\sigma \Phi(x,y)\nu(x)\cdot\nu(y)\alpha(x)\varphi(y)\,ds(x)\,ds(y)\\
&-\int_\sigma\int_\sigma \Phi(x,y)(\nabla\alpha(x)\times\nu(x))\cdot(\nabla\varphi(y)\times\nu(y))\,ds(x)\,ds(y).
\end{aligned}$$

1.4.2 Numerical results

We end the study of the direct problem by some numerical tests obtained by the scheme described above. To validate our algorithm, we also use FreeFem++ to solve the (ICP) problem using the FEM method. To this end, we discretize the disk of radius 10 times the wavelength by $P1$ elements. The scattering problem in the homogeneous case is used to generate the synthetic data that will be needed in the inverse problem in Chapter 3 and 4. Since in these two chapters we use the LSM and the Factorization method that require the data u^∞, then we should compare the measurements of u_∞ in the case of a homogeneous domain for the two methods (the method based on integral equations and that using FEM), where u^∞ is the far field pattern of the scattered wave, $x \in \mathbf{R}^m\backslash\overline{\sigma}$, $\hat{x} = x/|x|$ and $r = |x|$. We recall that the solution of the (ICP) problem has the asymptotic behavior of an outgoing spherical wave (see [34])

$$u^s(x,d) = r^{\frac{1-m}{2}}e^{ikr}u^\infty(\hat{x},d) + O(r^{-\frac{m+1}{2}}). \tag{1.48}$$

The comparison of the modulus of the far field pattern (see (4.58)) is computed by the two methods for 100 observation points, different crack shapes and different incident plane waves $u^i(x) = \exp(ik(x_1 cos(\theta) + x_2 sin(\theta)))$ with angle θ. We keep the wave number constant $k = 2\pi$ for all the tests and we choose two different values of the impedance $\lambda^- = \lambda^+ = 5 + i$ and $\lambda^- = \lambda^+ = 1 + i$.

The scattering problem in the non homogeneous case is used to generate the synthetic data that will be needed in the inverse problem in Chapter 5. In order to validate this case, we compare the scattered field measurements on a fixed boundary.

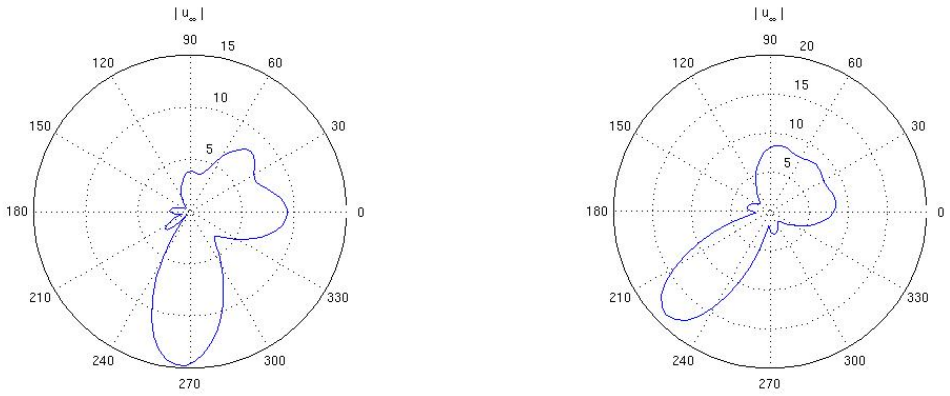

Figure 1.2: Reconstruction of the modulos of u_∞ associed to the scattering by the open arc centered in $(0,0)$ with radius $r=1$ and aperture $\pi/2$ for $\lambda^{\pm}=5+i$ where the angle of incidence $\theta=\pi/2$ (left) and $\theta=\pi/4$ (right).

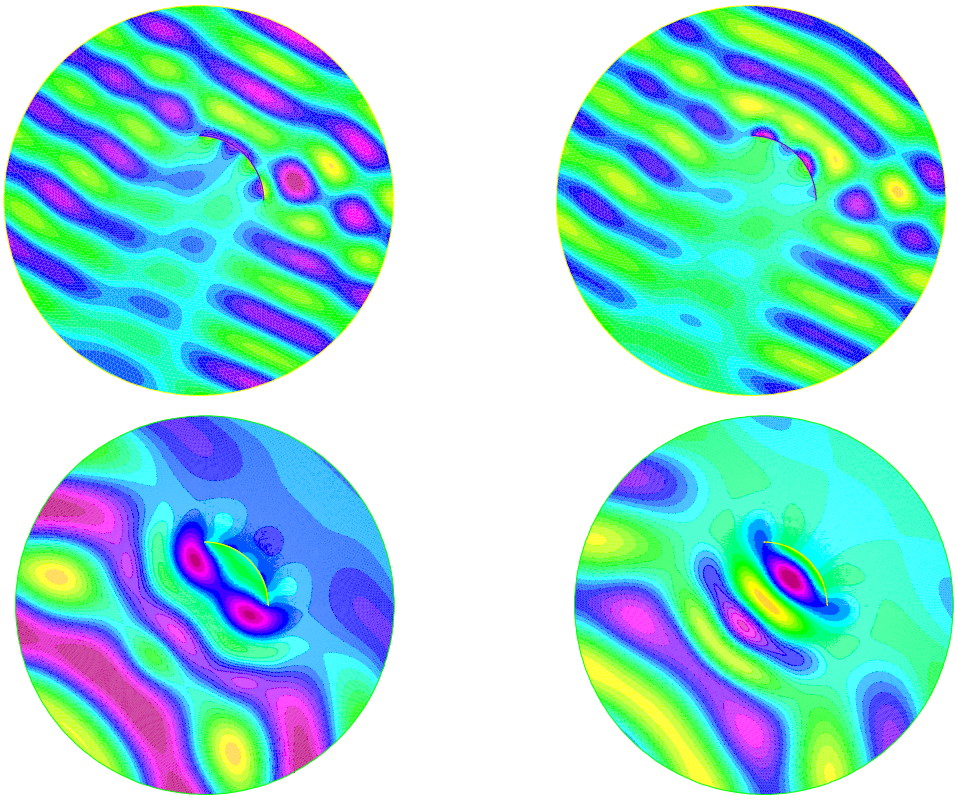

Figure 1.3: Reconstruction of the real part (left) and the imaginary part of the total field for $\lambda^{\pm}=5+i$ where $u_i=e^{ik(\cos(\theta)x,\sin(\theta)y)}$, with $\theta=\pi/3$ (in the first line) where $u_i=\Phi(.,x_0)$ with $x_0=(-2,-2)$ (in the second line). The crack is the open arc centered in $(0,0)$ with radius $r=1$ and aperture $\pi/2$.

Numerical results in the case of a homogeneous domain

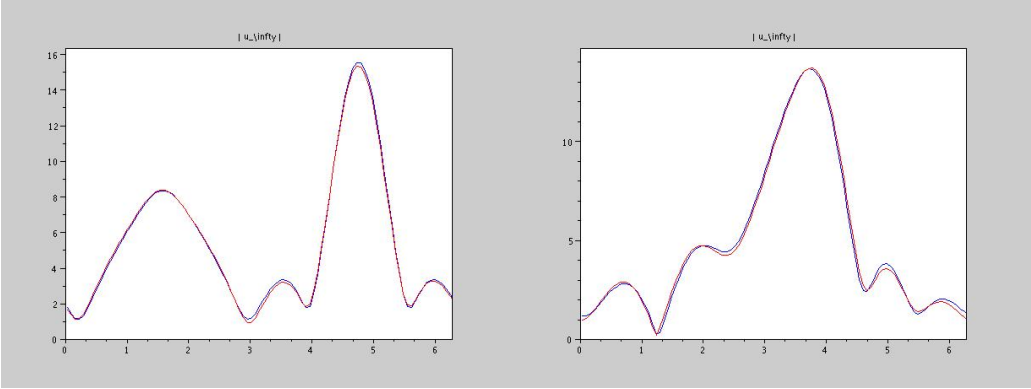

Figure 1.4: The modulus of u^∞ computed by Freefem++ (red) and by the integral equations method (blue) for $\lambda^- = \lambda^+ = 5 + i$. The angle of incidence $\theta = \pi/2$ (left) and $\theta = \pi/6$ (right). The crack is the segment $[-0.5,\ 0.5] \times \{0\}$.

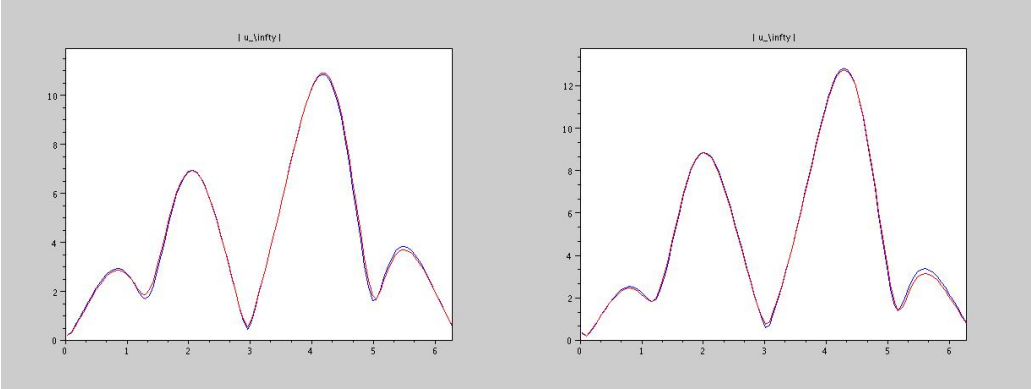

Figure 1.5: The modulus of u^∞ computed by Freefem++ (red) and by the integral equations method (blue) for $\lambda^- = \lambda^+ = 1 + i$. The angle of incidence $\theta = \pi/4$ (left) and $\theta = \pi/3$ (right). The crack is the segment $\{0\} \times [-0.5,\ 0.5]$.

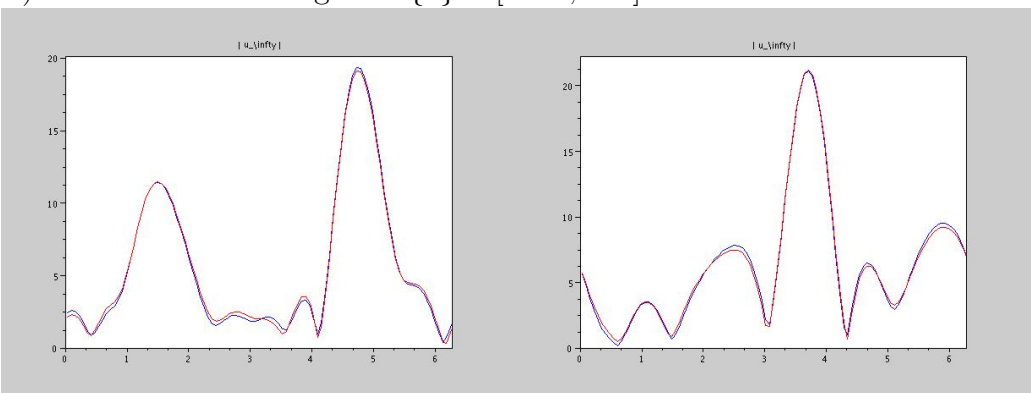

Figure 1.6: The modulus of u^∞ computed by Freefem++ (red) and by the integral equations method (blue) for $\lambda^- = \lambda^+ = 5 + i$. The angle of incidence $\theta = \pi/2$ (left) and $\theta = \pi/6$ (right). The crack is of shape L with peaks $(0, 1), (1, 1), (1, 0)$.

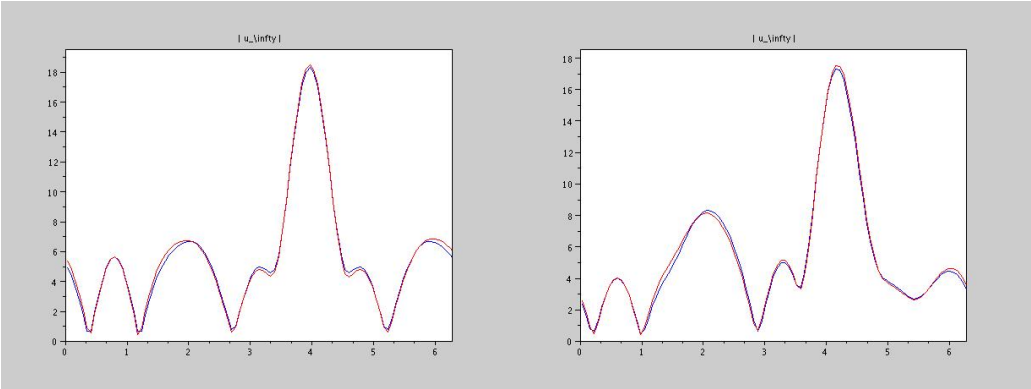

Figure 1.7: The modulus of u^∞ computed by Freefem++ (red) and by the integral equations method (blue) for $\lambda^- = \lambda^+ = 1 + i$, $\theta = \pi/4$ (left) and $\theta = \pi/3$ (right). The crack is of shape L with peaks $(0, 1), (1, 1), (1, 0)$.

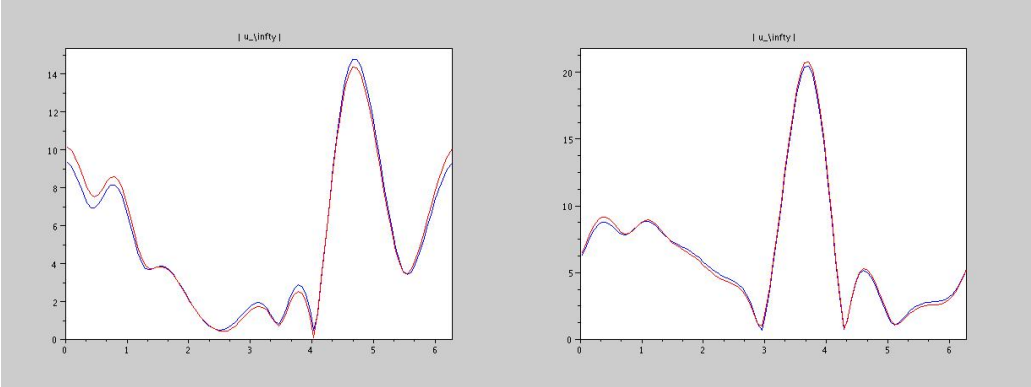

Figure 1.8: The modulus of u^∞ computed by Freefem++ (red) and by the integral equations method (blue) for $\lambda^- = \lambda^+ = 5 + i$, $\theta = \pi/2$ (left) and $\theta = \pi/6$ (right). The crack is an arc of the unit circle with an angle varying from 0 to 90 degrees.

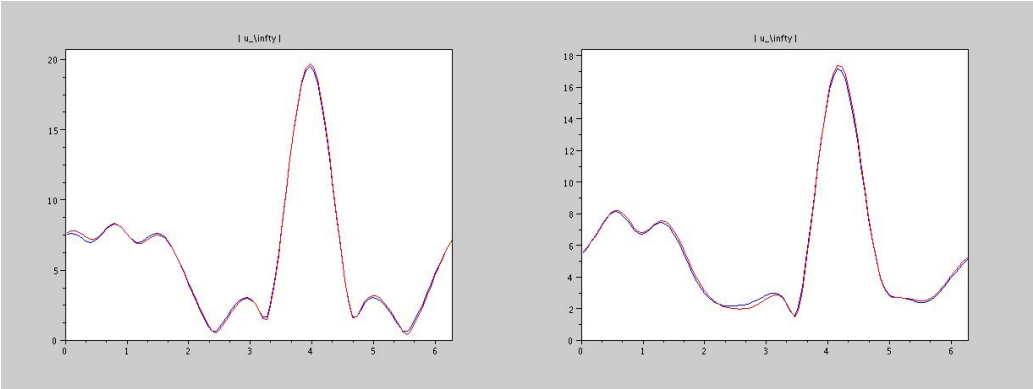

Figure 1.9: The modulus of u^∞ computed by Freefem++ (red) and by the integral equations method (blue) for $\lambda^- = \lambda^+ = 1 + i$, $\theta = \pi/4$ (left) and $\theta = \pi/3$ (right). The crack is an arc of the unit circle with an angle varying from 0 to 90 degrees.

Figures 1.4 to 1.9) clearly show that the two methods are very close which validates our scheme. Note that the integral equation method is much faster than the finite element method since the size of the linear system is much smaller (even though, the matrix is not sparse).

Numerical tests in the case of an inhomogeneous domain

In the case of an inhomogeneous domain, we compare the solution on a fixed boundary that contains the crack. We compare the results given by the variational method and the integral equations method for the two values of the impedance parameter $\lambda^+ = \lambda^- = 2+2i$ and $\lambda^+ = \lambda^- = 5+5i$ and for different locations of the point source. The measurements are done on the circle Γ_1 centered on $(0,0)$ and with radius 0.75. The crack is the segment $[-0.5, 0.5] \times \{0\}$ or an arc centered on $(0,0)$ with different apertures.

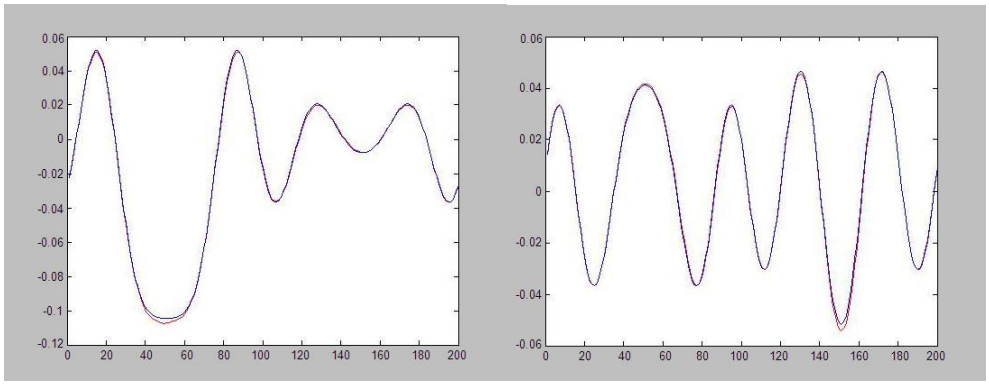

Figure 1.10: Representation of the real part (left) and the imaginary part (right) of the trace of u on Γ_1 computed by Freefem++ (red) and by the integral equations method (blue) for $\lambda^- = \lambda^+ = 2+2i$. The crack is a segment $[-0.5, 0.5] \times \{0\}$, the index of refraction $n = 2$ and the point source $x_0 = (0, 1)$.

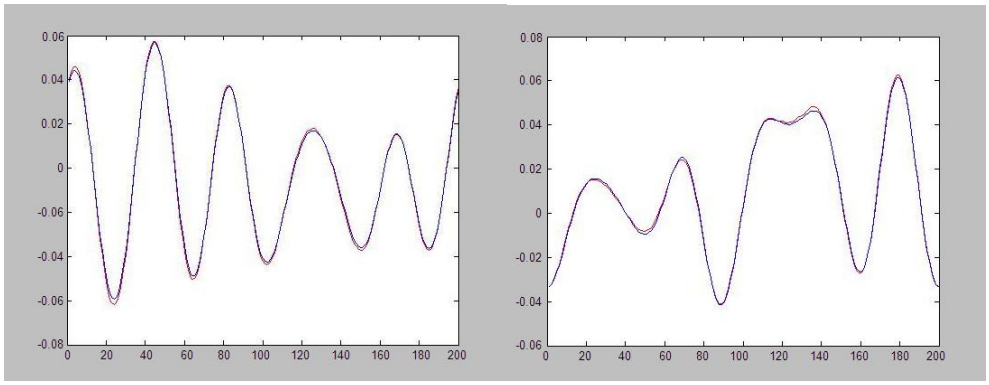

Figure 1.11: Representation of the real part (left) and the imaginary part (right) of the trace of u on Γ_1 computed by Freefem++ (red) and by the integral equations method (blue) for $\lambda^{\pm} = 2+2i$. The crack is a segment $[-0.5, 0.5] \times \{0\}$, the index of refraction $n = 2$ and the point source $x_0 = (-2, -2)$.

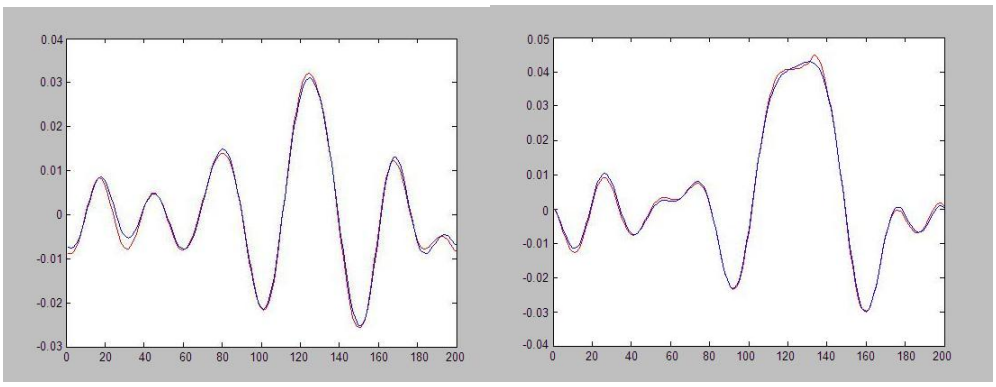

Figure 1.12: Representation of the real part (left) and the imaginary part (right) of the trace of u on Γ_1 computed by Freefem++ (red) and by the integral equations method (blue) for $\lambda^{\pm} = 5 + 5i$. The crack is an arc with radius 0.5 and aperture 180, the index of refraction $n = 4$ and the point source $x_0 = (-2, -2)$.

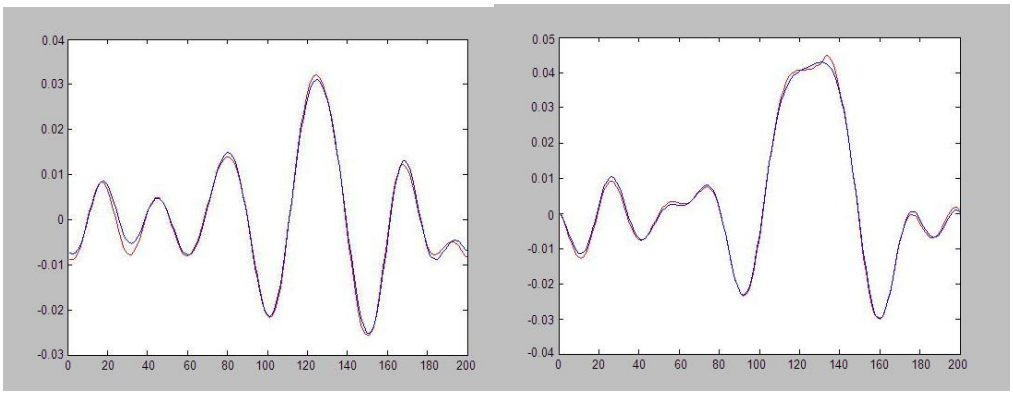

Figure 1.13: Representation of the real part (left) and the imaginary part (right) of the trace of u on Γ_1 computed by Freefem++ (red) and by the integral equations method (blue) for $\lambda^{\pm} = 10 + 10i$ the real part (left) and the imaginary part (right) The crack is an arc with radius 0.5 and aperture 90, the index of refraction $n = 4$, with point source $x_0 = (-2, -2)$.

We observe in Figures 1.10 to 1.13 that the two methods give close results for different shapes of cracks, segment or arc with different apertures and using different values of the impedance and the index of refraction, which validates our scheme in the inhomogeneous case.

CHAPTER 2

Generalities on the inverse problem

Contents

2.1 Introduction

After the study of the forward problem in Chapter 1, we now consider the associated inverse scattering problem, which consists in the crack identification by reconstructing the shape of the crack and the impedance values on both sides of the crack, using different qualitative methods. This requires the knowledge of far field measurements, as will be studied in Chapter 3 and 4, or the knowledge of all the Cauchy data on the boundary of a bounded domain that contains the crack, which will be studied in Chapter 5. To introduce these chapters, some definitions and properties necessary to the study of our inverse problem should be provided. Moreover, a general overview about this kind of problems should be presented. Note that there is a variety of inverse scattering problems that are considered in the literature. In fact, the problems depend on the different kind of data (e.g. one or multi-static far field data, one or several pairs of Cauchy measurements, etc.), the nature of the unknowns (e.g. a crack, an obstacle, etc.), the physical parameters of the unknowns (e.g. the impedance coefficient, the index of refraction of the inhomogeneous medium, etc.). In this chapter, we start by giving some properties of the far field pattern. Then, we present some uniqueness results of the solution of the inverse scattering problem. Finally, we provide a general overview of the different methods used to solve the inverse scattering problem for time-harmonic acoustic and electromagnetic waves at fixed frequency.

2.2 The far field pattern

For the setup of the inverse problem, usually the asymptotic behavior of the scattered field for large arguments is considered. Let $u^i(x,d) = e^{ikd\cdot x}$ for $x \in \mathbf{R}^m$, $m = 2, 3$, be an incident plane wave with a wave number $k > 0$ and a unit vector d giving the direction of propagation. The scattered field u^s is a solution of (1.1), (1.2) and (1.3), u^s has the asymptotic behavior of an outgoing spherical wave

$$u^s(x,d) = r^{\frac{1-m}{2}} e^{ikr} u^\infty(\hat{x},d) + O(r^{-\frac{m+1}{2}}), \tag{2.1}$$

as $r = |x| \to \infty$ uniformly in all directions $\hat{x} = x/|x|$. The function u^∞ is known as the far field pattern' of u^s. The fundamental solution Φ to the Helmholtz equation, given by

(1.8), has the following asymptotic behavior

$$\begin{aligned} m=2, \qquad \Phi(x,y) &= \frac{e^{i\frac{\pi}{4}}}{\sqrt{8\pi k}}\frac{e^{ik|x|}}{\sqrt{|x|}}(e^{-ik\hat{x}y}+\mathcal{O}(\frac{1}{|x|})) \\ \partial_{\nu(y)}\Phi(x,y) &= \frac{e^{i\frac{\pi}{4}}}{\sqrt{8\pi k}}\frac{e^{ik|x|}}{\sqrt{|x|}}(\partial_{\nu(y)}e^{-ik\hat{x}y}+\mathcal{O}(\frac{1}{|x|})) \\ m=3, \qquad \Phi(x,y) &= \frac{e^{ik|x|}}{4\pi|x|}(e^{-ik\hat{x}y}+\mathcal{O}(\frac{1}{|x|})) \\ \partial_{\nu(y)}\Phi(x,y) &= \frac{e^{ik|x|}}{4\pi|x|}(\partial_{\nu(y)}e^{-ik\hat{x}y}+\mathcal{O}(\frac{1}{|x|})) \end{aligned}$$

where $|x| \longrightarrow \infty$. Using these asymptotics and the expression (1.7) of the solution of (1.1), (1.2) and (1.3), the associated far field pattern is given by

$$u^{\infty}(\hat{x},d) = \gamma_m \int_{\sigma} \left(\partial_{\nu(y)}e^{-ik\hat{x}y}[u^s](y,d) - e^{-ik\hat{x}y}[\partial_{\nu}u^s](y,d)\right) ds(y), \qquad \forall \hat{x} \in \mathbf{S}^{m-1}. \quad (2.2)$$

where

$$\gamma_m = \begin{cases} \frac{e^{i\frac{\pi}{4}}}{\sqrt{8\pi k}} & , \quad \text{for} \quad m=2 \\ \frac{1}{4\pi} & , \quad \text{for} \quad m=3 \end{cases} \quad (2.3)$$

We now introduce one of the most important properties used in general to prove the uniqueness of the solution of some inverse problems.

Lemma 8. *[34, Lemma 2.11, p32](Rellich's Lemma)*
Assume the bounded set D as the open complement of an unbounded domain and let $u \in C^2(\mathbf{R}^m \setminus \bar{D})$ be a solution of the Helmholtz equation satisfying

$$\lim_{r\to\infty} \int_{|x=r|} |u(x)|^2 ds = 0. \quad (2.4)$$

Then $u = 0$ in $\mathbf{R}^m \setminus \bar{D}$.

Corollary 9. *[34, Theorem 2.13, p33] Let D as in Lemma 8 and let $u \in C^2(\mathbf{R}^m \setminus \bar{D})$ be a radiating solution to the Helmholtz equation for which the far field pattern vanishes identically. Then $u = 0$ in $\mathbf{R}^m \setminus \bar{D}$.*

Among the most important properties of the far field pattern that are needed to study the inverse problem, the two following reciprocity relations. The first one namely *First reciprocity relation* which can be physically explained by the fact that if we apply an incident wave with direction d to an object and we observe it in the direction $-\hat{x}$ is the same if we apply an incident wave with direction $\hat{x}$ and we observe it in the direction $-\theta$. The second one relates the scattered field to the far field.

Theorem 10. *[34, Theorem 8.8, p 223](First reciprocity principle) Let $u^\infty(\hat{x}, d)$ be the far field pattern with a direction of observation $\hat{x}$ and a direction d of the incident plane wave. Then*

$$u^\infty(-\hat{x}, d) = u^\infty(-d, \hat{x}), \qquad (\hat{x}, d) \in \mathbf{S}^{m-1}.$$

It follows from Theorem 10 the mixed reciprocity theorem (see [53, Theorem 1.7, p8]) which is very useful. We use it in the theoretical justification of the RG-LSM in Chapter 5. To this aim we adapt it to the case of cracks with impedance boundary conditions in Theorem 11.

Theorem 11. *(Second or mixed reciprocity principle)*
Let $u^s(z, d)$ be the scattered field at $z \in \mathbf{R}^m \setminus \overline{\sigma}$ that corresponds to the incident plane wave $u^i(x, d) = e^{ikx\cdot d}, \quad x \in \mathbf{R}^m$. Furthermore, let $v^\infty(d, z)$ be the far field pattern of the scattered field v^s corresponding to the incident point source $v^i(x, z) = \Phi(x, z)$, $x \in \mathbf{R}^m$. Then

$$v^\infty(d, z) = \gamma_m u^s(z, -d), \quad d \in \mathbf{S}^{m-1} \text{ and } z \notin \bar{\sigma}.$$

Proof. Given two incident fields u^i and v^i, the associated total fields u and v satisfy (1.1) and (1.2). Using the boundary condition (1.2) on σ, we obtain

$$\int_\sigma \partial_\nu u_2^+ u_1^+ - \int_\sigma \partial_\nu u_1^+ u_2^+ + \int_\sigma \partial_\nu u_1^- u_2^- - \int_\sigma \partial_\nu u_2^- u_1^- = \int_\sigma \lambda^+ u_1^+ u_2^+ - \int_\sigma \lambda^+ u_2^+ u_1^+ + \int_\sigma \lambda^- u_1^- u_2^- - \int_\sigma \lambda^- u_2^- u_1^- = 0$$

By using the decomposition $u_1 = u_1^i + u_1^s$ and $u_2 = u_2^i + u_2^s$ and the fact that the scattered fields solve the Helmholtz equation outside of σ as well as the radiation condition, we obtain

$$\int_\sigma \left([u_1^s]\, \partial_\nu u_2^i - u_2^i\, [\partial_\nu u_1^s] \right) ds = \int_\sigma \left([u_2^s]\, \partial_\nu u_1^i - u_1^i\, [\partial_\nu u_2^s] \right) ds. \tag{2.5}$$

Let $x \in \mathbf{R}^m \setminus \bar{\sigma}$, we recall the expression of u_2^s when the incident field is the point source wave $\Phi(., x)$

$$u_2^s(x, d) = \int_\sigma \left(\Phi(x, y)[\partial_\nu u_2^s](y, d) - \partial_{\nu(y)} \Phi(x, y)[u_2^s](y, d) \right) ds(y), \quad \forall x \in \mathbf{R}^m \setminus \bar{\sigma}.$$

By applying (2.5) when u_1^i is the plane wave with direction d and u_2^i is the point source wave $\Phi(., x)$ we obtain:

$$\gamma_m u_1^s(x, d) = u_2^\infty(-d, x), \tag{2.6}$$

where γ_m is given by (2.3). □

We propose to give some key properties of the scattering problem needed in the study of the inverse problem. We rewrite here the unique continuation principle proposed in [34, Lemma 8.5, p219].

Theorem 12. *(Unique continuation principle) Let $\mathcal{O}$ be an open set and $u \in H^2(\mathcal{O})$ such that there exists a constant C for which*

$$|\Delta u(x)| \leq C(|\nabla u(x)| + |u(x)|), \qquad \text{for a.e. } x \in \mathcal{O}.$$

If u vanishes a.e. in a neighborhood of a point $x_0 \in \mathcal{O}$ then u vanishes a.e in $\mathcal{O}$.

Corollary 13. *Let $\mathcal{O}$ be an open set and $\Sigma \subset \partial\mathcal{O}$ such that $|\Sigma| \neq 0$. We assume that u is a solution of*

$$\Delta u + k^2 u = 0 \quad \text{in } \mathcal{O}.$$

If $(u, \partial_\nu u)$ vanishes on Σ then u vanishes in $\mathcal{O}$.

Proof. Let $x_0 \in \Sigma$ and B_{x_0} be a ball centered on x_0 such that $B_{x_0} \cap \partial\mathcal{O} \subset \Sigma$. Let $B^-_{x_0}$ and $B^+_{x_0}$ be such that

$$B^-_{x_0} = B_{x_0} \cap \mathcal{O} \quad \text{and} \quad B^+_{x_0} = B_{x_0} \cap (\mathbf{R}^m \setminus \mathcal{O})$$

We define $\tilde{u} \in H^1(B_{x_0})$ by

$$\tilde{u} = u \quad \text{in} \quad B^-_{x_0} \qquad \text{and} \qquad \tilde{u} = 0 \quad \text{in} \quad B^+_{x_0}.$$

Since $(u, \partial_\nu u)_{|\Sigma} = 0$ and $\tilde{u}$ vanishes in $B^+_{x_0}$ and satisfies the Helmholtz equation in $B^-_{x_0}$, then $\Delta\tilde{u} + k^2\tilde{u} = 0$ in B_{x_0}. Consequently, $\tilde{u} \in H^2_{loc}(B_{x_0})$ and

$$|\Delta\tilde{u}(x)| \leq k^2|\tilde{u}(x)|, \qquad \text{for} \quad x \in B_{x_0}. \tag{2.7}$$

Therefore, using the unique continuation principle, $\tilde{u} = 0$ in B_{x_0} and consequently $u = 0$ in $B^-_{x_0}$. Applying the unique continuation principle to u, we get that u vanishes in $\mathcal{O}$. □

2.3 Uniqueness of the solution of the inverse problem

In this section we are interested in proving the uniqueness of the solution of the inverse problem of scattering by a crack with impedance boundary conditions from measurements of the far field pattern for all directions and observation points.
Colton and Sleeman [37] proved in 1983 that a sound-soft obstacle D is uniquely determined by the far field pattern for one incident plane wave if $k\ diam(D) < 2\pi$. In 1997, Liu [66] extended this result to the case of a sound soft ball. Cheng and Yamamoto [27] in 2003, Alessandrini and Rondi [2] in 2005, Elschner and Yamamoto [40] in 2006, Liu and Zou [67] in 2006 generalized the result given by Liu for the ball to the case of a polyhydral sound-soft obstacle.
When the far field pattern $u^\infty(\hat{x}, d)$ is given for all directions d and observation points $\hat{x}$, the first uniqueness theorem was given by Shiffer [83] in 1960 for the case of a sound-soft

obstacle. The main ingredient of the proof of Shiffer is the Rellich's Lemma. In 1988, Nachman, Novikov and Ramm [74, 76, 78] established the uniqueness results in the case of an inhomogeneous medium. We refer also to [29] and [34] for other uniqueness results of the inverse obstacle scattering problem, where it is assured that in principle the data is sufficient to uniquely determine the obstacle.
For the case of a sound soft or a sound hard crack, the uniqueness results are quite similar to those for the obstacle. L. Rondi [80] proved the uniqueness of the inverse problem for a sound soft defect. For the case of a crack with impedance boundary conditions, we prove the following uniqueness result.

Theorem 14. *Assume that σ_1, σ_2 are two cracks and λ_1, λ_2 two impedance functions satisfying the assumptions $\lambda_i^{\pm} \in L^\infty(\sigma_i)$ and $\lambda_i^+ + \lambda_i^- \neq 0$ a.e, for $i = 1:2$. If the far field patterns u_j^∞ of the scattered waves u_j^s solutions of the (1.1), (1.2) and (1.3) associated to σ_j, λ_j, for $j = 1, 2$, coincide for all incident directions d then $\sigma_1 = \sigma_2$ and $\lambda_1 = \lambda_2$.*

Proof. Assume that $u_1^\infty(., d) = u_2^\infty(., d)$ for all the directions $d \in \mathbf{S}^{m-1}$ of the incident plane waves $u^i(x, d) = e^{ikx\cdot d}$.
Then, by the Rellich's Lemma, $u_1^s(\cdot, d) = u_2^s(\cdot, d)$ in $\mathbf{R}^m \backslash (\overline{\sigma}_1 \cup \overline{\sigma}_2)$. Hence, using the mixed reciprocity relation,

$$u_j^s(z, d) = u_j^\infty(d, z), \qquad \text{for all } d \in \mathbf{S}^{m-1} \text{ and } z \notin \sigma_j,$$

for $j = 1, 2$, we get

$$u_1^\infty(\cdot, z) = u_2^\infty(\cdot, z), \qquad \text{for } z \in \mathbf{R}^m \backslash (\overline{\sigma}_1 \cup \overline{\sigma}_2).$$

where $u_i^\infty(\cdot, z)$ is associated to the incident point source $u^i = \Phi(\cdot, z)$ in the source point z. Thus, by the Rellich's Lemma, $u_1^s(x, z) = u_2^s(x, z)$, for $x, z \in \mathbf{R}^m \backslash (\overline{\sigma}_1 \cup \overline{\sigma}_2)$.

Let us assume that $\sigma_1 \neq \sigma_2$. Then, there exists $x^* \in \partial C$ such that $x^* \in \sigma_1$ and $x^* \notin \sigma_2$. In particular, $z_n := x^* + \frac{1}{n}\nu(x^*)$, belongs to C for integers n sufficiently small and $z_n \in \sigma_1$ for n sufficiently large.
The boundary condition on σ_1 reads

$$\partial_\nu u_{1,\pm}^s(x^*, z_n) + \lambda_1^{\pm} u_{1,\pm}^s(x^*, z_n) = -(\partial_\nu \pm \lambda_1^{\pm})\Phi(x^*, z_n).$$

Then, since u_2^s is analytic outside of σ_2 and $u_1^s(x^*, z_n) = u_2^s(x^*, z_n)$, we have

$$\partial_\nu u_{2,\pm}^s(x^*, z_n) + \lambda_1^{\pm} u_{2,\pm}^s(x^*, z_n) = -(\partial_\nu \pm \lambda_1^{\pm})\Phi(x^*, z_n). \tag{2.8}$$

For non vanishing $\lambda_i^{\pm} \in L^\infty(\sigma)$, $\quad i = 1:2$, the left hand side of (2.8) is bounded whereas the right hand side blows up when z_n tends to x^* which is a contradiction.

Finally, let $\sigma_1 = \sigma_2$ and assume that $(\lambda_1^+, \lambda_1^-) \neq (\lambda_2^+, \lambda_2^-)$. Then from Rellichs lemma, for a given incident field, the boundary condition writes

$$\partial_\nu u_{1,\pm} + \lambda_1^\pm u_{1,\pm} = \partial_\nu u_{2,\pm} + \lambda_2^\pm u_{2,\pm}, \quad \text{on } \sigma \tag{2.9}$$

using the fact that $u_1 = u_2$, we have

$$(\lambda_1^\pm - \lambda_2^\pm) u_{1,\pm} = 0, \quad \text{on } \sigma. \tag{2.10}$$

Therefore, since $(\lambda_1^+, \lambda_1^-) \neq (\lambda_2^+, \lambda_2^-)$, by the unique continuation principle $u_1^s = 0$ in $\mathbf{R}^m \setminus \bar{\sigma}$ and the associated far field vanishes which contradicts the hypothesis. Therefore, $\lambda_1 = \lambda_2$. □

2.4 Some reconstruction methods

The reconstruction methods for inverse scattering problems can be classified in three families, the iterative methods, the decomposition schemes and the qualitative methods. Let us provide a brief description of some identification methods of each family.

2.4.1 Iterative methods

The iterative methods give an identification of the unknown objects thanks to an appropriate parametrization of the boundary of the scatterer and by computing the parameters using iterative schemes. The principle of this kind of methods is to formulate the inverse problem as finding the zero of some operators expressed in function of the data. This problem is not linear which requires to use some iterative process to linearize it. This kind of methods are well-known for their high-quality reconstructions of the shape of the scatterer when the data are sufficiently good and the use of a small amount data which are necessary to ensure at least local uniqueness of the solution. For an inverse obstacle scattering, the methods work when a scatterer is illuminated by one time-harmonic wave only. However, the main drawbacks of these methods is the need of a priori information on the unknown object such as the type of the boundary conditions since the methods use some derivative tools as the Frechet derivative or topological derivative which requires to solve some direct problems in every iteration step which is computationally very expensive. These methods can also suffer from local minima for large nonlinear optimization functional. However, they offer the possibility of reconstructing only a part of the scatterer or to reconstruct only some of its properties.

The Newton method

In this subsection, we explain the principle of the Newton method. Let u^i be a fixed incident field. We define the far field operator $F : \partial D \longrightarrow u^\infty$ mapping the boundary ∂D

of the scatterer D, which can be an obstacle or a crack, onto the far field pattern u^∞ of the scattered wave u^s. The inverse problem consists in solving the operator equation

$$F(\partial D) = u^\infty. \tag{2.11}$$

This is an ill-posed and non linear problem. The inversion algorithm is based first on the linearization of (2.11) by solving, for a given initialization ∂D_0 in a class of admissible surfaces, the following equation

$$F'(\partial D_0)h + F(\partial D_0) \simeq u^\infty, \tag{2.12}$$

since we have

$$F(\partial D_0 + h) = F(\partial D_0) + F'(\partial D_0)h + O(h^2)$$

where $h = \partial D - \partial D_0$ is the increment and F' is the Fréchet derivative of F. By solving the equation (2.12), we find h that yields the new approximation of ∂D, given by $\partial D_1 = \partial D_0 + h$. The Newton method consists in iterating this procedure. A characterization of the Fréchet derivative is given by solving a scattering problem similar to the direct problem. For example, in the case of the Dirichlet boundary condition, the Fréchet derivative is given by

$$F'(\partial D_0)h = v_h^\infty,$$

where v_h^∞ is the far field pattern of the radiating solution v_h^∞ to the Helmholtz equation in $\mathbf{R}^m \setminus \overline{D}$ satisfying the Dirichlet boundary condition

$$v_h = -(\nu \cdot h)\partial_\nu u \quad \text{on } \partial D$$

in terms of the total field $u = u^i + u^s$. Solving (2.12) is an ill-posed problem. To this end, a regularization is needed. Using the Tikhonov regularization, the equation (2.12) is replaced by

$$\alpha h + [F'(\partial D_0)]^* F(\partial D_0)h = [F'(\partial D_0)]^* \{u^\infty - F(\partial D_0)\} \tag{2.13}$$

where α is a regularization parameter. The Newton method has been extended and successfully tested for other boundary conditions in the case of the obstacle [57, 58, 62, 70, 71, 63] and for scattering from cracks [59, 60, 72].

The Topological gradient method

The topological gradient method was introduced by A. Schumacher [82], J. Sokolowski and A. Zochowski [84]. It consists in studying the behavior of a shape functional when modifying the topology of the domain by the creation of a small trial flaw in a defect-free domain or in some cases a small hole. More precisely, the main idea of this method is to consider a variable domain D and a cost functional $j(D) = J(u_D)$ to be minimized, where

u_D is a solution to a given PDE defined in D. Let $x_0 \in D$ and $B(x_0, \rho)$ be a ball centered in x_0 with a small radius ρ, the perturbed domain is $D \setminus B(x_0, \rho)$. The topological sensitivity analysis provides the following asymptotic expansion of $j(D \setminus B(x_0, \rho))$ when ρ tends to zero

$$j(D \setminus B(x_0, \rho)) - j(D) = f(\rho)g(x_0) + O(f(\rho)),$$

where f is a positive function and g is the so-called topological gradient or topological derivative. Consequently, the defect is detected by the set of holes at some points x where g is negative. For cracks in the case of the Laplace equation, I. Horchani [46] used the previous concept and gave an algorithm to locate the crack which requires to solve the direct and adjoint problems for few iterations.
C. Bellis [7], C. Bellis and M. Bonnet [8] gave a time-domain topological derivative method to retrieve a crack Γ embedded in a domain Ω in linear elasticity and acoustics. By defining $z \to \mathbb{T}(z, \bar{\Gamma}, T)$ as the indicator function, the crack consists in the set of points $z \in \Omega$ at which $\mathbb{T}(z, \bar{\Gamma}, T)$ have a negative value. Here, $\mathbb{T}(z, \bar{\Gamma}, T)$ is the topological derivative field of a cost function $\mathbb{J}$ as

$$\mathbb{J}(\Omega_{\epsilon,z}, T) = \mathbb{J}(\Omega, T) + \eta(\epsilon)T(z, \bar{\Gamma}, T) + O(\eta(\epsilon)).$$

Considering an infinitesimal trial crack $\Gamma_\epsilon = z + \epsilon\Gamma$ centered at $z \in \Omega$ with characteristic size ϵ, whose shape is defined using a normalized open surface Γ, and setting $\Omega_\epsilon = \Omega \setminus \Gamma_\epsilon$. For the cost function $\mathbb{J}$ defined by

$$\mathbb{J} = \int_0^T \int_{S_{obs}} \varphi[u_\Gamma(\xi, t), \xi, t] dS_\xi dt,$$

where $S_{obs} \subset \partial\Omega$ is the measurement surface and

$$\varphi[w, \xi, t] = \frac{1}{2}\|w - u_{obs}(\xi, t)\|^2.$$

The misfit function φ is chosen so as the gap between measurements u^{obs} and the displacement u_Γ arising in a trial cracked solid Ω_Γ. The method proposed in [7] is not considered as an iterative method but as a qualitative method since the value of the indicator should be computed at each point of the sampling domain.

2.4.2 Decomposition methods

The main idea of the decomposition methods is to split the inverse scattering problem into a linear and ill-posed problem which consists in reconstructing the scattered wave from the far field pattern and a nonlinear well posed problem by determining the unknown boundary of the scatterer as the location where the boundary condition for the total field is satisfied. This idea was proposed by Colton and Monk in 1986 [35], Kirsch an Kress in 1987 [54] and

Potthast in 1996 [77] with the Point Source Method. Notice that the conformal mapping proposed by I. Akduman and R. Kress [1] is considered as a decomposition method in the case of the Laplace equation. The decomposition methods have the advantage of avoiding to solve any forward problem. Also, parts of the scatterer might be reconstructed and other parts neglected. In principle, with an appropriate set-up, these analytic continuation methods provide high-quality reconstructions. Some of their limitations are similar to those of iterative schemes since they need an a priori knowledge of the boundary conditions of the unknown objects whereas this information might not be available for some applications.

Decomposition method: Kirsch and Kress

For scattering by a sound soft obstacle, the scattered field u^s can be written as the single-layer potential

$$u^s(x) = \int_{\partial D} \varphi(y)\Phi(x,y)ds(y), \qquad x \in \mathbf{R}^m \setminus \overline{D}, \tag{2.14}$$

with an unknown density $\varphi \in L^2(\partial D)$. In this case, we have

$$u^\infty(\hat{x}) = \frac{1}{4\pi}\int_{\partial D} \varphi(y)e^{-ik\hat{x}.y}ds(y), \qquad x \in \mathbf{S}^{m-1}. \tag{2.15}$$

First, a linear ill-posed problem is solved which consists in computing the density φ from the measured far field pattern u^∞ by solving the linear integral equation of the first kind

$$S_\infty \varphi = u^\infty \tag{2.16}$$

with the compact integral operator $S_\infty : L^2(\partial D) \longrightarrow L^2(\mathbf{S}^{m-1})$ given by

$$(S_\infty\varphi)(\hat{x}) = \frac{1}{4\pi}\int_{\partial D} \varphi(y)e^{-ik\hat{x}\cdot y}ds(y), \qquad x \in \mathbf{S}^{m-1}.$$

Due to the fact that S_∞ is a compact operator since it is an integral operator with smooth kernel then the equation (2.16) is severely ill-posed. For a stable numerical solution of this equation, a regularization is needed. We can apply for example the Tikhonov regularization scheme by solving

$$\alpha\varphi_\alpha + S_\infty^* S_\infty \varphi_\alpha = S_\infty^* u^\infty \tag{2.17}$$

with a positive regularization parameter α where S_∞^* is the adjoint of S_∞. The second step consists in solving the nonlinear but well-posed problem of finding the unknown sound soft obstacle by finding the zeros of the total field. Hence, given an approximation of the scattered waves u_α^s obtained by inserting a solution φ_α of (2.17) into the potential (2.14) we search $u^i + u^s = 0$ in a last-squares sense, i.e. by minimizing

$$\|u^i + u_\alpha^s\|_{L^2(\Lambda)} \tag{2.18}$$

over a suitable set of admissible surfaces Λ. Instead of solving the two problems separately, which has a negative impact on the accuracy of the results, the two problems are coupled. This is achieved by combining the minimization of the Tikhonov function for (2.16) and the minimization (2.18) into one cost functional

$$\|S_\infty \varphi - u^\infty\|^2_{L^2(\partial D)} + \alpha \|\varphi\|^2_{L^2(\partial D)} + \gamma \|u^i + u^s_\alpha\|^2_{L^2(\Lambda)}. \tag{2.19}$$

Here $\gamma > 0$ denotes a coupling parameter which has to be chosen appropriately for the numerical implementation in order to make the two terms in (2.19) of the same magnitude, for example

$$\gamma = \|u^\infty\|_{L^2(\mathbf{S}^{m-1})} / \|u^i\|_\infty.$$

2.4.3 Sampling methods

The idea of the Sampling methods is to define an indicator function that provides information about the location, shape and properties of the unknown object. The main advantage of the Sampling methods is that they avoid to solve any sequence of forward problems as in the iterative methods and they can treat a large class of practically relevant problems where only limited knowledge about the scatterer is available. In fact, these methods do not require any a priori information on the physical properties of the unknown object. The numerical implementation is also extremely simple and fast in this case. However, in general the drawback of these methods is that they need a large number of data since one usually needs all measurements of the far-field pattern for all directions of incident plane waves and all observation points.

The Linear Sampling Method

Let's now describe the Linear Sampling Method, which has been first introduced by Kirsh and Colton in 1996 [33] and analyzed in [36]. For different applications of the LSM for obstacle detection with various boundary conditions in the case of Helmholtz or Maxwell equation we refer to [22, 23, 32, 31, 5, 6]. We summarize the main idea of this method in the case of the obstacle. Let ∂D be the boundary of the obstacle D with non empty interior. We assume that we have all the measurements of the far field pattern associated to the scattered field u^s satisfying the Helmholtz equation outside of the scatter and the radiation condition. To reconstruct D, we represent the sampling domain as a grid and we solve for every sampling point z the following equation

$$F(g) \simeq \Phi^\infty(., z) \tag{2.20}$$

where the far-field operator $F : L^2(\mathbf{S}^{m-1}) \longrightarrow L^2(\mathbf{S}^{m-1})$ is defined by

$$F(g)(\hat{x}) = \int_{\mathbf{S}^{m-1}} u^\infty(\hat{x}, d) g(d) ds(d) \tag{2.21}$$

and Φ^∞ is the far field pattern of the Green function Φ of the domain. The behavior of the solution of (2.20) gives a characterization of the scatterer. In fact, as a consequence of the equation (2.20), we have

$$u^s_{v_g}(z') = \Phi(z', z) \tag{2.22}$$

where $u^s_{v_g}$ is the scattered wave associated to the incident Herglotz wave v_g given by

$$v_g(x) = \int_{\mathbf{S}^{m-1}} e^{ikd\cdot x} g(d) ds(d).$$

Consequently, (2.20) may have a solution only if $z \in D$, since otherwise $|\Phi(z', z)|$ goes to infinity while $|u^s_{v_g}(z')|$ is finite for $z' \to z$. Let's now give a small idea about the theoretical justification. The equation (2.20) does not always have a solution since Φ^∞ is not always in the range of F. Hence, an approximated solution should be found. The operator can be factored as $F = G\mathcal{H}$ where

$$z \notin D \qquad \text{if and only} \qquad \Phi^\infty(., z) \in R(G),$$

and $R(G)$ is the range of G.
Consequently using the denseness of $R(\mathcal{H})$, the existence of an approximated solution is proved. Hence, we can deduce that the characterization of the scatterer is given by the $R(G)$.
For the numerical implementation, an approximate solution of (2.20) is computed using a regularization. For instance for Tikhonov this is equivalent to

$$(\alpha I + F^* F)g = F^* \Phi^\infty(., z).$$

We refer to [36] and [19] for the analysis of possible strategies to choose the regularization parameter α.

In the case of a crack, we use a similar process with a slight modification by changing the test function in the far field equation with the far field associated to the combinaison of single and double layer potentials on an arc and the sampling points by sampling arcs. We refer to Chapter 3 for detailed analysis of this method.

The Factorization method

The Factorization algorithm has been first introduced by A. Kirsh on 1998 [53]. It is inspired from the Linear Sampling Method. The main advantage of this method is to give an explicit function to characterize the scatterer contrary to the LSM which is based on an approximated solution. Moreover as a qualitative method, it does not require a priori knowledge of the physical properties of the scatterer. Despite considerable efforts [50, 51, 52, 55, 56], the Factorization method is still limited to a restricted class of scattering

problems. The method has not been established yet for limited aperture data or partially coated obstacles.
Recall that in the theoretical justification of the LSM, a factorization of F in the form of $F = G\mathcal{H}$ is required and a characterization of the obstacle is then given by the $R(G)$. The factorization method is based on the characterization of $R(G)$ in terms of the range of some operator function applied to F. For instance, we observe in some particular cases that G can be expressed as $G = \mathcal{H}^*T$ where $\mathcal{H}^*$ is the adjoint of $\mathcal{H}$ and T is an isomorphism. Therefore, we have $R(G) = R(\mathcal{H}^*)$. By replacing the expression of G in the expression of F, we prove that when F is normal $R(\mathcal{H}^*)$ is given by

$$R(\mathcal{H}^*) = R((FF^*)^{1/4})$$

and consequently, one can then show that the equation

$$(FF^*)^{1/4}(g) = \Phi^\infty(\cdot, z),$$

has a solution if and only if $z \in D$. Otherwise, when F fails to be normal such as in the case of an impedance boundary condition with positive imaginary part or when the imaginary part of the index medium is not zero, we have a characterization of $R(\mathcal{H}^*)$ using the so-called $F_\sharp$ operator defined as follows:

$$F_\sharp = |\Re F| + |\Im F|$$

where

$$\Re F := \frac{F + F^*}{2} \qquad \text{and} \qquad \Im F := \frac{F - F^*}{2i}.$$

In this case, we have $R(\mathcal{H}^*) = R(F_\sharp^{1/2})$ and consequently the equation that we solve is

$$(F_\sharp)^{1/2}(g) = \Phi^\infty(., z).$$

We refer to Chapter 4 for a detailed exposition of this method in the case of crack. For more applications of the factorization method, see [53] and for inverse scattering by a sound soft crack we refer to [55].

CHAPTER 3

The LSM to retrieve a crack with impedance boundary conditions

Contents

Abstract
We use the Linear Sampling Method (LSM) to detect a crack with impedance boundary conditions. This work extends the work of Cakoni and Colton [21] that uses the LSM to reconstruct a crack with mixed boundary conditions from measurements of the far field patterns associated with different incident plane waves. The performance of our method is illustrated through some numerical examples.

3.1 Introduction

In this chapter, we shall investigate the application of the Linear Sampling Method (LSM) to retrieve the geometry of the crack from multi-static far field data at a given frequency. As compared to previous works on this type of problem and methods [21, 38, 55, 85], the originality of the present one relies on considering the case of the impedance boundary conditions on both sides of the crack. This induces more technical difficulties in the justification of the method and also on the numerical side. For instance the algorithm proposed in [21] does not work if one of the impedance values is not infinite. The main difficulty relies on the choice of the orientation of the probing "small" crack. Based on the theoretical justification of the LSM we propose a minimization procedure that enforces the correct choice of this orientation. We not only stop at the reconstruction of cracks, but more than that we also find the value of the impedance parameter in both sides of the crack using two approaches. The first one, that we call the natural approach, is based on finding the scattered field from the far field pattern and the boundary conditions. The second one uses the solution of the far field equation founded on the linear sampling method.

This chapter is organized as follows. In Section 3.2 we present briefly the direct problem. This is followed in Section 3.3 by introducing the inverse problem and describing our formulation of the LSM along with the mathematical justifications. Section 3.3.2 is devoted to the numerical schemes and tests for different shapes of cracks and different values of the impedances. Finally, in the last Section 3.4 we find a reconstruction of the impedance values on both sides of the crack using the two approaches. We demonstrate the feasibility of the two approaches by some numerical results.

3.2 The direct problem

We give here a brief introduction of the direct problem. We recall that the study of this problem is given on the Chapter 1. Let $\sigma \subset \mathbf{R}^m$, $m = 2, 3$, be a smooth nonintersecting open arc. For further considerations, we assume that σ can be extended to an arbitrary smooth, closed curve $\partial\Omega$ enclosing a bounded domain Ω in $\mathbf{R}^m$. The normal vector ν on σ coincides with the outward normal vector to $\partial\Omega$, with simply connected complement.

Impedance type boundary conditions on σ lead to the following problem

$$\begin{cases} \Delta u + k^2 u = 0 & \text{in } \mathbf{R}^m \setminus \overline{\sigma} \\ \partial_\nu u_\pm \pm \lambda^\pm u_\pm = 0 & \text{on } \sigma \end{cases} \tag{3.1}$$

where the wave number k is positive and $\lambda^\pm \in L^\infty(\sigma)$ are the given (complex-valued) impedance functions with non-negative imaginary part and $(\lambda^+ + \lambda^-)^{-1} \in L^\infty(\sigma)$. Notice that $u_\pm(x) = \lim_{h\to 0^+} u(x \pm h\nu)$ and $\partial_\nu u_\pm = \lim_{h\to 0^+} \nu \cdot \nabla u(x \pm h\nu)$ for $x \in \sigma$.
The total field $u = u^i + u^s$ is decomposed into the given incident plane wave $u^i(x,d) = e^{ikd\cdot x}$ with unitary direction d and the unknown scattered field u^s which is required to satisfy the Sommerfeld radiation condition

$$\lim_{r=|x|\to+\infty} r^{\frac{m-1}{2}}(\partial_r u^s - iku^s) = 0, \tag{3.2}$$

uniformly in all directions $\hat{x} = \frac{x}{|x|}$.
This problem have a unique solution (see Chapter 1). Our inverse problem consists in reconstructing the crack σ by knowing all the measures of $u_\infty(\hat{x}, d)$ on all directions d and observations point $\hat{x}$. To this aim, we use the LSM.

3.3 The inverse problem

3.3.1 Settings and theoretical justification of the LSM

In this section, we adapt the LSM for scattering by a partially coated crack (see [21]) to the following inverse problem :

Inverse scattering by an Impedance Crack (IIC). Given the far field pattern $u^\infty(\hat{x}, d)$ for all $(\hat{x}, d) \in \mathbf{S}^{m-1} \times \mathbf{S}^{m-1}$ of the solution to (ICP), reconstruct the crack σ.

To solve the (IIC) by the LSM method, we first define the far field operator

$$\begin{array}{rccc} F: & L^2(\mathbf{S}^{m-1}) & \to & L^2(\mathbf{S}^{m-1}) \\ & g & \mapsto & \displaystyle\int_{\mathbf{S}^{m-1}} u^\infty(\cdot, y) g(y) ds(y) \end{array} \tag{3.3}$$

and consider the far field equation

$$F(g_L)(\hat{x}) = \Phi_L^\infty(\hat{x}) \qquad \text{for all} \quad \hat{x} \in \mathbf{S}^{m-1} \tag{3.4}$$

where $\Phi_L^\infty \in L^2(\mathbf{S}^{m-1})$ is given by

$$\Phi_L^\infty(\hat{x}) = \gamma \int_L \left(\alpha_L(y) \frac{\partial e^{-ik\hat{x}\cdot y}}{\partial \nu(y)} + \beta_L(y) e^{-ik\hat{x}\cdot y} \right) ds(y), \tag{3.5}$$

$$\text{with } \gamma = \begin{cases} \dfrac{e^{i\pi/4}}{\sqrt{8k\pi}} & \text{in } 2D \\ \dfrac{1}{4\pi} & \text{in } 3D \end{cases} \tag{3.6}$$

Notice that Φ_L^∞ is the far field pattern of the potential Φ_L defined by

$$\Phi_L(x) := \int_L \left(\alpha_L(y) \frac{\partial \Phi(x,y)}{\partial \nu(y)} + \beta_L(y) \Phi(x,y) \right) ds(y) \tag{3.7}$$

with densities $\alpha_L \in \tilde{H}^{\frac{1}{2}}(L)$ and $\beta_L \in \tilde{H}^{-\frac{1}{2}}(L)$, for any smooth non intersecting $(m-1)$ manifold $L \in \mathbf{R}^{m-1}$.
We will characterize the crack σ by the behavior of an approximate solution g_L of the far field equation (3.4).

To prove the existence of an approximate solution of (3.4), we factorize the operator F as $F = B\mathcal{H}$ where $B : H^{-1/2}(\sigma) \times \tilde{H}^{-1/2}(\sigma) \to L^2(\mathbf{S}^{m-1})$ maps the boundary data $(g^+, g^+ - g^-)$ to the far field pattern of the solution of (ICP) and $\mathcal{H}$ is the trace operator defined by

$$\begin{array}{rccc} \mathcal{H}: & L^2(\mathbf{S}^{m-1}) & \to & H^{-1/2}(\sigma) \times \tilde{H}^{-1/2}(\sigma) \\ & g & \mapsto & (-(\partial_\nu + \lambda^+)v_g, -(\lambda^+ + \lambda^-)v_g) \end{array}$$

where v_g is the Herglotz wave function of kernel $g \in L^2(\mathbf{S}^{m-1})$,

$$v_g(x) := \int_{\mathbf{S}^{m-1}} e^{ikx\cdot d} g(d)\, ds(d), \quad x \in \mathbf{R}^m. \tag{3.8}$$

We will show that the traces of the solution of the (ICP) on both sides of σ can be approximated by the appropriate traces of the Herglotz wave function v_g.

Lemma 15. *The operator $\mathcal{H}$ is injective and has a dense range.*

Proof. Let $g \in L^2(\mathbf{S}^{m-1})$ be an element of the kernel of $\mathcal{H}$. Then,

$$(\partial_\nu + \lambda^\pm)v_g = 0 \quad \text{and} \quad (\lambda^+ + \lambda^-)v_g = 0 \qquad \text{on } \sigma.$$

Since by assumption $(\lambda^+ + \lambda^-) \neq 0$ then $v_g = 0$ and $\partial_\nu v_g = 0$ on $\sigma_0 \subset \sigma$. From the unique continuation principle (see Corollary 13), it implies that $v_g = 0$ in $\mathbf{R}^m$ and therefore $g = 0$ which proves that $\mathcal{H}$ is one to one.
The main idea of the proof of the second part of the Lemma is to show that $\mathcal{H}^*$, the adjoint operator of $\mathcal{H}$, is injective.
To this end, we determine first the expression of $\mathcal{H}^*$. Let $g \in L^2(\mathbf{S}^{m-1})$ and $(\alpha, \beta) \in \tilde{H}^{1/2}(\sigma) \times H^{1/2}(\sigma)$, then $\mathcal{H}^* : \tilde{H}^{1/2}(\sigma) \times H^{1/2}(\sigma) \to L^2(\mathbf{S}^{m-1})$ satisfies

$$\langle \mathcal{H}(g), (\alpha, \beta) \rangle_{H^*, H} = \langle g, \mathcal{H}^*(\alpha, \beta) \rangle_{L^2(\mathbf{S}^{m-1}), L^2(\mathbf{S}^{m-1})}$$

where $H := \tilde{H}^{1/2}(\sigma) \times H^{1/2}(\sigma)$.
By changing the order of integration and using (3.8),

$$\begin{aligned} &\langle \mathcal{H}(g), (\alpha, \beta) \rangle_{H^*, H} \\ &= -\int_{\mathbf{S}^{m-1}} g(d) \overline{\left[\int_\sigma \left(\alpha(y) \left(\frac{\partial}{\partial \nu(y)} + \overline{\lambda^+} \right) + \beta(y) \overline{(\lambda^+ + \lambda^-)} \right) e^{-ikd\cdot y} ds(y) \right]} ds(d). \end{aligned}$$

Therefore, for $d \in \mathbf{S}^{m-1}$, the operator $\mathcal{H}^*$ is given by

$$\mathcal{H}^*(\alpha,\beta)(d) = -\left[\int_\sigma \left(\alpha(y)\left(\frac{\partial}{\partial\nu(y)} + \overline{\lambda^+}\right) + \beta(y)\overline{(\lambda^+ + \lambda^-)}\right) e^{-ikd\cdot y} ds(y)\right].$$

We observe that $\mathcal{H}^*$ is the far field pattern of the potential

$$\gamma^{-1}V(z) = -\int_\sigma \alpha(y)\frac{\partial\Phi(z,y)}{\partial\nu(y)} ds(y) - \int_\sigma \left(\overline{\lambda^+}\alpha + \overline{(\lambda^+ + \lambda^-)}\beta\right)\Phi(z,y) ds(y),$$

for $z \in \mathbf{R}^m \setminus \bar{\sigma}$. This function is well defined in $\mathbf{R}^m \setminus \bar{\sigma}$ since α and β can be extended by zero to functions in $H^{1/2}(\sigma)$. Moreover, $V \in H^1_{loc}(\mathbf{R}^m \setminus \bar{\sigma})$ satisfies the Helmholtz equation and the Sommerfeld radiation condition.
Therefore, if $\mathcal{H}^*(\alpha,\beta) = 0$, the far field pattern of V is zero and from Rellich's lemma and the unique continuation principle (see Corollary 13) we conclude that $V = 0$ in $\mathbf{R}^m \setminus \bar{\sigma}$. Then, by the jump relations of the layer potentials, we have $[V] = -\alpha$ and $[\partial_\nu V] = \overline{\lambda^+}\alpha + \overline{(\lambda^+ + \lambda^-)}\beta$. This implies that

$$\alpha = 0 \quad \text{and} \quad \overline{\lambda^+}\alpha + \overline{(\lambda^+ + \lambda^-)}\beta = 0.$$

Finally, since by assumption $(\lambda^+ + \lambda^-)^{-1} \in L^\infty(\sigma)$, then $\alpha = \beta = 0$ and the operator $\mathcal{H}^*$ is injective. □

In the next step, we provide some properties of the operator B. We need to introduce the operators $\mathcal{F} : \tilde{H}^{1/2}(\sigma) \times \tilde{H}^{-1/2}(\sigma) \to L^2(\mathbf{S}^{m-1})$ given by

$$\mathcal{F}(\varphi,\psi)(\hat{x}) := \gamma \int_\sigma \left(\varphi(y)\frac{\partial e^{-ik\hat{x}y}}{\partial\nu(y)} + \psi(y)e^{-ik\hat{x}y}\right) ds(y) \tag{3.9}$$

and $M : \tilde{H}^{1/2}(\sigma) \times \tilde{H}^{-1/2}(\sigma) \to H^{-1/2}(\sigma) \times \tilde{H}^{-1/2}(\sigma)$ defined by

$$M := \begin{pmatrix} T + \lambda^+(K + \frac{1}{2}I) & -\lambda^+ S - K' + \frac{1}{2}I \\ (\lambda^+ + \lambda^-)K + \frac{(\lambda^+ - \lambda^-)}{2}I & -(\lambda^+ + \lambda^-)S - I \end{pmatrix}. \tag{3.10}$$

Lemma 16. *The operator M has a bounded inverse and $B = \gamma\mathcal{F}M^{-1}$.*

Proof. For a given $(\varphi,\psi) \in \tilde{H}^{1/2}(\sigma) \times \tilde{H}^{-1/2}(\sigma)$, the function $\mathcal{F}(\varphi,\psi)(\hat{x})$ is the far field pattern of the potential

$$P(\varphi,\psi)(x) := \int_\sigma \varphi(y)\frac{\partial\Phi(x,y)}{\partial\nu(y)} ds(y) + \int_\sigma \psi(y)\Phi(x,y) ds(y).$$

The function $P \in H^1_{loc}(\mathbf{R}^m \setminus \bar{\sigma})$ satisfies the Helmholtz equation in $\mathbf{R}^m \setminus \bar{\sigma}$ and the Sommerfeld radiation condition. In addition, following the proof of Lemma 3, we show that $\varphi = [P]$, $\psi = -[\partial_\nu P]$ and

$$\begin{pmatrix} (\partial_\nu + \lambda^+)P^+(\varphi,\psi) \\ [\partial_\nu P](\varphi,\psi) + \lambda^+ P^+(\varphi,\psi) + \lambda^- P^-(\varphi,\psi) \end{pmatrix} = M \begin{pmatrix} \varphi \\ \psi \end{pmatrix}$$

where $M : \tilde{H}^{1/2}(\sigma) \times \tilde{H}^{-1/2}(\sigma) \to H^{-1/2}(\sigma) \times \tilde{H}^{-1/2}(\sigma)$ is given by (3.10). This operator is related to the matrix A_σ defined by (1.10). More precisely,

$$A_\sigma = \begin{pmatrix} (\lambda^+ + \lambda^-)I & -\lambda^+ I \\ 0 & I \end{pmatrix} M$$

and by Lemma 4, $M^{-1} : H^{-1/2}(\sigma) \times \tilde{H}^{-1/2}(\sigma) \to \tilde{H}^{1/2}(\sigma) \times \tilde{H}^{-1/2}(\sigma)$ exists and is bounded. Moreover, M^{-1} is given by

$$M^{-1} = A_\sigma^{-1} \begin{pmatrix} (\lambda^+ + \lambda^-)I & -\lambda^+ I \\ 0 & I \end{pmatrix}. \tag{3.11}$$

□

Lemma 17. *The operator $\mathcal{F} : \tilde{H}^{1/2}(\sigma) \times \tilde{H}^{-1/2}(\sigma) \to L^2(\mathbf{S}^{m-1})$ is injective and has a dense range in $L^2(\mathbf{S}^{m-1})$.*

Proof. The injectivity of $\mathcal{F}$ can be proved in the same way as in Lemma 15, by replacing the potential V by P.
Proceeding again as in the proof of Lemma 15, let $g \in L^2(\mathbf{S}^{m-1})$ and $(\alpha, \beta) \in \tilde{H}^{1/2}(\sigma) \times \tilde{H}^{-1/2}(\sigma)$,

$$\langle \mathcal{F}(\alpha,\beta), g\rangle = \int_{\mathbf{S}^{m-1}} g(d)\mathcal{F}(\alpha,\beta)(d)ds(d)$$

$$= \gamma \int_{\mathbf{S}^{m-1}} g(d) \left(\int_\sigma \alpha(y) \frac{\partial e^{-ikd\cdot y}}{\partial \nu(y)} ds(y) + \int_\sigma \beta(y) e^{-ikd\cdot y} ds(y) \right) ds(d)$$

$$= \gamma \int_\sigma \alpha(y) \int_{\mathbf{S}^{m-1}} g(d) \frac{\partial e^{-ikd\cdot y}}{\partial \nu(y)} ds(d)ds(y) + \gamma \int_\sigma \beta(y) \int_{\mathbf{S}^{m-1}} g(d) e^{-ikd\cdot y} ds(d)ds(y).$$

Therefore, $\mathcal{F}^*(g) = \gamma(\partial_\nu v_g, v_g)$.
Now, if $\mathcal{F}^*(g) = 0$ then $v_g = \partial_\nu v_g = 0$.
Thus, as in Lemma 15, $g = 0$ which proves the density of the range of $\mathcal{F}$. □

Summarizing the previous results, the operator F defined by (5.9) is factorized as $F = \mathcal{F}M^{-1}\mathcal{H}$. Hence, the range of F is included in the range of $\mathcal{F}$. Therefore, thanks to the following Lemma, there exists an approximated solution of the equation (3.4).

Lemma 18. *For any smooth non intersecting arc L and functions $\alpha_L \in \tilde{H}^{\frac{1}{2}}(L)$, $\beta_L \in \tilde{H}^{-\frac{1}{2}}(L)$ such that $(\alpha_L, \beta_L) \neq (0,0)$, the function Φ_L^∞ given by (3.5) belongs to $R(\mathcal{F})$, the range of $\mathcal{F}$, if and only if $L \subset \sigma$.*

Proof. First assume that $L \subset \sigma$. Since $\tilde{H}^{\pm\frac{1}{2}}(L) \subset \tilde{H}^{\pm\frac{1}{2}}(\sigma)$, it follows from (3.9) that $\Phi_L^\infty(\hat{x}) \in R(\mathcal{F})$.

Now let $L \not\subset \sigma$ and assume, on the contrary, that $\Phi_L^\infty \in R(\mathcal{F})$. Hence, there exists $\varphi \in \tilde{H}^{\frac{1}{2}}(\sigma)$ and $\psi \in \tilde{H}^{-\frac{1}{2}}(\sigma)$ such that

$$\Phi_L^\infty(\hat{x}) = \gamma \int_L \left(\varphi(y) \frac{\partial e^{-ik\hat{x}\cdot y}}{\partial \nu(y)} + \psi(y) e^{-ik\hat{x}\cdot y}(y) \right) ds(y).$$

Thus Φ_L^∞ is the far field pattern of the potential

$$P(x) = \int_\sigma \left(\varphi(y) \frac{\partial \Phi(x,y)}{\partial \nu(y)} + \psi(y)\Phi(x,y) \right) ds(y), \quad x \in \mathbf{R}^m \setminus \overline{\sigma}.$$

Since by definition Φ_L^∞ is also the far field pattern of the potential Φ_L given by (3.7) then using the Rellich lemma and the unique continuation principle (see Corollary 13), the potentials Φ_L and P coincide in $\mathbf{R}^m \setminus (\bar{\sigma} \cup \bar{L})$.
Let $x_0 \in L \backslash \overline{\sigma}$ and B_ϵ a small neighborhood of x_0 with $B_\epsilon \cap \sigma = \emptyset$. Then, P is analytic in B_ϵ while Φ_L or its normal derivative is not continuous across L which is a contradiction. This proves that $\Phi_L^\infty \notin R(\mathcal{F})$. □

Theorem 19. *We assume that L is a nonintersecting smooth open arc. The following is true:*

1. *If $L \subset \sigma$; there exists a sequence $(g_n)_{n\in\mathbf{N}}$ on $L^2(\mathbf{S^{m-1}})$ such that*

$$\lim_{n\to+\infty} \|F(g_n) - \Phi_L^\infty\|_{L^2(\mathbf{S^{m-1}})} = 0$$

and

$$\lim_{n\to+\infty} ||v_{g_n}||_* < \infty,$$

where $\|v_{g_n}\|_* := \|\partial_\nu v_{g_n} + \lambda^+ v_{g_n}\|_{H^{-\frac{1}{2}}(\sigma)} + \|(\lambda^+ + \lambda^-) v_{g_n}\|_{\tilde{H}^{-\frac{1}{2}}(\sigma)}$.

2. *Otherwise, for any sequence $(g_n)_{n\in\mathbf{N}} \subset L^2(\mathbf{S^{m-1}})$ that satisfies*

$$\lim_{n\to+\infty} \|F(g_n) - \Phi_L^\infty\|_{L^2(\mathbf{S^{m-1}})} = 0$$

we have

$$\lim_{n\to+\infty} ||v_{g_n}||_* = +\infty.$$

Proof. • If $L \subset \sigma$, it is easy to find a bounded solution of the far field equation (3.4). In fact, we have $\tilde{H}^{\frac{1}{2}}(L) \subset \tilde{H}^{\frac{1}{2}}(\sigma)$ and $\tilde{H}^{-\frac{1}{2}}(L) \subset \tilde{H}^{-\frac{1}{2}}(\sigma)$.
Thus, $\Phi_L^\infty \in R(\mathcal{F})$ there exists a unique $(\alpha, \beta) \in \tilde{H}^{\frac{1}{2}}(\sigma) \times \tilde{H}^{-\frac{1}{2}}(\sigma)$ such that

$$\Phi_L^\infty = \mathcal{F}(\alpha, \beta)$$

Therefore by Lemma 16 there exists a unique $(\tilde{\alpha}, \tilde{\beta}) \in \tilde{H}^{\frac{1}{2}}(\sigma) \times \tilde{H}^{-\frac{1}{2}}(\sigma)$ such that

$$\Phi_L^\infty = \mathcal{F}M^{-1}(\tilde{\alpha}, \tilde{\beta})^T.$$

Moreover by Lemma 15 the range of $\mathcal{H}$ is dense on $H^{-1/2}(\sigma) \times \tilde{H}^{-1/2}(\sigma)$, hence there exists $(\alpha_n, \beta_n)_{n\in\mathbf{N}} \subset R(\mathcal{H})$ such that $\lim_{n\to+\infty}(\alpha_n, \beta_n) = (\tilde{\alpha}, \tilde{\beta})$. Using the continuity of $\mathcal{H}$, we show the existence of a sequence $(g_n)_{n\in\mathbf{N}} \subset L^2(\mathbf{S^{m-1}})$ verifying $\lim_{n\to\infty} \mathcal{H}g_n = (\tilde{\alpha}, \tilde{\beta})$ which proves that

$$\lim_{n\to+\infty} \|F(g_n) - \Phi_L^\infty\|_{L^2(\mathbf{S^{m-1}})} = 0.$$

- Let $L \not\subset \sigma$ and let us assume that $\|v_{g_n}\|_* < \infty$. Therefore,

$$\|\partial_\nu v_{g_n} + \lambda^+ v_{g_n}\|_{H^{-\frac{1}{2}}(\sigma)} + \|(\lambda^+ + \lambda^-)v_{g_n}\|_{\tilde{H}^{-\frac{1}{2}}(\sigma)} < \infty. \tag{3.12}$$

Let $(\alpha_n, \beta_n) \in R(\mathcal{H})$. Since $\mathcal{H}$ is injective there exists a sequence $(g_n)_{n\in\mathbf{N}} \subset L^2(\mathbf{S}^{m-1})$ such that $\mathcal{H}(g_n) = (\alpha_n, \beta_n)$. From (3.12), the sequence (α_n, β_n) is bounded in $H^{-\frac{1}{2}}(\sigma) \times \tilde{H}^{-\frac{1}{2}}(\sigma)$. Therefore we can extract a subsequence, that we still denote (α_n, β_n) which weakly converges to (α, β).
The integral operator $\mathcal{F}$ is compact since it has a regular kernel and M^{-1} is a bounded operator, so that the operator $\mathcal{F}M^{-1}$ is a compact operator. Consequently,

$$\lim_{n\to+\infty} \|F(g_n) - \mathcal{F}M^{-1}(\alpha, \beta)\|_{L^2(\mathbf{S^{m-1}})} = 0$$

and by the uniqueness of the limit, we have

$$\mathcal{F}M^{-1}(\alpha, \beta) = \Phi_L^\infty.$$

We deduce that $\Phi_L^\infty \in R(\mathcal{F})$ and $L \subset \sigma$ which is a contradiction.

□

3.3.2 Numerical schemes and results

For the purpose of the numerical experiments, we cannot give a crack characterization by using the norm of v_g as suggested in Theorem 19 since this norm depends on the impedance values and on the crack σ. However, we expect that $L \mapsto \|v_{g_L}\|_*$ has the same behavior as $L \mapsto \|g_L\|_{L^2(\mathbf{S^{m-1}})}$ in the sense that $\|g_L\|_{L^2(\mathbf{S^{m-1}})}$ has smaller values when $L \subset \sigma$, where g_L denotes a nearby solution of (3.4). The latter heuristic argument can be for instance justified by the fact that, at the discrete level, the Herglotz operator $\mathcal{H}$ is invertible. Our indicator function will then be based on $L \mapsto \|g_L\|_{L^2(\mathbf{S^{m-1}})}$.

Regularization.
In order to construct a nearby solution to (3.4) we use a Tikhonov regularization. Therefore we solve the following equation

$$(\eta I + F^*F)g_\eta = F^*\Phi_L^\infty$$

where η is a parameter of regularization. By the singular value decomposition (SVD) we mean a representation of F in the form

$$F(g) = \sum_i \sigma_i(g, f_i)l_i,$$

where (f_i), (l_i) are orthonormal systems in $L^2(S^1)$, and σ_i are positive constants, the singular values of F. The adjoint of F is given by

$$F^*(g) = \sum_i \sigma_i(g, l_i)f_i,$$

Thus, the operator F^*F is given by

$$F^*F(g) = \sum_i \sigma_i^2(g, f_i)f_i,$$

On the other hand, we have

$$F^*(\Phi_L^\infty) = \sum_i \sigma_i(\Phi_L^\infty, l_i)f_i.$$

Finally, we get the expression of g_η, the solution of (3.4)as

$$g_\eta = \sum_i \frac{\sigma_i(\Phi_L^\infty, l_i)}{\eta + \sigma_i^2} f_i \tag{3.13}$$

The regularization parameter is chosen using the Morozov discrepancy principle.

Discretization.
The numerical experiments are conducted in a 2D setting of the problem. We consider n equally distant observation points $(\hat{x}_l)_{1\leq l\leq n}$ of the far field on the unit circle $\mathbb{S}^1$.

$$Fg(\hat{x}_l) \simeq \sum_{j=1}^{n} w_j u^\infty(\hat{x}_l, \hat{x}_j)g(\hat{x}_j) \tag{3.14}$$

where w_j is the arclengh between two adjacent points. Let L be a small segment of center z and with normal ν. Then

$$\Phi_L^\infty(\hat{x}_l) \simeq \gamma|L|(\alpha(z)e^{-ik\hat{x}_l z} + \beta(z)(-ik\hat{x}_l.\nu)e^{-ik\hat{x}_l z}) \tag{3.15}$$

The discrete equation to solve is then

$$Fg(\hat{x}_l) \simeq \Phi_L^{\infty}(\hat{x}_l) \qquad \forall \hat{x}_l \tag{3.16}$$

using the Tikhonov procedure explained above. The sampling procedure will consist then in varying the z and ν in (3.15). According to Theorem 3 we expect $\|g\|$ (where g is a solution to (3.16)) to be large except when $z \in \sigma$ and ν is the normal to σ at z.
We shall consider two types of solutions: the first one denoted by g_z corresponds to $\alpha(z) = 1$ and $\beta(z) = 0$, the second one denoted by $g_{z,\nu}$ corresponds to $\alpha(z) = 0$ and $\beta(z) = 1$.

First criterion
Let us consider two independent normals for instance $\nu_1 = (0,1)^t$ and $\nu_2 = (1,0)^t$. At each sampling point z we compute

$$z \quad \longrightarrow \quad \frac{1}{\|g_z\|} + \frac{1}{\|g_{z,\nu_1}\|} + \frac{1}{\|g_{z,\nu_2}\|}. \tag{3.17}$$

However, as we shall observe later, this criterion may not be efficient if ν_1 or ν_2 do not coincide with the exact normal to σ at z (see the numerical tests in section 3.3.3).

Second criterion
Let us define the normal ν as follows:

$$\nu = \zeta\nu_1 + \sqrt{1-\zeta^2}\nu_2 \qquad \text{with } 0 \le \zeta \le 1$$

Therefore, by linearity of the equation (4.72)

$$g_{z,\nu} = \zeta g_{z,\nu_1} + \sqrt{1-\zeta^2} g_{z,\nu_2}.$$

Based on the theoretical justification, the normal ν to σ at $z \in \sigma$ corresponds with the value ζ that minimizes

$$\|g_{z,\nu}\|^2 = \zeta^2\|g_{z,\nu_1}\|^2 + (1-\zeta^2)\|g_{z,\nu_2}\|^2 + 2\zeta(1-\zeta^2)\,\langle g_{z,\nu_1}\,, g_{z,\nu_2}\rangle \tag{3.18}$$

The proposed criterion will be the determination on each point z of

$$z \quad \longrightarrow \quad \frac{1}{\|g_z\|} + \frac{1}{\|g_{z,\nu}\|} \tag{3.19}$$

where $g,\ g_{z,\nu}$ corresponds with ζ that minimizes (3.18).

3.3.3 Numerical tests

The efficiency of our approach is tested using both criteria for several ranges of the impedance values and for different shapes, namely arc-shaped cracks, L-shaped cracks and angular cracks. We present in the following figures the isovalues of the right hand side of (3.17) and (3.19). The location of the crack would corresponds with the red isovalues in the figures.
In all the numerical tests we use 100 observation points of the far field pattern and the same number of incident plane waves.

Case of Large impedances
Both criteria give a good reconstruction of the crack for the case of large impedances (see Figures 3.1 and 3.2).

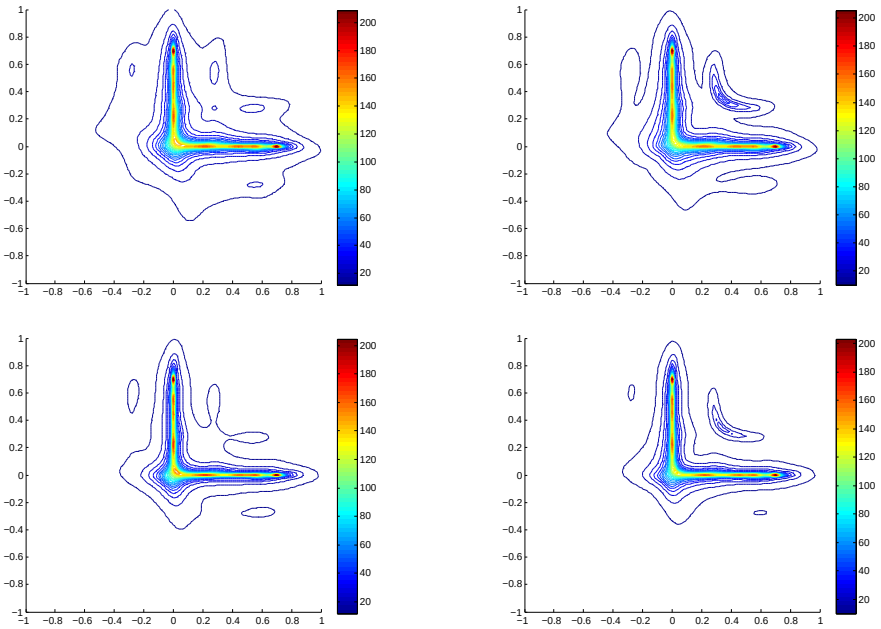

Figure 3.1: Reconstruction of an L-shaped crack with peaks $(0.75, 0), (0, 0), (0, 0.75)$ for $\lambda^{\pm} = 10^2(1+i)$ (first line), $\lambda^{\pm} = 10^3(1+i)$ (second line), using the first criterion (left) and the second criterion (right)

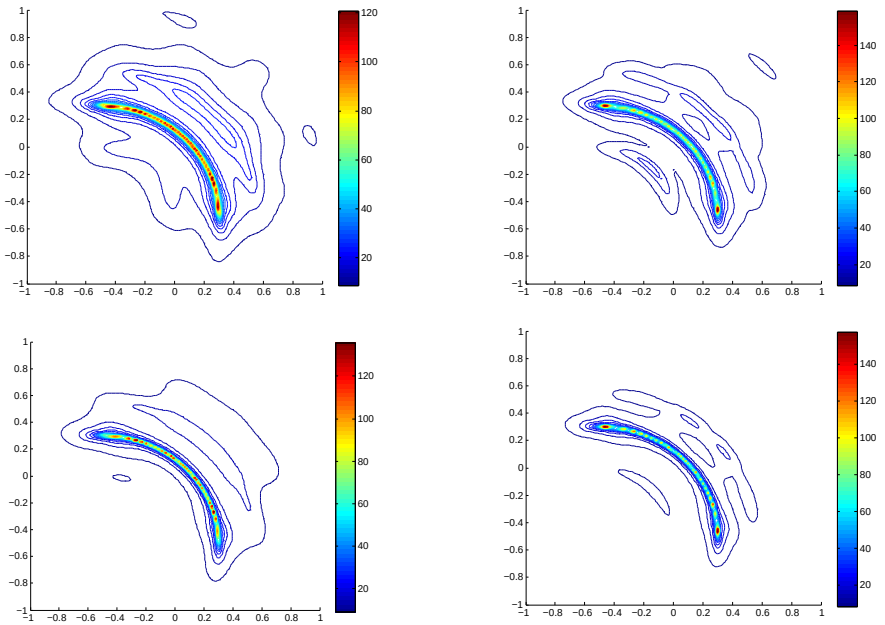

Figure 3.2: Reconstruction of an arc-shaped crack with center $(-0.5,-0.5)$, radius 0.8 and aperture 90 degrees for $\lambda^{\pm} = 10^2(1+i)$ (first line), $\lambda^{\pm} = 10^3(1+i)$ (second line), using the first criterion (left) and the second criterion (right)

Case of small impedances

In this case, using the first criterion, the results are not satisfactory for all geometries. This is due to the fact that for large impedances we are close to the Dirichlet case, hence the dominant term in (3.17) is $\frac{1}{\|g_z\|}$ whereas for small impedances we are close to the Neumann case where the dominant term is the one that contains the normal derivatives. Figure 3.3 shows that if ν_1 or ν_2 coincides with the exact normal to the crack we have a good reconstruction otherwise only the part of the crack for which the normal coincides with ν_1 or ν_2 is correctly reconstructed (see Figures 3.4 and 3.5). Hence having a good approximation of ν is very important for the precision of the result. This problem is fixed by the use of the second criterion as demonstrated by the reconstruction shown in Figure 3.1 to Figure 3.5.

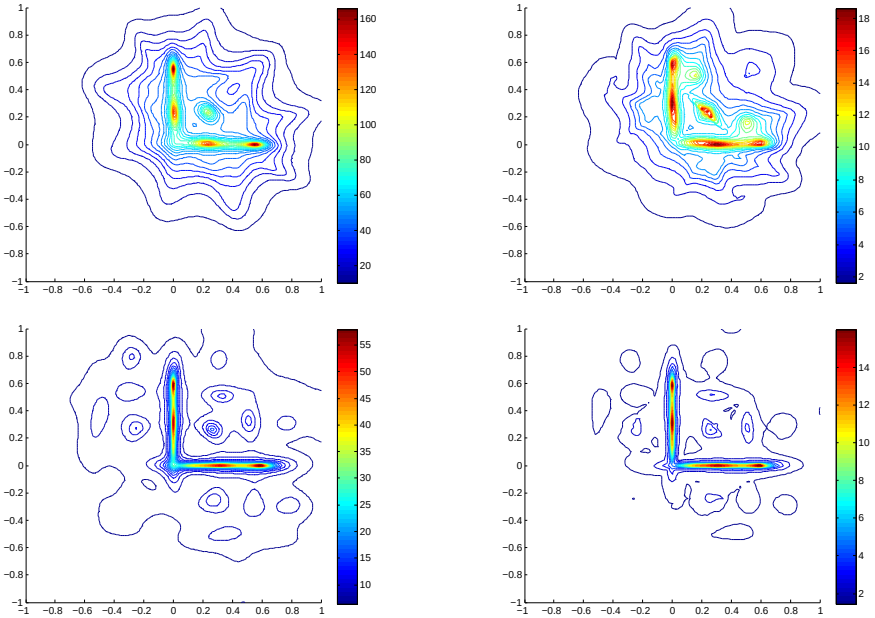

Figure 3.3: Reconstruction of an L-shaped crack with peaks $(0.75, 0), (0, 0), (0, 0.75)$ for $\lambda^{\pm} = 10^{-1}(1 + i)$ (first line), $\lambda^{\pm} = 10^{-2}(1 + i)$ (second line), using the first criterion (left) and the second criterion (right)

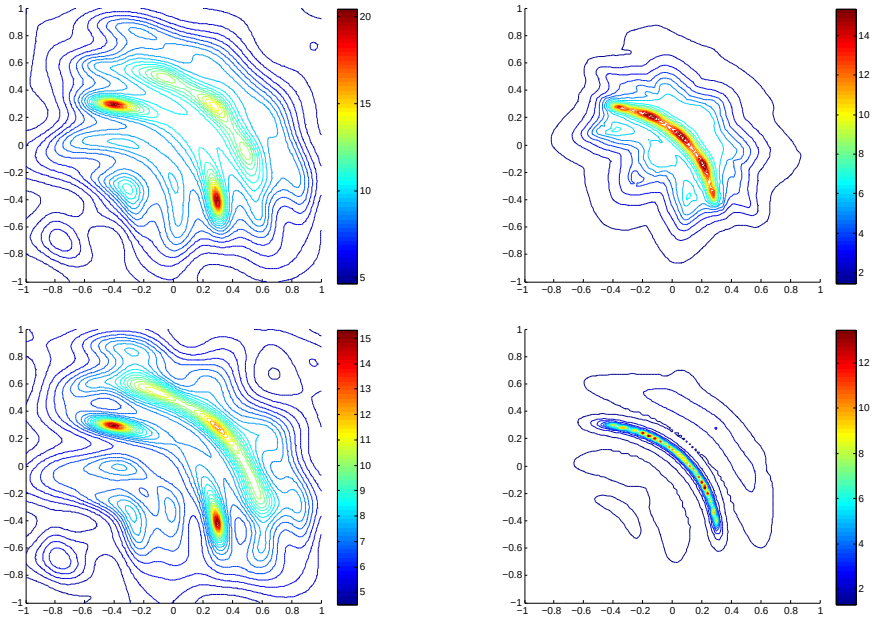

Figure 3.4: Reconstruction of an arc-shaped crack with center $(-0.5, -0.5)$, radius 0.8 and aperture 90 degrees for $\lambda^{\pm} = 10^{-1}(1 + i)$ (first line), $\lambda^{\pm} = 10^{-2}(1 + i)$ (second line), using the first criterion (left) and the second criterion (right)

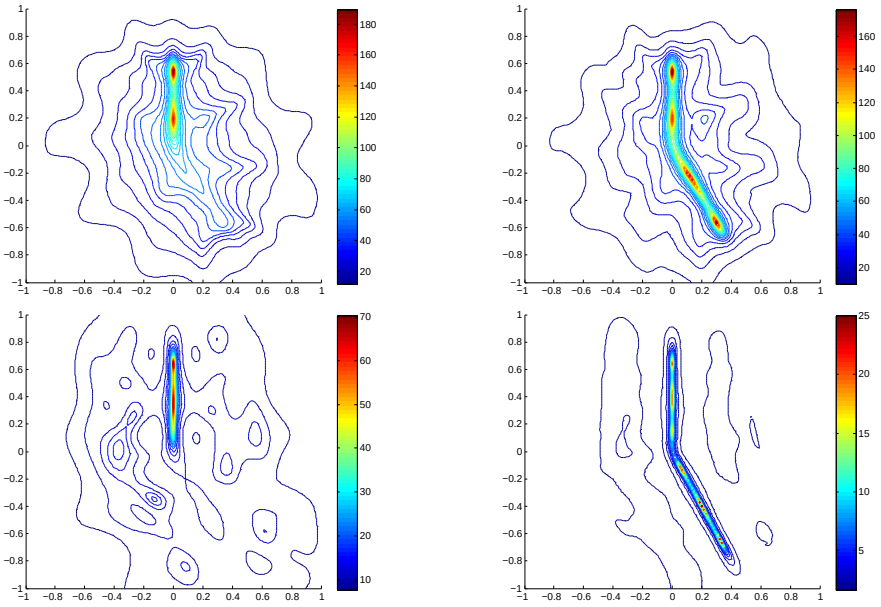

Figure 3.5: Reconstruction of two segments $\{0\} \times [0, 0.8]$ and $[0, 0.4] \times [0, -0.8]$ for $\lambda^{\pm} = 10^{-1}(1 + i)$ (first line), $\lambda^{\pm} = 10^{-2}(1 + i)$ (second line), using the first criterion (left) and the second criterion (right)

Case of impedances with " moderate values "

We observe that the quality of the results slightly deteriorates when the impedance values are intermediate between high and small magnitudes (see Figures 3.6 to 3.8).

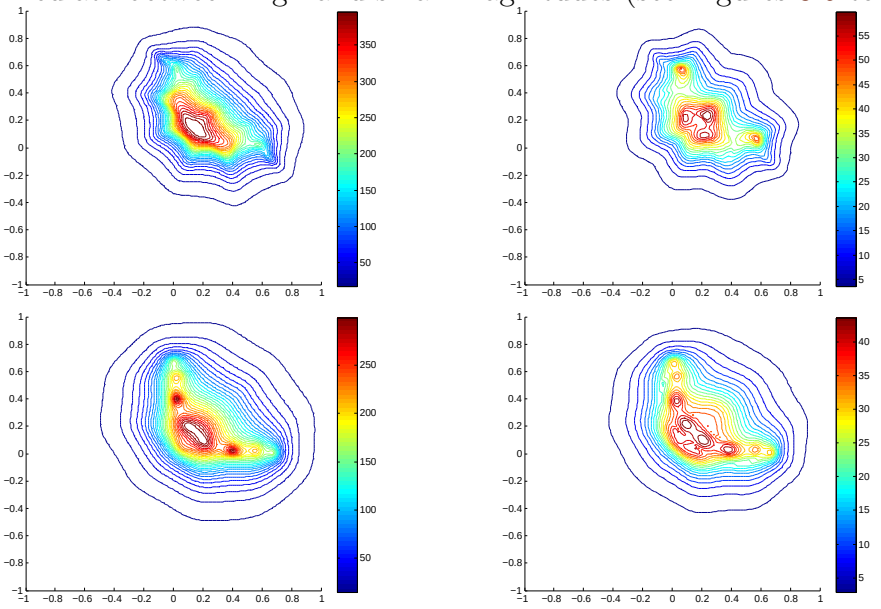

Figure 3.6: Reconstruction of two segments an L-shaped crack with peaks $(0, 0.75), (0, 0), (0.75, 0)$ for $\lambda^{-} = 1.5 + 1$ and $\lambda^{+} = 2 + 1.2i$ (first line), $\lambda^{\pm} = 10(1 + i)$ (second line), using the first criterion (left) and the second criterion (right)

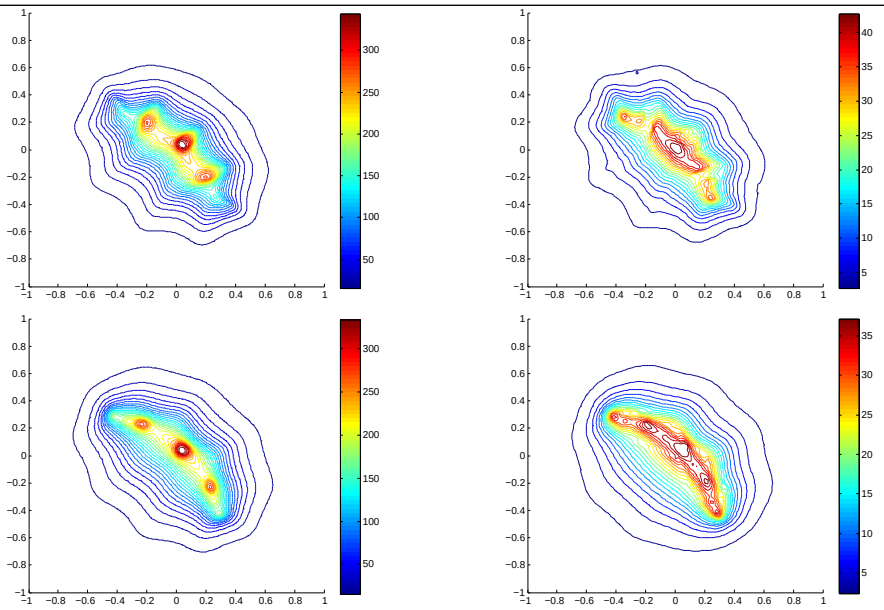

Figure 3.7: Reconstruction of an arc-shaped crack with center $(-0.5, -0.5)$, radius 0.8 and aperture 90 degrees for $\lambda^- = 1.5 + 1$ and $\lambda^+ = 2 + 1.2i$ (first line), $\lambda^\pm = 10(1 + i)$ (second line), using the first criterion (left) and the second criterion (right)

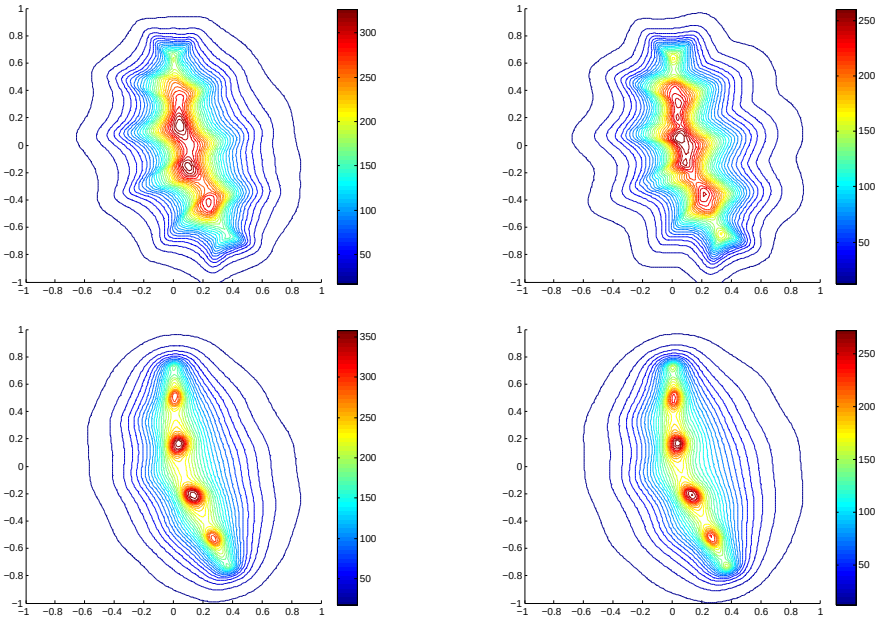

Figure 3.8: Reconstruction of two segments $\{0\} \times [0, 0.8]$ and $[0, 0.4] \times [0, -0.8]$ for $\lambda^- = 1.5 + 1$ and $\lambda^+ = 2 + 1.2i$ (first line), $\lambda^\pm = 10(1 + i)$ (second line), using the first criterion (left) and the second criterion (right)

As in the case of one crack, we have a good reconstruction even when we have multiple cracks. Figure 3.9 shows that we can observe separately the shape of all reconstructed cracks for various values of the impedance parameter.

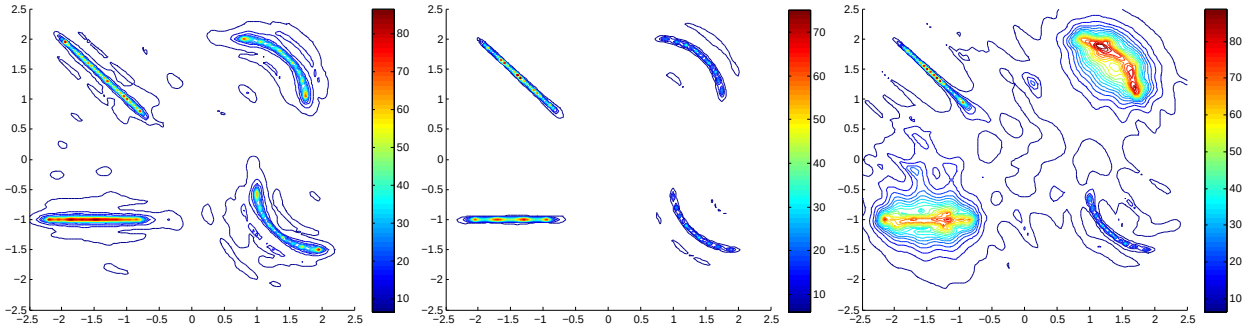

Figure 3.9: Reconstruction of multiple cracks for $\lambda_1^{\pm} = \lambda_2^{\pm} = \lambda_3^{\pm} = \lambda_4^{\pm} = 10^4(1+i)$ (left), $\lambda^{\pm} = 10^{-2}(1+i)$ (middle), $\lambda_3^{\pm} = \lambda_1^{\pm} = 10(1+i)$ (right).

Reconstruction of the normals.

To illustrate the correlation between the reconstruction of the normals (that is the ν that minimizes (3.18)) and the precision of the crack reconstruction, we represent these vectors in Figure 3.10 to Figure 3.12. We observe that the best crack reconstructions for intermediate values of the impedances correspond with the cases where the normals at the crack are close to the exact ones. For large values of the impedances, the reconstruction of the normal is not correct but has negligible influence on the crack reconstruction.

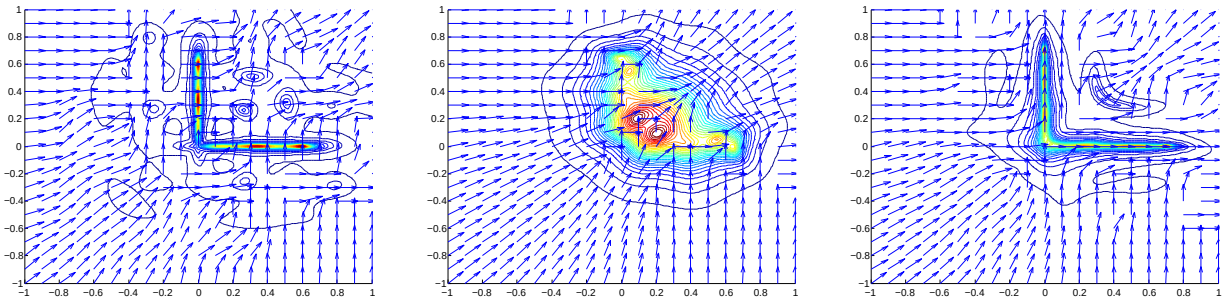

Figure 3.10: Reconstruction of the normals for $\lambda^- = \lambda^+ = 0.001 + 0.001i$ (left), $\lambda^- = \lambda^+ = 5 + 5i$ (middle), $\lambda^- = \lambda^+ = 10(1+i)$ (right).

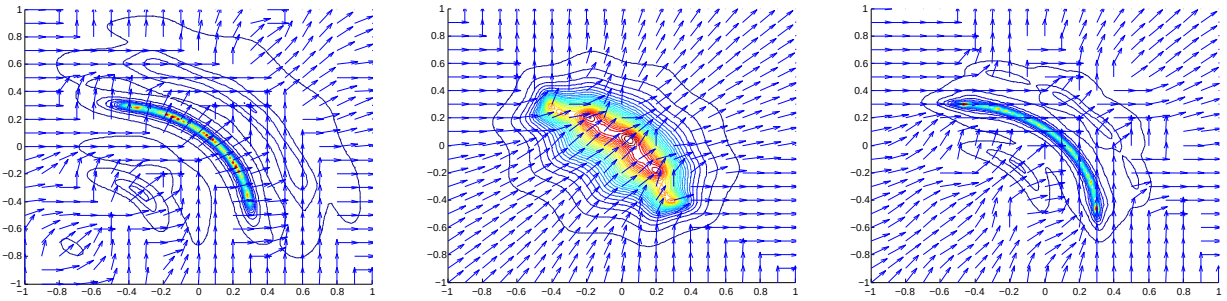

Figure 3.11: Reconstruction of the normals for $\lambda^- = \lambda^+ = 0.001 + 0.001i$ (left), $\lambda^- = \lambda^+ = 5 + 5i$ (middle), $\lambda^- = \lambda^+ = 10(1 + i)$ (right).

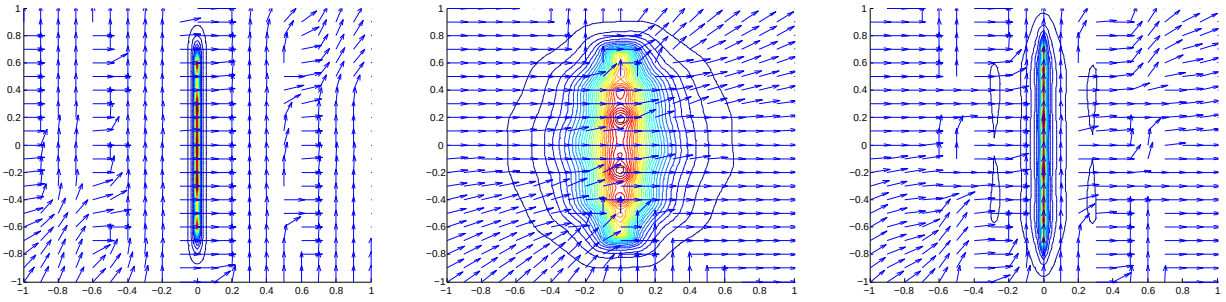

Figure 3.12: Reconstruction of the normals for $\lambda^- = \lambda^+ = 0.001 + 0.001i$ (left), $\lambda^- = \lambda^+ = 5 + 5i$ (middle), $\lambda^- = \lambda^+ = 10(1 + i)$ (right).

Influence of the frequency

A more relevant physical model for the impedance boundary conditions would be

$$\partial_\nu u_\pm \pm k\tilde{\lambda}^\pm u_\pm = 0 \qquad \text{on} \quad \sigma$$

where now $\lambda^\pm$ are dimensionless constants. We shall study the influence of the frequency on the reconstructions for these type of conditions. Figures 3.13 and 3.14 show the reconstructions of the normals for two different choices of the frequency. We observe that the best orientation for the normals are given by the smaller frequency. This then suggests to use the small frequency to first reconstruct the normal fields then use these normals to evaluate the criterion (3.19). This procedure improves the results obtained for the higher frequency: compare Figures 3.15–3.17 to Figures 3.6–3.8 respectively.

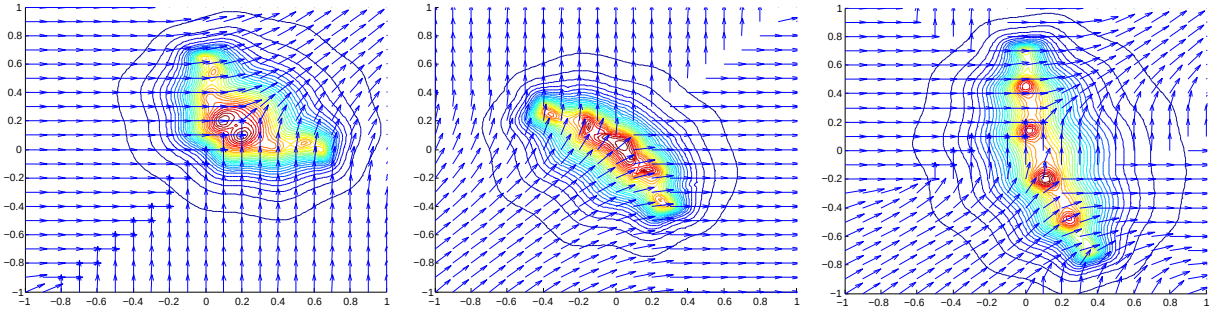

Figure 3.13: Reconstruction of the normals for $\tilde{\lambda}^- = \tilde{\lambda}^+ = 0.79(1+i)$, $k = \pi/2$.

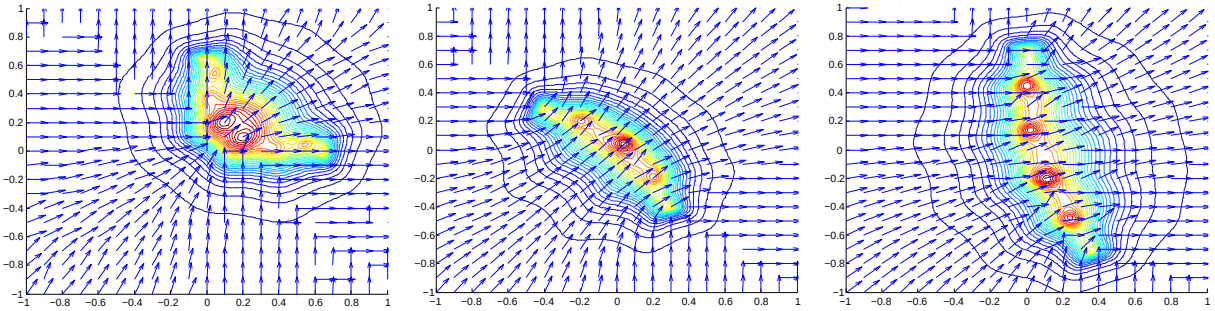

Figure 3.14: Reconstruction of the normals for $\tilde{\lambda}^- = \tilde{\lambda}^+ = 0.79(1+i)$, $k = 4\pi$.

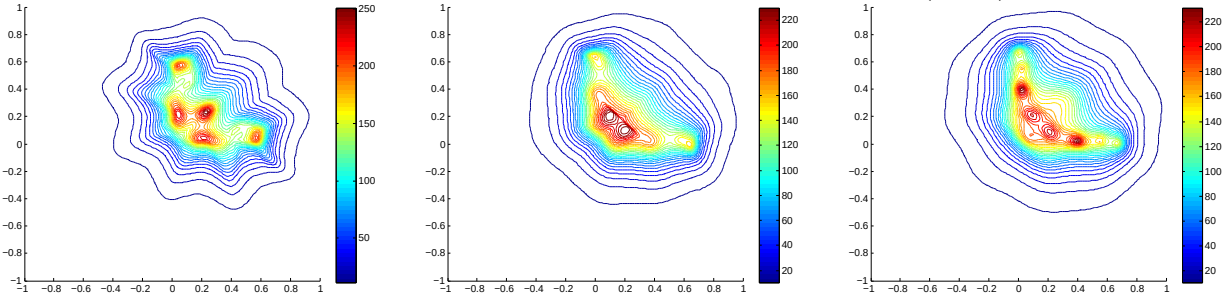

Figure 3.15: Reconstruction of an L-shaped crack with peaks $(0, 0.75), (0, 0), (0.75, 0)$ for $\tilde{\lambda}^+ = 0.23 + 0.15i \quad \tilde{\lambda}^- = 0.31 + 0.19i$ (left) $\tilde{\lambda}^- = \tilde{\lambda}^+ = 0.79(1+i)$ (middle) $\tilde{\lambda}^- = \tilde{\lambda}^+ = 1.58(1+i)$ (right) with $k = 2\pi$.

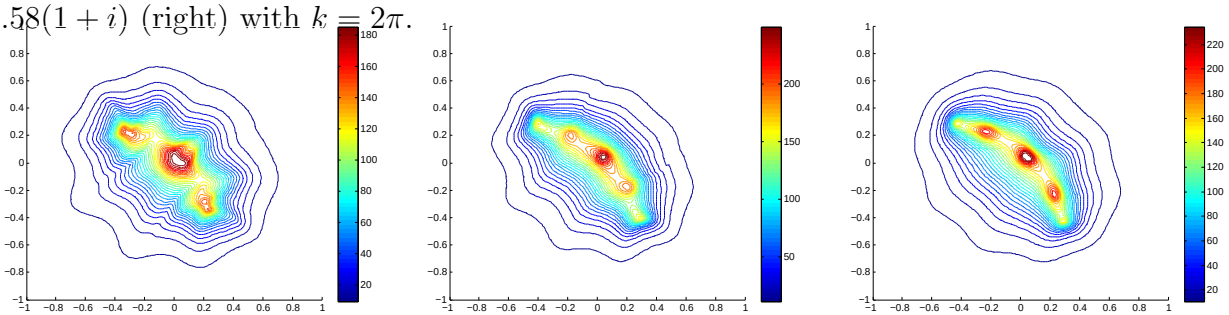

Figure 3.16: Reconstruction of arc-shaped crack for $\tilde{\lambda}^+ = 0.23 + 0.15i \quad \tilde{\lambda}^- = 0.31 + 0.19i$ (left) $\tilde{\lambda}^- = \tilde{\lambda}^+ = 0.79(1+i)$ (middle) $\tilde{\lambda}^- = \tilde{\lambda}^+ = 1.58(1+i)$ (right) with $k = 2\pi$.

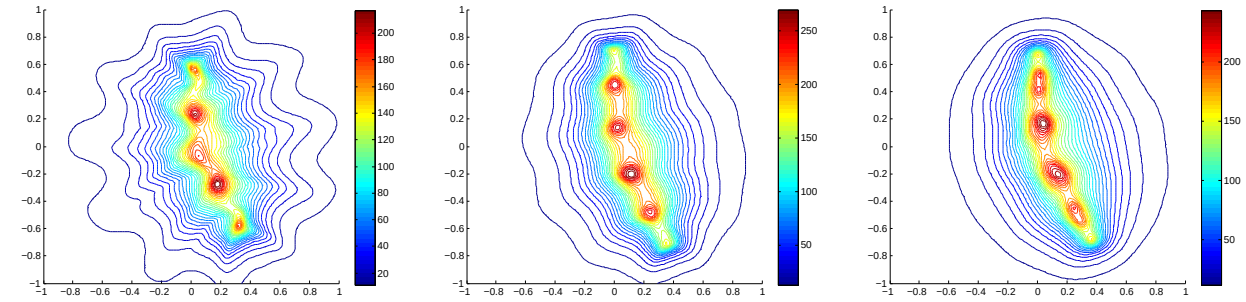

Figure 3.17: Reconstruction of two segments $\{0\} \times [0, 0.8]$ and $[0, 0.4] \times [0, -0.8]$ for $\tilde{\lambda}^+ = 0.23+0.15i \quad \tilde{\lambda}^- = 0.31+0.19i$ (left) $\tilde{\lambda}^- = \tilde{\lambda}^+ = 0.79(1+i)$ (middle) $\tilde{\lambda}^- = \tilde{\lambda}^+ = 1.58(1+i)$ (right) with $k = 2\pi$.

3.4 Determination of the impedance values

After having reconstructed the geometry of the crack, it would be interesting to obtain more information on the crack for example by determining the impedance values. This problem has been the subject of numerous investigations and it has led to the development of a variety of mathematical and numerical tools. J. Liu and M. Sini [68] have proposed a method to reconstruct the shape of the crack and the value of the impedance parameter knowing all the measurements of the far field data and using a direct formula which links the far field data to the unknown ingredients of the cracks through an asymptotic expansion. That gives an explicit formula for the impedance values in the two sides of the crack. We can also refer to the result given by F. Delbary [38] where he gives a reconstruction of the crack's shape using the reciprocity gap method and the value of the impedance parameter through both the computed jump of the solution of the scattered problem and its normal derivative and by considering the boundary condition. This approach gives a good reconstruction in 2D and also in 3D.

We also refer to some results concerning the reconstruction of the impedance parameter in the case of scattering by an obstacle. In fact, O. Ivanyshyn and R. Kress [49] have proposed a comparison between the regularized Newton-type method and a direct method for reconstructing the surface impedance function based on a formula using the spherical harmonics, where it has been assumed that both methods know the shape of the obstacle and all the measurements of the far field pattern for a fixed incident wave. F. Cakoni and D. Colton [22] have provided an explicit formula of the impedance value based on the solution given by the linear sampling method and the fact that the Herglotz wave can be approached by a solution of the Helmholtz equation inside the obstacle satisfying the same boundary condition as in the direct problem. Another approach proposed by R. Kress and W. Rundell [62] consists in recovering the shape of the obstacle given the information about the far field pattern of the scattered wave from each of a set of incident fields. This has been done by using an iterative process based on the Newton method. In the case of an obstacle with the Laplace equation, F. Cakoni, R. kress and C. Schuft [25]

have proposed a method to recover simultaneously the shape and the impedance of a part on the boundary of an inaccessible inclusion. This has been done by using two pairs of Cauchy data and an iterative method which is an extension of the work of W. Rundell [81].

In our case, we have applied two approaches. The first one is a natural approach based on the expression of the far field pattern and on the scattering problem. Measures of the far field pattern are first used to find $[u_s]$ and $[\partial_\nu u_s]$ on σ which are then used to retrieve the total field $u^\pm = {u_s}^\pm + u_i^\pm$ and $\partial_\nu u^\pm$ on each part of the crack. From the boundary conditions, an estimate of the impedance values can be obtained. This kind of approach is similar to that used in [38] for planar cracks but where the reconstruction of $[u]$ and $[\partial_\nu u]$ was done using the Fourrier expansion.

The second approach is deduced directly from the main theorem of the linear sampling method, using the solution of the far-field equation g, the test function Φ_L and the reconstructed crack σ. This approach is similar to the one used in [20] for an obstacle with impedance boundary condition. In the following sub-sections, we develop the two approaches and we present the numerical results associated to each approach. The results of the two approaches are also compared.

3.4.1 The natural approach

This approach is based on the expression of the far field pattern. We recall that

$$u^\infty(\hat{x}, d) = \int_\sigma \left([u^s](y)\partial_\nu e^{ik\hat{x}\cdot y} - [\partial_\nu u^s](y)e^{ik\hat{x}\cdot y}\right) ds(y) \tag{3.20}$$

$$= \int_\sigma \left([u](y)\partial_\nu e^{ik\hat{x}\cdot y} - [\partial_\nu u](y)e^{ik\hat{x}\cdot y}\right) ds(y) \tag{3.21}$$

Since $[u^i] = 0$ and $[\partial_\nu u^i] = 0$ on σ.
By knowing the crack σ, we can deduce $([u], [\partial_\nu u])$ on σ by inverting the operator $\mathcal{F} : \tilde{H}^{1/2}(\sigma) \times \tilde{H}^{-1/2}(\sigma) \longrightarrow L^2(S^1)$ defined by

$$\mathcal{F}([u], [\partial_\nu u]) := \int_\sigma \left([u](y)\partial_\nu e^{ik\hat{x}\cdot y} - [\partial_\nu u](y)e^{ik\hat{x}\cdot y}\right) ds(y)$$

This is an ill posed problem since $\mathcal{F}$ is a compact operator. Consequently a regularization is needed. We shall use a Tikhonov regularisation by solving

$$(\zeta I + \mathcal{F}^*\mathcal{F})([u][\partial_\nu u]) = \mathcal{F}^* u^\infty(\hat{x})$$

where ζ is a regularization parameter chosen by using the Morozov criterion. Let us recall that $\mathcal{F}$ is injective with dense range (see Lemma 17). By using the integral representation

of the scattered solution one deduces

$$u^s_\pm = K_\sigma([u]) - S_\sigma([\partial_\nu u]) \pm \frac{[u]}{2}$$
$$\partial_\nu u^s_\pm = T_\sigma([u]) - K'_\sigma([\partial_\nu u]) \pm \frac{[\partial_\nu u]}{2}$$

Finally, by considering the boundary conditions on σ,

$$\lambda^\pm = \mp \frac{\partial_\nu u_\pm}{u_\pm}$$

In the case of constant impedance values we prefer using the formula

$$\lambda^\pm = \mp \frac{\int_L \partial_\nu u_\pm \bar{u}_\pm}{\int_L |u_\pm|^2} \tag{3.22}$$

which is less sensitive to pointwise small values of $u_\pm(x)$. This approach is tested for different shapes, namely a segment, an arc and a broken line (see Figure 3.18). These results are presented in the following Tables.

In Table 3.1 we fix the geometry as a segment and we provide different estimates of the impedance for different incident plane waves $u^i(x,\theta) = e^{ik\theta x}$ with direction θ. The results show that a good estimate is obtained if the direction of the incident plane wave is perpendicular to the crack.

λ_e^+	λ_e^-	θ	λ_a^+	λ_a^-
2	1i	0	2.00+ 0.09i	0.97i
2	1i	90	1.95+0.17i	0.13+0.93i
2	1i	180	2.02-0.04i	-0.38+ 1.62 i
2	1i	270	2.07+0.03i	0.16+1.39i
5+5i	5+5i	0	4.78+5.75 i	4.86+ 5.28 i
5+5i	5+5i	90	3.43+ 4.52i	5.15+4.30 i
5+5i	5+5i	180	5.05+4.47i	3.20+ 4.04i
5+5i	5+5i	270	5.00+5.40 i	5.46+6.24 i
0.5+1i	0.2+0.4i	0	0.32+1.33i	0.25+0.38 i
0.5+1i	0.2+0.4i	90	0.41+ 1.31 i	0.27+0.35i
0.5+1i	0.2+0.4i	180	0.56+ 0.93i	0.16+0.60 i
0.5+1i	0.2+0.4i	270	0.54+1.01i	0.81i

Table 3.1: Reconstruction of the average of $\lambda^\pm$ given by formula (3.22) on $\sigma = [-0.5, 0.5] \times \{0\}$, with the wave length $\lambda = 1$, θ is the direction of the incident plane wave .

In Tables 3.2 and 3.3, we provide different estimates of the average of n reconstructed impedance values where n is the number of the different directions of u^i for segment and arc-shaped cracks respectively. Both Tables show good estimates of the impedance values.

λ_e^+	λ_e^-	n	λ_a^+	λ_a^-
2	1i	4	2.01+0.06i	-0.02+1.23 i
2	1i	100	1.99+0.06i	-0.06+1.18i
5+5i	5+5i	4	4.57+ 5.04 i	4.67+4.96 i
5+5i	5+5i	100	4.68+ 5.19 i	4.77+ 5.22i
0.5+1i	0.2+0.4i	4	0.46+ 1.15 i	0.17+0.54 i
0.5+1i	0.2+0.4i	100	0.44+ 1.13 i	0.15+0.51 i

Table 3.2: Reconstruction of the average of λ^+ and λ^- given by formula (3.22) on $\sigma = [-0.5, 0.5] \times \{0\}$ for n equidistant directions of plane wave starting from $\theta = 0$ to $\theta = 2\pi$ with the wave length $\lambda = 1$.

λ_e^+	λ_e^-	n	λ_a^+	λ_a^-
2	1i	4	2.07+1.50 i	0.37+0.82 i
2	1i	100	2.06+0.0 38i	0.22+ 1.01i
5+5i	5+5i	4	5.53+ 2.18 i	7.69+ 5.07 i
5+5i	5+5i	100	5.08+2.30 i	7.07+5.01i
0.5+1i	0.2+0.4i	4	0.46+ 0.99 i	0.15+ 0.41 i
0.5+1i	0.2+0.4i	100	0.47+ 1.08i	0.18+ 0.41 i

Table 3.3: Reconstruction of the average of $\lambda^\pm$ given by formula (3.22) on σ where σ is the arc centered on $(0, 0)$ with aperture $\frac{\pi}{2}$ for n equidistant directions of plane waves starting from $\theta = 0$ to $\theta = 2\pi$ with the wave length $\lambda = 1$.

We next test whether the reconstructed impedance is sensitive to the errors on the cracks geometries. To do so, we make a small perturbation of the geometry of the cracks by shifting its vertical position with ε. The results shown in Tables 3.4 and 3.5 below indicate that a stable approximation is obtained only for $k\varepsilon$ small enough.

λ_e^+	λ_e^-	n	λ_a^-	λ_a^+
2	1i	4	14.21-0.45 i	12.57+ 1.15 i
2	1i	100	10.10-0.38 i	9.24+ 1.18 i
5+5i	5+5i	4	29.12+ 3.42 i	12.01+ 2.12 i
5+5i	5+5i	100	25.96+ 3.54 i	12.39+ 2.28i
0.5+1i	0.2+0.4i	4	17.29+0.08 i	11.14+ 0.82 i
0.5+1i	0.2+0.4i	100	12.28+ 0.18 i	7.92+ 0.80 i

Table 3.4: Reconstruction of the average of $\lambda^{\pm}$ given by formula (3.22) on σ with the perturbed geometry $\sigma = [-0.5, 0.5] \times \{0.1\}$ (the wavelength $\lambda = 1$) and the exact crack is $\sigma = [-0.5, 0.5] \times \{0\}$ for n equidistant directions of plane wave starting from $\theta = 0$ to $\theta = 2\pi$.

λ_e^+	λ_e^-	n	λ_a^-	λ_a^+
2	1i	4	2.04+0.0 1i	1.33i
2	1i	100	2.03+0.04 i	-0.02+ 1.21 i
5+5i	5+5i	100	4.33+ 5.39i	5.24+ 4.97i
5+5i	5+5i	4	4.17+ 5.24 i	5.11+ 4.71 i
0.5+1i	0.2+0.4i	100	0.56+1.05 i	0.20+0.55 i
0.5+1i	0.2+0.4i	4	0.60+ 1.03 i	0.26+ 0.62 i

Table 3.5: Reconstruction of the average of $\lambda^{\pm}$ given by formula (3.22) on σ with the perturbed geometry $\sigma = [-0.5, 0.5] \times \{0.01\}$ (the wavelength $\lambda = 1$) and the exact crack is $\sigma = [-0.5, 0.5] \times \{0\}$ for n equidistant directions of plane wave starting from $\theta = 0$ to $\theta = 2\pi$.

The results show that a good approximation of the crack is needed to obtain a good estimate of the impedance values. However, this issue can be tackled by increasing the wave length as can be seen in Table 3.6 and 3.7

λ_e^+	λ_e^-	n	λ_a^-	λ_a^+
2	1i	100	2.01+0.0 4 i	-0.02+1.07 i
5+5i	5+5i	100	4.15+ 5.20 i	4.67+ 4.73 i
0.5+1i	0.2+0.4i	100	0.45+ 1.03 i	0.22+0.42 i

Table 3.6: Reconstruction of the average of $\lambda^{\pm}$ given by formula (3.22) on σ with the perturbed geometry $\sigma = [-0.5, 0.5] \times \{0.01\}$ (the wavelength $\lambda = 4$) and the exact crack is $\sigma = [-0.5, 0.5] \times 0$ for n equidistant directions of plane wave starting from $\theta = 0$ to $\theta = 2\pi$

λ_e^+	λ_e^-	n	λ_a^-	λ_a^+
2	1i	100	1.99+0.06 i	1.65+ 0.90 i
5+5i	5+5i	100	1.06+4.11 i	5.48+ 2.97 i
0.5+1i	0.2+0.4i	100	0.38+0.80 i	0.68+ 0.52 i

Table 3.7: Reconstruction of the average of $\lambda^{\pm}$ given by formula (3.22) on σ with the perturbed geometry $\sigma = [-0.5, 0.5] \times \{0.1\}$ (the wavelength $\lambda = 4$) and the exact crack is $\sigma = [-0.5, 0.5] \times \{0\}$ for n equidistant directions of plane wave starting from $\theta = 0$ to $\theta = 2\pi$.

3.4.2 An approach inspired by the LSM algorithm

According to the proof of the main Lemma of the Linear Sampling Method (see Theorem 19), if $L \subset \sigma$ then Φ_L is an approximation of the scattered wave associated to an incident Herglotz wave with the kernel g_L solution of the equation (3.4) the LSM equation. Hence we have the following relations

$$\partial_\nu \Phi_L^{\pm} \pm \lambda^{\pm} \Phi_L^{\pm} \simeq -(\partial_\nu v_g \pm \lambda^{\pm} v_g) \qquad \text{on} \quad \sigma \tag{3.23}$$

We recall that

$$\Phi_L^{\infty}(\hat{x}) = \int_L \left(\alpha(y) \frac{\partial e^{-ik\hat{x}\cdot y}}{\partial \nu(y)} + \beta(y) e^{-ik\hat{x}\cdot y} \right) ds(y).$$

where $(\alpha, \beta) \in \tilde{H}^{1/2}(\sigma) \times H^{-1/2}(\sigma)$. Hence to estimate the value of the impedance over the small crack L, the following formulas can be used, which can be directly deduced from (3.23) for constant impedance values over L

$$\lambda^{\pm} \simeq \mp \frac{\int_L (\partial_\nu \Phi_L^{\pm} + \partial_\nu v_g) \overline{(\Phi_L^{\pm} + v_g)}}{\int_L |\Phi_L^{\pm} + v_g|^2} \tag{3.24}$$

The main advantage of this procedure as compared to the previous one is that a complete knowledge of σ is not required to obtain an approximation of $\lambda^{\pm}$ on L. This is particularly attractive for cases where the reconstructed geometry is good only in some parts of the crack. This has been observed for instance for complex geometries with impedances having "intermediate" values.

Before investigating the cases where L is a part of σ let us consider similar configurations as for the previous approach. Namely we take $L = \sigma = [-0.5, 0.5] \times \{0\}$. Since (α, β) should be in $\tilde{H}^{1/2}(L) \times \tilde{H}^{-1/2}(L)$, we can choose β as a constant function and α as a function that vanishes on the vertices of σ given by

$$\alpha(x) = \frac{(x + 0.5)}{0.5} \quad \text{if } x \in [-0.5, 0] \qquad \text{else} \qquad \alpha(x) = -\frac{(x - 0.5)}{0.5}.$$

The results of Table 3.8 show that a good reconstruction of the impedance values is obtained when using this criterion, however the accuracy of the results depends on the values of β.

λ_e^+	λ_e^-	β	λ_a^+	λ_a^-
2	1i	1	2.03	0.01 +0.95 i
2	1i	2	2.02	-0.01+ 1 i
2	1i	5	2.01	1 i
5+5i	5+5i	6	5.02+4.97 i	4.88+4.99 i
0.5+1i	0.2+0.4i	6	0.50+ 1.01 i	0.20+0.40 i
0.5+1i	0.2+0.4i	1	0.53+1.01 i	0.19+0.38 i

Table 3.8: Reconstruction of the average of $\lambda^{\pm}$ using formula (3.24) on $L = \sigma = [-0.5, 0.5] \times \{0\}$.

Then, we assume that $L = \sigma$ where σ is an arc centered on $(0, 0)$, with radius 1 and opening aperture $\left[0, \frac{\pi}{2}\right]$, β is constant and

$$\alpha(x, y) = 10(x - 1)(y - 1).$$

Table 3.9 shows that a good estimate of the impedance values is obtained by using different values of β.

λ_e^+	λ_e^-	β	λ_a^-	λ_a^+
2	1i	1	2.03	-0.06 + 1.02i
2	1i	2	2.03	-0.04+ 1.01 i
2	1i	5	2.03	-0.02+ 0.99i
5+5i	5+5i	6	5.02+ 5.05 i	4.99+ 4.98 i
0.5+1i	0.2+0.4i	6	0.49+ 1.01 i	0.20+ 0.39i
0.5+1i	0.2+0.4i	1	0.50+ 1.01i	0.20+ 0.40i

Table 3.9: Reconstruction of the average of $\lambda^{\pm}$ using formula (3.24) on $L = \sigma = e^{i\theta'}$, $\theta' \in [0, 2\pi]$.

As done in the first approach we test also the sensibility of this approach to small perturbation of the exact geometry (see Tables 3.10 to Table 3.13). We qualitatively observe similar behavior as in the first approach, namely $k\varepsilon$ should be small enough to ensure a good accuracy. However we can state that the second method seems to be more sensitive to error in the geometry than the first one.

λ_e^+	λ_e^-	β	λ_a^-	λ_a^+
2	1i	6	6.72-1.14i	-5.14+ 2.08 i
5+5i	5+5i	6	7.95+ 4.63 i	-3.10+ 0.51 i
0.5+1i	0.2+0.4i	6	4.96+0.75i	-4.44+0.22i

Table 3.10: Reconstruction of the average of $\lambda^{\pm}$ using formula (3.24) on σ with the perturbed geometry $\sigma = [-0.5, 0.5] \times \{0.1\}$ (the wave length $\lambda = 1$) and the exact crack is $\sigma = [-0.5, 0.5] \times \{0\}$.

λ_e^+	λ_e^-	β	λ_a^-	λ_a^+
2	1i	6	2.37	-0.42+ 1.06 i
5+5i	5+5i	6	5.11+ 4.92 i	3.66+ 4.50 i
0.5+1i	0.2+0.4i	6	0.88+0.96 i	-0.20+ 0.39 i

Table 3.11: Reconstruction of the average of $\lambda^{\pm}$ using formula (3.24)on σ with the perturbed geometry $\sigma = [-0.5, 0.5] \times \{0.01\}$ (the wave length $\lambda = 1$) and the exact crack is $\sigma = [-0.5, 0.5] \times \{0\}$.

λ_e^+	λ_e^-	β	λ_a^-	λ_a^+
2	1i	6	2.01-0.02 i	0.03+1.03 i
5+5i	5+5i	6	4.41+ 5.27 i	5.28+ 4.08 i
0.5+1i	0.2+0.4i	6	0.48+ 0.96 i	0.20+ 0.43

Table 3.12: Reconstruction of the average of $\lambda^{\pm}$ using formula (3.24)on σ with the perturbed geometry $\sigma = [-0.5, 0.5] \times \{0.01\}$ (the wave length $\lambda = 4$) and the exact crack is $\sigma = [-0.5, 0.5] \times \{0\}$.

We now consider the cases where L is only a part of σ (recall that for intermediary impedance values we don't have a high precision in the reconstructed cracks). We test this issue for three different geometries given in Figure 3.18.
In the first experiment we assume that $L = [-0.5, 0.5] \times \{0\}$ is a part of the exact crack $\sigma = [-2, 0.75] \times \{0\}$. Table 3.4.2 shows that a good estimate of the impedance is also obtained in this case.

λ_e^+	λ_e^-	β	λ_a^-	λ_a^+
2	1i	5	2.12-0.08 i	0.44+ 1.05i
5+5i	5+5i	6	-0.33+ 8.64 i	4.38+ 1.95 i
0.5+1i	0.2+0.4i	6	0.49+ 0.96 i	0.15+0.46i

Table 3.13: Reconstruction of the average of $\lambda^{\pm}$ using formula (3.24)on σ with the perturbed geometry $\sigma = [-0.5, 0.5] \times \{0.1\}$ (the wave length $\lambda = 4$) and the exact crack is $\sigma = [-0.5, 0.5] \times \{0\}$.

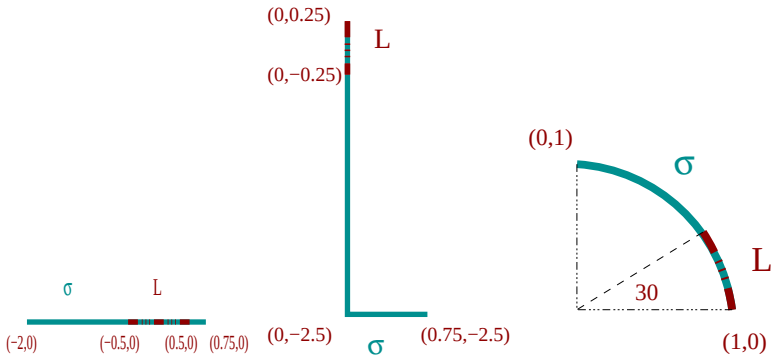

Figure 3.18: The three geometries used on the following test, In blue we represent the exact crack σ and on red we represent the part of crack L.

λ_e^+	λ_e^-	β	λ_a^-	λ_a^+
2	1i	6	2.03+0.01i	0.10+1.02 i
5+5i	5+5i	6	5.12+ 4.967i	5.33+ 4.57i
0.5+1i	0.2+0.4i	6	0.52+1.02 i	0.22+ 0.43 i

Table 3.14: Reconstruction of the average of the impedance values $\lambda^{\pm}$ using formula (3.24)on L where $L = [-0.5, 0.5] \times \{0\}$ is a part of the exact crack $\sigma = [-2, 0.75] \times \{0\}$ (see Fig 3.18, left).

In the following test we show that even for a complex shape as the L-shaped crack we can get good reconstructions. In Table 3.15, σ is an L-shaped crack with vertices $(0, 0.25), (0, -2.5), (0.75, -2.5)$ and $L = \{0\} \times [-0.25, 0.25]$ for a constant β and

$$\alpha(y) = i\frac{(y + 0.25)}{0.25} \quad \text{if } y \in [-0.25, 0] \qquad \text{else} \qquad \alpha(y) = -i\frac{(y - 0.25)}{0.25}.$$

λ_e^+	λ_e^-	β	λ_a^-	λ_a^+
2	2	6	2.13-0.01i	2.12
2	2+1i	2	2.58-0.04 i	2.34+ 0.98 i
5+5i	5+5i	1	5.81+3.92 i	5.38+4.38 i
0.5+1i	0.2+0.4i	6	0.54+1.05 i	0.23+0.43 i
0.5+1i	0.2+0.4i	1	1.09+1.03 i	0.34+ 0.39i

Table 3.15: Reconstruction of the average of the impedance values using formula (3.24) on $L = \{0\} \times [-0.25, 0.25]$ is a part of the exact crack σ the L-shape crack (see Fig 3.18, center) for the wave length $\lambda = 1$.

Finally, let L be a part of the arc shown in Figure 3.18 (right). The results in Table 3.16 show that a good approximation of the exact values of the impedance is obtained on the known part of the exact crack.

λ_e^+	λ_e^-	β	λ_a^-	λ_a^+
2	1i	10	2.21- 0.07 i	-0.05+0.98 i
5+5i	5+5i	10	5.72 +4.86 i	5.20+ 4.69 i
0.5+1i	0.2+0.4i	10	0.59+1.13i	0.19+ 0.36i

Table 3.16: Reconstruction of the average of $\lambda^{\pm}$ on L using formula (3.24) where L is the arc centered on $(0, 0)$ with aperture $\frac{\pi}{6}$ is a part of the exact crack σ (see Fig 3.18, right) for the wave length $\lambda = 1$.

3.5 Conclusion

The first part of this chapter presents an application of the LSM to reconstruct a crack with impedance boundary conditions on both sides of the crack. Compared to the inverse scattering problem by an impenetrable obstacle with smooth closed boundary, the crack detection problems are much more complex due to the joint effects of the tips of the crack, the concave side of the crack and the inhomogeneous surface impedance distributions. Our method provides a good crack reconstruction, with a relatively less precision in the case of

intermediate impedance values. This latter issue can be explained physically by the multiple reflection of waves in the cavity. Note also that in addition to the good reconstruction, the LSM has other advantages, such as the fact that it does not require any information about the crack and it gives a fast algorithm with a simple numerical implementation. However, the LSM has some drawbacks. In fact, it requires many measurements of the far field data. In our case, in the sampling process we have a difficulty in the numerical implementation due to the fact that we use a double layer potential on the expression of the test function Φ_L^∞ where L is considered as a sampling point z. In fact, the sampling process requires to find a good approximation of the exact normal on z. We provide a criterion to tackle this problem that works and give a good normal approximation but it is very sensitive to the impedance values since the precision depends on the values of the frequency. Recall also that in the theoretical justification we give a characterization of the crack using the behavior of a norm of the Herglotz wave that depends on the values of the impedance parameter which can impact the accuracy of the crack reconstruction. This leads to an idea of using another method that tackles these issues by giving an explicit indicator function, which motivates our choice of the application of the Factorization method in the following chapter.

In the second part of this chapter, we have proposed two approaches for the reconstruction of the impedance values. The first approach which is the natural approach that consists in finding the impedance parameter by computing the trace and the normal trace of the total field on σ, knowing the direction of the incident applied wave and the measurement of the associated far field. Using this approach, the results show a good estimate if several directions of the incident plane wave are used. However, it should be noted that this approach is very sensitive to the presence of noise but this issue can be tackled by decreasing the frequency. The second approach use the trace and the normal trace of the test function Φ_L used in the LSM algorithm and the solution g of the far field equation given by the LSM. The performance of this approach depends on three parameters, namely the choice of (α, β) the density function of Φ_L, the reconstructed crack and L. The results show that by using this approach a better estimate is obtained as compared to the first approach, especially when $L = \sigma$. Note that the sensitivity to the presence of noise is similar to that in the first approach but the main advantage of the second one is that it can be applied when L is only a part of the crack geometry while keeping the quality of the estimate. Note that the two approaches for the reconstruction of the impedance values can also be applied using other crack reconstruction methods such as the RG-LSM. In the latter, if the first approach is applied, a small modification should be introduced which consists in computing the trace and the normal trace of the total field, knowing the point source of the incident wave and the measurement of the Cauchy data on a fixed boundary that contains the crack.

CHAPTER 4

Application of the Factorization method to the inverse crack problem

Contents

Abstract
We use the Factorization method to retrieve the shape of cracks with impedance boundary conditions from far fields associated with incident plane waves at a fixed frequency. This work is an extension of the study initiated in [55] where the case of sound soft cracks is considered. We recall that this method is known to be a sampling method that gives an exact charcterization of the scatterer using an exact indicator function. We provide theoretical and numerical validations of the method.

4.1 Introduction

In this chapter we are concerned with the reconstruction of the shape of cracks with impedance boundary conditions from acoustic measurements using the so-called Factorization method [53]. The data for the considered inverse problem is formed by the far fields associated with incident plane waves at a fixed frequency. This work is an extension of the study initiated in [55] where the case of sound soft cracks is addressed. Two difficulties on the theoretical level had to be faced. The first one is due to the fact that the far field operator is no longer normal when the impedance values are not real. Therefore, only the second version of the Factorization method (the so called $F_\sharp$ version) can be considered. To do so, a slight modification of the main theoretical tool behind this method has been introduced. The second one is related to the geometrical nature of the crack problem. For instance as opposed to the case of an obstacle with a non empty interior [53], two boundary unknowns are needed in the factorization of the far field operator. This required in particular a non intuitive choices of the unknowns and the functional spaces associated with. The case of impedance boundary conditions also causes difficulties in designing the numerical algorithm associated with the theoretical part. The latter requires a proper choice of the orientation of the probing "small" crack. In order to fix this problem a minimization procedure with respect to the normal is incorporated. For an overview of recent works on other sampling methods applied to crack identification we refer to [21, 68, 14, 85] and the references therein. This chapter is organized as follows. We start by a brief introduction of the direct and the inverse problem in Section 4.2 and Section 4.3. This is followed in Section 4.4 by giving some factorization of the far field operator which is required later in theoretical justification of the method. In Section 4.7 and 4.3.2 we introduce two scheme to retrieve the shape of the crack. The first one using the so-called the $F_\sharp$ method and the second one using the inf criterion. Both methods give an exact characterization of the crack but the first one are more simple from the numerical point of view. For this end, we perform in the last Section different tests for different shapes of cracks and different values of the impedances using the $F_\sharp$ method. A comparison between the $F_\sharp$ method and the LSM developed in chapter 3 is also presented, which prove the efficiency of this method.

4.2 The forward and inverse scattering problem

We consider the same forward problem introduced for the LSM, in Chapter 3 that we recall here. Let $\sigma \subset \mathbf{R}^m$, $m = 2, 3$, be a smooth nonintersecting open arc embedded in a homogeneous domain. For further considerations, we assume that σ can be extended to an arbitrary smooth, simply connected, closed curve $\partial\Omega$ enclosing a bounded domain Ω in $\mathbf{R}^m$. The normal vector ν on σ coincides with the outward normal vector to $\partial\Omega$.
The total field u satisfies

$$\begin{cases} \Delta u + \kappa^2 u = 0 & \text{in } \mathbf{R}^m \setminus \overline{\sigma}, \\ \partial_\nu u_\pm \pm \lambda^\pm u_\pm = 0 & \text{on } \sigma, \end{cases} \tag{4.1}$$

where the wave number κ is positive and $\lambda^\pm \in L^\infty(\sigma)$ are the given (complex-valued) impedance functions with non-negative imaginary part. The total field $u = u^i + u^s$ is decomposed into the given incident plane wave $u^i(x, d) = e^{ikd\cdot x}$ with unitary direction d and the unknown scattered field u^s which is required to satisfy the Sommerfeld radiation condition

$$\lim_{r=|x|\to+\infty} r^{\frac{m-1}{2}}(\partial_r u^s - i\kappa u^s) = 0, \tag{4.2}$$

uniformly in all directions $\hat{x} = \frac{x}{|x|}$.
Problem (4.1)-(4.2) can be seen as a special case of the following problem:

Find $u^s \in H^1_{loc}(\mathbf{R}^m \setminus \overline{\sigma})$ satisfying the Sommerfeld radiation condition (4.2) and

$$\begin{cases} \Delta u^s + \kappa^2 u^s &= 0 \quad \text{in } \mathbf{R}^m \setminus \overline{\sigma}, \\ \partial_\nu u^s_\mp \pm \lambda^\pm u^s_\pm &= g^\pm \quad \text{on } \sigma. \end{cases} \tag{4.3}$$

where $g^\pm \in H^{-1/2}(\sigma)$ such that $(g^+ - g^-) \in \tilde{H}^{-1/2}(\sigma)$ and $(\lambda^+ + \lambda^-)^{-1} \in L^\infty(\sigma)$ with $\Im(\lambda^\pm) \geq 0$, We recall the variational formulation since we will use it in the study of the inverse problem given by: find $u^s \in H^1(B_R \setminus \bar{\sigma})$ satisfying for all $v \in H^1(B_R \setminus \bar{\sigma})$ the following equation

$$\begin{aligned} \int_{B_R\setminus\bar{\sigma}} \nabla u^s \overline{\nabla v} - \kappa^2 \int_{B_R\setminus\bar{\sigma}} u^s \bar{v} - \int_\sigma \lambda^+ u^s_+ \overline{v_+} - \int_\sigma \lambda^- u^s_- \overline{v_-} - \left\langle T_R(u^s_{|S_R}), v \right\rangle_{S_R} \\ = -\left\langle g^+, [v] \right\rangle_{H^{-1/2}(\sigma), \tilde{H}^{1/2}(\sigma)} - \left\langle (g^+ - g^-), v^- \right\rangle_{\tilde{H}^{-1/2}(\sigma), H^{1/2}(\sigma)} \end{aligned} \tag{4.4}$$

where B_R is a sufficiently large ball with radius R containing $\bar{\sigma}$ and by S_R its boundary and $\langle , \rangle_{S_R}$ denotes the duality product between $H^{-1/2}(S_R)$ and $H^{1/2}(S_R)$ and $T_R : H^{1/2}(S_R) \to H^{-1/2}(S_R)$ is the Dirichlet to Neumann operator defined on (1.24).

We recall that in section 1.2.3 in chapter 1 we have proved that (4.4) has a unique solution that depends continuously on the boundary data $g^\pm$ (see Lemma 5).

Our inverse problem consists in giving the far field pattern $u^\infty(\cdot,\cdot)$ on $\mathbf{S}^{m-1}\times\mathbf{S}^{m-1}$ of the solution to (4.3), reconstruct the crack σ. where u^∞ is the far field pattern defined by

$$u^\infty(\hat{x},d)=\gamma\int_\sigma\left([u^s](y)\frac{\partial e^{ik\hat{x}y}}{\partial\nu(y)}-[\partial_\nu u^s](y)e^{ik\hat{x}y}\right)ds(y),\qquad\forall(\hat{x},d)\in\mathbf{S}^{m-1}\times\mathbf{S}^{m-1}.\quad(4.5)$$

with $\gamma=\frac{e^{i\pi/4}}{\sqrt{8k\pi}},\frac{1}{4\pi}$ respectively for $m=2,3$.

4.3 The far field operator and the $F_\sharp$ method

4.3.1 Definition and properties of the far field operator

We recall that the far field operator is defined by

$$\begin{array}{rccl}F:&L^2(\mathbf{S}^{m-1})&\to&L^2(\mathbf{S}^{m-1})\\&\varphi&\mapsto&\displaystyle\int_{\mathbf{S}^{m-1}}u^\infty(\cdot,y)\varphi(y)ds(y)\end{array}\qquad(4.6)$$

Let us give some properties of this operator in the following theorem which is a slight modification of [53, Theorem 3.3, p73]

Theorem 20.
a) F is a compact operator.
b) F satisfies the relations

$$F-F^*-2ik|\gamma|^2F^*F=2iR,\qquad(4.7)$$
$$F^*-F+2ik|\gamma|^2FF^*=2iJ\bar{R}J,\qquad(4.8)$$

where $\gamma=\frac{e^{i\pi/4}}{\sqrt{8k\pi}},\frac{1}{4\pi}$ respectively for $m=2$ and $m=3$, and $R:L^2(\mathbf{S}^{m-1})\to L^2(\mathbf{S}^{m-1})$ is the self-adjoint non-negative operator defined for $\eta\in\mathbf{S}^{m-1}$ by

$$(R\psi)(\eta)=\int_{\mathbf{S}^{m-1}}\left(\int_\sigma u^+(x,\theta)\overline{u^+(x,\eta)}\Im(\lambda^+)+\int_\sigma u^-(x,\theta)\overline{u^-(x,\eta)}\Im(\lambda^-)\right)\psi(\theta)ds(\theta),\qquad(4.9)$$

and $u(.,\theta)=u^i(.,\theta)+u^s(.,\theta)$ is the total scattered field on σ corresponding to the incident plane wave $u^i(.,\theta)$ of direction θ.
We denote by $J:L^2(\mathbf{S}^{m-1})\to L^2(\mathbf{S}^{m-1})$ the self adjoint involution $J(g)(\theta)=g(-\theta)$.
c) The scattering operator

$$\mathcal{S}=I+2ik|\gamma|^2F,\qquad(4.10)$$

satisfies

$$\mathcal{S}^*\mathcal{S}=I-2ik|\gamma|^2R.$$

If $\lambda^\pm$ is real-valued then the far field operator F is normal, and the scattering operator $\mathcal{S}$ is unitary.

Proof. The proof of *a)* is standard since F is an integral operator with a smooth kernel. *b)* For $g,\ h \in L^2(\mathbf{S}^{m-1})$, define the Herglotz wave functions v^i and w^i by

$$\begin{aligned} v^i(x) &= \int_{\mathbf{S}^{m-1}} e^{ikx.\theta} g(\theta), \quad x \in \mathbf{R}^m, \\ w^i(x) &= \int_{\mathbf{S}^{m-1}} e^{ikx.\theta} h(\theta), \quad x \in \mathbf{R}^m, \end{aligned}$$

respectively. Let v and w be the solution of (4.3) corresponding to incidents fields v^i and w^i, By superposition, we conclude that

$$\begin{aligned} v(x) &= \int_{\mathbf{S}^{m-1}} u(x,\theta) g(\theta) ds(\theta), \quad x \notin \sigma. \\ w(x) &= \int_{\mathbf{S}^{m-1}} u(x,\theta) h(\theta) ds(\theta), \quad x \notin \sigma. \end{aligned}$$

where $u(.,\theta) = u^i(.,\theta) + u^s(.,\theta)$ is the total scattering field on σ solution of (4.3) corresponding to the incident plane wave $u^i(.,\theta)$ of direction θ. We denote by $v^s = v - v^i$, $w^s = w - w^i$ the scattered field and $v^\infty,\ w^\infty$ the far field patterns corresponding respectively with v and w. Then, by linearity, $v^\infty = Fg$ and $w^\infty = Fh$. Green's formula in $D_r = \{x \in \mathbf{R}^2 \setminus \bar{\sigma} : \quad |x| < r\}$ and the boundary conditions yield

$$\int_\sigma \left[v_+ \overline{w_+} \Im(\lambda^+) + v_- \overline{w_-} \Im(\lambda^-) \right] ds = \int_{D_r} \left[v \Delta \bar{w} - w \Delta \bar{v} \right] ds = \int_{|x|=r} \left[v \partial_\nu \bar{w} - \bar{w} \partial_\nu v \right] ds. \tag{4.11}$$

The integral on the right hand side is split into four parts by decomposing $v = v^i + v^s$ and $w = w^i + w^s$. The integral

$$\int_{|x|=r} \left[v^i \partial_\nu \overline{w^i} - \overline{w^i} \partial_\nu v^i \right] ds$$

vanishes by Green's second theorem in $\{x : |x| < r\}$ since v^i and $\overline{w^i}$ are two solutions of the Helmholtz equation. We note that by our normalization of the far field pattern

$$v^s(x) \frac{\partial \overline{w^s(x)}}{\partial r} - \overline{w^s(x)} \frac{\partial v^s(x)}{\partial r} = -2ik|\gamma|^2 r^{-(m-1)} v^\infty(\hat{x}) \overline{w^\infty(\hat{x})} + \mathcal{O}\left(\frac{1}{r^m}\right).$$

In fact, using the asymptotic behavior of w^s and w^s we have

$$v^s(x,d) = \gamma r^{\frac{1-m}{2}} e^{ikr} v^\infty(\hat{x},d) + O(r^{-\frac{m+1}{2}}),$$

Therefore we have

$$\int_{|x|=r} \left[v^s \frac{\partial \overline{w^s}}{\partial \nu} - \overline{w^s} \frac{\partial v^s}{\partial \nu} \right] ds \longrightarrow -2ik|\gamma|^2 \int_{\mathbf{S^{m-1}}} v^\infty \overline{w^\infty} ds = -2ik|\gamma|^2 \left(Fg, Fh\right)_{L^2(\mathbf{S^{m-1}})}$$

as r tends to infinity. Finally, we use the definition of v^i and w^i and by changing the order of integration we have

$$\begin{aligned}\int_{|x|=r}\left[v^i\partial_\nu\overline{w^s}-\overline{w^s}\partial_\nu v^i\right]ds &= \int_{\mathbf{S^{m-1}}}g(\theta)\int_{|x|=r}\left[e^{ikx\theta}\partial_\nu\overline{w^s}-\overline{w^s}\partial_\nu e^{ikx\theta}\right]ds\\ &= -\int_{\mathbf{S^{m-1}}}g(\theta)\overline{w^\infty(\theta)}d(\theta)\\ &= -(g,Fh)_{L^2(\mathbf{S^{m-1}})}.\end{aligned}$$

Analogously, we have that

$$\int_{|x|=r}\left[v^s\partial_\nu\overline{w^i}-\overline{w^i}\partial_\nu v^s\right]ds=-(Fg,h)_{L^2(\mathbf{S^{m-1}})}.$$

Interchanging the orders of integration in the left hand side of (4.11) yields

$$\begin{aligned}&\int_\sigma\left[v_+\overline{w_+}\Im(\lambda^+)+v_-\overline{w_-}\Im(\lambda^-)\right]ds=\\ &\int_{\mathbf{S^{m-1}}}\int_{\mathbf{S^{m-1}}}\left[\int_\sigma u^+(x,\theta)\overline{u^+(x,\eta)}\Im(\lambda^+)(x)ds(x)+\int_\sigma u^-(x,\theta)\overline{u^-(x,\eta)}\Im(\lambda^-)(x)ds(x)\right]\\ &\qquad g(\theta)\overline{h(\eta)}ds(\theta)ds(\eta)=(Rg,h)_{L^2(\mathbf{S}^{m-1})}.\end{aligned}$$

Finally, taking the limit $r\to\infty$ yields

$$\begin{aligned}2i\,(Rg,h)_{L^2(\mathbf{S^{m-1}})} &= -2ik|\gamma|^2\,(Fg,Fh)_{L^2(\mathbf{S^{m-1}})}-(g,Fh)_{L^2(\mathbf{S^{m-1}})}+(Fg,h)_{L^2(\mathbf{S^{m-1}})}\\ &= -2ik|\gamma|^2\,(F^*Fg,h)_{L^2(\mathbf{S^{m-1}})}-(F^*g,h)_{L^2(\mathbf{S^{m-1}})}+(Fg,h)_{L^2(\mathbf{S^{m-1}})},\end{aligned}$$

which prove (4.7), for the prof of (4.8) we can deduce it directly from (4.7) using the reciprocity relation and the fact that

$$F^*=J\overline{F}J$$

Hence we have

$$\overline{F}-\overline{F^*}-2ik|\gamma|^2\overline{F^*F} = -2i\overline{R}$$

that's implies

$$J\overline{F}J-J\overline{F^*}J+2ik|\gamma|^2J\overline{F^*F}J=-2iJ\overline{R}J$$

and consequently

$$F^*-F+2ik|\gamma|^2FF^*=-2iJ\overline{R}J.$$

c) We just compute

$$\begin{aligned}\mathcal{S}^*\mathcal{S} &= \left(I - 2ik|\gamma|^2F^*\right)\left(I + 2ik|\gamma|^2F\right) = I + \frac{ik}{8\pi^2}\left[(F - F^*) - 2ik|\gamma|^2F^*F\right] \\ &= I + 2ik|\gamma|^2 2iR = I - 2k|\gamma|^2R.\end{aligned}$$

□

According to the previous lemma, for general complex impedance values (i.e when $\Im(\lambda^\pm) \neq 0$) the far field operator fails to be normal. Hence we cannot expect the classical form of the Factorization method i.e the $(F^*F)^{1/4}$ method to apply in this case. We shall rather consider the so called $F_\sharp$ version. A characterization of σ will be obtained using the solvability of equation (4.12).

$$(F_\sharp)^{1/2}(g_L)(\hat{x}) = \Phi_L^\infty(\hat{x}) \qquad \text{for all} \quad \hat{x} \in \mathbf{S}^{m-1} \tag{4.12}$$

where $F_\sharp$ is defined by

$$F_\sharp = |\Re F| + \Im F$$

with $\Re F = \frac{1}{2}(F + F^*)$, and $\Im F = \frac{1}{2i}(F - F^*)$ and where $\Phi_L^\infty \in L^2(\mathbf{S}^{m-1})$ is defined by

$$\Phi_L^\infty(\hat{x}) := \gamma \int_L \left(-i\kappa\ \hat{x}.\nu(y)\alpha_L(y) + \beta_L(y)\right) e^{-i\kappa\hat{x}\cdot y} ds(y), \tag{4.13}$$

for any smooth non intersecting open arc $L \subset \mathbf{R}^{m-1}$, where $\gamma = \frac{e^{i\pi/4}}{\sqrt{8\pi\kappa}}, \frac{1}{4\pi}$ respectively for $m = 2$ and $m = 3$ and with densities $\alpha_L \in \tilde{H}^{\frac{1}{2}}(L)$ and $\beta_L \in \tilde{H}^{-\frac{1}{2}}(L)$. The proof of this result is based on the factorization of the operator F in the form $F = \mathcal{H}^*T\mathcal{H}$ where $T : H \to H^*$ is a linear bounded operator and $\mathcal{H} : L^2(\mathbf{S}^{m-1}) \longrightarrow H^*$ is a compact operator with dense range. More precisely we shall prove the following Theorem 22.

4.3.2 The $F_\sharp$ characterization

The main theorem behind the inversion algorithm proposed belows is the following characterization of σ using the range of $F_\sharp^{1/2}$.

Theorem 21. *For any smooth non intersecting arc L and functions $\alpha_L \in \tilde{H}^{\frac{1}{2}}(L)$ and $\beta_L \in \tilde{H}^{-1/2}(L)$ such that $(\alpha_L, \beta_L) \neq (0, 0)$, the following is true*

$$L \subset \sigma \qquad \textit{if and only if} \qquad \Phi_L^\infty \in R(F_\sharp^{1/2}). \tag{4.14}$$

We recall that (4.14) is verified iff

$$\sum_{n=1}^{\infty} \frac{|\left(\Phi_L^\infty, \psi_n\right)_{L^2(S^2)}|^2}{\lambda_n} < +\infty$$

where $\{\lambda_n, \psi_n\}_{n\in\mathbf{N}}$ is an eigensystem of the self-adjoint, positive and compact operator $F_\sharp$.

Proof. The proof of this Theorem can be deduced from Theorem 22, Lemma 28, Lemma29, Lemma 30 and Lemma 31. It can be also proved using Theorem 22, Lemma 23 and Lemma 42.

□

Theorem 22. *Let $H \subset U \subset H^*$ be a Gelfand triple with a Hilbert space U and a reflexive Banach space H such that the embedding is dense. Moreover, let Y be a second Hilbert space and let $F : Y \longrightarrow Y, \mathcal{H} : H \longrightarrow Y$, and $T : H^* \longrightarrow H$ be linear bounded operators such that*

$$F = \mathcal{H}^* T \mathcal{H}$$

We make the following assumptions:
(A1) $\mathcal{H}^*$ is compact with dense range.
(A2) We have $\Re[T] = C + K$ with some compact operator K and some self-adjoint and coercive operator $C : H^* \longrightarrow H$, i.e, there exists $c > 0$ with

$$\langle \varphi, C\varphi \rangle \geq \|\varphi\|^2 \qquad \text{for all} \qquad \varphi \in H^*$$

And $\Im T$ is non-negative on $R(\mathcal{H}^*) \subset H^*$. Then the operator $F_\sharp = |\Re F| + \Im F$ is positive, and the ranges of $\mathcal{H}^* : H^* \longrightarrow Y$ and $F_\sharp{}^{1/2} : Y \longrightarrow Y$ coincide.

Proof. This theorem is a slight modification of [53, Theorem 2.15, p57]. The two first assumptions of the previous theorem $(A1)$ and $(A2)$ are needed to give of a factorization of $F_\sharp$ in the form $F_\sharp = GT_\sharp G^*$ (see the proof on [53]). The fact that $\Im T$ is non-negative on $R(G^*) \subset X^*$ is sufficient to prove the coercivity of $T_\sharp$ unlike to the classical $F_\sharp$ method where we need an extra condition which consists on proving that $\Im T$ is a compact operator.

In fact, as in the proof given in [53], $T_\sharp$ is a self-adjoint operator defined by

$$T_\sharp := T_R^R(Q^+ - Q^-) + \Im T \tag{4.15}$$

with $T_R^R = \Re[T]$ and $Q^\pm : U \longrightarrow U^\pm$ are two projectors onto $U^\pm$ parallel to $U^\mp$, where $U = U^+ \oplus U^-$, for $U^- = \mathcal{H}(Y^-)$ and $Y^- = span\{\psi_j : \lambda_j \leq 0\}$.
On the other hand, using (A_2) we have $T_R^R = C+K$ and consequently $T_\sharp$ can be decomposed as follows:

$$T_\sharp := C(Q^+ + Q^-) - 2CQ^- + K(Q^+ - Q^-) + \Im T \tag{4.16}$$

Since $(Q^+ + Q^-) = I$ then $C(Q^+ + Q^-)$ is also coercive, and using the fact that $(Q^+ - Q^-)$ is an isomorphism and K is compact, so we have $K(Q^+ - Q^-)$ is also compact, Q^- has a finite range hence is compact and $2CQ^-$ is also compact.Finally, $\Im T$ is non negative hence $C(Q^+ + Q^-) + \Im T$ is coercive. That proves that $T_\sharp$ is a Freedholm operator. As T_R^R and

$\Im T$ are non negative then $T_\sharp$ has a bounded inverse $T_\sharp^{-1}$.
From the positivity of the form

$$\langle T_\sharp(\varphi + t\psi), (\varphi + t\psi)\rangle_U = \langle T_\sharp\varphi, \varphi\rangle_U + 2\Re[t\,\langle \psi, T_\sharp\rangle_U] + |t|^2\,\langle T_\sharp\psi, \psi\rangle_U$$

For any $\varphi, \psi \in U$ and any $t \in \mathbf{C}$ we conclude that

$$|\,\langle T_\sharp\varphi, \psi\rangle\,| \leq \langle T_\sharp\varphi, \varphi\rangle_U\,\langle T_\sharp\psi, \psi\rangle_U\,.$$

For $\psi = T_\sharp^{-1}\varphi$ this yields to

$$\|\varphi\|_U^4 = |\,\left\langle T_\sharp\varphi, T_\sharp^{-1}\varphi\right\rangle_U|^2 \leq \langle T_\sharp\varphi, \varphi\rangle_U\left\langle \varphi, T_\sharp^{-1}\varphi\right\rangle_U \leq \langle T_\sharp\varphi, \varphi\rangle_U\,\|T_\sharp^{-1}\|\|\varphi\|_U^2,$$

i.e.,

$$\|T_\sharp^{-1}\|^{-1}\|\varphi\|_U^2 \leq \langle T_\sharp\varphi, \varphi\rangle_U$$

which proves the coercivity of $T_\sharp$ with $c = \|T_\sharp^{-1}\|^{-1}$.

□

The goal of the next section is to give two possible factorizations of the operator F in the indicated forms.

4.4 Example of factorizations of the far field operator

As explained above in this subsection we need a special factorization of the operator F in the form $F = \mathcal{H}^*T\mathcal{H}$, where $\mathcal{H}^*$ is a compact operator with dense range and T is an isomorphism. We present in the following some example of factorization choices.

4.4.1 A natural choice

We recall that F is the far field of the solution $\tilde{u}^s$ satisfying the following system

$$\begin{array}{rcccl} \Delta\tilde{u}^s + \kappa^2\tilde{u}^s & = & 0 & \text{in} & \mathbf{R}^m \setminus \overline{\sigma} \\ \partial_\nu\tilde{u}^s_\pm \pm \lambda^\pm\tilde{u}^s_\pm & = & g^\pm & \text{on} & \sigma \end{array} \tag{4.17}$$

and the radiation condition

$$\lim_{r=|x|\to+\infty} r^{\frac{m-1}{2}}(\partial_r\tilde{u}^s - ik\tilde{u}^s) = 0$$

uniformly in all directions $\hat{x} = \frac{x}{|x|}$.
whith $g^\pm = -(\partial_\nu v_\varphi \pm \lambda^\pm v_\varphi)$ and v_φ is the Herglotz wave of kernel φ defined by

$$v_\varphi(x) := \int_{\mathbf{S}^{m-1}} e^{i\kappa x\cdot\theta}\varphi(\theta)\,ds(\theta), \quad x \in \mathbf{R}^m.$$

For $H_1 := \{g^{\pm} \in H^{-1/2}(\sigma) \quad \text{such that} \quad (g^+ - g^-) \in \tilde{H}^{-1/2}(\sigma)\}$, we can deduce therefore the following factorization

$$F = \mathcal{G}_1 \mathcal{H}_1,$$

where the operator $\mathcal{G}_1 : H_1 \to L^2(\mathbf{S}^{m-1})$ maps the boundary data (g^+, g^-) to the far field pattern of the solution of (4.3), which can be defined by:

$$\mathcal{G}_1(g^+, g^-)(\hat{x}) = \int_\sigma \left([u^s](y) \frac{\partial e^{ik\hat{x}y}}{\partial \nu(y)} - [\partial_\nu u^s](y) e^{ik\hat{x}y} \right) ds(y). \tag{4.18}$$

and $\mathcal{H}_1 : L^2(\mathbf{S}^{m-1}) \to H_1$ is the trace operator defined by

$$\mathcal{H}_1(\varphi) = (-(\partial_\nu + \lambda^+) v_{\varphi|\sigma}, -(\partial_\nu - \lambda^-) v_{\varphi|\sigma}) \tag{4.19}$$

From (4.19), we observe that for $d \in \mathbf{S}^{m-1}$ and $(\alpha, \beta) \in H_1^*$, the operator $\mathcal{H}_1^*$ is given by

$$\mathcal{H}_1^*(\alpha, \beta)(d) = -\int_\sigma \left((\alpha(y) + \beta(y)) \frac{\partial e^{-\imath\kappa d \cdot y}}{\partial \nu(y)} + \left(\overline{\lambda^+} \alpha(y) - \overline{\lambda^-} \beta(y) \right) e^{-\imath\kappa d \cdot y} \right) ds(y). \tag{4.20}$$

In fact, for $\varphi \in L^2(\mathbf{S}^{m-1})$ and $\alpha, \beta \in H_1^*$, then $\mathcal{H}_1^* : H_1^* \to L^2(\mathbf{S}^{m-1})$ satisfies

$$\langle \mathcal{H}_1(\varphi), (\alpha, \beta) \rangle_{H_1^*, H_1} = \langle \varphi, \mathcal{H}_1^*(\alpha, \beta) \rangle_{L^2(\mathbf{S}^{m-1}), L^2(\mathbf{S}^{m-1})}$$

By changing the order of integration in the left hand side of the previous equation we have

$$\begin{aligned}
& \langle \mathcal{H}_1(\varphi), (\alpha, \beta) \rangle_{H_1^*, H_1} \\
= & -\int_{\mathbf{S}^{m-1}} \varphi(d) \overline{\left[\int_\sigma \left(\alpha(y) \left(\frac{\partial}{\partial \nu(y)} + \overline{\lambda^+} \right) e^{-\imath\kappa d \cdot y} + \beta(y) \left(\frac{\partial}{\partial \nu(y)} - \overline{\lambda^-} \right) e^{-i\kappa d \cdot y} \right) ds(y) \right]} ds(d) \\
= & -\int_{\mathbf{S}^{m-1}} \varphi(d) \overline{\left[\int_\sigma \left((\alpha(y) + \beta(y)) \frac{\partial e^{-\imath\kappa d \cdot y}}{\partial \nu(y)} + \left(\overline{\lambda^+} \alpha(y) - \overline{\lambda^-} \beta(y) \right) e^{-\imath\kappa d \cdot y} \right) ds(y) \right]} ds(d)
\end{aligned}$$

Note that $\mathcal{H}_1^*$ is the far field pattern of the potential

$$V(z) = -\gamma \int_\sigma \left((\alpha(y) + \beta(y)) \frac{\partial \Phi(z, y)}{\partial \nu(y)} ds(y) + \left(\overline{\lambda^+} \alpha(y) - \overline{\lambda^-} \beta(y) \right) \Phi(z, y) \right) ds(y),$$

for $z \in \mathbf{R}^m \setminus \bar{\sigma}$, where $\gamma = \frac{e^{i\pi/4}}{\sqrt{8k\pi}}, \frac{1}{4\pi}$ respectively for $m = 2$ and $m = 3$.
From the expression of $\mathcal{G}_1$ given in (4.18) V can be seen as a solution $\tilde{u}^s$ for some (g^+, g^-) of (4.3) if α and β are such that

$$\alpha + \beta = -[\tilde{u}^s]_{|\sigma} \quad \text{and} \quad \overline{\lambda^+} \alpha - \overline{\lambda^-} \beta = [\partial_\nu \tilde{u}^s]_{|\sigma}.$$

The latters are equivalent to

$$\alpha = \frac{1}{\lambda^+ + \lambda^-} [\partial_\nu \tilde{u}^s]_{|\sigma} - \frac{\overline{\lambda^-}}{\lambda^+ + \lambda^-} [\tilde{u}^s]_{|\sigma} \quad \text{and} \quad \beta = -\frac{1}{\lambda^+ + \lambda^-} [\partial_\nu \tilde{u}^s]_{|\sigma} - \frac{\overline{\lambda^+}}{\lambda^+ + \lambda^-} [\tilde{u}^s]_{|\sigma}.$$

Therefore, $\mathcal{G}_1 = \mathcal{H}_1^* T_1$, where the operator $T_1 : H \to H^*$ is defined by

$$T_1(g^+, g^-) = \left(T_1^1(g^+, g^-),\ \ T_1^2(g^+, g^-)\right), \tag{4.21}$$

where

$$T_1^1(g^+, g^-) := \frac{1}{\lambda^+ + \lambda^-}[\partial_\nu \tilde{u}^s]_{|\sigma} - \frac{\overline{\lambda^-}}{\lambda^+ + \lambda^-}[\tilde{u}^s]_{|\sigma}, \tag{4.22}$$

and

$$T_1^2(g^+, g^-) := -\frac{1}{\lambda^+ + \lambda^-}[\partial_\nu \tilde{u}^s]_{|\sigma} - \frac{\overline{\lambda^+}}{\lambda^+ + \lambda^-}[\tilde{u}^s]_{|\sigma}, \tag{4.23}$$

with $\tilde{u}^s \in H^1_{loc}(\mathbf{R}^m \setminus \sigma)$ is a solution of (4.17). Finally, a factorization of the operator F is given by

$$F = \mathcal{H}_1^* T_1 \mathcal{H}_1. \tag{4.24}$$

The issue with this factorization is that $H_1 := \{g^\pm \in H^{-1/2}(\sigma) \quad \text{such that} \quad (g^+ - g^-) \in \tilde{H}^{-1/2}(\sigma)\}$, and we cannot prove in this case that the operator $T_1 : H_1 \to H_1^*$ is continuous whith $H_1^* = \{f^\pm \in H^{1/2}(\sigma) \quad \text{such that} \quad (f^+ + f^-) \in \tilde{H}^{1/2}(\sigma)\}$.
To tackle this issue we need to change the space on which T_1 is defined. This approach will be developed in Section 4.6.

4.4.2 A "better" choice of the factorization

We remark that (4.17) can be written as

$$\begin{cases} \Delta \tilde{u}^s + \kappa^2 \tilde{u}^s = 0 & \text{in } \mathbf{R}^m \setminus \overline{\sigma} \\ \partial_\nu \tilde{u}^s_+ + \lambda^+ \tilde{u}^s_+ = h^+ & \text{on } \sigma \\ [\partial_\nu \tilde{u}^s] + \lambda^+ \tilde{u}^s_+ + \lambda^- \tilde{u}^s_- = h^- & \text{on } \sigma \end{cases} \tag{4.25}$$

where $h^+ = g^+$, $h^- = g^+ - g^-$. For $(\lambda^+ + \lambda^-)^{-1} \in L^\infty(\sigma)$ we already proved that (4.25) problem is well posed for $(h^+, h^-) \in H_2$, where $H_2 := H^{-1/2}(\sigma) \times L^2(\sigma)$ since $L^2(\sigma) \subset \tilde{H}^{1/2}(\sigma)$. We observe that $H_2^* := \tilde{H}^{1/2}(\sigma) \times L^2(\sigma)$. We recall that solving (4.25) is equivalent to solve the following variational problem

$$\begin{aligned} \int_{B_R \setminus \bar{\sigma}} \nabla \tilde{u}^s \overline{\nabla v} - \kappa^2 \int_{B_R \setminus \bar{\sigma}} \tilde{u}^s \bar{v} - \int_\sigma \lambda^+ \tilde{u}^s_+ \overline{v_+} - \int_\sigma \lambda^- \tilde{u}^s_- \overline{v_-} - \left\langle T_R(u_{|S_R}), v \right\rangle_{S_R} \\ = -\left\langle h^+, [v] \right\rangle_{H^{-1/2}(\sigma), \tilde{H}^{1/2}(\sigma)} - \int_\sigma h^- \overline{v_-} \end{aligned} \tag{4.26}$$

Proceeding as in the natural choice we deduce the following factorization $F = \mathcal{G}_2 \mathcal{H}_2$ from the expression of the operator F by rewriting the operator $\mathcal{G}_2 : H_2 \to L^2(\mathbf{S}^{m-1})$ which maps the boundary data (h^+, h^-) to the far field pattern of the radiation solution of (4.25) and $\mathcal{H}_2 : L^2(\mathbf{S}^{m-1}) \to H_2$ is the trace operator defined by

$$\mathcal{H}_2(\varphi) = \left(-(\partial_\nu + \lambda^+) v_{\varphi_{|\sigma}}, -(\lambda^- + \lambda^+) v_{\varphi_{|\sigma}}\right), \tag{4.27}$$

where v_φ is the Herglotz wave function of kernel $\varphi \in L^2(\mathbf{S}^{m-1})$, We denote by $\mathcal{H}_2^*$ the adjoint of the operator $\mathcal{H}_2$. Let $(\alpha, \beta) \in H_2^*$ and $d \in \mathbf{S}^{m-1}$, proceeding as in the case of the natural choice, the expression of the operator $\mathcal{H}_2^*$ is given by

$$\mathcal{H}_2^*(\alpha,\beta)(d) = -\int_\sigma \alpha(y)\frac{\partial e^{-i\kappa d\cdot y}}{\partial \nu(y)}ds(y) - \int_\sigma \left(\bar{\lambda}^+\alpha(y) + \overline{(\lambda^+ + \lambda^-)}\beta(y)\right) e^{-i\kappa d\cdot y}ds(y). \tag{4.28}$$

We note that $\mathcal{H}_2^*$ is the far field pattern of the potential

$$V(z) = -\int_\sigma \alpha(y)\frac{\partial \Phi(z,y)}{\partial \nu(y)}ds(y) - \int_\sigma \left(\bar{\lambda}^+\alpha(y) + \overline{(\lambda^+ + \lambda^-)}\beta(y)\right) \Phi(z,y))ds(y), \tag{4.29}$$

V can be a solution $\tilde{u}^s$ for some (h^+, h^-) of (4.25), where

$$\alpha = -[\tilde{u}^s] \qquad \text{and} \qquad \bar{\lambda}^+\alpha + \overline{(\lambda^+ + \lambda^-)}\beta = [\partial_\nu \tilde{u}^s],$$

which is equivalent to $\alpha = -[\tilde{u}^s]$ and

$$\beta = \frac{h^-}{\overline{\lambda^+ + \lambda^-}} - \frac{2i\Im(\lambda^+)}{\lambda^+ + \lambda^-}\tilde{u}^s_+ - \frac{\lambda^- + \bar{\lambda}^+}{\lambda^+ + \lambda^-}\tilde{u}^s_-.$$

Therefore, $\mathcal{G}_2$ can be expressed as follows

$$\mathcal{H}_2^* T_2 = \mathcal{G}_2, \tag{4.30}$$

where $T_2 : H_2 \to H_2^*$ is the bounded linear operator defined by

$$T_2(h^+, h^-) = (-[\tilde{u}^s], \frac{h^-}{\overline{\lambda^+ + \lambda^-}} - \frac{2i\Im(\lambda^+)}{\lambda^+ + \lambda^-}\tilde{u}^s_+ - \frac{\lambda^- + \bar{\lambda}^+}{\lambda^+ + \lambda^-}\tilde{u}^s_-); \tag{4.31}$$

where $\tilde{u}^s \in H^1_{loc}(\mathbf{R}^m \setminus \bar{\sigma})$ is the radiating solution to (4.25). Finally, by replacing the expression of $\mathcal{G}_2$ on the decomposition of F by (4.30), we find a new factorization of F as a function of $\mathcal{H}_2$, $\mathcal{H}_2^*$ and T_2

$$F = \mathcal{H}_2^*\, T_2\, \mathcal{H}_2. \tag{4.32}$$

For the study of this factorization see section 4.5.

4.5 Analysis of the factorization (4.32)

Let now prove that the operator T_2 is an isomorphism

Lemma 23. *Let $H_2 = H^{-1/2}(\sigma) \times L^2(\sigma)$, the operator $T_2 : H_2 \to H_2^*$ can be decomposed as $T_2 = T_2^C + T_2^K$ where T_2^K is a compact operator and T_2^c is defined by*

$$T_2^c(h^+, h^-) = (-[u^0], \frac{h^-}{\overline{\lambda^+ + \lambda^-}} - u^0_-), \tag{4.33}$$

with $u^0 \in H^1_{loc}(B_R \setminus \bar{\sigma})$ is the solution of the variational problem (4.34)

$$\int_{B_R\setminus\bar{\sigma}} \nabla u^0 \overline{\nabla v} + \kappa^2 \int_{B_R\setminus\bar{\sigma}} u^0_- \bar{v} - \langle T_R u^0, v\rangle_{S_R} = -\langle h^+, [v]\rangle_{H^{-1/2}(\sigma),\tilde{H}^{1/2}(\sigma)} - \int_\sigma h^- \overline{v_-}. \quad (4.34)$$

and T_R is the Dirichlet to Neuman operator defined in Theorem 6.

Proof. The operator T_2 can be splitted in the form $T_2 = T_2^c + T_2^K$ where $T_2^c : H_2 \to H_2^*$ which is coercive, since we have

$$\begin{aligned}
\langle (h^+,h^-), T_2^c(h^+,h^-)\rangle &= -\langle h^+, [u^0]\rangle_{H^{-1/2}(\sigma),\tilde{H}^{1/2}(\sigma)} - \int_\sigma h^- \overline{u^0_-} + \int_\sigma \frac{|h^-|^2}{\lambda^+ + \lambda^-} \\
&\geq \Re\left(\int_{B_R\setminus\bar{\sigma}} |\nabla u^0|^2 + \kappa^2 \int_{B_R\setminus\bar{\sigma}} |u^0|^2 + \int_\sigma \frac{|h^-|^2}{\lambda^+ + \lambda^-}\right) \\
&\geq \left(\|u^0\|^2_{H^1(B_R\setminus\bar{\sigma})} + \|h^-\|^2_{L^2(\sigma)}\right)
\end{aligned}$$

The variational solution u^0 of (4.34) satisfies

$$\left\{\begin{array}{lcll}
\Delta u^0 - \kappa^2 u^0 & = & 0 & \text{in } B_r \setminus \overline{\sigma} \\
\partial_\nu u^0_+ & = & h^+ & \text{on } \sigma \\
\partial_\nu u^0_- & = & (h^+ - h^-) & \text{on } \sigma \\
\partial_\nu u^0 - T_R(u^0) & = & 0 & \text{on } S_R
\end{array}\right. \quad (4.35)$$

Moreover, from the continuity of the trace application and the fact that $\Delta u^0 \in L^2(B_R \setminus \bar{\sigma})$ so we have

$$\begin{aligned}
\|\partial_\nu u^0\|^2_{H^{-1/2}(\sigma)} &\leq K(\|\Delta u^0\|^2_{L^2(B_R\setminus\bar{\sigma})} + \|\nabla u^0\|^2_{L^2(B_R\setminus\bar{\sigma})}) \\
&\leq K(\kappa^2\|u^0\|^2_{L^2(B_R\setminus\bar{\sigma})} + \|\nabla u^0\|^2_{L^2(B_R\setminus\bar{\sigma})}) \\
&\leq K'\|u^0\|^2_{H^1(B_R\setminus\bar{\sigma})}
\end{aligned}$$

Consequently

$$\|h^+\|^2_{H^{-1/2}(\sigma)} \leq K'\|u^0\|^2_{H^1(B_R\setminus\bar{\sigma})}$$

Finally, we have

$$\langle (h^+,h^-), T_2^c(h^+,h^-)\rangle \geq K_0(||h^+||^2_{H^{-1/2}(\sigma)} + ||h^-||^2_{L^2(\sigma)})$$

Moreover, the operator $T_2^K = T_2 - T_2^c$ is a compact operator. In fact,

$$\begin{array}{rccl} T_2^K: & H_2 & \to & H_2^* \\ & (h^+,h^-) & \mapsto & (-[w], -\dfrac{2i\Im(\lambda^+)}{\overline{\lambda^+ + \lambda^-}}w_+ - \dfrac{2i\Im(\lambda^-)}{\overline{\lambda^+ + \lambda^-}}w_- - w_-) \end{array} \tag{4.36}$$

with $w = \tilde{u}^s - u^0$ and u^0 solution of (4.34). Hence we have

$$A(u^0, v) = l(v) \tag{4.37}$$

$$A(\tilde{u}^s, v) + B(\tilde{u}^s, v) = l(v) \tag{4.38}$$

where

$$A(\tilde{u}^s, v) = \int_{B_R\setminus\bar{\sigma}} \nabla\tilde{u}^s\nabla\bar{v} + \kappa^2 \int_{\mathbf{R}^2\setminus\sigma} \tilde{u}^s\bar{v} - \langle T_R\tilde{u}^s, v\rangle$$

$$B(\tilde{u}^s, v) = -2\kappa^2 \int_{B_R\setminus\bar{\sigma}} \tilde{u}^s\bar{v} + \int_\sigma \lambda^- \tilde{u}^s_- \overline{v_-} - \int_\sigma \lambda^+ \tilde{u}^s_+ \overline{v_+}$$

$$l(v) = -\left\langle h^+, [v]\right\rangle_{H^{-1/2}(\sigma), \tilde{H}^{1/2}(\sigma)} - \int_\sigma h^- \overline{v_-}$$

(4.65)-(4.64) give:

$$A(w, v) = -B(\tilde{u}^s, v)$$

Using the fact that $\tilde{u}^s$ depends continuously on the boundary data we have

$$\|\tilde{u}^s\|_{H^1(B_R\setminus\bar{\sigma})} \leq K(\|h^+\|_{H^{-1/2}(\sigma)} + \|h^-\|_{L^2(\sigma)}) \tag{4.39}$$

Let $(h_n)_{n\in\mathbf{N}}$ be a bounded sequence in H_2 and let us prove the existence of a subsequence $(h_{\varphi_n})_n$ such that

$$\text{If} \qquad h_{\varphi_n} \rightharpoonup h \qquad \text{Then} \qquad T_2^K(h_{\varphi_n}) \longrightarrow T_2^K(h)$$

Using the fact that $(h_n)_{n\in\mathbf{N}}$ is a bounded sequence, then $\tilde{u}^s$ is also a bounded sequence on the Hilbert space $H^1(B_R \setminus \bar{\sigma})$, so we can extract a subsequence $(\tilde{u}^s_{\varphi_n})_n$ such that

$$\tilde{u}^s_{\varphi_n} \rightharpoonup \tilde{u}^s \qquad \text{on } H^{1/2}(\sigma) \tag{4.40}$$

$$\tilde{u}^s_{\varphi_n} \rightharpoonup \tilde{u}^s \qquad \text{on } H^1(B_R \setminus \bar{\sigma}) \tag{4.41}$$

As the injection $H^{1/2}(\sigma) \hookrightarrow L^2(\sigma)$ is compact then

$$\tilde{u}^s_{\varphi_n} \longrightarrow \tilde{u}^s \qquad \text{on } L^2(\sigma) \tag{4.42}$$

$$\tilde{u}^s_{\varphi_n} \longrightarrow \tilde{u}^s \qquad \text{on } L^2(B_R \setminus \bar{\sigma}) \tag{4.43}$$

On the other hand,we have

$$\|A(w,v)\| = \|B(\tilde{u}^s, v)\|$$

and we have

$$\|B(u,w)\| \leq K_1(\|\tilde{u}^s\|_{L^2(\sigma)} + \|\tilde{u}^s\|_{L^2(B_R\setminus\bar{\sigma})})\|w\|_{H^1(B_R\setminus\bar{\sigma})}$$

Using the coercivity of $\|A(.,.)\|$, hence we

$$\|w\|_{H^1(\mathbf{R}^2\setminus\sigma)} \leq K_2(\|\tilde{u}^s\|_{L^2(\sigma)} + \|\tilde{u}^s\|_{L^2(B_R\setminus\bar{\sigma})}) \tag{4.44}$$

Hence $(w_n)_n$ is a bounded sequence on $H^1(B_R\setminus\bar{\sigma})$, so we can extract a subsequence $(w_{\varphi n})_n$ such that

$$w_{\varphi_n} \rightharpoonup w \qquad \text{on } H^1(B_R\setminus\bar{\sigma})$$

Using the continuity of the operator A and B

$$B(\tilde{u}^s_{\varphi_n}, v) \longrightarrow B(\tilde{u}^s, v) \tag{4.45}$$
$$A(w_{\varphi_n}, v) \longrightarrow A(w, v) \tag{4.46}$$

and using (4.44), we have

$$\|w_n - w\|_{H^1(B_R\setminus\bar{\sigma})} \leq K_2(\|\tilde{u}^s_n - \tilde{u}^s\|_{L^2(\sigma)} + \|\tilde{u}^s_n - \tilde{u}^s\|_{L^2(B_R\setminus\bar{\sigma})}) \tag{4.47}$$

Finally, we can deduce that

$$w_{\varphi_n} \longrightarrow w \qquad \text{on } H^1(B_R\setminus\bar{\sigma})$$

□

Lemma 24. *For all $(h^+,h^-)\in H_2$, where $H_2 = H^{-1/2}(\sigma)\times L^2(\sigma)$ such that $(h^+,h^-)\neq 0$ we have*

$$\Im\left\langle (h^+,h^-), T_2(h^+,h^-)\right\rangle < 0$$

Proof. In fact, we note that solving (4.25) is equivalent to solve the following variational problem.
Find $\tilde{u}^s \in H^1(B_R\setminus\bar{\sigma})$ verifying for all $v\in H^1(B_R\setminus\bar{\sigma})$

$$\int_{B_R\setminus\bar{\sigma}} \nabla\tilde{u}^s\overline{\nabla v} - \kappa^2\int_{B_R\setminus\bar{\sigma}} \tilde{u}^s\bar{v} - \int_\sigma \lambda^-\tilde{u}^s_-\overline{v_-} - \int_\sigma \lambda^+\tilde{u}^s_+\overline{v_+} - \left\langle T_R(\tilde{u}^s_{|S_R}), v\right\rangle = -\left\langle h^+, [v]\right\rangle_{H^{-1/2}(\sigma),\tilde{H}^{1/2}(\sigma)} - \int_\sigma h^-\overline{v_-}.$$

On the other hand, let $(h^+, h^-) \in H_2$

$$\left\langle (h^+,h^-), T_2(h^+,h^-)\right\rangle = -\left\langle h^+, [\tilde{u}^s]\right\rangle_{H^{-1/2}(\sigma),\tilde{H}^{1/2}(\sigma)} + \int_\sigma \frac{|h^-|^2}{\lambda^+ + \lambda^-} - \int_\sigma \frac{2i\Im(\lambda^+)h^-}{\lambda^+ + \lambda^-}\overline{\tilde{u}^s_+} - \int_\sigma h^- \frac{\lambda^+ + \bar{\lambda}^-}{\lambda^+ + \lambda^-}\overline{\tilde{u}^s_-}.$$

Hence

$$\left\langle (h^+,h^-), T_2(h^+,h^-)\right\rangle = -\left\langle h^+, [\tilde{u}^s]\right\rangle_{H^{-1/2}(\sigma),\tilde{H}^{1/2}(\sigma)} - \int_\sigma h^-\overline{\tilde{u}^s_+} + \int_\sigma \frac{|h^-|^2}{\lambda^+ + \lambda^-} - \int_\sigma \frac{2i\Im(\lambda^+)h^-}{\lambda^+ + \lambda^-}\overline{\tilde{u}^s_+} - \int_\sigma \frac{2i\Im(\lambda^-)h^-}{\lambda^+ + \lambda^-}\overline{\tilde{u}^s_-}$$

Therefore using the variational formulation of (ICP) we have

$$\left\langle (h^+,h^-), T_2(h^+,h^-)\right\rangle = \int_{B_R\setminus\bar{\sigma}} |\nabla\tilde{u}^s|^2 - \kappa^2\int_{B_R\setminus\bar{\sigma}} |\tilde{u}^s|^2 - \int_\sigma \lambda^-|\tilde{u}^s_-|^2 - \int_\sigma \lambda^+|\tilde{u}^s_+|^2 - \langle T_R\tilde{u}^s, \tilde{u}^s\rangle_{S_R} + \int_\sigma \frac{|h^-|^2}{\lambda^+ + \lambda^-} - \int_\sigma \frac{2i\Im(\lambda^+)h^-}{\lambda^+ + \lambda^-}\overline{\tilde{u}^s_+} - \int_\sigma \frac{2i\Im(\lambda^-)h^-}{\lambda^+ + \lambda^-}\overline{\tilde{u}^s_-}$$

Consequently

$$\Im\left\langle (h^+,h^-), T_2(h^+,h^-)\right\rangle = -\int_\sigma \Im(\lambda^-)|\tilde{u}^s_-|^2 - \int_\sigma \Im(\lambda^+)|\tilde{u}^s_+|^2 - \Im\left\langle T_R\tilde{u}^s, \tilde{u}\right\rangle_{S_R} + \int_\sigma \frac{\Im(\overline{\lambda^+ + \lambda^-})|h^-|^2}{|\lambda^+ + \lambda^-|^2} - \int_\sigma 2\Im(\lambda^+)\Re(\frac{h^-}{\lambda^+ + \lambda^-}\overline{\tilde{u}^s_+}) - \int_\sigma 2\Im(\lambda^-)\Re(\frac{h^-}{\lambda^+ + \lambda^-}\overline{\tilde{u}^s_-})$$

Finally we have

$$\Im\left\langle (h^+,h^-), T(h^+,h^-)\right\rangle = -\int_\sigma \Im(\lambda^-)\left|\tilde{u}^s_- + \frac{h^-}{\lambda^+ + \lambda^-}\right|^2 - \Im\left\langle T_R(\tilde{u}^s), \tilde{u}^s\right\rangle_{S_R} - \int_\sigma \Im(\lambda^+)\left|\tilde{u}^s_+ + \frac{h^-}{\lambda^+ + \lambda^-}\right|^2$$

Using the fact that

$$\Im\left\langle (h^+,h^-), T_2(h^+,h^-)\right\rangle = -\left\langle (h^+,h^-), \Im T(h^+,h^-)\right\rangle,$$

we prove finally that $\Im T_2$ is non negative.
Now suppose that $\Im\left\langle (h^+,h^-), T_2(h^+,h^-)\right\rangle = 0$ then we have

$$\Im\left\langle T_R(\tilde{u}^s), \tilde{u}^s\right\rangle = 0$$

Hence, $(\partial_\nu\tilde{u}^s, \tilde{u}^s) = (0,0)$ on S_R. Then, by using the unique continuation principle (see Corollary 13), $\tilde{u}^s$ vanishes on $B_R \setminus \bar{\sigma}$ consequently $(h^+, h^-) = (0,0)$. □

Lemma 25. *Assume that* $(\lambda^+ + \lambda^-)^{-1} \in L^\infty(\sigma)$. *The operator* $\mathcal{H}_2^*$ *defined by (4.28) is one to one and has a dense range.*

Proof. Let $(\alpha, \beta) \in H_2^*$ such that $\mathcal{H}_2^*(\alpha, \beta) = 0$. We note that $\mathcal{H}_2^*$ is the far field pattern of the potential

$$\gamma^{-1} V(z) = \int_\sigma (-\alpha(y)\partial_{\nu(y)}\Phi(x,y) + (\overline{\lambda^+}\alpha(y) - (\overline{\lambda^+ + \lambda^-})\beta(y))\Phi(x,y))ds(y),$$

for $z \in \mathbf{R}^m \setminus \bar{\sigma}$, where $\gamma = \frac{e^{i\pi/4}}{\sqrt{8k\pi}}, \frac{1}{4\pi}$ respectively for $m = 2$ and $m = 3$. This function is well defined in $\mathbf{R}^m \setminus \bar{\sigma}$ since the kernel of the double and the single layer potential are respectively defined on $\tilde{H}^{1/2}(\sigma)$ and $\tilde{H}^{-1/2}(\sigma)$. Moreover, $V \in H^1_{loc}(\mathbf{R}^m \setminus \bar{\sigma})$ satisfies the Helmholtz equation and the Sommerfeld radiation condition.
Therefore, if $\mathcal{H}_2^*(\alpha, \beta) = 0$, the far field of V is zero and from Rellich's lemma and the unique continuation principle (see Corollary 13), we conclude that $V = 0$ in $\mathbf{R}^m \setminus \bar{\sigma}$. then by the jump relations of the layer potentials, we have $[V] = -\alpha$ and $[\partial_\nu V] = -\overline{\lambda^+}\alpha(y) + (\overline{\lambda^+ + \lambda^-})\beta(y)$. This implies that

$$\alpha = 0 \qquad \text{and} \qquad -\overline{\lambda^+}\alpha(y) + (\overline{\lambda^+ + \lambda^-})\beta(y) = 0.$$

Finally, since by assumption $(\lambda^+ + \lambda^-)^{-1} \in L^\infty(\sigma)$, $\alpha = \beta = 0$ and that proves that $\mathcal{H}^*$ is one to one.
In the aim to prove the density of the range of the operator $\mathcal{H}^*{}_2$, we should prove the injectivity of his adjoint $\mathcal{H}_2$.
Let $g \in L^2(S^{m-1})$ be an element of the kernel of $\mathcal{H}_2$. Then,

$$(-\partial_\nu + \lambda^+)v_g = 0 \qquad \text{and} \qquad (\lambda^+ + \lambda^-)v_g = 0 \qquad \text{on} \quad \sigma.$$

Since by assumption $(\lambda^+ + \lambda^-)^{-1} \in L^\infty(\sigma)$ then $v_g = 0$ and $\partial_\nu v_g = 0$ on $\sigma_0 \subset \sigma$. From the unique continuation principle it implies that $v_g = 0$ in $\mathbf{R}^m$ and therefore $g = 0$ which proves that $\mathcal{H}_2$ is one to one and consequently the density of the range of $\mathcal{H}_2^*$. □

Lemma 26. *For any smooth non intersecting arc* L *and functions* $\alpha_L \in \tilde{H}^{\frac{1}{2}}(L)$, $\beta_L \in \tilde{H}^{-\frac{1}{2}}(L)$, *the operator* Φ_L^∞ *given by (4.13) belongs to* $R(\mathcal{H}_2^*)$ *the range of* $\mathcal{H}_2^*$ *if and only* $L \subset \sigma$.

Proof. First assume that $L \subset \sigma$. Since $\tilde{H}^{1/2}(L) \subset \tilde{H}^{1/2}(\sigma)$ and $L^2(L) \subset L^2(\sigma)$, it follows from the expression of Φ_L^∞ and $\mathcal{H}^*{}_2$ that $\Phi_L^\infty(\hat{x}) \in R(\mathcal{H}^*{}_2)$.

Now let $L \not\subset \sigma$ and assume, on the contrary, that $\Phi_L^\infty \in R(\mathcal{H}^*{}_2)$. Hence, there exists $\varphi \in \tilde{H}^{1/2}(\sigma)$ and $\psi \in \tilde{L}^2(\sigma)$ such that

$$\Phi_L^\infty(\hat{x}) = \gamma \int_L \left(-\varphi(y)\frac{\partial e^{-i\kappa\hat{x}\cdot y}}{\partial\nu(y)} + (\overline{\lambda^+}\varphi(y) - \overline{(\lambda^+ + \lambda^-)}\psi(y))e^{-i\kappa\hat{x}\cdot y}(y) \right) ds(y).$$

Thus Φ_L^∞ is the far field pattern of the potential

$$P(x) = \int_\sigma \left(-\varphi(y) \frac{\partial \Phi(x,y)}{\partial \nu(y)} + (\overline{\lambda^+}\varphi(y) - \overline{(\lambda^+ + \lambda^-)}\psi(y))\Phi(x,y) \right) ds(y), \quad x \in \mathbf{R}^m \setminus \overline{\sigma}.$$

Since by definition Φ_L^∞ is also the far field pattern of the potential Φ_L given by

$$\Phi_L(x) = \int_L (\alpha(y)\partial_{\nu(y)}\Phi(x,y) + \beta(y)\Phi(x,y))ds(y) \qquad \text{for all} \quad x \in \mathbf{R}^m \setminus L \tag{4.48}$$

then using the Rellich lemma and the unique continuation principle (see Corollary 13), the potentials Φ_L and P coincide in $R^{m-1} \setminus (\bar{\sigma} \cup \bar{L})$.
Let $x_0 \in L \backslash \overline{\sigma}$ and B_ϵ a small neighborhood of x_0 with $B_\epsilon \cap \sigma = \emptyset$. Then, P is analytic in B_ϵ while Φ_L and his normal derivative is not continuous on L due to the non continuity of the trace of the double layer potential and the trace of the derivative of the single layer potential present on the expression of Φ_L which is a contradiction. This proves that $\Phi_L^\infty \notin R(\mathcal{H}_2^*)$.

□

4.6 Analysis of the factorization (4.24)

We recall that the problem of the natural factorization consists on the choice of the space on which the operator T_1 is defined. The main idea is to find a special space H_1 such that $T_1 : H_1 \to H_1^*$ defined as in (4.21) should be an isomorphism. To this aim let us express T_1 in function of $g^\pm$. it follows

$$T_1(g^+, g^-) = \left(T_1^1(g^+,\ g^-),\ T_1^2(g^+,\ g^-) \right) \tag{4.49}$$

where

$$T_1^1(g^+,\ g^-) \ = \ \frac{(g^+ - g^-)}{\overline{\lambda^+ + \lambda^-}} - \frac{2i\Im(\lambda^-)}{\overline{\lambda^+ + \lambda^-}}\tilde{u}_-^s - \frac{\lambda^+ + \overline{\lambda^-}}{\overline{\lambda^+ + \lambda^-}}\tilde{u}_+^s \tag{4.50}$$

and

$$T_1^2(g^+,\ g^-) \ = \ -\frac{(g^+ - g^-)}{\overline{\lambda^+ + \lambda^-}} + \frac{\overline{\lambda^+} + \lambda^-}{\overline{\lambda^+ + \lambda^-}}\tilde{u}_-^s + \frac{2i\Im(\lambda^+)}{\overline{\lambda^+ + \lambda^-}}\tilde{u}_+^s \tag{4.51}$$

In fact, using the boundary conditions we have

$$[\partial_\nu \tilde{u}^s] + \lambda^+ \tilde{u}_+^s + \lambda^- \tilde{u}_-^s = (g^+ - g^-) \tag{4.52}$$

By replacing the expression of $[\partial_\nu \tilde{u}^s]$ respectively in the expression of T_1^1 and T_1^2 given by (4.54)and (4.53) by (4.52) we have

$$\begin{aligned} T_1^1(g^+,\ g^-) &= \frac{1}{\overline{\lambda^+ + \lambda^-}}[\partial_\nu \tilde{u}^s] - \frac{\overline{\lambda^-}}{\overline{\lambda^+ + \lambda^-}}[\tilde{u}^s] \\ &= \frac{1}{\overline{\lambda^+ + \lambda^-}}\left[(g^+ - g^-) - \lambda^+\tilde{u}_+^s - \lambda^-\tilde{u}_-^s - \overline{\lambda^-}\tilde{u}_+^s + \overline{\lambda^-}\tilde{u}_-^s\right] \\ &= \frac{(g^+ - g^-)}{\overline{\lambda^+ + \lambda^-}} - \frac{2i\Im(\lambda^-)}{\overline{\lambda^+ + \lambda^-}}\tilde{u}_-^s - \frac{\lambda^+ + \overline{\lambda^-}}{\overline{\lambda^+ + \lambda^-}}\tilde{u}_+^s \end{aligned} \tag{4.53}$$

and

$$\begin{aligned} T_1^2(g^+,\ g^-) &= -\frac{1}{\overline{\lambda^+ + \lambda^-}}[\partial_\nu \tilde{u}^s] - \frac{\overline{\lambda^+}}{\overline{\lambda^+ + \lambda^-}}[\tilde{u}^s] \\ &= -\frac{1}{\overline{\lambda^+ + \lambda^-}}\left[(g^+ - g^-) - \lambda^+\tilde{u}_+^s - \lambda^-\tilde{u}_-^s + \overline{\lambda^+}\tilde{u}_+^s - \overline{\lambda^+}\tilde{u}_-^s\right] \\ &= -\frac{(g^+ - g^-)}{\overline{\lambda^+ + \lambda^-}} + \frac{\overline{\lambda^+} + \lambda^-}{\overline{\lambda^+ + \lambda^-}}\tilde{u}_-^s + \frac{2i\Im(\lambda^+)}{\overline{\lambda^+ + \lambda^-}}\tilde{u}_+^s \end{aligned} \tag{4.54}$$

From the expressions (4.54) and (4.53) of T_1. In this case, $T_1(g^+, g^-)$ will be in $\mathcal{X}$ where

$$\mathcal{X} := \left\{(f^+, f^-) \in (L^2(\sigma))^2 :\ f^+ + f^- \in \tilde{H}^{1/2}(\sigma)\right\}$$

with

$$\|f\|_{\mathcal{X}} = \|f^+\|_{L^2(\sigma)} + \|f^-\|_{L^2(\sigma)} + \|f^+ + f^-\|_{H^{1/2}(\sigma)} \tag{4.55}$$

We define

$$H_1 := \left\{(g^+, g^-) \in (H^{-1/2}(\sigma))^2 :\ g^+ - g^- \in L^2(\sigma)\right\}$$

with

$$\|g\|_{H_1} = \|g^+\|_{\tilde{H}^{-1/2}(\sigma)} + \|g^-\|_{H^{-1/2}(\sigma)} + \|g^+ - g^-\|_{L^2(\sigma)} \tag{4.56}$$

We have the following theorem.

Theorem 27. *The space H_1 is the dual space of $H_1^* = \mathcal{X}$ with the dual product $\langle ., . \rangle_{H_1, H_1^*}$ defined by :*

$$\langle g, f\rangle_{H_1, H_1^*} := \left\langle g^+, (f^+ + f^-)\right\rangle_{H^{-1/2}(\sigma), \tilde{H}^{1/2}(\sigma)} - \left\langle (g^+ - g^-), f^-\right\rangle_{L^2(\sigma), L^2(\sigma)},$$

for all $(g, f) \in H_1 \times H_1^*$.

Proof. • Let $f \in \mathcal{X}$ and θ be the linear application defined on H_1 by

$$\theta : g \to \mathcal{R}(g, f) \tag{4.57}$$

where $\mathcal{R}$ is the application given by

$$\mathcal{R}(g,f) := \left\langle g^+, (f^+ + f^-)\right\rangle_{H^{-1/2}(\sigma),\tilde{H}^{1/2}(\sigma)} - \left\langle (g^+ - g^-), f^-\right\rangle_{L^2(\sigma),L^2(\sigma)},$$

It is clear that $\mathcal{R}$ is a bilinear and continuous application satisfying

$$\mathcal{R}(g,f) \leq \|g\|_{H_1} + \|f\|_{\mathcal{X}}, \qquad \forall (f,g) \in H_1 \times \mathcal{X}$$

Consequently, θ is a linear and continuous application in H_1. On the other hand $f \in \mathcal{X}$, hence $f \in L^2(\sigma) \times L^2(\sigma)$. Using Riesz Theorem we have

$$f \equiv \theta' : \tilde{g} \to \int_\sigma \tilde{g}^+ \overline{f^+} + \int_\sigma \tilde{g}^- \overline{f^-}, \qquad \forall (\tilde{g}^+, \tilde{g}^-) \in L^2(\sigma) \times L^2(\sigma) \tag{4.58}$$

Moreover, for f and $\tilde{g}$ in $(L^2(\sigma))^2$, we can identify the dual product on $\langle ., . \rangle_{H^{-1/2} \times \tilde{H}^{1/2}}$ with the scalar product in $L^2(\sigma)$ and consequently

$$\mathcal{R}(f,\tilde{g}) = \int_\sigma \tilde{g}^+ \overline{f^+} + \int_\sigma \tilde{g}^- \overline{f^-}.$$

Then we have $\tilde{\theta}(\tilde{g}) = \theta(\tilde{g})$ for all $\tilde{g}^\pm \in L^2(\sigma)$. Using the fact that $L^2(\sigma) \times L^2(\sigma)$ is dense in H_1 and (4.58), there exists a linear and continuous application $\tilde{f}$ defined on H_1 such that $\tilde{f} = f$ in $L^2(\sigma) \times L^2(\sigma)$ hence $\tilde{f} \in H_1^*$ which proves that $\mathcal{X} \subset H_1^*$

- Let $l \in H_1^*$, then l is a linear and continuous application on H_1:

$$|l(g)| \leq C(\|\tilde{g}^+\|_{H^{-1/2}(\sigma)} + \|\tilde{g}^+ - \tilde{g}^-\|_{L^2(\sigma)}), \qquad \forall (\tilde{g}^+, \tilde{g}^-) \in H_1^*.$$

We have an equivalence between the norm given by (4.56) and the right hand side of the previous inequality. Let $(h^+, h^-) = (\tilde{g}^+, \tilde{g}^+ - \tilde{g}^-)$. We define the linear application $\tilde{l}$

$$\tilde{l} : (h^+, h^-) \to l(h^+, h^-), \qquad \forall (h^+, h^-) \in H^{-1/2} \times L^2(\sigma)$$

$\tilde{l}$ is continuous, therefore $\tilde{l} \in (\tilde{H}^{-1/2} \times L^2(\sigma))^*$. Hence there exists $(\theta, \gamma) \in H^{1/2} \times L^2(\sigma)$ such that $\tilde{l} = (\theta, \gamma)$.
For $g^+ = h^+$ and $g^+ - g^- = h^-$ we have

$$\tilde{l}(h^+, h^-) = l(\tilde{g}^+, \tilde{g}^-)$$

which leads to

$$\tilde{l}(h^+, h^-) = l(\tilde{g}^+, \tilde{g}^-) = \left\langle \theta, \tilde{g}^+ \right\rangle_{\tilde{H}^{1/2}, H^{-1/2}} + \left\langle \gamma, \tilde{g}^+ - \tilde{g}^- \right\rangle_{L^2(\sigma)}$$

On the other hand $l \in H_1^*$, then $l \in L^2(\sigma) \times L^2(\sigma)$. Using Riez Theorem and the identification of $L^2(\sigma)$ to his dual, we have for all $(\tilde{g}^+, \tilde{g}^-) \in L^2(\sigma) \times L^2(\sigma)$

$$l(\tilde{g}^+, \tilde{g}^-) = \int_\sigma l^+ \tilde{g}^+ + \int_\sigma l^- \tilde{g}^- \tag{4.59}$$

Furthermore we have

$$l(\tilde{g}^+, \tilde{g}^-) = \int_\sigma (\theta + \gamma)\tilde{g}^+ + \int_\sigma (-\gamma)\tilde{g}^-. \tag{4.60}$$

By uniqueness we have

$$l^+ = \theta + \gamma \qquad \text{and} \qquad l^- = -\gamma$$

which proves that $l \in \mathcal{X}$.

□

It is easy to see that $T_1 : H_1 \to H_1^*$ continuous. The next step is to prove that T_1 is an isomorphism.

Lemma 28. *The operator $T_1 : H_1 \to H_1^*$ is an isomorphism.*

Proof. The operator T_1 can be decomposed as $T_1 = T_1^c + T_1^k$, where $T_1^c : H_1 \to H_1^*$ is a coercive operator defined by

$$T_1^c(g^+, g^-) = (\frac{(g^+ - g^-)}{\overline{\lambda^+ + \lambda^-}} - u_+^0, -\frac{(g^+ - g^-)}{\overline{\lambda^+ + \lambda^-}} + u_-^0), \tag{4.61}$$

where $u^0 \in H^1_{loc}(B_R \setminus \bar{\sigma})$ is the solution of

$$\int_{B_R\setminus\bar{\sigma}} \nabla\tilde{u}^s\overline{\nabla v} + \kappa^2 \int_{B_R\setminus\bar{\sigma}} \tilde{u}^s\bar{v} - \langle T_R\tilde{u}^s, v\rangle = -\left\langle g^+, [v]\right\rangle_{H^{-1/2},\tilde{H}^{1/2}} - \int_\sigma (g^+ - g^-)\overline{v_-} \tag{4.62}$$

Which is the "coercive part" of the variational formulation of (4.3). $T_1^K : H_1 \to H_1^*$ is the compact operator defined as follows

$$T_1^K(h^+, h^-) = (-\frac{2i\Im(\lambda^+)}{\overline{\lambda^+ + \lambda^-}}w_+ - \frac{2i\Im(\lambda^-)}{\overline{\lambda^+ + \lambda^-}}w_- - w_+, \frac{2i\Im(\lambda^+)}{\overline{\lambda^+ + \lambda^-}}w_+ + \frac{2i\Im(\lambda^-)}{\overline{\lambda^+ + \lambda^-}}w_- + w-) \tag{4.63}$$

with $w = \tilde{u}^s - u^0$ and u^0 solution of (4.62). Hence we have

$$A(u^0, v) = l(v) \tag{4.64}$$

$$A(\tilde{u}^s, v) + B(\tilde{u}^s, v) = l(v) \tag{4.65}$$

where

$$A(\tilde{u}^s, v) = \int_{B_R\setminus\bar{\sigma}} \nabla\tilde{u}^s\nabla\overline{v} + \kappa^2 \int_{B_R\setminus\bar{\sigma}} \tilde{u}^s\overline{v} - \langle T_R\tilde{u}^s, v\rangle \tag{4.66}$$

$$B(\tilde{u}^s, v) = -2\kappa^2 \int_{B_R\setminus\bar{\sigma}} \tilde{u}^s\overline{v} + \int_\sigma \lambda^-\tilde{u}_-^s\overline{v_-} - \int_\sigma \lambda^+\tilde{u}_+^s\overline{v_+}, \tag{4.67}$$

and

$$l(v) = -\left\langle g^+, [v]\right\rangle_{H^{-1/2},\tilde{H}^{1/2}} - \int_\sigma (g^+ - g^-)\overline{v_-}. \tag{4.68}$$

For the proof of the compactness of T_1^K and the coercivity of T_1^c, we proceed in the same way as in the proof of Theorem 23. Moreover T_1 is injective since if we have $T_1(g^+, g^-) = (0, 0)$ then from the expression of T_1 we deduce that

$$[\partial_\nu \tilde{u}^s] = \overline{\lambda^+}[\tilde{u}^s] \qquad \text{and} \qquad [\partial_\nu \tilde{u}^s] = \overline{\lambda^-}[\tilde{u}^s] \tag{4.69}$$

using the fact that $\lambda^+ \neq \lambda^-$ then we prove that

$$[\tilde{u}^s] = 0 \qquad \text{and} \qquad [\partial_\nu \tilde{u}^s] = 0$$

as $\tilde{u}^s$ is a solution of the Helmholtz equation satisfying the radiation condition then $\tilde{u}^s = 0$ in $\mathbf{R}^m$ and consequently $g^\pm = 0$.

□

Lemma 29. *For all $(g^+, g^-) \in H_1$, such that $(g^+, g^-) \neq 0$ we have*

$$\Im \left\langle (g^+, g^-), T_1(g^+, g^-) \right\rangle < 0$$

Proof. In fact, we note that solving (4.25) is equivalent to solve the following variational problem.
Find $\tilde{u}^s \in H^1(B_R \setminus \bar{\sigma})$ verifying for all $v \in H^1(B_R \setminus \bar{\sigma})$

$$\int_{B_R \setminus \bar{\sigma}} \nabla \tilde{u}^s \overline{\nabla v} - \kappa^2 \int_{B_R \setminus \bar{\sigma}} \tilde{u}^s \bar{v} - \int_\sigma \lambda^- \tilde{u}^s_- \overline{v_-} - \int_\sigma \lambda^+ \tilde{u}^s_+ \overline{v_+} - \langle T_R(\tilde{u}^s), v \rangle_{S_R} = - \left\langle g^+, [v] \right\rangle_{H^{-1/2}, \tilde{H}^{1/2}} - \int_\sigma (g^+ - g^-) \overline{v_-}.$$

On the other hand, let $(g^+, g^-) \in H_1$, using the expression of T_1 given in (4.49)

$$\left\langle (g^+, g^-), T_1(g^+, g^-) \right\rangle_{H_1, H_1^*} = - \left\langle g^+, [\tilde{u}^s] \right\rangle_{H^{-1/2}, \tilde{H}^{1/2}} + \int_\sigma \frac{|g^+ - g^-|}{\lambda^+ + \lambda^-} - \int_\sigma \frac{(g^+ - g^-)}{\lambda^+ + \lambda^-} (\lambda^+ + \overline{\lambda^-}) \overline{\tilde{u}^s_-} - \int_\sigma (g^+ - g^-) \frac{2i\Im(\lambda^+)}{\lambda^+ + \lambda^-} \overline{\tilde{u}^s_+}$$

Hence

$$\left\langle (g^+, g^-), T_1(g^+, g^-) \right\rangle_{H_1, H_1^*} = - \left\langle g^+, [\tilde{u}^s] \right\rangle_{H^{-1/2}, \tilde{H}^{1/2}} - \int_\sigma (g^+ - g^-) \overline{\tilde{u}^s_-} + \int_\sigma \frac{|g^+ - g^-|^2}{\lambda^+ + \lambda^-} - \int_\sigma (g^+ - g^-) \frac{2i\Im(\lambda^+)}{\lambda^+ + \lambda^-} \overline{\tilde{u}^s_+} + \int_\sigma (g^+ - g^-) \frac{2i\Im(\lambda^-)}{\lambda^+ + \lambda^-} \overline{\tilde{u}^s_-}$$

Consequently

$$\begin{aligned} \Im \left\langle (g^+, g^-), T_1(g^+, g^-) \right\rangle_{H_1, H_1^*} &= -\Im \langle T_R(\tilde{u}^s), \tilde{u}^s \rangle_{S_R} - \int_\sigma \Im(\lambda^+) |\tilde{u}^s_+|^2 - \int_\sigma \Im(\lambda^-) |\tilde{u}^s_-|^2 \\ &\quad - \int_\sigma \Im(\lambda^+ + \lambda^-) \frac{|g^+ - g^-|^2}{|\lambda^+ + \lambda^-|^2} - \int_\sigma 2\Im(\lambda^+) \Re \left(\frac{(g^+ - g^-)}{\lambda^+ + \lambda^-} \overline{\tilde{u}^s_+} \right) \\ &\quad + \int_\sigma 2\Im(\lambda^-) \Re \left(\frac{(g^+ - g^-)}{\lambda^+ + \lambda^-} \overline{\tilde{u}^s_-} \right) \end{aligned}$$

Finally

$$\Im\left\langle (g^+,g^-), T_1(g^+,g^-)\right\rangle_{H_1,H_1^*} = -\Im\left\langle T_R(\tilde{u}^s),\tilde{u}^s\right\rangle_{S_R} - \int_\sigma \Im(\lambda^+)\left|\frac{(g^+-g^-)}{\lambda^++\lambda^-}+\tilde{u}^s_+\right|^2 - \int_\sigma \Im(\lambda^-)\left|\frac{(g^+-g^-)}{\lambda^++\lambda^-}-\tilde{u}^s_-\right|^2.$$

□

Lemma 30. *Assume that* $(\lambda^+ + \lambda^-)^{-1} \in L^\infty$. *The operator* $\mathcal{H}_1^*$ *defined by (4.20) is one to one and has a dense range.*

For the proof of this theorem we proceed similar to the proof of Lemma 25.

Lemma 31. *For any smooth non intersecting arc* L *and functions* $\alpha_L \in \tilde{H}^{\frac{1}{2}}(L)$, $\beta_L \in \tilde{H}^{-\frac{1}{2}}(L)$, *the operator* Φ_L^∞ *given by (4.13) belongs to* $R(\mathcal{H}_1^*)$ *the range of* $\mathcal{H}_1^*$ *if and only* $L \subset \sigma$.

Proof. First assume that $L \subset \sigma$. Since $\tilde{H}^{1/2}(L) \subset \tilde{H}^{1/2}(\sigma)$ and $L^2(L) \subset L^2(\sigma)$, it follows from the expression of Φ_L^∞ and $\mathcal{H}^*{}_1$ that $\Phi_L^\infty(\hat{x}) \in R(\mathcal{H}_1^*)$.

Now let $L \not\subset \sigma$ and assume, on the contrary, that $\Phi_L^\infty \in R(\mathcal{H}_1^*)$. Hence, there exists $\varphi \in \tilde{H}^{1/2}(\sigma)$ and $\psi \in \tilde{L}^2(\sigma)$ such that

$$\Phi_L^\infty(\hat{x}) = -\gamma \int_L \left((\varphi(y)+\psi(y))\frac{\partial e^{-i\kappa\hat{x}\cdot y}}{\partial\nu(y)} + (\overline{\lambda^+}\varphi(y) - \overline{\lambda^-}\psi(y))e^{-i\kappa\hat{x}\cdot y}(y)\right) ds(y).$$

Thus Φ_L^∞ is the far field pattern of the potential

$$P(x) = -\int_\sigma \left(\varphi(y)\frac{\partial\Phi(x,y)}{\partial\nu(y)} + (\overline{\lambda^+}\varphi(y) - \overline{\lambda^-}\psi(y))\Phi(x,y)\right) ds(y), \quad x \in \mathbf{R}^m \setminus \overline{\sigma}.$$

Since by definition Φ_L^∞ is also the far field pattern of the potential Φ_L given by

$$\Phi_L(x) = \int_L (\alpha(y)\partial_{\nu(y)}\Phi(x,y) + \beta(y)\Phi(x,y))ds(y) \qquad \text{for all} x \in \mathbf{R}^m \setminus L \tag{4.70}$$

then using the Rellich lemma and the unique continuation principle (see Corollary 13), the potentials Φ_L and P coincide in $R^{m-1} \setminus (\bar{\sigma} \cup \bar{L})$.
Let $x_0 \in L\backslash\overline{\sigma}$ and B_ϵ a small neighborhood of x_0 with $B_\epsilon \cap \sigma = \emptyset$. Then, P is analytic in B_ϵ while Φ_L is not continuous on L due to the non continuity of the double layer potential present on the expression of Φ_L. which is a contradiction. This proves that $\Phi_L^\infty \notin R(\mathcal{H}_1^*)$.
□

4.7 Numerical algorithm and results

The numerical experiments are conducted in a 2 D setting of the problem. We consider n equally distant observation points of the far field $(\hat{x}_l)_{1\leq l\leq n}$ on the unit circle.

$$Fg(\hat{x}_l) \simeq \sum_{j=1}^{n} w_j u_\infty(\hat{x}_l, \hat{x}_j) g(\hat{x}_j) \tag{4.71}$$

where w_j is the arclengh between two adjacent points. Let L be a small segment of center z and with normal ν. Then

$$\Phi_L^\infty(\hat{x}_l) \simeq \gamma|L|(-ik\ \hat{x}_l.\nu\ \alpha(z) + \beta(z))e^{-ik\hat{x}_l z}$$

The discrete equation to solve is then

$$(F_\sharp)^{1/2} g_L(\hat{x}_l) \simeq \Phi_L^\infty(\hat{x}_l) \qquad \forall \hat{x}_l \tag{4.72}$$

Using a regularization by truncation, the solution of (4.72) is given by

$$\|g_L\|^2_{L^2(S^1)} \simeq \sum_{k=1}^{M} \frac{|\,(\Phi_L^\infty, \psi_k)_{L^2(S^1)}\,|^2}{\lambda_k} \tag{4.73}$$

where $\{\lambda_n, \psi_n\}_{n\in\mathbf{N}}$ is an eigensystem of the self-adjoint and positive operator $F_\sharp$ and M is a regularization parameter. We shall consider two types of solutions. The first one denoted by g_z corresponds to $\alpha(z) = 1$ and $\beta(z) = 0$ whereas the second one denoted by $g_{z,\nu}$ corresponds to $\alpha(z) = 0$ and $\beta(z) = 1$.
Let us also consider the two independent normals $\nu_1 = (0, 1)^t$ and $\nu_2 = (1, 0)^t$. We define the normal ν as follows

$$\nu = \zeta\nu_1 + \sqrt{1-\zeta^2}\nu_2$$

with $-1 \leq \zeta \leq 1$. Therefore, by linearity of the equation (4.72),

$$g_{z,\nu} = \zeta g_{z,\nu_1} + \sqrt{1-\zeta^2} g_{z,\nu_2}.$$

Hence according to Theorem Reftheoreme1, the normal ν to σ at $z \in \sigma$ corresponds to the value ζ that minimizes

$$\|g_{z,\nu}\|^2 = \zeta^2\|g_{z,\nu_1}\|^2 + (1-\zeta^2)\|g_{z,\nu_2}\|^2 + 2\zeta\sqrt{1-\zeta^2}\,\langle g_{z,\nu_1}\ , g_{z,\nu_2}\rangle\,. \tag{4.74}$$

The proposed criterion will be the determination on each point z of

$$z \to \frac{1}{\|g_z\|} + \frac{1}{\|g_{z,\nu}\|},$$

where $g_{z,\nu}$ corresponds with ζ that minimizes (4.74) . In Figures 4.1, 4.3 and 4.5 we show the efficiency of this algorithm for the reconstruction of cracks for different values of the impedance of different shapes type of the cracks in the vacuum, given by:

- (a) The union of two segments with respective peaks $(0, 0.8)$, $(0, 0)$ and $(0.4, -0.8)$,
- (b) An arc shape crack centered on $(-0.5, 0.5)$ with radius 0.75 and angle $\theta \in [0,\ \pi/2]$,
- (c) an L shape cracks with vertices $(0.75, 0), (0, 0)$ and $(0, 0.75)$,

Similar to the LSM case, we observe that a very good reconstruction of the crack is obtained when the impedance is relatively small or high. The case of impedances with "intermediate" values is less accurate but it still better than the result given by the LSM since we can see the exact shape of the crack. In general these observations are in concordance with the conclusions made in [14] for the case of the Linear Sampling Method, although better reconstructions are obtained using the Factorization method.

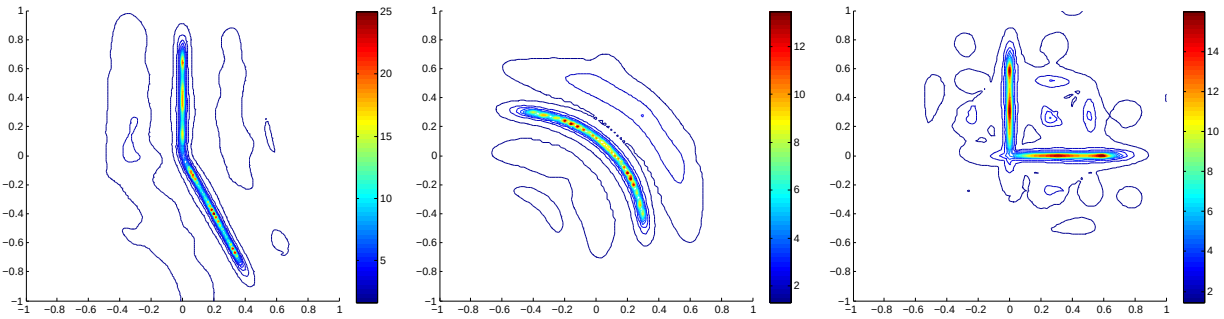

a)Crack reconstruction using the LSM

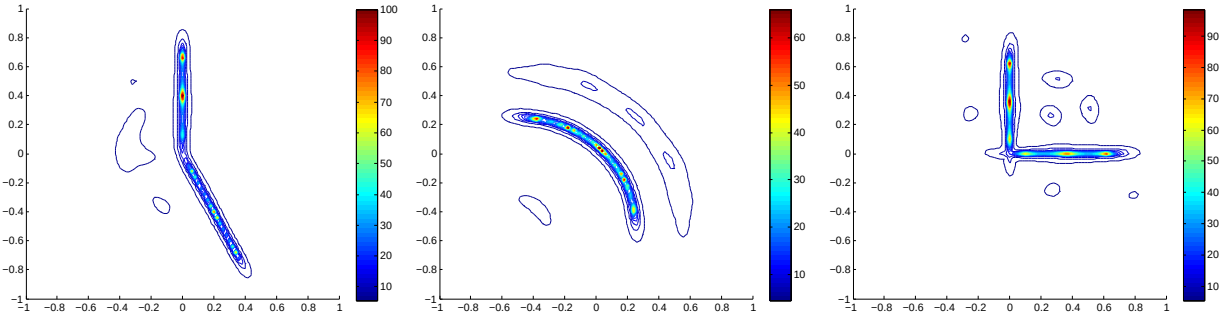

b)Crack reconstruction using the Factorization method

Figure 4.1: Reconstruction of cracks geometries type (a)(right), (b) (middle) and (c) (left) for $\lambda^- = \lambda^+ = 10^{-2}(1 + i)$ and the wave lenght $\lambda = 1$

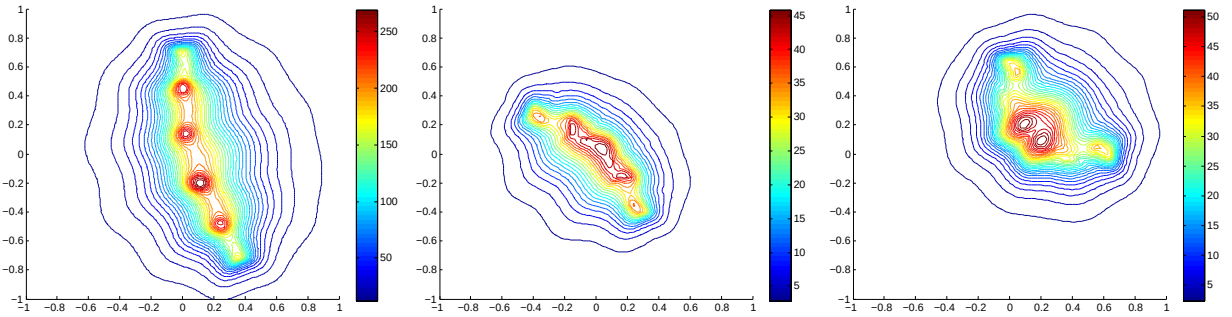

a)Crack reconstruction using the LSM

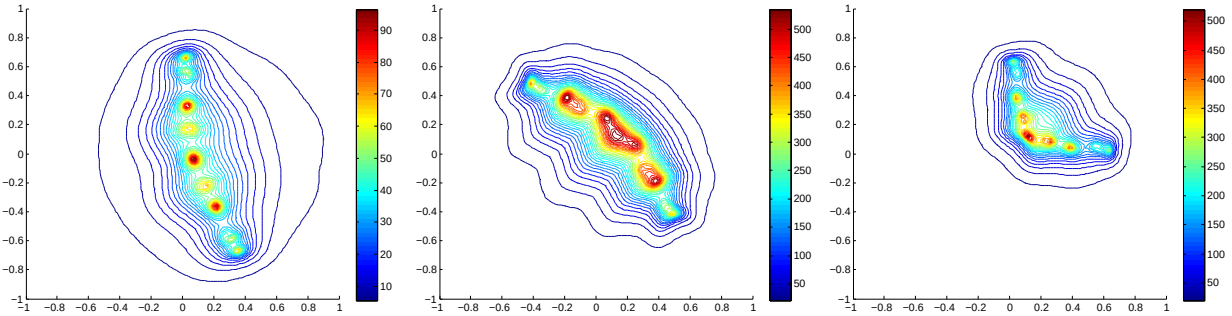

b)Crack reconstruction using the Factorization method

Figure 4.2: Reconstruction of cracks geometries type (a)(right), (b) (middle) and (c) (left) for $\lambda^- = \lambda^+ = 5 + 5i$.

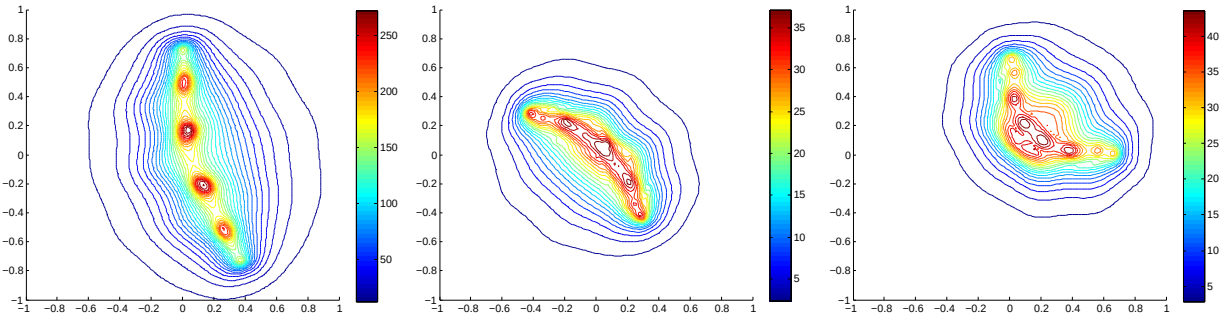

a)Crack reconstruction using the LSM.

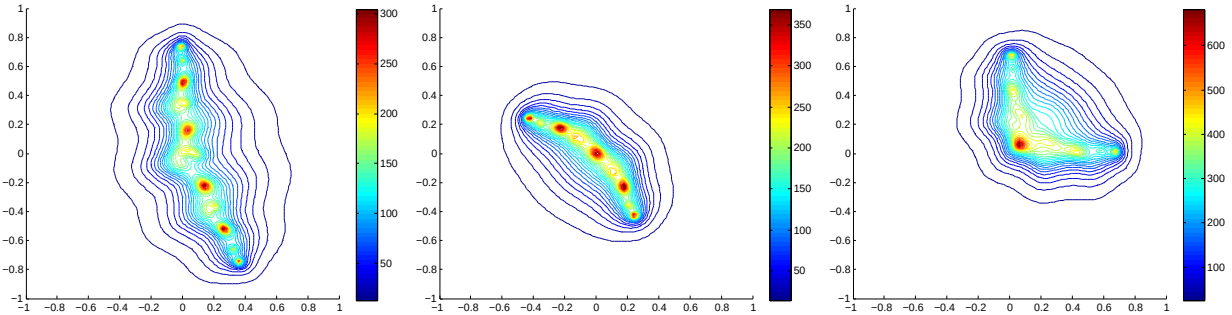

b)Crack reconstruction using the Factorization method

Figure 4.3: Reconstruction of cracks geometries type (a)(right), (b) (middle) and (c) (left) for $\lambda^- = \lambda^+ = 10 + 10i$.

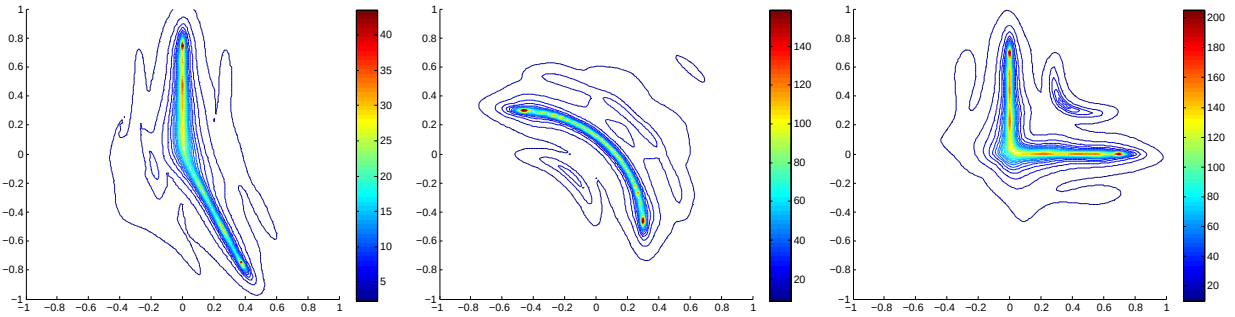

a)Crack reconstruction using the LSM

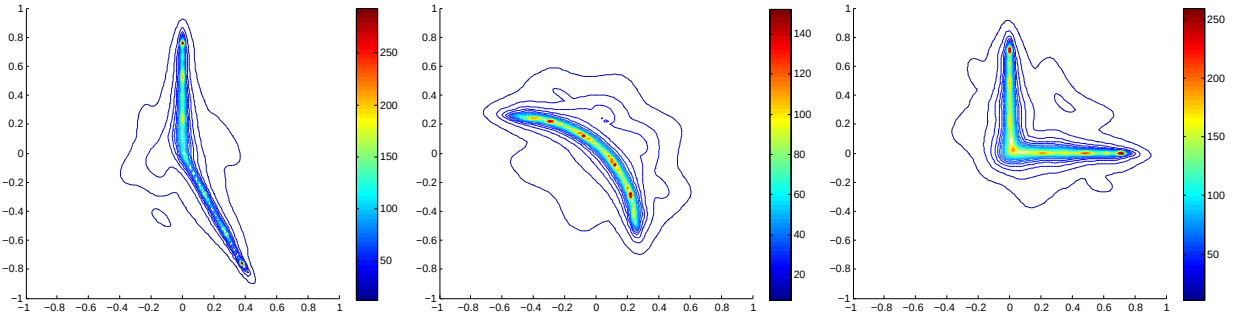

b)Crack reconstruction using the Factorization method

Figure 4.4: Reconstruction of cracks geometries type (a) (right), (b) (middle) and (c) (left) for $\lambda^- = \lambda^+ = 10^2(1+i)$.

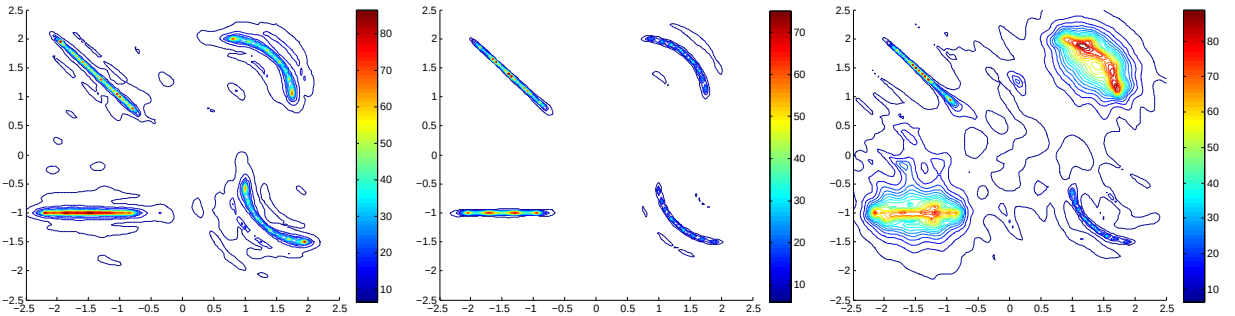

a)Crack reconstruction using the LSM

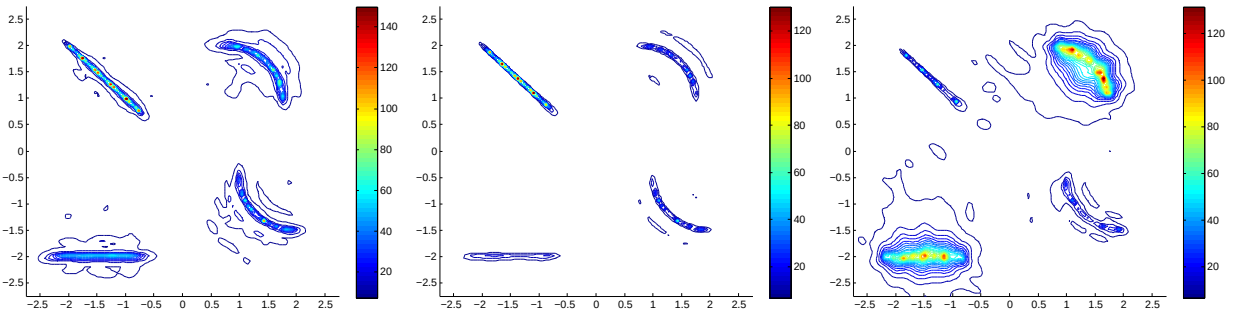

b)Crack reconstruction using the Factorization method

Figure 4.5: Reconstruction of multiple cracks for $\lambda_1^\pm = \lambda_2^\pm = \lambda_3^\pm = \lambda_4^\pm = 10^2(1+i)$(right), $\lambda_1^\pm = \lambda_2^\pm = \lambda_3^\pm = \lambda_4^\pm = 10^{-2}(1+i)$(middle) and $\lambda_1^\pm = \lambda_4^\pm = 10^{-2}$ and$\lambda_3^\pm = \lambda_2^\pm = 10(1+i)$ (left) .

Appendix: On the inf criterion

This criterion gives also an exact characterization of the crack using the special factorization of the far field operator $F = \mathcal{H}^* T \mathcal{H}$ and the coercivity of the operator T. Therefore, we don't need to prove different properties of this operators. The main advantage of this method is that the theoretical study is very simple but the principal drawback of this criterion is that it is very costly in the numerical implementation. This method is based on the following theorem

Theorem 32. *[53, Theorem 1.16, p19]*
Let X, Y be (complex) reflexive Bannach spaces with duals X^*, Y^* respectively, and dual forms $< .,. >$ in X, X^* and Y, Y^*. furthermore, let $F : Y^* \longrightarrow Y$ and $B : X \longrightarrow Y$ linear operator with $F = BAB^*$ for some linear operator $A : X \longrightarrow X^*$. Which satisfies a coercivity condition of the form : There exists $c > 0$ with

$$| \langle \varphi, A\varphi \rangle | \geq c ||\varphi||^2_{X^*} \qquad \text{for all} \quad \varphi \in R(B^*) \subset X^* \tag{4.75}$$

Then, for any $\varphi \in Y^*$, $\varphi \neq 0$

$$\varphi \in R(B) \qquad \text{if and only if} \qquad inf\{\| < \psi, F\psi > \| : \psi \in Y^*, < \psi, \varphi >= 1\} > 0. \tag{4.76}$$

Here again, $R(B)$ denotes the range of the operator $B : X \longrightarrow Y$. Furthermore, if $\varphi = B\varphi_0 \in R(B)$ for some $\varphi_0 \in X$ then

$$inf\{\| < \psi, F\psi > \| : \psi \in Y^*, < \psi, \varphi >= 1\} \geq \frac{c}{\|\varphi_0\|^2_X}. \tag{4.77}$$

In our case it is no simple to prove the coercivity of the operator T_2, to do so we introduce some modification on the [53, Lemma 1.17, p20] gives as follows

Lemma 33. *Let X be a reflexive Bannach space and $A, A_0 : X^* \longrightarrow X$ be linear and bounded operators such that*
$(i) \Im \langle \varphi, A\varphi \rangle \in \mathbf{R}^*$ for$\varphi \neq 0$ has the same sign with $\Im \langle \varphi, A_0\varphi \rangle$.
(ii) there exists $c_0 > 0$ such that

$$| \langle \varphi, A_0\varphi \rangle | \geq \|\varphi\|^2_{X^*} \qquad \text{for all} \qquad \varphi \in R(B^*) \tag{4.78}$$

$(iii) A - A_0$ is compact.
Then there exists $c > 0$ with

$$| \langle \varphi, A\varphi \rangle | \geq c ||\varphi||^2_{X^*} \qquad \text{for all} \qquad \varphi \in R(B^*) \subset X^* \tag{4.79}$$

Proof. Let suppose that we have $A_0,\ A$ two operators satisfying the three conditions $(i),(ii),(iii)$ and suppose that there no exists a constant with (4.79), then there exists a sequence$(\varphi_n)_{n\in\mathbf{N}} \subset R(\mathcal{H}^*)$, with $\|\varphi_n\|_{H^*} = 1$ and satisfying

$$\forall n \in \mathbf{N}, \qquad |\langle \varphi_n, A\varphi_n\rangle| < \frac{1}{n} \tag{4.80}$$

Hence

$$\langle \varphi_n, A\varphi_n\rangle \longrightarrow 0 \qquad \text{when} \qquad n \longrightarrow +\infty \tag{4.81}$$

Using the fact that $(\varphi_n)_{n\in\mathbf{N}}$ is a bounded sequence on a Hilbert space then there exists a subsequence $(\varphi_n)_{\psi_{n\in\mathbf{N}}}$ which converges weakly to some $\varphi \in R(\mathcal{H}^*)$.
On the other hand, by linearity we have

$$\langle \varphi-\varphi_n, A_0(\varphi-\varphi_n)\rangle = \langle \varphi_n, A_0(\varphi-\varphi_n)\rangle - \langle \varphi_n, (A_0-A)(\varphi-\varphi_n)\rangle + \langle \varphi_n, A\varphi_n\rangle - \langle \varphi_n, A\varphi\rangle \tag{4.82}$$

The operator $(A-A_0)$ is compact hence $(A-A_0)\varphi_n$ converges to $(A-A_0)\varphi$ and we have

$$\langle \varphi_n, (A-A_0)(\varphi-\varphi_n)\rangle \longrightarrow 0 \qquad \text{when} \qquad n \longrightarrow +\infty \tag{4.83}$$

Using the continuity of the operator A_0, and (4.81), (4.83)

$$\lim_{n\to+\infty} \langle \varphi-\varphi_n, A_0(\varphi-\varphi_n)\rangle = \langle \varphi, A\varphi\rangle \tag{4.84}$$

$$\Longrightarrow \lim_{n\to+\infty} \Im\langle \varphi-\varphi_n, A_0(\varphi-\varphi_n)\rangle = -\Im\langle \varphi, A\varphi\rangle \tag{4.85}$$

A_0 and A satisfy the condition (i), hence we have $\Im\langle \varphi, A\varphi\rangle = 0$ and $\varphi = 0$.
We have

$$\begin{aligned} |\langle \varphi-\varphi_n, A_0(\varphi-\varphi_n)\rangle| &\leq |\langle \varphi_n, A_0(\varphi-\varphi_n)\rangle| + |\langle \varphi_n, (A_0-A)(\varphi-\varphi_n)\rangle| \\ &+ |\langle \varphi_n, A\varphi_n\rangle| + |\langle \varphi_n, A\varphi\rangle| \end{aligned}$$

Using (ii) we have

$$\begin{aligned} \|\varphi-\varphi_n\|^2 &\leq |\langle \varphi_n, A_0(\varphi-\varphi_n)\rangle| + |\langle \varphi_n, (A_0-A)(\varphi-\varphi_n)\rangle| \\ &+ |\langle \varphi_n, A\varphi_n\rangle| + |\langle \varphi_n, A\varphi\rangle| \end{aligned}$$

Finally we have $\varphi_n \longrightarrow 0$ when $n \longrightarrow +\infty$ which contradicts the assumption $\|\varphi_n\|_{H^*} = 1$ □

Theorem 34. *For any smooth non intersecting arc L and functions $\alpha_L \in \tilde{H}^{\frac{1}{2}}(L)$ and $\beta_L \in \tilde{H}^{-1/2}(L)$ the following is true*

$$L \subset \sigma \qquad \textit{if and only if} \qquad inf\{\| < \psi, F\psi > \| : \psi \in Y^*, < \psi, \Phi_L^\infty >= 1\} > 0. \tag{4.86}$$

Proof. the proof of this theorem is proved using for the first factorization Lemma 31, Lemma 29 and the fact that $\Im\langle(g^+,g^-)^t,T_1(g^+,g^-)^t\rangle$ and $\Im\langle(g^+,g^-)^t,T_1^c(g^+,g^-)^t\rangle$ have both a positive sign. In fact we have

$$\begin{aligned}\Im\left\langle(g^+,g^-)^t,T_1^c(g^+,g^-)^t\right\rangle &= \Im(-\int_\sigma g^+\frac{\overline{g^+-g^-}}{\lambda^++\lambda^-}+\int_\sigma g^+\overline{u_+^0}+\int_\sigma g^-\frac{\overline{g^+-g^-}}{\lambda^++\lambda^-}-\int_\sigma g^-\overline{u_-^0})\\ &= \Im(-\int_\sigma\frac{|g^+-g^-|^2}{\lambda^++\lambda^-}+\int_\sigma g^+\overline{u_+^0}-\int_\sigma g^-\overline{u_-^0})\\ &= \int_\sigma\Im(\lambda^++\lambda^-)\frac{|g^+-g^-|^2}{|\lambda^++\lambda^-|^2}+\Im\left\langle T_Ru^0,u^0\right\rangle\end{aligned}$$

and T_1^c satisfy the condition (ii) of Lemma 33 and $T_1-T_1^c$ is compact, hence the operator T_1 is coercive such that there exists $c>0$ with

$$|\langle\varphi,T_1\varphi\rangle|\leq C\|\varphi\|^2_{H_1^*}\qquad\text{for all}\qquad\varphi\in R(\mathcal{H}_1^*)\tag{4.87}$$

Consequently

$$\Phi_L^\infty\in R(\mathcal{H}_1^*)\qquad\text{if and only}\qquad inf\{\|<\psi,F\psi>\|:\psi\in Y^*,<\psi,\Phi_L^\infty>=1\}>0.$$

For the second factorization using Lemma 26, Lemma 42 and the fact $\Im\langle(h^+,h^-)^t,T_2(h^+,h^-)^t\rangle$ and $\Im\langle(h^+,h^-)^t,T_2^c(h^+,h^-)^t\rangle$ have both a non positive sign since we have

$$\begin{aligned}\Im\left\langle(h^+,h^-)^t,T_2^c(h^+,h^-)^t\right\rangle &= \Im(-\int_\sigma h^+\overline{\tilde{u}_+^s}+\int_\sigma(h^+-h^-)\overline{\tilde{u}_-^s}+\int_\sigma\frac{|h^-|^2}{\lambda^++\lambda^-})\\ &= -\int_\sigma\Im(\lambda^+)|\tilde{u}_+^s|^2-\int_\sigma\Im(\lambda^-)|\tilde{u}_-^s|^2-\Im\left\langle T_R\tilde{u}^s,\tilde{u}^s\right\rangle\\ &\quad-\int_\sigma\frac{\Im(\lambda^++\lambda^-)}{|\lambda^++\lambda^-|^2}|h^-|^2\end{aligned}$$

and T_2^c satisfy the condition (ii) of Lemma 33 and $T_2-T_2^c$ is compact, hence the operator T_2 is coercive such that there exists $c>0$ with

$$|\langle\varphi,T_2\varphi\rangle|\leq C\|\varphi\|^2_{H_2^*}\qquad\text{for all}\qquad\varphi\in R(\mathcal{H}_2^*)\tag{4.88}$$

Finally, using Theorem 32 we prove that

$$\Phi_L^\infty\in R(\mathcal{H}_2^*)\qquad\text{if and only}\qquad inf\{\|<\psi,F\psi>\|:\psi\in Y^*,<\psi,\Phi_L^\infty>=1\}>0.$$

□

4.8 Conclusion

In this Chapter, we give an application of the Factorization method in the case of scattering by a crack with impedance boundary conditions in both side of the crack. This method is known to be simple since it gives a simple algorithm and it provides a simple formula for the characteristic function of the crack. From the numerical point of view, compared to the LSM both methods are equally simple and fast, but the numerical results in this chapter show that the Factorization method gives a reconstruction with a higher accuracy than that obtained using the LSM. Note that in the sampling process of the Factorization method we have used the same criterion to find a good approximation of the normal as in the LSM.

From the theoretical point of view, the justification of the Factorization is more complex than that of the LSM since a special factorization of the far field operator is needed and some properties of the operator used in the factorization should be proved. In the counterpart, the justification of the Factorization method is stronger than that of the LSM since an explicit function to characterize the crack is given. We have also proved in this chapter that we can use another criterion to reconstruct the crack, which is the inf criterion but we don't give numerical results in that case since they are difficult to generate. Note that both the LSM and the Factorization method have been applied in this thesis in the case of a homogeneous domain. In the case of an inhomogeneous domain the two methods are very costly since the Green function of the whole domain should be computed. To this end, we will apply in the next chapter the RG-LSM which is a qualitative method suitable to the case of an inhomogeneous domain without the need to compute the Green function of the domain.

CHAPTER 5

The case of an inhomogeneous background and RG-LSM algorithm

Contents

Abstract
We use the Reciprocity Gap-Linear Sampling Method (RG-LSM) to identify cracks with impedance boundary conditions. This is an extension of the work of F. Delbary [38] and the work of N. Zeev et al [85] that use the RG-LSM to reconstruct cracks by using several pairs of Cauchy data corresponding to near field electromagnetic or acoustic time harmonic measurements. The former has considered the case of sound soft cracks, whereas the latter has considered cracks with mixed boundary condition, a Dirichlet boundary condition in one side and an impedance boundary condition in the other side. An application of the RG-LSM for the case of a crack with impedance boundary condition is presented in this chapter and its performance is illustrated through some numerical examples

5.1 Introduction

This chapter is devoted to study the identification of cracks with an impedance boundary condition using the RG-LSM method. The RG-LSM algorithm has been first introduced by D. Colton and H. Haddar in [30] as a reformulation of the Linear Sampling Method for near-field measurements in an inhomogeneous domain by using the concept of reciprocity gap. The main advantage of this algorithm is to avoid the computation of the $\mathbf{R}^m$ background Green function if one assumes that Cauchy data is available on the boundary of homogeneous part containing the target (see experimental setting Figure 5.3.1). Moreover as a qualitative method, it does not require a priori knowledge of the physical properties of the scattering object. The RG-LSM is a coupling between the use of the reciprocity gap functional and the Linear Sampling Method. In fact, D. Colton and H. Haddar in [30] give a relation in the case of homogeneous domain between the farfield operator used in the study of the LSM, the reciprocity gap functional applied to the scattered field and a test function, that can be the Herglotz wave, on a boundary of a subdomain that contains the crack and with a constant index of a medium. As in the LSM, this method allows to retrieve the crack using the behavior of an approximated solution of a linear equation. The equation solved in the RG-LSM is defined by the reciprocity gap functional. We recall that the reciprocity gap functional is employed in a variety of areas in inverse problems. The well known one is the reciprocity gap (RG) method introduced by S. Andrieux et al [4]. This method allows the reconstruction of planar cracks in two steps. The first step consists in finding the plane recovering the crack and the second one consists in locating the crack by finding the support of the jump of the solution across this plane. The jump is recovered by computing the Fourier transform. The RG method has also been used by [3], [11] and [10]). Note that the latter considers the case of the scattering by a crack with impedance boundary conditions. In our research work, we focus on the reconstruction of cracks with impedance boundary conditions with different shapes from several pairs of

Cauchy data corresponding to electromagnetic or acoustic time harmonic measurements at the boundary of a domain containing the cracks. We show that the RG-LSM scheme has a comparable accuracy as the results given by the LSM (see Chapter 4). We also provide a theoretical justification of the method and a numerical validation.
The remainder of this chapter is organized as follows. The forward scattering problem is briefly presented in Section 5.2. We focus in Section 5.3.2 on the theoretical justification of the use of the RG-LSM scheme along with a description of our method to solve the inverse problem. The results are validated through some numerical examples in Section 5.4. For an overview of a recent literature that deals with the use of the RG-LSM, we refer to [39, 24, 73, 38, 85] and references therein.

5.2 The forward scattering problem

We start this section by introducing the direct problem of scattering of an incident point source wave by an impedance crack in an inhomogeneous medium. We assume that the index of refraction n is piecewise-constant complex-valued function with non-negative imaginary part. Moreover,

$$n(x) = \begin{cases} n_0 & \text{for } x \in \Omega \\ 1 & \text{for } |x| \geq R \end{cases} \tag{5.1}$$

where $R > 0$ is sufficiently large and $\Omega \in \mathbf{R}^m$ is a domain with a constant index n_0 containing the crack σ. For further considerations, we assume that σ is a smooth non-intersecting open arc which can be extended to an arbitrary smooth, simply connected and closed curve $\partial\Omega_\sigma$ enclosing a bounded domain $\Omega_\sigma \subset\subset \Omega$. The normal vector ν on σ coincides with the outward normal vector to $\partial\Omega_\sigma$.
For a source point $x_0 \in \mathbf{R}^m \setminus \bar{\Omega}$, the incident point source $G(\cdot, x_0)$ is the fundamental solution of the Helmholtz equation

$$\Delta G(\cdot, x_0) + k^2 n G(\cdot, x_0) = -\delta_{x_0} \quad \text{in } \mathbf{R}^m,$$

satisfying the Sömmerfeld radiation condition

$$\lim_{r=|x|\to+\infty} r^{\frac{m-1}{2}} (\partial_r G(\cdot, x_0) - ikn G(\cdot, x_0)) = 0, \qquad \text{uniformly for all } \hat{x} = \frac{x}{|x|}.$$

The direct scattering problem is to find a scattered field $u_s(\cdot, x_0) \in H^1_{loc}(\mathbf{R}^m \setminus \overline{\sigma})$ solution of the Helmholtz equation

$$\Delta u_s(\cdot, x_0) + k^2 n u_s(\cdot, x_0) = 0 \qquad \text{in } \mathbf{R}^m \setminus \overline{\sigma}, \tag{5.2}$$

which satisfies the Sömmerfeld radiation condition

$$\lim_{r=|x|\to+\infty} r^{\frac{m-1}{2}} (\partial_r u_s(\cdot, x_0) - ikn u_s(\cdot, x_0)) = 0 \tag{5.3}$$

uniformly for all $\hat{x} = \frac{x}{|x|}$ and such that the total field $u(\cdot, x_0) = G(\cdot, x_0) + u_s(\cdot, x_0)$ satisfies the impedance boundary condition

$$\partial_\nu u^\pm(\cdot, x_0) \pm \lambda^\pm u^\pm(\cdot, x_0) = 0 \quad \text{on } \sigma, \tag{5.4}$$

where $\lambda^\pm \in L^\infty(\sigma)$ are the given (complex-valued) impedance functions with non-negative imaginary part. Notice that $u^\pm(x, x_0) := \lim_{h\to 0^+} u(x \pm h\nu, x_0)$ and $\partial_\nu u^\pm(x, x_0) := \lim_{h\to 0^+} \nu \cdot \nabla u(x \pm h\nu, x_0)$ for $x \in \sigma$.
Using the notation

$$g^\pm_{x_0} = -\left(\partial_\nu G(\cdot, x_0) \pm \lambda^\pm G(\cdot, x_0)\right), \tag{5.5}$$

the impedance boundary condition reads

$$\partial_\nu u^\pm_s(\cdot, x_0) \pm \lambda^\pm u^\pm_s(\cdot, x_0) = g^\pm_{x_0} \quad \text{on } \sigma. \tag{5.6}$$

We recall that in section 1.3.1 in chapter 1 we have proved that the direct problem has a unique solution that depends continuously on the boundary data $g^\pm_{x_0}$ (see Lemma 7).

5.3 The inverse problem

5.3.1 Setting of the inverse problem

We apply several incident point source waves and we measure the Cauchy data associated with the total wave at $\partial\Omega$. We assume that the set of point sources x_0 lies on the boundary C of an open domain $B \supset \bar{\Omega}$.
The data of our inverse problem is then $u(x, x_0)$ and $\partial_\nu u(x, x_0)$ for all $(x, x_0) \in \partial\Omega \times C$. Recall that we assumed that the index $n = n_0$ is constant inside Ω.

We define the *Reciprocity Gap functional* $R : H(\Omega) \to L^2(C)$, where

$$H(\Omega) = \{v \in H^1(\Omega);\ \Delta v + k^2 n_0 v = 0 \text{ in } \Omega\}.$$

It is given by

$$R(v)(x_0) := \int_{\partial\Omega} \left(u(x, x_0)\partial_\nu v(x) - v(x)\partial_\nu u(x, x_0)\right) ds(x), \qquad \text{for} \quad x_0 \in C, \tag{5.7}$$

and for all $v \in H(\Omega)$. As for the Linear Sampling Method, the RG-LSM consists in computing the solution of a linear equation at each point of a given grid. The behavior of

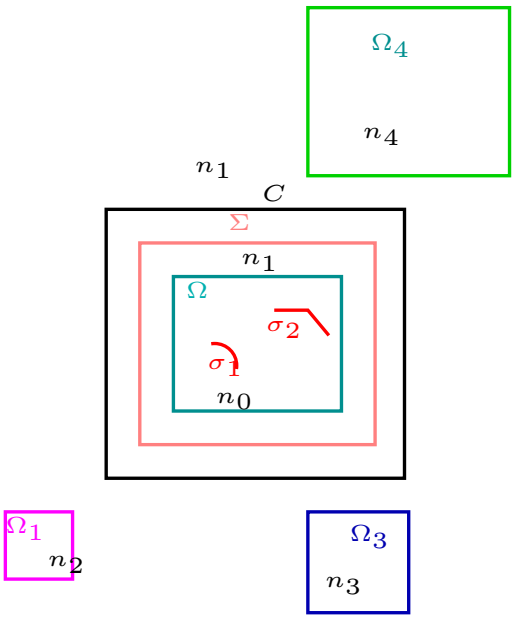

Figure 5.1: Representation of the domain

the computed solution shows if the grid point is on the crack or not. In our case, for any smooth and non intersecting arc L, the linear equation to solve is

$$R(S_g)(x_0) \simeq R(\Phi_L)(x_0), \tag{5.8}$$

where

$$\Phi_L(x) = \int_L \varphi_L(y)\Phi(x,y)ds(y) + \int_L \beta_L(y)\partial_\nu\Phi(x,y)ds(y), \quad \text{for } x \in \mathbf{R}^m \setminus L,$$

with densities $\varphi_L \in \tilde{H}^{-\frac{1}{2}}(L)$ and $\beta_L \in \tilde{H}^{\frac{1}{2}}(L)$ and S_g is the single layer potential on Σ with density $g \in L^2(\Sigma)$,

$$S_g(x) = \int_\Sigma g(y)\Phi(x,y)ds(y)$$

where Σ is a surface enclosing a domain containing $\overline{\Omega}$ and Φ is the free-space fundamental solution of the Helmholtz equation in $\mathbf{R}^m$ with wave number $k^2 n_0$.
We show in this section how we use an approximation of the solution g of (5.8) to reconstruct the crack σ.

5.3.2 Theoretical justification of the RG-LSM

To justify the use of the RG-LSM to identify an impedance crack from near-field measurements, we should prove the existence of an approximate solution of (5.8). Let us first

define the operator N by

$$\begin{array}{rccc} N: & L^2(\Sigma) & \longrightarrow & L^2(C) \\ & g & \longmapsto & R(S_g) \end{array} \tag{5.9}$$

N is an integral operator with kernel A.

$$\begin{aligned} N(g)(x_0) = & \int_{\partial\Omega} (u(x,x_0)\partial_\nu S_g(x) - \partial_\nu u(x,x_0) S_g(x)) ds(x) \\ = & \int_{\partial\Omega} u(x,x_0) \left(\int_\Sigma g(y) \partial_{\nu(x)} \Phi(x,y) ds(y) \right) ds(x) \\ & - \int_{\partial\Omega} \partial_{\nu(x)} u(x,x_0) \left(\int_\Sigma g(y) \Phi(x,y) ds(y) \right) ds(x) \\ = & \int_\Sigma g(y) A(x_0,y) ds(y) \end{aligned}$$

with

$$A(x_0,y) := \int_{\partial\Omega} u(x,x_0)\partial_{\nu(x)}\Phi(x,y) - \partial_{\nu(x)} u(x,x_0)\Phi(x,y) ds(x) \quad \text{for} \quad (x_0,y) \in C \times \Sigma \tag{5.10}$$

Since $\partial\Omega \cap C = \emptyset$ and $\partial\Omega \cap \Sigma = \emptyset$ then $A(.,.) \in L^2(C \times \Sigma)$. Thus, N is a compact operator. For any smooth non intersecting arc L, the equation (5.8) can be written as

$$Ng = \Lambda_L \tag{5.11}$$

where

$$\Lambda_L(x_0) = R(\Phi_L)(x_0) \quad \text{for } x_0 \in C. \tag{5.12}$$

In order to prove the existence of a nearby solution of the equation (5.11), a factorization of the operator N is needed. Using the fact that $u(\cdot, x_0)$ and S_g satisfy the Helmholtz equation with wave number $k^2 n_0$ in $\Omega \backslash \sigma$, the Green formula shows that

$$N(g)(x_0) = \int_\sigma \partial_\nu S_g(x)[u](x,x_0) ds(x) - \int_\sigma S_g(x)[\partial_\nu u](x,x_0) ds(x).$$

Hence a factorization of N is given by

$$N = P \circ H \tag{5.13}$$

where H is the operator defined by

$$\begin{array}{rccc} H: & L^2(\Sigma) & \longrightarrow & H^{1/2}(\sigma) \times H^{-1/2}(\sigma) \\ & g & \longmapsto & (S_g, \partial_\nu S_g) \end{array} \tag{5.14}$$

and P is the operator given by

$$\begin{aligned} P: \quad H^{1/2}(\sigma) \times H^{-1/2}(\sigma) \quad &\longrightarrow \quad L^2(C) \\ (\alpha\ ,\ \beta) \qquad\qquad &\longmapsto \quad \int_\sigma \beta(x)[u](x,x_0)ds(x) - \int_\sigma \alpha(x)[\partial_\nu u](x,x_0)ds(x) \end{aligned} \tag{5.15}$$

Theorem 35. *The operator H defined by (5.14) is one to one and has a dense range.*

Proof. We first prove the injectivity of H. Let $g \in L^2(\Sigma)$ such that

$$S_g(x) = 0 \qquad \text{and} \qquad \partial_\nu S_g(x) = 0 \qquad \text{for } x \in \sigma.$$

Since S_g is a solution of the Helmholtz equation in Ω with vanishing Cauchy data on σ, then using the unique continuation principle (see Corollary 13), S_g vanishes on a neighborhood of σ. Consequently, by the unique continuation principle and the continuity of the single layer potential, S_g vanishes also on Σ. Finally using the fact that S_g is the unique solution of the Helmholtz equation in $\mathbf{R}^m \setminus \Sigma$ satisfying the radiation condition we deduce that $S_g = 0$ in $\mathbf{R}^m$. Therefore by the jump relation of the normal derivative of S_g on Σ we have $g = 0$ which proves the injectivity of the operator H.
Next, to prove the denseness of the range of H, we show that the adjoint H^* of H is one to one. Let z_1 and z_2 be two functions in $L^2(\sigma)$, then

$$\langle H(g),\ (z_1, z_2)\rangle_{K,K^*} = \int_\sigma S_g \bar{z}_1 + \int_\sigma \partial_\nu S_g\ \bar{z}_2$$

where $\langle\cdot,\cdot\rangle_{K,K^*}$ denotes the duality pairing between $K = H^{1/2}(\sigma) \times H^{-1/2}(\sigma)$ and K^*.
By changing the order of integration we obtain

$$H^*(z_1, z_2)(y) = \int_\sigma \left(z_1(x)\bar{\Phi}(x,y) + z_2(x)\partial_\nu \bar{\Phi}(x,y)\right) ds(x).$$

for $y \in \Sigma$. We define the function Z in $\mathbf{R}^m \setminus \bar{\sigma}$ by

$$Z(y) = \int_\sigma \left(z_1(x)\bar{\Phi}(x,y) + z_2(x)\partial_\nu \bar{\Phi}(x,y)\right) ds(x).$$

The function Z is a solution of the Helmholtz equation in $\mathbf{R}^m \setminus \bar{\sigma}$ that satisfies the following radiation condition

$$\lim_{r=|x|\to+\infty} r^{\frac{m-1}{2}}(\partial_r u^s + inku^s) = 0, \tag{5.16}$$

uniformly in all directions $\hat{x} = \frac{x}{|x|}$.
If $Z = 0$ on Σ then by the uniqueness of the solution of the scattering problem and the unique continuation principle (see Corollary 13), we have $Z = 0$ on $\mathbf{R}^m \setminus \bar{\sigma}$. Finally by the jump relation of Z and its normal derivative, we have $z_1 = z_2 = 0$ on σ. That proves that H^* is one to one and consequently that H has a dense range. □

Theorem 36. *Assume that* $(\lambda^+ + \lambda^-)^{-1} \in L^\infty(\sigma)$. *Then, the operator* N *is one to one.*

Proof. Since H is injective, it remains to prove that P is one to one. Let $(\alpha, \beta) \in H^{1/2}(\sigma) \times H^{-1/2}(\sigma)$ such that $P(\alpha, \beta) = 0$. Then, for $x_0 \in C$

$$\int_\sigma \beta(x)[u](x, x_0)ds(x) - \int_\sigma \alpha(x)[\partial_\nu u](x, x_0)ds(x) = 0. \tag{5.17}$$

Here the integrals are considered as the duality pairing between $H^{-1/2}(\sigma)$, $\tilde{H}^{1/2}(\sigma)$ and $H^{1/2}(\sigma)$, $\tilde{H}^{-1/2}(\sigma)$. We denote by $W = H^{-1/2}(\sigma) \times H^{1/2}(\sigma)$, $f^+_{x_0} := -(\lambda^+ + \lambda^-)\partial_\nu G(\cdot, x_0)$ and $f^-_{x_0} := -(\lambda^+ + \lambda^-)G(\cdot, x_0)$. Then from the integral equations (1.40), the equation (5.17) can be written as

$$\left\langle (\alpha, \beta), (A^n_\sigma)^{-1}(f^+_{x_0}, f^-_{x_0}) \right\rangle_{W,W^*} = 0$$

where A^n_σ is the matrix given by (1.41). Since A^n_σ is invertible, we have for $x_0 \in C$

$$\left\langle ((A^n_\sigma)^*)^{-1}(\alpha, \beta), (f^+_{x_0}, f^-_{x_0}) \right\rangle_{W,W^*} = 0$$

and there exists a unique $(\alpha_1, \beta_1) \in W$ such that $(A^n_\sigma)^*(\alpha_1, \beta_1) = (\alpha, \beta)$. Hence

$$\left\langle (\alpha_1, \beta_1), (f^+_{x_0}, f^-_{x_0}) \right\rangle_{W,W^*} = 0$$

We set

$$Z_2(x_0) = \int_\sigma \left((\lambda^+ + \lambda^-)(y)\alpha_1(y)\frac{\partial G(y, x_0)}{\partial \nu} + (\lambda^+ + \lambda^-)(y)\beta_1(y)G(y, x_0) \right) ds(y).$$

Therefore, Z_2 is a solution of the Helmholtz equation in $\mathbf{R}^m \setminus \bar{\sigma}$ which vanishes on C. Then by using the uniqueness of the solution of the scattering problem and the unique continuation principle (see Corollary 13), we show that $Z_2 = 0$ on $\mathbf{R}^m \setminus \bar{\sigma}$. Thus, applying the jump relations on σ gives $[Z_2] = [\partial_\nu Z_2] = 0$ and $(\lambda^+ + \lambda^-)\alpha_1 = (\lambda^+ + \lambda^-)\beta_1 = 0$. Since $(\lambda^+ + \lambda^-)^{-1} \in L^\infty(\sigma)$, then $\alpha_1 = \beta_1 = 0$. Finally as $(A^n_\sigma)^*$ is invertible we conclude that $\alpha = \beta = 0$. □

Theorem 37. *Assume that* $(\lambda^+ + \lambda^-)^{-1} \in L^\infty(\sigma)$, *then the operator* N *has a dense range.*

Proof. We have proved in Theorem 35 that H has a dense range. It remains to prove the denseness of the range of the operator P. From (5.15), we have

$$\begin{aligned}
\langle P(\alpha, \beta), h \rangle_{L^2(C),L^2(C)} &= \int_C h(x_0) \left(\int_\sigma (-\alpha(x)[\partial_\nu u](x, x_0) + \beta(x)[u](x, x_0)ds(x) \right) ds(x_0) \\
&= \int_\sigma \alpha(x) \left(-\int_C h(x_0)[\partial_\nu u](x, x_0)ds(x_0) \right) + \\
&\quad \int_\sigma \beta(x) \left(\int_C h(x_0)[u](x, x_0)ds(x_0) \right) ds(x)
\end{aligned}$$

Hence, the adjoint operator of P is given by

$$P^*(h)(x) = \left(-\int_C h(x_0)[\partial_\nu u](x,x_0)ds(x_0),\ \int_C h(x_0)[u](x,x_0)ds(x_0) \right)$$

for $x \in \sigma$. Assume that there exists $h \in L^2(C)$ such that $P^*(h) = 0$. Then,

$$\int_C h(x_0)[\partial_\nu u](x,x_0)ds(x_0) = \int_C h(x_0)[u](x,x_0)ds(x_0) = 0, \qquad \text{for } x \in \sigma. \tag{5.18}$$

Let $V(x) := \int_C u(x,x_0)h(x_0)ds(x)$,for $x \in \mathbf{R}^m \setminus \bar{\sigma}$. Then V satisfies the Helmholtz equation in $\mathbf{R}^m \setminus \bar{\sigma}$. It can be seen as the total field associated to the incident wave $V_i(x) = \int_C G(x,x_0)h(x_0)ds(x_0)$ and to the scattered field $V_s(x) = \int_C u_s(x,x_0)h(x_0)ds(x_0)$. As $[V_i] = [\partial_\nu V_i] = 0$ on σ, we deduce by using (5.18) that

$$[V_s] = [\partial_\nu V_s] = 0 \qquad \text{on } \sigma.$$

Since V_s satisfies the Helmholtz equation in $\mathbf{R}^m$ and the Sommerfeld radiation condition, then it vanishes in $\mathbf{R}^m$. On the other hand

$$\begin{cases} \partial_\nu {V_s}^+ + \lambda^+ {V_s}^+ &= -(\partial_\nu V_i + \lambda^+ V_i) \\ \partial_\nu {V_s}^- - \lambda^- {V_s}^- &= -(\partial_\nu V_i - \lambda^- V_i) \end{cases}$$

Therefore, $\partial_\nu V_i + \lambda^+ V_i = \partial_\nu V_i - \lambda^- V_i = 0$ on σ. Since $(\lambda^+ + \lambda^-)^{-1} \in L^\infty(\sigma)$, then V_i and $\partial_\nu V_i$ vanish on σ. Hence, by the unique continuation principle (see Corollary 13) $V_i = 0$ in B. Thus the continuity of the single layer potential V_i implies that $V_i = 0$ on $C = \partial B$. Now, using the uniqueness of the solution of the scattering problem we conclude that $V_i = 0$ in $\mathbf{R}^m \setminus C$. Finally, by the jump relation of $\partial_\nu V_i$ on C we show that $h = 0$. This proves that P^* is one to one and consequently the operator N has a dense range. □

Theorem 38. *Let L be a smooth and non intersecting arc such that $\bar{L} \subset \Omega$, $\varphi_L \in \tilde{H}^{-1/2}(L)$ and $\beta_L \in \tilde{H}^{1/2}(L)$ such that $(\varphi_L, \beta_L) \neq (0,0)$. Then the function Λ_L defined in (5.12) belongs to the range of the operator P if and only if $supp(\varphi_L) \subset \bar{\sigma}$ and $supp(\beta_L) \subset \bar{\sigma}$.*

Proof. We first consider the straightforward case where $\varphi_L \in \tilde{H}^{-1/2}(L)$ and $\beta_L \in \tilde{H}^{1/2}(L)$. Under these assumptions, it is clear that φ_L and β_L can be extended by zero outside of σ. The result follows directly from the definition of P.
Now assume that $supp(\varphi_L) \nsubseteq \bar{\sigma}$ or $supp(\beta_L) \nsubseteq \bar{\sigma}$ and that $\Lambda_L \in Range(P)$. Let $\tilde{\Omega} \subset\subset \Omega$ such that $L \cup \sigma \subset \tilde{\Omega}$. Since, for $x_0 \in C$, $u(\cdot, x_0)$ and Φ_L are two solutions of the Helmholtz equation in $\Omega \setminus \tilde{\Omega}$, then the Green formula gives

$$R(\Phi_L)(x_0) = \int_{\partial\tilde{\Omega}} (u(x,x_0)\partial_\nu \Phi_L(x) - \partial_\nu u(x,x_0)\Phi_L(x))ds(x), \qquad \text{for } x_0 \in C. \tag{5.19}$$

Now, we define the function φ in $\mathbf{R}^m \setminus \tilde{\Omega}$ by

$$\varphi(x_0) = \int_{\partial\tilde{\Omega}} (u(x, x_0)\partial_\nu \Phi_L(x) - \partial_\nu u(x, x_0)\Phi_L(x))ds(x). \tag{5.20}$$

By reciprocity, $u(x, .)$ is a radiating solution of the following Helmholtz equation

$$\Delta_{x_0} u(x, x_0) + k^2 n(x_0) u(x, x_0) = -\delta_x \qquad \text{for } x_0 \in \mathbf{R}^m \setminus (\{x\} \cup \sigma).$$

Hence φ is a radiating solution satisfying

$$\Delta\varphi + k^2 n\varphi = 0 \qquad \text{in } \mathbf{R}^m \setminus \tilde{\Omega}.$$

Using the fact that $\Lambda_L \in Range(P)$ then there exists $(\alpha, \beta) \in H^{1/2}(\sigma) \times H^{-1/2}(\sigma)$ such that

$$R(\Phi_L)(x_0) = \int_\sigma (\beta(y) [\partial_\nu u] (y, x_0) - \alpha(y) [u] (y, x_0))ds(y) \tag{5.21}$$

We define the function f in $\mathbf{R}^m \setminus \sigma$ by

$$f(x_0) = \int_\sigma (\beta(y) [\partial_\nu u] (y, x_0) + \alpha(y) [u] (y, x_0))ds(y).$$

Therefore by (5.19) and (5.20), $f(x_0) = \varphi(x_0)$ for $x_0 \in C$. By reciprocity f satisfies the same equation as φ in $\mathbf{R}^m \setminus \tilde{\Omega}$ and the uniqueness of the solution of the scattering problem gives

$$f(x_0) = \varphi(x_0), \qquad \text{for } x_0 \in \mathbf{R}^m \setminus B.$$

By the unique continuation principle (see Corollary 13) we obtain

$$f(x_0) = \varphi(x_0), \qquad \text{for } x_0 \in \mathbf{R}^m \setminus \tilde{\Omega}.$$

Now let $\tilde{u}^s(\cdot, x_0) := u^s(\cdot, x_0) + \Phi^d(\cdot, x_0)$, where $\Phi^d := G - \Phi$. using the Green theorem we get for $x_0 \in \Omega \setminus \tilde{\Omega}$

$$\begin{aligned} \varphi(x_0) = R(\Phi_L)(x_0) \quad = \quad & \int_{\tilde{\partial}\Omega} (\tilde{u}^s(x, x_0)\partial_\nu \Phi_L(x) - \partial_\nu \tilde{u}^s(x, x_0)\Phi_L(x))ds(x) \\ & + \int_{\tilde{\partial}\Omega} (\Phi(x, x_0)\partial_\nu \Phi_L(x) - \partial_\nu \Phi(x, x_0)\Phi_L(x))ds(x) \end{aligned}$$

Let v be the function defined in defined $\Omega \setminus \bar{\sigma}$ by

$$v(x_0) := \int_{\tilde{\partial}\Omega} (\tilde{u}^s(x, x_0)\partial_\nu \Phi_L(x) - \partial_\nu \tilde{u}^s(x, x_0)\Phi_L(x))ds(x).$$

Then we have

$$\varphi(x_0) = v(x_0) - \Phi_L(x_0), \qquad \text{for } x_0 \in \Omega \setminus \tilde{\Omega} \tag{5.22}$$

Since f, v, Φ_L are solutions of the Helmholtz equation associated to k_0, then the unique continuation principle (see Corollary 13) gives

$$f(x) = v(x) + \Phi_L(x) \qquad \text{for } x \in \Omega \setminus (\sigma \cup L)$$

The right hand side of this equation is not continuous across L. In fact we cannot have at once the continuity across L of the double layer potential and the derivative of the single layer potential present in Φ_L. Whereas, f and its derivative are continuous across L which is a contradiction. □

The following theorem is the fundamental result of the RG-LSM method.

Theorem 39. *Let L be a non intersecting smooth open arc, $\varphi_L \in \tilde{H}^{-\frac{1}{2}}(L)$ and $\beta_L \in \tilde{H}^{\frac{1}{2}}(L)$, such that $(\varphi_L, \beta_L) \neq (0,0)$.*

1. *If $L \subset \sigma$, there exists a sequence $(g_n)_{n\in\mathbf{N}} \in L^2(\Sigma)$ such that*

$$\lim_{n\to+\infty} \|N(g_n) - \Lambda_L\|_{L^2(C)} = 0. \tag{5.23}$$

Furthermore, we have

$$\lim_{n\to+\infty} ||S_{g_n}||_* < +\infty$$

where $\|S_{g_n}\|_* = \|\partial_\nu S_{g_n}\|_{H^{-\frac{1}{2}}(\sigma)} + \|S_{g_n}\|_{H^{\frac{1}{2}}(\sigma)}$.

2. *Otherwise, for any sequence $(g_n)_{n\in\mathbb{N}} \in L^2(\Sigma)$ satisfying (5.23),*

$$\lim_{n\to+\infty} ||S_{g_n}||_* = \infty$$

Proof. • If $L \subset \sigma$ then we can find a bounded solution to the equation (5.11). In fact we have $H^{\frac{1}{2}}(L) \subset H^{\frac{1}{2}}(\sigma)$ and $H^{-\frac{1}{2}}(L) \subset H^{-\frac{1}{2}}(\sigma)$. Hence Λ_L belongs to the range of P. Therefore, there exists $(\alpha, \beta) \in H^{\frac{1}{2}}(\sigma) \times H^{-\frac{1}{2}}(\sigma)$ such that $\Phi_L = P(\alpha, \beta)$. Moreover the range of H is dense in $H^{1/2}(\sigma) \times H^{-\frac{1}{2}}(\sigma)$. Thus there exists two sequences $(\alpha_n, \beta_n)_{n\in\mathbf{N}}$ in the range of H such that $\lim_{n\to+\infty}(\alpha_n, \beta_n) = (\alpha, \beta)$. Using the continuity of H, we show the existence of a sequence $(g_n)_{n\in\mathbf{N}} \subset L^2(\Sigma)$ satisfying $\lim_{n\to+\infty} H(g_n) = (\alpha, \beta)$. That proves finally that

$$\lim_{n\to+\infty} \|R(S_{g_n}) - R(\Phi_L)\|_{L^2(C)} = 0.$$

• Now let $L \not\subset \sigma$ and assume that $\|S_{g_n}\|_* < +\infty$. Then, there exists a pair $(\alpha_n, \beta_n) \in H^{-\frac{1}{2}}(\sigma) \times H^{\frac{1}{2}}(\sigma)$ such that $\partial_\nu S_{g_n} = \alpha_n$ and $S_{g_n} = \beta_n$. Hence (α_n, β_n) belongs to the range of H. Since H is one to one and continuous, then $H(g_n) = (\alpha_n, \beta_n)$. The

sequence $(\alpha_n, \beta_n)_{n\in\mathbb{N}}$ is bounded in $H^{-\frac{1}{2}}(\sigma)\times H^{\frac{1}{2}}(\sigma)$ which is a complete space. Therefore we can extract a subsequence that weakly converges to (α, β) in $H^{-\frac{1}{2}}(\sigma)\times H^{\frac{1}{2}}(\sigma)$. The integral operator P has a regular kernel so P is compact. Consequently, $\lim_{n\to+\infty} \|P\cdot H(g_n) - P(\alpha,\beta)\|_{L^2(C)} = 0$. Hence $\lim_{n\to+\infty} \|R(S_{g_n}) - P(\alpha,\beta)\|_{L^2(C)} = 0$. Then from (5.23) and by uniqueness of the limit $P(\alpha,\beta) = \Lambda_L$. Finally Λ_L belongs to the range of P and $L \subset \sigma$ which is a contradiction.

□

5.4 Numerical experiments and results

5.4.1 Numerical schemes

For the purpose of the numerical experiments, we construct a nearby solution to (5.11) using a Tikhonov regularization. Therefore we solve the following equation

$$(\eta I + N^*N)g_\eta(x_0) = N^*\Lambda_L(x_0) \qquad \text{for } x_0 \in C \tag{5.24}$$

where η is a parameter of regularization chosen using the Morozov discrepancy principle. **Discretization:** The numerical experiments are conducted in 2D. We consider m measures of Cauchy data $(u(.,x_0), \partial_\nu u(.,x_0))_{|\partial\Omega}$, l equally distant points on Σ and n equally distant source points on C.

$$Ng(x_0^i) \simeq \sum_{k=1}^{l} \Sigma_k g(y_k) A(x_0^i, y_k), \qquad \text{for } 1 \le i \le n, \tag{5.25}$$

where

$$A(x_0^i, y_k) = -\sum_{j=1}^{m} \partial\Omega_j \left[u(x_j, x_0^i) \frac{(x_j - y_k, \nu)}{\|x_j - y_k\|} H_1^{(1)}(k\|x_j - y_k\|) + \partial_\nu u(x_j, x_0^i) H_0^{(1)}(k\|x_j - y_k\|) \right], \tag{5.26}$$

and

$$\Lambda(x_0^i) \simeq \sum_{j=1}^{m} \partial\Omega_j \left[u(x_j, x_0^i)\partial_\nu \Phi_L(x_j) - \partial_\nu u(x_j, x_0^i)\Phi_L(x_j) \right], \qquad \text{for } 1 \le i \le n \tag{5.27}$$

with Σ_k and $\partial\Omega_j$ are respectively the arc-length between two adjacent points on Σ and $\partial\Omega$ and $H_0^{(1)}$ and $H_1^{(1)}$ are the Hankel functions of first kind. Let L be a small segment of center z and with normal ν. Then

$$\Phi_L(x_j) \simeq \gamma|L| \left[\alpha(z) H_0^{(1)}(k\|x_j - z\|) - \beta(z) \frac{(x_j - z, \nu)}{\|x - z\|} H_1^{(1)}(k\|x_j - z\|) \right]. \tag{5.28}$$

The discrete equation to solve is then

$$Ng(x_0^i) \simeq \Lambda_L(x_0^i) \qquad \text{for } 1 \leq i \leq n, \tag{5.29}$$

using the Tikhonov procedure explained above. The sampling procedure will consist in varying z and ν in (5.28). According to Theorem 39 we expect that $\|g\|$, solution to (5.29)), to be large except when $z \in \sigma$ and ν is the normal to σ at z.
We shall consider two types of solutions. The first one denoted by g_z corresponds to $\alpha(z) = 1$ and $\beta(z) = 0$, the second one denoted by $g_{z,\nu}$ corresponds to $\alpha(z) = 0$ and $\beta(z) = 1$).
Let us also consider the two independent normals $\nu_1 = (0,1)^t$ and $\nu_2 = (1,0)^t$. We define the normal $\nu := \zeta\nu_1 + \sqrt{1-\zeta^2}\nu_2$ with $0 \leq \zeta \leq 1$. Therefore, by linearity of the equation (5.29)

$$g_{z,\nu} = \zeta g_{z,\nu_1} + \sqrt{1-\zeta^2} g_{z,\nu_2}.$$

Based on the theoretical justification, the normal ν to σ at $z \in \sigma$ corresponds with the value ζ that minimizes

$$\|g_{z,\nu}\|^2 = \zeta^2 \|g_{z,\nu_1}\|^2 + (1-\zeta^2)\|g_{z,\nu_2}\|^2 + 2\zeta\sqrt{1-\zeta^2}\,\langle g_{z,\nu_1}\ , g_{z,\nu_2}\rangle \tag{5.30}$$

The proposed criterion will be the determination on each point z of

$$z \quad \longrightarrow \quad \frac{1}{\|g_z\|} + \frac{1}{\|g_{z,\nu}\|} \tag{5.31}$$

where g, $g_{z,\nu}$ corresponds with ζ that minimizes (5.30).

5.4.2 Numerical results

The efficiency of this approach is tested for different shapes, namely arc-shaped cracks, L-shaped cracks and the union of two segments having an oblique angle between them and for several impedance values, also for different examples of media. We present in the following figures the isovalues of the right hand side of (5.31). The red isovalues correspond to the highest values whereas the blue ones represent the smallest ones. This means that the crack corresponds to red isovalues in the figures.
In all the numerical tests we use 500 measures of Cauchy data on the $\partial\Omega$.
The given results are similar to those given by the LSM in the case of a crack in the vacuum (see [14]). We represent the border of the search domain by the square with dashed line and $\partial\Omega$ by the square with continuous line.

Example 1

In this example, the target object is a crack having different shapes embedded in a medium Ω with index n. This medium is surrounded by small inhomogeneities. To locate the target object we use 80 point sources uniformly distributed around Ω represented by the blue square (see Figure 5.4).

In sequel, the wavelength in vacuum is denotes by λ_0

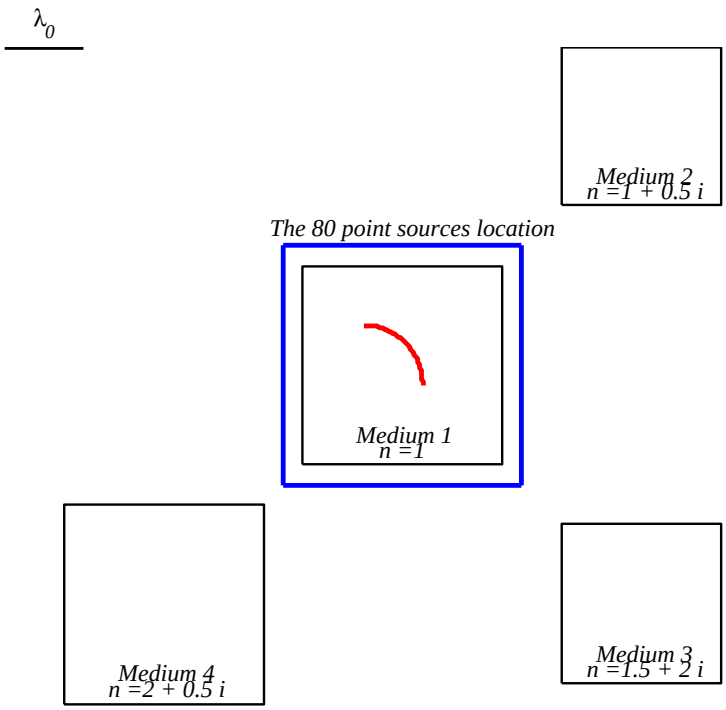

Figure 5.2: Geometry of the problem. The measurements are taken on the boundary of the *Medium 1*.

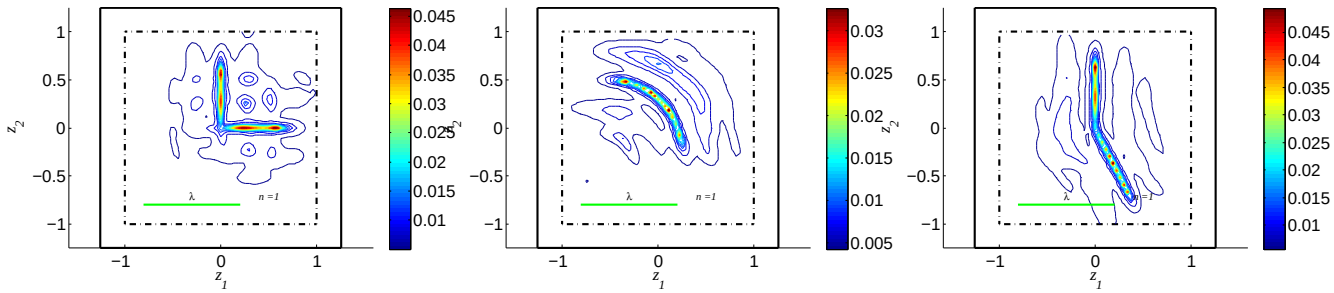

Figure 5.3: Reconstruction of different cracks for $\lambda^- = \lambda^+ = 10^{-2}(1+i)$, included in the *Medium 1*.

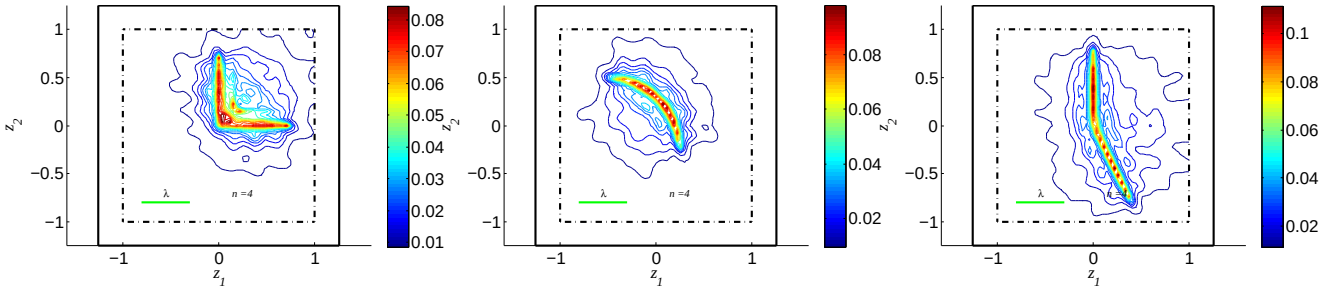

Figure 5.4: Reconstruction of different cracks for $\lambda^- = \lambda^+ = 10^2(1+i)$, included in the *Medium 1* where $n = 4$.

Example 2

In this example we test the precision of the reconstructed crack's shape with respect to the impedance values. To this aim we fix the medium index of Ω ($n = 2$) and we vary the value of the impedance.

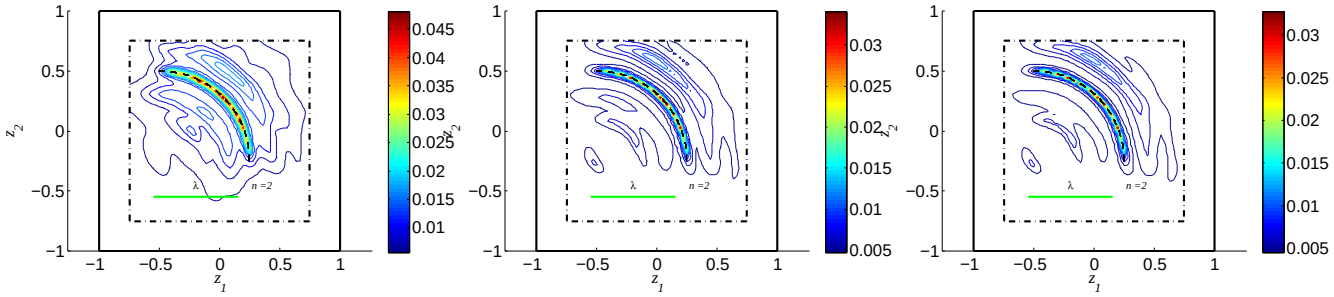

Figure 5.5: Reconstruction of an arc centered on $(-0.5, 0.5)$ and with radius 0.75 for $\lambda^- = \lambda^+ = 10^{-1}(1+i)$(left), $\lambda^- = \lambda^+ = 10^{-2}(1+i)$ (middle), $\lambda^- = \lambda^+ = 10^{-5}(1+i)$ (right).

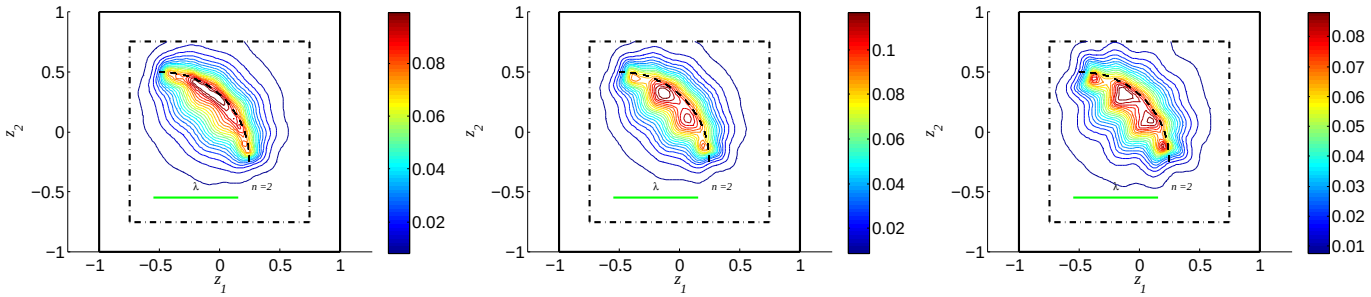

Figure 5.6: Reconstruction of an arc centered on $(-0.5, 0.5)$ and with radius 0.75 for $\lambda^- = \lambda^+ = 10 + 10i$(left), $\lambda^- = \lambda^+ = 5 + 5i$ (middle), $\lambda^- = 1.2 + 2i\tilde{\lambda}^+ = 2 + 1.2i$ (right).

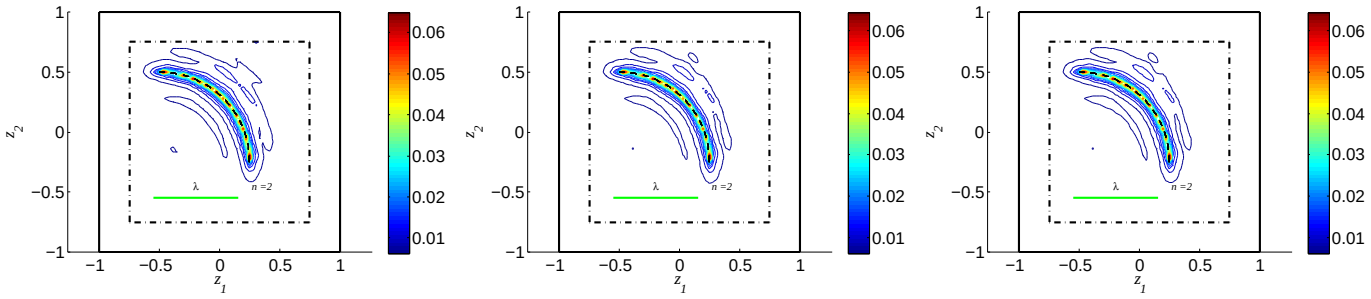

Figure 5.7: Reconstruction of an arc centered on $(-0.5, 0.5)$ and with radius 0.75 for $\lambda^- = \lambda^+ = 10^2(1+i)$(left), $\lambda^- = \lambda^+ = 10^3(1+i)$ (middle), $\lambda^- = \lambda^+ = 10^6(1+i)$ (right).

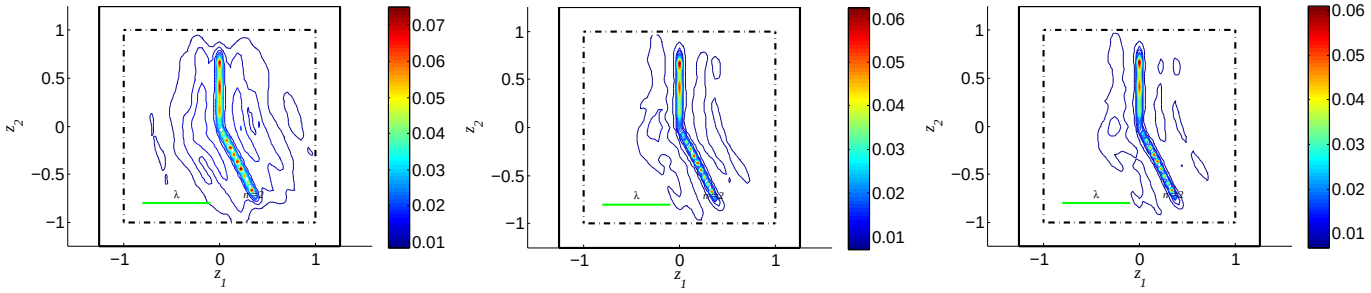

Figure 5.8: Reconstruction of two segments $[0.8, 0] \times \{0\}$ and $[-0.8, 0] \times \{0, 0.4\}$for $\lambda^- = \lambda^+ = 10^{-1}(1+i)$(left), $\lambda^- = \lambda^+ = 10^{-3}(1+i)$ (middle), $\lambda^- = \lambda^+ = 10^{-6}(1+i)$ (right).

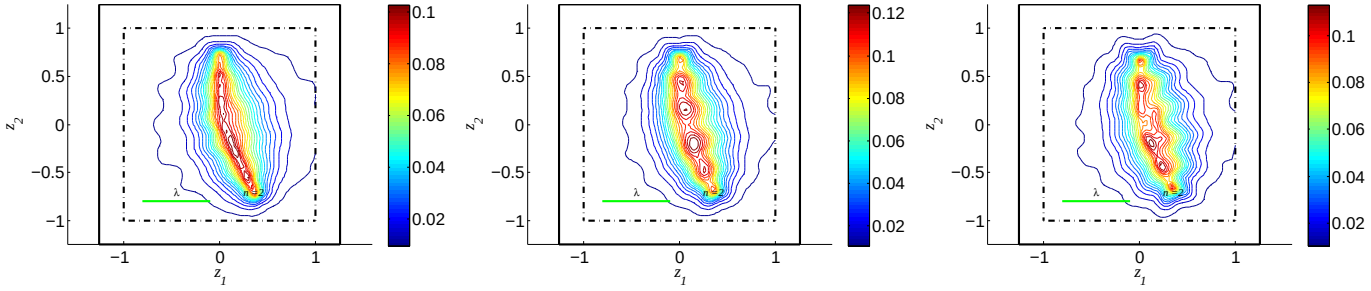

Figure 5.9: Reconstruction of two segments $[0.8, 0] \times \{0\}$ and $[-0.8, 0] \times \{0, 0.4\}$for $\lambda^- = \lambda^+ = 10 + 10i$(left), $\lambda^- = \lambda^+ = 5 + 5i$ (middle), $\lambda^- = 1.2 + 2i\tilde{\lambda}^+ = 2 + 1.2i$ (right).

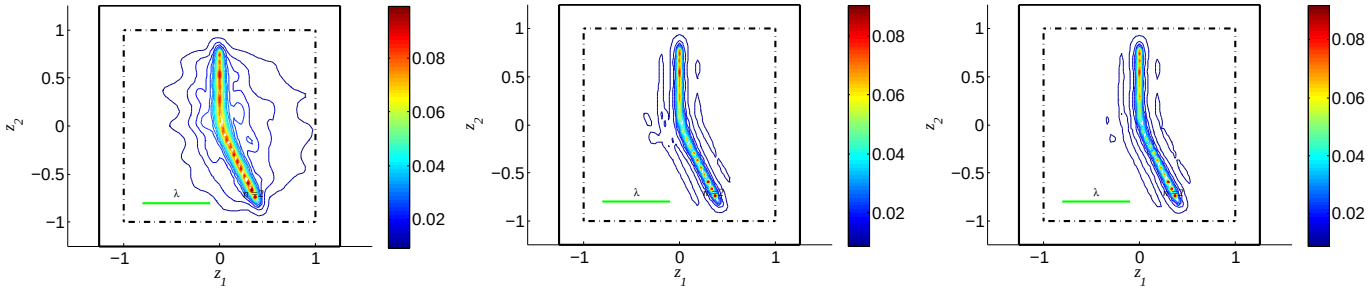

Figure 5.10: Reconstruction of two segments $[0.8, 0] \times \{0\}$ and $[-0.8, 0] \times \{0, 0.4\}$for $\lambda^- = \lambda^+ = 10^2(1+i)$(left), $\lambda^- = \lambda^+ = 10^3(1+i)$ (middle), $\lambda^- = \lambda^+ = 10^6(1+i)$ (right).

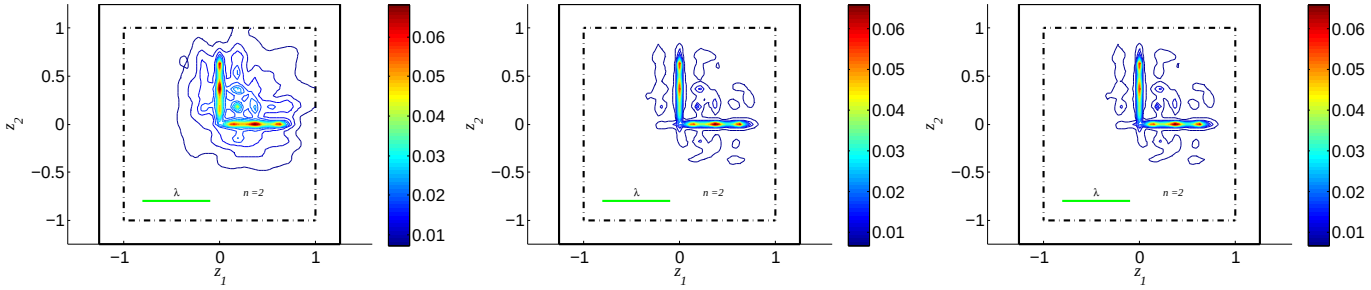

Figure 5.11: Reconstruction of an L-shaped crack with peaks $(0.75, 0)$, $(0, 0)$ and $(0, 0.75)$for $\lambda^- = \lambda^+ = 10^{-1}(1 + i)$(left), $\lambda^- = \lambda^+ = 10^{-3}(1 + i)$ (middle), $\lambda^- = \lambda^+ = 10^{-6}(1 + i)$ (right).

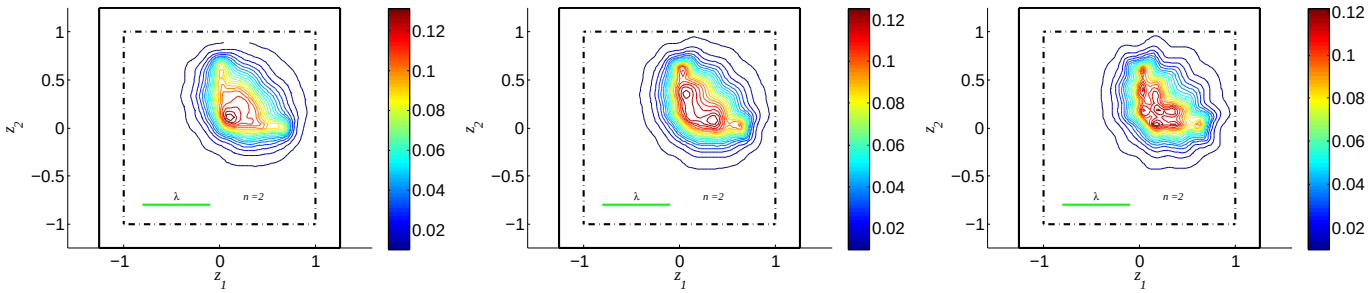

Figure 5.12: Reconstruction of an L-shaped crack with peaks $(0.75, 0)$, $(0, 0)$ and $(0, 0.75)$for $\lambda^- = \lambda^+ = 10(1 + i)$(left), $\lambda^- = \lambda^+ = 5(1 + i)$ (middle), $\lambda^- = 1.2 + 2i$ $\lambda^+ = 2 + 1.2i$ (right).

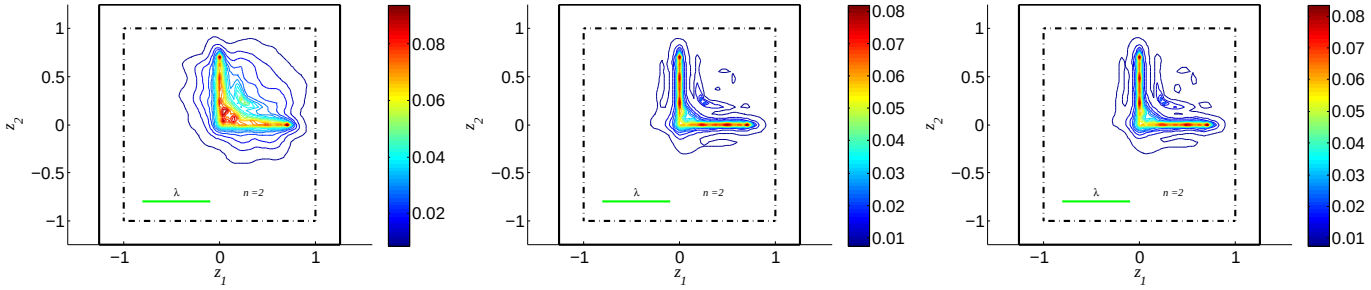

Figure 5.13: Reconstruction of an L-shaped crack with peaks $(0.75, 0)$, $(0, 0)$ and $(0, 0.75)$for $\lambda^- = \lambda^+ = 10^2(1+i)$(left), $\lambda^- = \lambda^+ = 10^3(1+i)$ (middle), $\lambda^- = \lambda^+ = 10^3(1+i)$ (right).

Figure 5.5 to 5.13 show that the RG-LSM give a good crack reconstruction for a fixed index of medium by varying the shape of the crack and the impedance values. Note that similar to the LSM reconstruction given in Chapter 3 we have the same observation, a height quality of the reconstruction for the large and small impedance values and the results is less better in the case of the intermediate impedance value.

Example 3

In this example we add a small amount of absorption to the host medium for different shapes of cracks and impedance values. As shown in Figures 5.14, 5.15 and 5.16 we have also a good reconstruction.

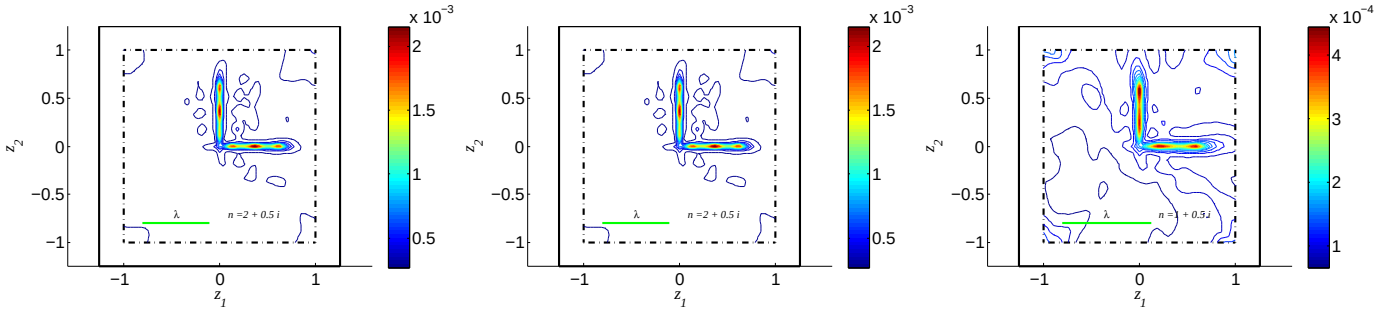

Figure 5.14: Reconstruction of an L-shaped crack with peaks $(0.75, 0)$, $(0, 0)$ and $(0, 0.75)$for $\lambda^- = \lambda^+ = 10^{-1}(1 + i)$ and the medium index $n = 2 + 0.1i$ (left), $n = 2 + 0.5i$ (in the middle) and $n = 1 + 0.5 * i$ (right)

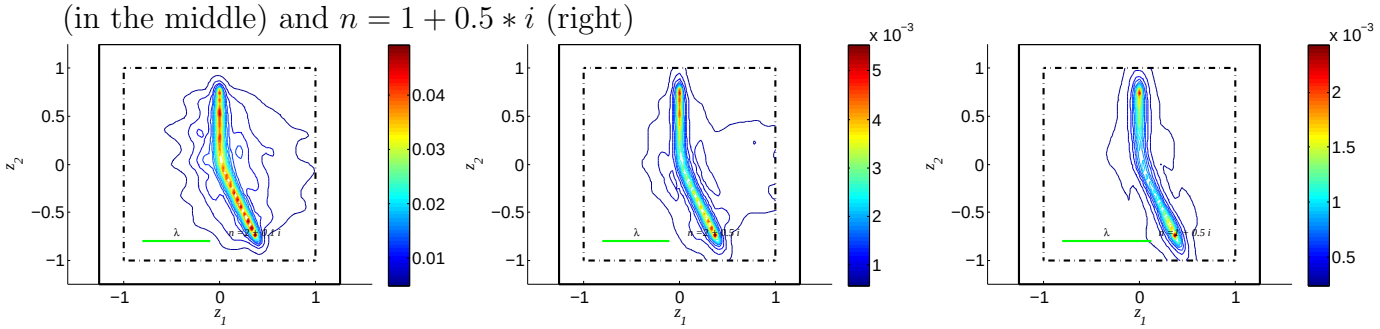

Figure 5.15: Reconstruction of a union of two segments for $\lambda^- = \lambda^+ = 10^2(1 + i)$(left) and the medium index $n = 2 + 0.1i$ (left), $n = 2 + 0.5i$ (in the middle) and $n = 1 + 0.5 * i$ (right)

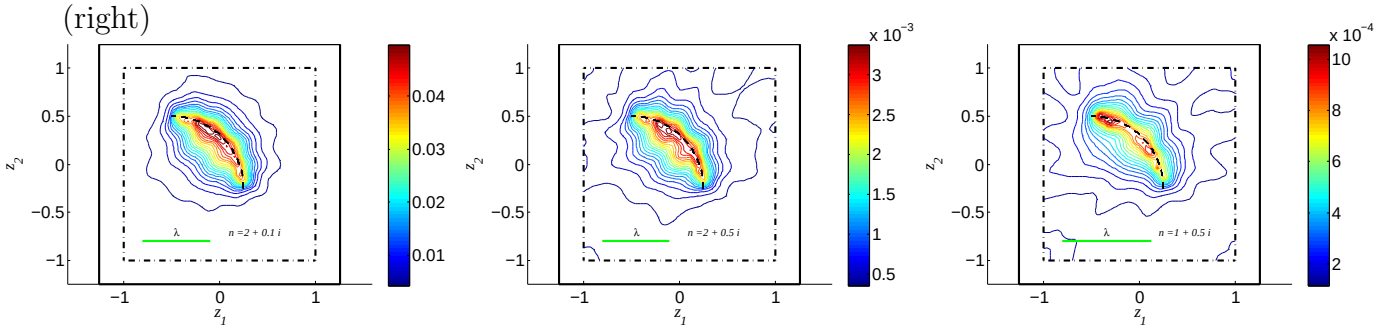

Figure 5.16: Reconstruction of an arc centered on $(-0.5, 0.5)$ and with radius 0.75, for $\lambda^- = \lambda^+ = 10(1 + i)$ and the medium index $n = 2 + 0.1i$ (left), $n = 2 + 0.5i$ (in the middle) and $n = 1 + 0.5 * i$ (right).

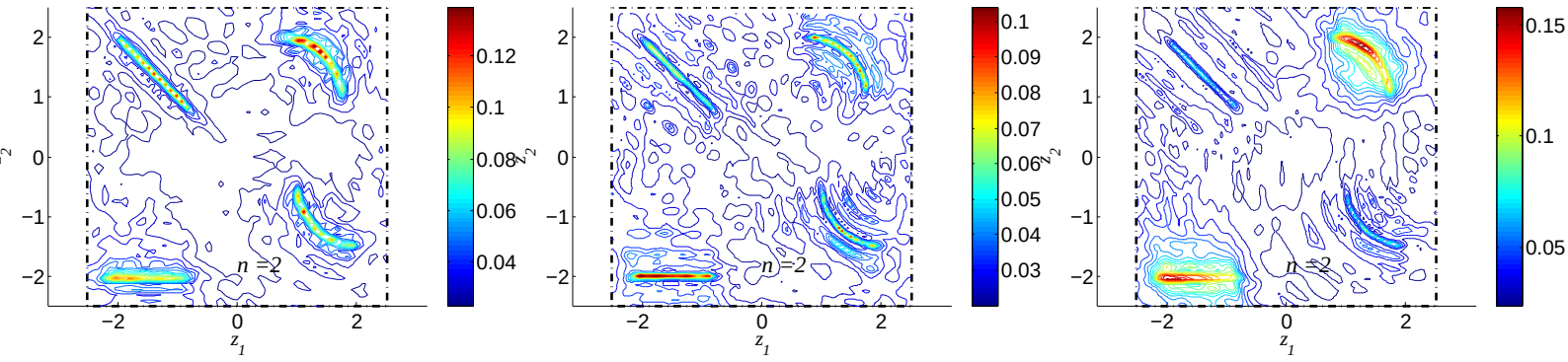

Figure 5.17: Reconstruction of multiple cracks for $\lambda_1^{\pm} = \lambda_2^{\pm} = \lambda_3^{\pm} = \lambda_4^{\pm} = 10^2(1+i)$(right), $\lambda_1^{\pm} = \lambda_2^{\pm} = \lambda_3^{\pm} = \lambda_4^{\pm} = 10^{-2}(1+i)$(middle) and $\lambda_1^{\pm} = \lambda_4^{\pm} = 10^{-2}$ and$\lambda_3^{\pm} = \lambda_2^{\pm} = 10(1+i)$ (left) for $n = 2$ (right).

Figures 5.14 to 5.16 show the efficiency of this method for different impedance values and crack shapes and even with an adding absorption in the domain. In Figure 5.17, we observe that even with multiple cracks we also have a good reconstruction since the shape of each crack can be clearly identified.

5.5 Conclusion

In this Chapter, we present an application of the RG-LSM in the case of scattering by crack with impedance boundary conditions in both side of the crack. The RG-LSM gives a simple algorithm as in the LSM and the Factorization method, but it is less faster since an integration of the test function on the border of the subdomain that contains the crack should be computed on each point of the sampling domain. The theoretical justification of the RG-LSM is close to that of the LSM but the characterization of the crack in the RG-LSM is given by the behavior of the norm of the potential S_g without using the impedance parameter as in the case of the LSM in the homogeneous case. For the numerical experiment, we show that the crack reconstruction is similar to the LSM reconstruction given in Chapter 3. The numerical tests show that a good crack reconstruction is given for different crack shapes, domain types and impedance values. A good reconstruction is given even with the presence of an absorption in the host medium. Note that since the method is restricted to the case of a crack embedded in a domain with constant index of refraction, the application of this method remains limited. Therefore, it would be more

interesting to extend the application of this method to the case of a stratified domain or to the case when there are limited data in a part of the boundary of the domain. To this end, a data completion algorithm is needed which constitutes the objective of the next chapter.

CHAPTER 6

A data completion algorithm: Application to RG-LSM

Contents

Abstract

In order to generalize the application of the RG-LSM introduced in the previous chapter to more realistic cases, a recovering data tool is needed. To illustrate that, let us consider the case of a crack buried in the earth or in some stratified domain with a regular exterior

boundary and suppose that we only have access to the Cauchy data on this exterior boundary. As explained in the previous chapter, the RG-LSM cannot be simply applied in this case since all the measurements of Cauchy data are required on a subdomain that contain the crack and have a constant refractive index. To overcome this difficulty we propose a data completion algorithm that determines the Cauchy data needed by the RG-LSM from available Cauchy data measurements. Our algorithm is based on the representation of the solution in terms of surface integral operators. We shall first provide a general overview on the Cauchy problem along with the relevant literature, then we develop our recovering data method and finally give some numerical results that validate our approach.

6.1 Introduction

We are mainly concerned here with solving the Cauchy problem in the framework of the Helmholtz equation. More specifically we would like to determine the Cauchy data associated with a solution of the Helmholtz equation in a part of a boundary of a bounded domain from the knowledge of the Cauchy data on the complementary part. This problem is known to be ill-posed since 1953 (Hadamard, 1953) [42]. Hadamard has given an explicit example to illustrate the instability of the results in the case of the Laplace equation in a squared shape domain. This work has been extended by F. Ben Belgacem and H. El Fekih [13] in 2005 where they generalize the results of instability for a more general domain. For more details about the study of the stability of the Cauchy problems we refer to [44, 47, 12]. It should be noted that there is a considerable literature that deals with the approaches for solving such an inverse problem. We first provide the example of the quasi-reversibility [17, 16, 26] method that was proposed by Lattes and Lions [64] in 1967. This method consists in replacing the Cauchy problem by a well-posed problem that is used to find the quasi-solutions. In 1976, another approach using the Tikhonov regularization was proposed, which consists first in solving a linear equation in the form $\mathcal{A}u = f$ with unknown the missing data and then in solving this equation using a Tikhonov minimization. In 2001, A.Cimetire et al. [28] proposed an Evanescent regularization method using an iterated Tikhonov method. There are also some iterative methods such as the method introduced by Kozlov 1991 which is based on solving a sequence of elliptic problems using a regularization with the regularization parameter that is the number of iterations and the initial choice of the algorithm. The method consists in replacing the Cauchy problem by a sequence of mixed well-posed problems and in alternating the use of the Dirichlet and the Neumann data on the part of the border that contains the data. Another interesting work is that by A. Ben abda et all [9] in the case of the Helmholtz equation. In the latter, the authors have used an iterative method using the decomposition domain tools and the Steklov Poincarré operator and they have solved a point fixe scheme via a preconditioned

Richardson algorithm with dynamic relaxation. Furthermore, under the framework of the Helmholtz equation, an iterative algorithm based on the Landweber method in combination with the Boundary Element Method (BEM) was developed by Marina et al. [69] in 2004. This latter method reduces the Cauchy problem to solving a sequence of well-posed boundary value problems in the space of square integrable functions, which provides accurate, convergent and stable numerical solutions. T. Reginska and K. Reginski in [79] have also presented a solution of the Cauchy problem for the Helmholtz equation using a regularization method based on truncated Fourier transform.
The aim of the present work is to solve Cauchy problem for the Helmholtz using a non iterative method based on the surface representation of the solution. We derive a linear integral equation system that has to be verified by the missing Cauchy data. The ill posedness of the problem shows up in the compactness of the component of the operator that has to be inverted. We prove injectivity and densness of the range of this operator in appropriate Sobolev spaces. Moreover, we also prove that our method naturally handle the case of noisy data. More precisely, in our formulation the available Cauchy data is multiplied by an operator that has the same range as the operator to be inverted. This makes possible the use of classical regularization techniques for noisy data. Then we provide some numerical results that prove the efficiency of this method for different shapes of the domain and also for noisy data. In the last part, we couple the use of the completion data algorithm with the reciprocity gap algorithm and we show how one is able to reconstruct cracks embedded in layered media.

6.2 Data completion algorithm

6.2.1 A data completion algorithm based on integral equations

We start this section by introducing our Cauchy problem. Let $\Omega_1 \subset \mathbf{R}^m$ be a bounded domain with connected complement and let $\Omega_2 \subset \mathbf{R}^m$ be a regular subdomain of Ω_1. We shall assume that Ω_2 is strictly included in Ω_1. We denote by Γ_1 and Γ_2 respectively the boundary of Ω_1 and Ω_2 and ν is the normal vector on $\Gamma_1 \cup \Gamma_2$ directed to the exterior of Ω_1 and Ω_2 (see Figure 6.1). Let $u \in H^1(\Omega_1 \setminus \Omega_2)$ solution of the following Helmholtz equation:

$$\Delta u + k^2 n u = 0 \quad \text{in } \Omega_1 \setminus \Omega_2, \tag{6.1}$$

where n denotes the index of refraction inside $\Omega_1 \setminus \Omega_2$, that we assume to be constant and where k denotes the wave number. Our data completion problem consists in determining $(u, \partial_\nu u)_{|\Gamma_2}$ from the knowledge of $(f, g) := (u, \partial_\nu u)_{|\Gamma_1}$.

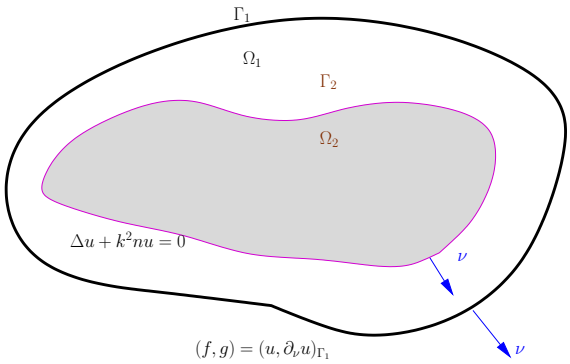

Figure 6.1: Representation of the domain

Our algorithm is based on the inversion of the surface representation of u in terms of the boundary values $(u, \partial_\nu u)_{|\Gamma_1}$ and $(u,\ \partial_\nu u)_{|\Gamma_2}$. More precisely, since $u \in H^1(\Omega_1 \setminus \Omega_2)$ satisfies the Helmholtz equation in $\Omega_1 \setminus \Omega_2$, then u has the following representation:

$$u(x) = -DL_{\Gamma_1}(u_{|\Gamma 1}) + SL_{\Gamma_1}(\partial_\nu u_{|\Gamma 1}) + DL_{\Gamma_2}(u_{|\Gamma 2}) - SL_{\Gamma_2}(\partial_\nu u_{|\Gamma 2}), \qquad \forall x \in \Omega_1 \setminus \Omega_2 \quad (6.2)$$

where

$$SL_{\Gamma_i}\psi(x) := \int_{\Gamma_i} \psi(y)\Phi(x,y)ds(y), \quad DL_{\Gamma_i}\varphi(x) := \int_{\Gamma_i} \varphi(y)\frac{\partial\Phi(x,y)}{\partial\nu(y)}ds(y),$$

for $x \in \mathbf{R}^m \setminus \Gamma_i,\ i = 1, 2$, with Φ the Green function defined by

$$\Phi(x,y) := \begin{cases} \dfrac{1}{4\pi}\dfrac{e^{ik\sqrt{n}|x-y|}}{|x-y|} & m = 3 \\ \dfrac{i}{4}H_0^{(1)}(k\sqrt{n}|x-y|) & m = 2 \end{cases} \quad (6.3)$$

for $x \neq y$ and $H_0^{(1)}$ being the Hankel function of the first kind of order zero. Taking the trace and the normal trace of u on Γ_1 and using the trace properties of double and single layer potentials, we obtain the following identities

$$f = -K_{\Gamma_1}(f) + \frac{f}{2} + S_{\Gamma_1}(g) + DL_{\Gamma_2\to\Gamma_1}(u_{|\Gamma_2}) - SL_{\Gamma_2\to\Gamma_1}(\partial_\nu u_{|\Gamma_2}) \quad (6.4)$$

$$g = -T_{\Gamma_1}(f) + K'_{\Gamma_1}(g) + \frac{g}{2} + TL_{\Gamma_2\to\Gamma_1}(u_{|\Gamma_2}) - DL'_{\Gamma_2\to\Gamma_1}(\partial_\nu u_{|\Gamma_2}) \quad (6.5)$$

We recall that the boundary integral operators

$$S_{\Gamma_i} : H^{-1/2}(\Gamma_i) \to H^{1/2}(\Gamma_i) \qquad K_{\Gamma_i} : H^{1/2}(\Gamma_i) \to H^{1/2}(\Gamma_i)$$
$$K'_{\Gamma_i} : H^{-1/2}(\Gamma_i) \to H^{-1/2}(\Gamma_i) \qquad T_{\Gamma_i} : H^{1/2}(\Gamma_i) \to H^{-1/2}(\Gamma_i)$$

are defined for regular densities ψ and φ by

$$S_{\Gamma_i}\psi(x) := \int_{\Gamma_i} \psi(y)\Phi(x,y)ds(y), \qquad K_{\Gamma_i}\varphi(x) := \int_{\Gamma_i} \varphi(y)\frac{\partial\Phi(x,y)}{\partial\nu(y)}ds(y),$$
$$K'_{\Gamma_i}\psi(x) := \int_{\Gamma_i} \psi(y)\frac{\partial\Phi(x,y)}{\partial\nu(x)}ds(y), \quad T_{\Gamma_i}\varphi(x) := \lim_{\epsilon\longrightarrow 0}\frac{\partial}{\partial\nu(x)}\int_{\Gamma_i,|x-y|>\epsilon} \varphi(y)\frac{\partial\Phi(x,y)}{\partial\nu(y)}ds(y)$$

for $x \in \Gamma_i$. The boundary integral operators for $i \neq j, \quad i,j = 1,2$

$$SL_{\Gamma_i\to\Gamma_j} : H^{-1/2}(\Gamma_i) \longrightarrow H^{1/2}(\Gamma_j) \qquad DL_{\Gamma_i\to\Gamma_j} : H^{1/2}(\Gamma_i) \longrightarrow H^{1/2}(\Gamma_j)$$
$$DL'_{\Gamma_i\to\Gamma_j} : H^{-1/2}(\Gamma_i) \longrightarrow H^{-1/2}(\Gamma_j) \qquad TL_{\Gamma_i\to\Gamma_j} : H^{1/2}(\Gamma_i) \longrightarrow H^{-1/2}(\Gamma_j)$$

are defined for regular densities ψ and φ by

$$SL_{\Gamma_i\to\Gamma_j}\psi(x) := \int_{\Gamma_i} \psi(y)\Phi(x,y)ds(y), \qquad DL_{\Gamma_i\to\Gamma_j}\varphi(x) := \int_{\Gamma_i} \varphi(y)\frac{\partial\Phi(x,y)}{\partial\nu(y)}ds(y),$$
$$DL'_{\Gamma_i\to\Gamma_j}\psi(x) := \int_{\Gamma_i} \psi(y)\frac{\partial\Phi(x,y)}{\partial\nu(x)}ds(y), \quad TL_{\Gamma_i\to\Gamma_j}\varphi(x) := \frac{\partial}{\partial\nu(x)}\int_{\Gamma_i} \varphi(y)\frac{\partial\Phi(x,y)}{\partial\nu(y)}ds(y)$$

for $x \in \Gamma_j$.

We observe that, since $\Gamma_i \neq \Gamma_j$, the kernels of $DL_{\Gamma_i\to\Gamma_j}, SL_{\Gamma_i\to\Gamma_j}, DL'_{\Gamma_i\to\Gamma_j}, TL_{\Gamma_i\to\Gamma_j}$ are continuous and therefore these operators are compact.

Equations (6.4) and (6.5) can be written in a matrix form as

$$-\begin{bmatrix} DL_{\Gamma_2\to\Gamma_1} & -SL_{\Gamma_2\to\Gamma_1} \\ TL_{\Gamma_2\to\Gamma_1} & -DL'_{\Gamma_2\to\Gamma_1} \end{bmatrix}\begin{bmatrix} u_{|\Gamma_2} \\ \partial_\nu u_{|\Gamma_2} \end{bmatrix} = \begin{bmatrix} -K_{\Gamma_1} - \frac{I}{2} & S_{\Gamma_1} \\ -T_{\Gamma_1} & K'_{\Gamma_1} - \frac{I}{2} \end{bmatrix}\begin{bmatrix} f \\ g \end{bmatrix}$$

Using the Calderón projector $P_{\Gamma_1} : H^{1/2}(\Gamma_1) \times H^{-1/2}(\Gamma_1) \longrightarrow H^{1/2}(\Gamma_1) \times H^{-1/2}(\Gamma_1)$ that satisfies $P^2_{\Gamma_1} = P_{\Gamma_1}$ (see [65]) defined by

$$P_{\Gamma_1}\begin{bmatrix} f \\ g \end{bmatrix} := \begin{bmatrix} -K_{\Gamma_1} + \frac{I}{2} & S_{\Gamma_1} \\ -T_{\Gamma_1} & K'_{\Gamma_1} + \frac{I}{2} \end{bmatrix}\begin{bmatrix} f \\ g \end{bmatrix} \tag{6.6}$$

and the operator $T_{\Gamma_2\to\Gamma_1} : H^{1/2}(\Gamma_2) \times H^{-1/2}(\Gamma_2) \longrightarrow H^{1/2}(\Gamma_1) \times H^{-1/2}(\Gamma_1)$ defined by

$$T_{\Gamma_2\to\Gamma_1}\begin{bmatrix} \varphi \\ \psi \end{bmatrix} := -\begin{bmatrix} DL_{\Gamma_2\to\Gamma_1} & -SL_{\Gamma_2\to\Gamma_1} \\ TL_{\Gamma_2\to\Gamma_1} & -DL'_{\Gamma_2\to\Gamma_1} \end{bmatrix}\begin{bmatrix} \varphi \\ \psi \end{bmatrix},$$

we obtain the following equation

$$T_{\Gamma_2\to\Gamma_1}\begin{bmatrix} u_{|\Gamma_2} \\ \partial_\nu u_{|\Gamma_2} \end{bmatrix} = (P_{\Gamma_1} - I)\begin{bmatrix} f \\ g \end{bmatrix}. \tag{6.7}$$

Similarly, taking the trace and the normal trace of u on Γ_2, we obtain a second relationship between (f, g) and $(u, \partial_\nu u)_{\Gamma_2}$

$$u_{|\Gamma_2} = -DL_{\Gamma_1\to\Gamma_2}(f) + SL_{\Gamma_1\to\Gamma_2}(g) + K_{\Gamma_2}(u_{|\Gamma_2}) + \frac{u_{|\Gamma_2}}{2} - S_{\Gamma_2}(\partial_\nu u_{|\Gamma_2}) \tag{6.8}$$

$$\partial_\nu u_{|\Gamma_2} = -TL_{\Gamma_1\to\Gamma_2}(f) + DL'_{\Gamma_1\to\Gamma_2}(g) + T_{\Gamma_2}(u_{|\Gamma_2}) - K'_{\Gamma_2}(\partial_\nu u_{|\Gamma_2}) + \frac{\partial_\nu u_{|\Gamma_2}}{2} \tag{6.9}$$

Therefore, we also have

$$P_{\Gamma_2}\begin{bmatrix} u_{|\Gamma_2} \\ \\ \partial_\nu u_{|\Gamma_2} \end{bmatrix} = T_{\Gamma_2\to\Gamma_1}\begin{bmatrix} f \\ \\ g \end{bmatrix} \tag{6.10}$$

with $P_{\Gamma_2} : H^{1/2}(\Gamma_2) \times H^{-1/2}(\Gamma_2) \longrightarrow H^{1/2}(\Gamma_2) \times H^{-1/2}(\Gamma_2)$ defined by

$$P_{\Gamma_2}\begin{bmatrix} \varphi \\ \\ \psi \end{bmatrix} = \begin{bmatrix} -K_{\Gamma_2} + \frac{I}{2} & S_{\Gamma_2} \\ \\ -T_{\Gamma_2} & K'_{\Gamma_2} + \frac{I}{2} \end{bmatrix}\begin{bmatrix} \varphi \\ \\ \psi \end{bmatrix} \tag{6.11}$$

and $T_{\Gamma_1\to\Gamma_2} : H^{1/2}(\Gamma_1) \times H^{-1/2}(\Gamma_1) \longrightarrow H^{1/2}(\Gamma_2) \times H^{-1/2}(\Gamma_2)$

$$T_{\Gamma_1\to\Gamma_2}\begin{bmatrix} f \\ \\ g \end{bmatrix} = -\begin{bmatrix} DL_{\Gamma_1\to\Gamma_2} & -SL_{\Gamma_1\to\Gamma_2} \\ \\ TL_{\Gamma_1\to\Gamma_2} & -DL'_{\Gamma_1\to\Gamma_2} \end{bmatrix}\begin{bmatrix} f \\ \\ g \end{bmatrix}$$

Regrouping (6.7) and (6.10) we end up with the following system

$$\begin{bmatrix} T_{\Gamma_2\to\Gamma_1} \\ \\ P_{\Gamma_2} \end{bmatrix}\begin{bmatrix} u_{|\Gamma_2} \\ \\ \partial_\nu u_{|\Gamma_2} \end{bmatrix} = \begin{bmatrix} (P_{\Gamma_1} - I) \\ \\ T_{\Gamma_1\to\Gamma_2} \end{bmatrix}\begin{bmatrix} f \\ \\ g \end{bmatrix} \tag{6.12}$$

In order to simplify the notation, we define
$A : H^{1/2}(\Gamma_2) \times H^{-1/2}(\Gamma_2) \longrightarrow H^{1/2}(\Gamma_1) \times H^{-1/2}(\Gamma_1) \times H^{1/2}(\Gamma_2) \times H^{-1/2}(\Gamma_2)$ by:

$$A\begin{bmatrix} \varphi \\ \\ \psi \end{bmatrix} = \begin{bmatrix} T_{\Gamma_2\to\Gamma_1} \\ \\ P_{\Gamma_2} \end{bmatrix}\begin{bmatrix} \varphi \\ \\ \psi \end{bmatrix} \tag{6.13}$$

and $B : H^{1/2}(\Gamma_1) \times H^{-1/2}(\Gamma_1) \longrightarrow H^{1/2}(\Gamma_1) \times H^{-1/2}(\Gamma_1) \times H^{1/2}(\Gamma_2) \times H^{-1/2}(\Gamma_2)$ by:

$$B\begin{bmatrix} \varphi \\ \\ \psi \end{bmatrix} = \begin{bmatrix} (P_{\Gamma_1} - I) \\ \\ T_{\Gamma_1\to\Gamma_2} \end{bmatrix}\begin{bmatrix} \varphi \\ \\ \psi \end{bmatrix} \tag{6.14}$$

So that our problem can be simply written as

$$A \begin{bmatrix} u_{|\Gamma_2} \\ \\ \partial_\nu u_{|\Gamma_2} \end{bmatrix} = B \begin{bmatrix} f \\ \\ g \end{bmatrix}. \tag{6.15}$$

Solving our Cauchy problem then consists in inverting the operator A. The ill-posedness of this problem can be seen in the compactness of the operator $T_{\Gamma_2 \to \Gamma_1}$ (as indicated previously all of its components are integral operators with smooth kernels). There is also another issue due to the fact that this operator is not injective. Moreover, the operator P_{Γ_2} is a Calderón projector (see [65]) and is only invertible from the complementary of its kernel to itself. Consequently, a regularization is needed. Before the use of a regularization method, the injectivity of the operator A should be proved. We also prove that $\overline{Range(A)} = \overline{Range(B)}$ which ensures that the right hand side of (6.15) is always in the closure of the range of A. To tackle this latter issue and the issue of the injectivity, we first need to characterize the range and the kernel of $T_{\Gamma_i \to \Gamma_j}, i \neq j$.
To simplify the notation we introduce the following spaces ($i = 1, 2$):

$$\begin{aligned} \mathcal{H}(\Omega_i) &:= \{u \in H^1(\Omega_i), \quad \Delta u + k^2 n u = 0 \quad \text{in} \quad \Omega_i\} \\ \tilde{\mathcal{H}}(\Omega_i) &:= \{u \in H^1_{loc}(\mathbf{R}^m \setminus \Omega_1), \quad \Delta u + k^2 n u = 0 \quad \text{in} \quad \mathbf{R}^m \setminus \Omega_i \quad \text{and } u \text{ satisfies } \textit{the R.C}\} \end{aligned}$$

where $R.C$ refers to the following radiation condition

$$\lim_{r=|x| \to +\infty} r^{\frac{m-1}{2}} (\partial_r u - ikn u) = 0, \tag{6.16}$$

uniformally in all directions $\hat{x} = \frac{x}{|x|}$.

Lemma 40.

$$\begin{aligned} a) \quad Ker(T_{\Gamma_2 \to \Gamma_1}) &= \{(u, \partial_\nu u)_{|\Gamma_2}, \quad \textit{such that} \quad u \in \mathcal{H}(\Omega_2)\} \\ &= Ker(P_{\Gamma_2} - I) \\ b) \quad Ker(T_{\Gamma_1 \to \Gamma_2}) &= \{(u, \partial_\nu u)_{|\Gamma_1}, \quad \textit{such that} \quad u \in \tilde{\mathcal{H}}(\Omega_1)\} \\ &= Ker(P_{\Gamma_1}) \end{aligned}$$

Proof. We start by proving a).
• Let $(\varphi, \psi) \in H^{1/2}(\Gamma_2) \times H^{-1/2}(\Gamma_2)$ such that $T_{\Gamma_2 \to \Gamma_1}(\varphi, \psi) = 0$.
We denote by v the solution of the Helmholtz equation in $\mathbf{R}^m \setminus \Gamma_2$ given by:

$$v = -DL_{\Gamma_2}(\varphi) + SL_{\Gamma_2}(\psi), \qquad \text{in} \quad \mathbf{R}^m \setminus \Gamma_2. \tag{6.17}$$

Knowing that $T_{\Gamma_2\to\Gamma_1}(\varphi,\psi)=0$, it is clear that $(v,\partial_\nu v)$ vanishes on Γ_1. Using the unique continuation principle (see Corollary 13), we get that $v=0$ in $\mathbf{R}^m\setminus\Omega_2$.
Consequently, we obtain

$$(v^+,\partial_\nu v^+)_{|\Gamma_2}=(0,0)\qquad\text{on }\Gamma_2$$

where the following notation will be used

$$v^{\pm}_{\Gamma_i}(x):=\lim_{h\to 0^+}v(x\pm h\nu)\quad\text{and}\quad\partial_\nu v^{\pm}_{\Gamma_i}(x):=\lim_{h\to 0^+}\nu\cdot\nabla v(x\pm h\nu)\quad\text{for}\quad x\in\Gamma_2.$$

Therefore

$$[v]_{|\Gamma_2}=v^+_{|\Gamma_2}-v^-_{|\Gamma_2}=v^-_{|\Gamma_2}=\varphi\qquad\text{and}\qquad[\partial_\nu v]_{|\Gamma_2}=\partial_\nu v^+_{|\Gamma_2}-\partial_\nu v^-_{|\Gamma_2}=\partial_\nu v^-_{|\Gamma_2}=\psi$$

Then we obtain $Ker(T_{\Gamma_2\to\Gamma_1})\subset\{(u,\partial_\nu u)_{|\Gamma_2},\quad\text{such that}\quad u\in\mathcal{H}(\Omega_2)\}$.
• Let $(\varphi,\psi)=(u,\partial_\nu u)_{|\Gamma_2}$ where $u\in\mathcal{H}(\Omega_2)$ For $x\in\Omega_1\setminus\Omega_2$ we have, using the Green formula in Ω_2

$$\int_{\Gamma_2}\partial_\nu u(y)\Phi(x,y)ds(y)-\int_{\Gamma_2}u(y)\partial_\nu\Phi(x,y)ds(y)=0$$

Therefore, the function v be defined by (6.17) satisfies $v=0$ in $\Omega_1\setminus\Omega_2$. Hence we have:

$$(\partial_\nu v^-,v^-)_{\Gamma_1}=0\qquad\text{and}\qquad T_{\Gamma_2\to\Gamma_1}(\varphi,\psi)=(0,0).$$

Consequently

$$Ker(T_{\Gamma_2\to\Gamma_1})=\{(u,\partial_\nu u)_{\Gamma_2},\quad\text{such that}\quad u\in\mathcal{H}(\Omega_2)\}.$$

We can give another characterization of $Ker(T_{\Gamma_2\to\Gamma_1})$ using the Calderón projector P_{Γ_2}. In fact, if $(\varphi,\psi)\in Ker(T_{\Gamma_2\to\Gamma_1})$ then $(\varphi,\psi)=(v,\partial_\nu v)_{|\Gamma_2}$ where v satisfies the Helmholtz equation inside Ω_2 and be represented as follows:

$$v=-DL_{\Gamma_2}(v_{|\Gamma_2})+SL_{\Gamma_2}(\partial_\nu v_{|\Gamma_2})\qquad\text{in}\quad\Omega_2.$$

Using the trace and the normal derivative trace of v on Γ_2 we obtain

$$\begin{aligned}v_{|\Gamma_2}&=-K_{\Gamma_2}(v_{|\Gamma_2})+\frac{v_{|\Gamma_2}}{2}+S_{|\Gamma_2}(\partial_\nu v_{|\Gamma_2}),\\ \partial_\nu v_{|\Gamma_2}&=-T_{\Gamma_2}(v_{|\Gamma_2})+K'_{|\Gamma_2}(\partial_\nu v_{|\Gamma_2})+\frac{\partial_\nu v_{|\Gamma_2}}{2}.\end{aligned}$$

Consequently

$$\begin{aligned}-K_{\Gamma_2}(v_{|\Gamma_2})-\frac{v_{|\Gamma_2}}{2}+S_{|\Gamma_2}(\partial_\nu v_{|\Gamma_2})&=0\\ -T_{\Gamma_2}(v_{|\Gamma_2})+K'_{|\Gamma_2}(\partial_\nu v_{|\Gamma_2})-\frac{\partial_\nu v_{|\Gamma_2}}{2}&=0\end{aligned}$$

which proves that $(v, \partial_\nu v)_{\Gamma_2} \in Ker(P_{\Gamma_2} - I)$. On the other hand let $(\varphi, \psi) \in Ker(P_{\Gamma_2} - I)$ and let the function v be defined by

$$v = -DL_{\Gamma_2}(\psi) + SL_{|\Gamma_2}(\varphi), \qquad \text{in} \quad \mathbf{R}^m \setminus \Gamma_2.$$

v satisfies the Helmholtz equation with index n in $\mathbf{R}^m \setminus \Gamma_2$ and satisfying the radiation condition. Using trace formulas for double and single layer potential, we obtain

$$\begin{pmatrix} v^+_{\Gamma_2} \\ \\ \partial_\nu v^+_{\Gamma_2} \end{pmatrix} = (P_{\Gamma_2} - I) \begin{pmatrix} \psi \\ \\ \varphi \end{pmatrix}$$

Since $(\varphi, \psi) \in Ker(P_{\Gamma_2} - I)$ then we have

$$(v^+, \partial_\nu v^+)_{|\Gamma_2} = (0, 0)$$

Using the unique continuation principle (see Corollary 13), then we have v is zero outside Ω_2 which prove that $(v, \partial_\nu v)_{|\Gamma_1}$ is also zero and consequently $(\varphi, \psi) \in Ker(T_{\Gamma_2 \to \Gamma_1})$.
The proof of b) follows the same lines as the proof of a). □

We now characterize the range of the operator $T_{\Gamma_2 \to \Gamma_1}$. We recall that we have

$$\overline{Range(T_{\Gamma_2 \to \Gamma_1})} = (Ker(T^*_{\Gamma_2 \to \Gamma_1}))^\perp$$

Let $(\varphi, \psi) \in H^{1/2}(\Gamma_2) \times H^{-1/2}(\Gamma_2)$, and $(\varphi', \psi') \in H^{-1/2}(\Gamma_1) \times H^{1/2}(\Gamma_1)$, so we have:

$$\begin{aligned} \langle T_{\Gamma_2 \to \Gamma_1}(\varphi, \psi), (\varphi', \psi') \rangle = & \int_{\Gamma_1} \int_{\Gamma_2} \partial_{\nu(y)} \Phi(x, y) \varphi(y) \overline{\varphi'(x)} - \int_{\Gamma_1} \int_{\Gamma_2} \Phi(x, y) \psi(y) \overline{\varphi'(x)} \\ & + \int_{\Gamma_1} \int_{\Gamma_2} \partial_{\nu(x)} \partial_{\nu(y)} \Phi(x, y) \varphi(y) \overline{\varphi'(x)} - \int_{\Gamma_1} \int_{\Gamma_2} \partial_\nu(x) \Phi(x, y) \psi(y) \overline{\psi'(x)} \end{aligned} \quad (6.18)$$

Therefore,

$$\langle T_{\Gamma_2 \to \Gamma_1}(\varphi, \psi), (\varphi', \psi') \rangle = \int_{\Gamma_2} \varphi(y) \overline{\left[K'(\varphi') + \overline{T}(\psi')\right]} - \int_{\Gamma_2} \psi(y) \overline{\left[\overline{S}(\varphi') + \overline{K}(\psi')\right]} \quad (6.19)$$

Consequently, $T^*_{\Gamma_2 \to \Gamma_1}$ is given by:

$$T^*_{\Gamma_2 \to \Gamma_1} \begin{bmatrix} \varphi' \\ \\ \psi' \end{bmatrix} = \begin{bmatrix} \overline{DL'}_{\Gamma_1 \to \Gamma_2} & \overline{TL}_{\Gamma_1 \to \Gamma_2} \\ \\ -\overline{SL}_{\Gamma_1 \to \Gamma_2} & -\overline{DL}_{\Gamma_1 \to \Gamma_2} \end{bmatrix} \begin{bmatrix} \varphi' \\ \\ \psi' \end{bmatrix}$$

$\overline{DL'}_{\Gamma_1 \to \Gamma_2}$, $\overline{SL}_{\Gamma_1 \to \Gamma_2}$, $\overline{TL}_{\Gamma_1 \to \Gamma_2}$, $\overline{DL}_{\Gamma_1 \to \Gamma_2}$ have the same definition as $DL'_{\Gamma_1 \to \Gamma_2}$, $SL_{\Gamma_1 \to \Gamma_2}$, $TL_{\Gamma_1 \to \Gamma_2}$, $DL_{\Gamma_1 \to \Gamma_2}$ with Φ replaced by $\overline{\Phi}$. The next step is to characterize $Ker(T^*_{\Gamma_2 \to \Gamma_1})$.

We shall use the adjoint $P^*_{\Gamma_1}$ of P_{Γ_1}. Similar calculations as above show that $P^*_{\Gamma_1}$: $H^{-1/2}(\Gamma_1) \times H^{1/2}(\Gamma_1) \longrightarrow H^{-1/2}(\Gamma_1) \times H^{1/2}(\Gamma_1)$ is given by

$$P_{\Gamma_1^*} \begin{bmatrix} \varphi \\ \\ \psi \end{bmatrix} := \begin{bmatrix} -\overline{K'_{\Gamma_1}} + \frac{I}{2} & -\overline{T_{\Gamma_1}} \\ \\ \overline{S}_{\Gamma_1} & \overline{K_{\Gamma_1}} + \frac{I}{2} \end{bmatrix} \begin{bmatrix} \varphi \\ \\ \psi \end{bmatrix} \tag{6.20}$$

where $\overline{K'}_{\Gamma_1\to\Gamma_2}$, $\overline{S}_{\Gamma_1\to\Gamma_2}$, $\overline{T}_{\Gamma_1\to\Gamma_2}$, $\overline{K}_{\Gamma_1\to\Gamma_2}$ have the same definition as $K'_{\Gamma_1\to\Gamma_2}$, $S_{\Gamma_1\to\Gamma_2}$, $T_{\Gamma_1\to\Gamma_2}$, $K_{\Gamma_1\to\Gamma_2}$ with Φ replaced by $\overline{\Phi}$. $P_{\Gamma_1^*}$ is also a projector i.e $P_{\Gamma_1^*}P_{\Gamma_1^*} = P_{\Gamma_1^*}$.
We prove the following lemma:

Lemma 41.

$$\begin{aligned} Ker(T^*_{\Gamma_2\to\Gamma_1}) &= \{(\partial_\nu \bar{u}, -\bar{u})_{|\Gamma_1} \quad \textit{such that} \quad u \in \tilde{\mathcal{H}}(\Omega_1)\} \\ &= Ker(P^*_{\Gamma_1} - I). \end{aligned}$$

$$Ker(T^*_{\Gamma_2\to\Gamma_1}) = Ker(P^*_{\Gamma_2}).$$

Proof. • Let $(\varphi', \psi') \in H^{-1/2}(\Gamma_2) \times H^{1/2}(\Gamma_2)$ such that $T^*_{\Gamma_2\to\Gamma_1}(\varphi', \psi') = 0$. We define v by:

$$v(x) = -\overline{SL}_{\Gamma_1}(\varphi') - \overline{DL}_{\Gamma_1}(\psi'), \qquad \text{for all} \quad x \in \mathbf{R}^m \setminus \Gamma_1 \tag{6.21}$$

v satisfies the Helmholtz equation with index $\bar{n}$ in $\mathbf{R}^m \setminus \Gamma_1$ and $\bar{v}$ satisfies the radiation condition. Using the fact that

$$T^*_{\Gamma_2\to\Gamma_1}(\varphi', \psi') = 0 \qquad \Longleftrightarrow (v, \partial_\nu v)_{|\Gamma_2} = (0, 0)$$

Using the unique continuation principle (see Corollary 13), we obtain $v = 0$ in Ω_1 and consequently

$$(v^-, \partial_\nu v^-)_{|\Gamma_1} = (0, 0) \quad \text{on} \quad \Gamma_1$$

On the other hand

$$[v]_{|\Gamma_1} = v^+_{|\Gamma_1} - v^-_{|\Gamma_1} = v^+_{|\Gamma_1} = -\psi' \qquad \text{and} \qquad [\partial_\nu v]_{|\Gamma_1} = \partial_\nu v^+_{|\Gamma_1} - \partial_\nu v^-_{|\Gamma_1} = \partial_\nu v^+_{|\Gamma_1} = \varphi'$$

Finally we have

$$(\varphi', \psi') = (\overline{\partial_\nu \overline{v^+}}, \overline{-\overline{v^+}})_{|\Gamma_1} \qquad \Longrightarrow \qquad (\varphi', \psi') = (\overline{\partial_\nu u^+}, -\overline{u^+})_{|\Gamma_1}$$

where $u = \bar{v} \in \tilde{\mathcal{H}}(\Omega_1)$. Hence

$$Ker(T^*_{\Gamma_2\to\Gamma_1}) \subset \{(\partial_\nu \bar{u}, -\bar{u})_{|\Gamma_1} \quad \text{such that} \quad u \in \tilde{\mathcal{H}}(\Omega_1)\}$$

• Let $(\varphi', \psi') = (\partial_\nu \bar{u}, -\bar{u})_{|\Gamma_1}$, where $u \in \tilde{\mathcal{H}}(\Omega_1)$. We recall that

$$\forall x \in \Omega_1, \qquad \Delta\Phi(.,x) + k^2 n \Phi(.,x) = 0 \quad \text{in} \quad \mathbf{R}^m \setminus \overline{\Omega_1}$$

Using the fact that both functions Φ and u satisfy the same Helmholtz equation in $\mathbf{R}^m \setminus \overline{\Omega_1}$ and the radiation condition then we have

$$\int_{\Gamma_1} \left(\partial_\nu \bar{u}(y) \overline{\Phi}(x,y) - \partial_\nu \overline{\Phi}(x,y) \bar{u}(y) \right) ds(y) = 0 \qquad \forall x \in \Omega_1.$$

Hence the function v defined by (6.21) is zero in Ω_1. Consequently

$$T^*_{\Gamma_2 \to \Gamma_1}(\varphi', \psi') = 0.$$

This proves that

$$Ker(T^*_{\Gamma_2 \to \Gamma_1}) = \{(\partial_\nu \bar{u}, -\bar{u})_{|\Gamma_1} \quad \text{such that,} \quad u \in \tilde{\mathcal{H}}(\Omega_1)\}.$$

We now prove that $Ker(T^*_{\Gamma_2 \to \Gamma_1}) = Ker(P^*_{\Gamma_1} - I)$. In fact, if $(\varphi, \psi) \in Ker(T^*_{\Gamma_2 \to \Gamma_1})$ then $(\varphi, \psi) = (\partial_\nu v, -v)_{|\Gamma_1}$ where $\bar{v} \in \tilde{\mathcal{H}}(\Omega_1)$ and using the integral equation v can be represented as follows:

$$v(x) = \overline{DL}_{\Gamma_1}(v_{|\Gamma_1})(x) - \overline{SL}_{\Gamma_1}(\partial_\nu v_{|\Gamma_1})(x). \qquad \forall x \in \mathbf{R}^m \setminus \Omega_1. \tag{6.22}$$

Using the trace and the normal derivative trace of v on Γ_1 we obtain

$$\begin{aligned} v_{|\Gamma_1} &= \overline{K}_{\Gamma_1}(v_{|\Gamma_1}) + \frac{v_{|\Gamma_1}}{2} - \overline{S}_{|\Gamma_1}(\partial_\nu v_{|\Gamma_1}), \\ \partial_\nu v_{|\Gamma_1} &= \overline{T}_{\Gamma_1}(v_{|\Gamma_1}) - \overline{K'}_{\Gamma_1}(\partial_\nu v_{|\Gamma_1}) + \frac{\partial_\nu v_{|\Gamma_1}}{2}. \end{aligned}$$

Hence

$$\begin{aligned} \psi &= \overline{K}_{\Gamma_1}(\psi) + \frac{\psi}{2} + \overline{S}_{|\Gamma_1}(\varphi), \\ \varphi &= -\overline{T}_{\Gamma_1}(\psi) - \overline{K'}_{\Gamma_1}(\varphi) + \frac{\varphi}{2}. \end{aligned}$$

Consequently

$$\begin{aligned} \overline{K}_{\Gamma_1}(\psi) - \frac{\psi}{2} + \overline{S}_{|\Gamma_1}(\varphi) &= 0 \\ -\overline{T}_{\Gamma_1}(\psi) - \overline{K'}_{\Gamma_1}(\varphi) - \frac{\varphi}{2} &= 0 \end{aligned}$$

which proves that $(\varphi, \psi) \in Ker(P^*_{\Gamma_1} - I)$ and consequently $Ker(T^*_{\Gamma_2 \to \Gamma_1}) \subset Ker(P^*_{\Gamma_1} - I)$. On the other hand let $(\varphi, \psi) \in Ker(P^*_{\Gamma_1} - I)$ and let the function v defined by

$$v = \overline{DL}_{\Gamma_1}(\psi) + \overline{SL}_{|\Gamma_1}(\varphi), \qquad \text{in} \quad \mathbf{R}^m \setminus \Gamma_1$$

This function satisfies the Helmholtz equation with index $\bar{n}$ in $\mathbf{R}^m \setminus \Gamma_1$. Using the trace formulas of the double layer and simple layer potential on Γ_1, we obtain

$$\begin{pmatrix} \partial_\nu v^-_{\Gamma_1} \\ \\ v^-_{\Gamma_1} \end{pmatrix} = \left(P^*_{\Gamma_1} - I\right) \begin{pmatrix} \varphi \\ \\ \psi \end{pmatrix}$$

Since $(\varphi, \psi) \in Ker(P^*_{\Gamma_1} - I)$ then we have

$$(v^-, \partial_\nu v^-)_{|\Gamma_1} = (0, 0)$$

Using the unique continuation principle (see Corollary 13), then we have v is zero in Ω_1 which prove that $(v, \partial_\nu v)_{|\Gamma_2}$ and consequently $(\varphi, \psi) \in Ker(T^*_{\Gamma_2 \to \Gamma_1})$.
The proof of $Ker(T^*_{\Gamma_1 \to \Gamma_2})$ follows the same lines as the proof of $Ker(T^*_{\Gamma_2 \to \Gamma_1})$. □

Corollary 42.

$$\begin{array}{lll} \overline{Range(T_{\Gamma_2 \to \Gamma_1})} = & Ker(P_{\Gamma_1}) & = Range(P_{\Gamma_1} - I) \\ \overline{Range(T_{\Gamma_1 \to \Gamma_2})} = & Ker(P_{\Gamma_2} - I) & = Ker(P_{\Gamma_2}) \end{array}$$

Proof. the proof of this corollary can be deduced directly from Lemma 41 and using the fact that both of P_{Γ_1}, $P^*_{\Gamma_1}$, P_{Γ_2} and $P^*_{\Gamma_2}$ are a Calderón projector. We recall that we have

$$\begin{array}{rcl} \overline{Range(T_{\Gamma_2 \to \Gamma_1})} & = & \left(Ker(T^*_{\Gamma_2 \to \Gamma_1})\right)^\perp, \\ \overline{Range(T_{\Gamma_1 \to \Gamma_2})} & = & \left(Ker(T^*_{\Gamma_1 \to \Gamma_2})\right)^\perp \end{array}$$

On the other hand we have

$$\begin{array}{lll} \left(Ker(T^*_{\Gamma_2 \to \Gamma_1})\right)^\perp = & \left(Ker(P^*_{\Gamma_1} - I)\right)^\perp = \overline{Range(P_{\Gamma_1} - I)} & = Ker(P_{\Gamma_1}), \\ \left(Ker(T^*_{\Gamma_1 \to \Gamma_2})\right)^\perp = & \left(Ker(P^*_{\Gamma_2})\right)^\perp = \overline{Range(P_{\Gamma_2})} & = Ker(P_{\Gamma_1} - I). \end{array}$$

□

Lemma 43. *The operator $A : X \to Y$ defined by expression (6.13) is one to one and has a dense range, where $X = H^{1/2}(\Gamma_2) \times H^{-1/2}(\Gamma_2)$ and $Y = Ker(P_{\Gamma_1}) \times Ker(P_{\Gamma_2} - I)$. Moreover $\overline{Range(A)} = \overline{Range(B)}$ where B is defined by (6.14).*

Proof. We start by proving the injectivity of the operator A. Since P_{Γ_2} is a projector then

$$X = Ker(P_{\Gamma_2}) \oplus Range(P_{\Gamma_2}), \quad \text{and for all} \quad u \in X, \quad u = u_1 + u_2$$

where $u_1 \in Ker(P_{\Gamma_2})$ and $u_2 \in Range(P_{\Gamma_2})$. Let $u \in X$ such that $A(u) = 0$ then we have

$$T(u) = 0 \qquad \text{and} \qquad P_{\Gamma_2}(u) = 0.$$

Hence, by linearity

$$T(u) = T(u_1) + T(u_2).$$

Using Lemma 40 then $u_2 \in Ker(T_{\Gamma_2 \to \Gamma_1})$ and consequently we have

$$T(u_1) = 0 \quad \Longrightarrow \quad u_1 = 0. \tag{6.23}$$

On the other hand, we have

$$P_{\Gamma_2}(u) = 0 \quad \Longrightarrow \quad P_{\Gamma_2}(u_2) = 0 \tag{6.24}$$

Since $u_2 \in Range(P_{\Gamma_2})$ and P_{Γ_2} is a projector then

$$P_{\Gamma_2}(u_2) = u_2 \quad \Longrightarrow \quad u_2 = 0.$$

This proves the injectivity of the operator A. On the other hand, for the characterization of the range of the operator A we use Corollary **??** in which we have proved that $\overline{Range(T_{\Gamma_2 \to \Gamma_1})} = Ker(P_{\Gamma_1})$. For the Calderón projector P_{Γ_2} we have $Range(P_{\Gamma_2}) = Ker(P_{\Gamma_2} - I)$ and Consequently we obtain

$$\overline{Range(A)} = Ker(P_{\Gamma_1}) \times Ker(P_{\Gamma_2} - I)$$

Using Corollary 42 we deduce that $\overline{Range(B)} = Ker(P_{\Gamma_1}) \times \overline{Range(T_{\Gamma_1 \to \Gamma_2})}$.

□

Corollary 44. *Let* $(f, g) \in H^{1/2}(\Gamma_1) \times H^{-1/2}(\Gamma_1)$ *and* $(u_{|\Gamma_2}, \partial_\nu u_{|\Gamma_2}) \in H^{1/2}(\Gamma_2) \times H^{-1/2}(\Gamma_2)$ *such that*

$$A \begin{pmatrix} u_{|\Gamma_2} \\ \partial_\nu u_{|\Gamma_2} \end{pmatrix} = B \begin{pmatrix} f \\ g \end{pmatrix}. \tag{6.25}$$

$(f^\delta, g^\delta) \in H^{1/2}(\Gamma_1) \times H^{-1/2}(\Gamma_1)$ *such that*

$$\left\| \begin{pmatrix} f^\delta \\ g^\delta \end{pmatrix} - \begin{pmatrix} f \\ g \end{pmatrix} \right\| \leq \delta$$

Let the Tikhonov solution $(u^\delta, \partial_\nu u^\delta)$ *satisfying*

$$(\alpha(\delta) + A^* A) \begin{pmatrix} u^\delta \\ \partial_\nu u^\delta \end{pmatrix} = A^* B \begin{pmatrix} f^\delta \\ g^\delta \end{pmatrix} \tag{6.26}$$

where $\alpha(\delta)$ is determined using the Morozov discrepancy principle, i.e $\alpha(\delta)$ is the unique solution of

$$\left\| A \begin{pmatrix} u^\delta \\ \partial_\nu u^\delta \end{pmatrix} - B \begin{pmatrix} f^\delta \\ g^\delta \end{pmatrix} \right\| = \delta \|B\| < \left\| B \begin{pmatrix} f^\delta \\ g^\delta \end{pmatrix} \right\| \tag{6.27}$$

Then

$$\left\| \begin{pmatrix} u^\delta \\ \partial_\nu u^\delta \end{pmatrix} - \begin{pmatrix} u \\ \partial_\nu u \end{pmatrix} \right\| \longrightarrow 0 \qquad as \qquad \delta \longrightarrow 0 \tag{6.28}$$

Proof. The proof of this Corollary can be deduced directly from Lemma 43 using the Tikhonov regularization theory and Morozov discrepancy principle. For more details see [41, Theorem 4.17, p 85] □

6.2.2 Numerical validation

The numerical experiments are conducted in a $2D$ setting of the problem. We recall that our algorithm is based on solving the equation (6.26). The efficiency of this approach is tested against synthetic data by solving the scattering problem from a crack illustrated by Figure 6.2.2. The data on Γ_1 is generated using the integral equation approach of Chapter 1. We use 100 discretization points on each boundary with three tests for the crack $\sigma = [-0.25, 0.25] \times \{0\}$ and the point source $x_0 = (-2.5, -2, 5)$.
The first test (a) on which both Γ_1 and Γ_2 are the interior and exterior boundary of an annulus. The second one (b) where the outer geometry is a circle and the inner is a square The third test (c) is where the exterior is the circle and the interior geometry is an ellipse. Test (a) gives a good reconstruction with high precision even when the two circles are not very close (see Figures 6.3, 6.5), which prove that the algorithm is not very sensitive to the distance between the two boundary. Figure 6.4, 6.7, 6.10 show the stability of the algorithm since in the three tests geometry we have a reconstructed data close to the exact data. Note that in the case of a non circular geometry, all tests give also a good approximation but with less precision as compared to the circular case (see Figure 6.8, 6.10). This issue can be tackled by increasing the index of refraction as shown in Figure 6.6, 6.8.

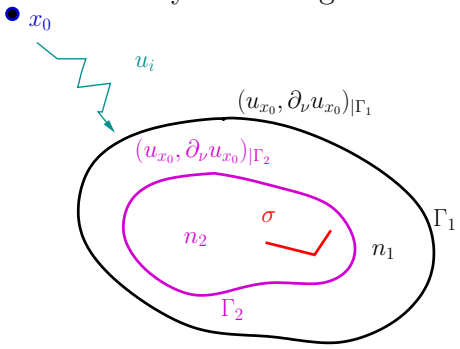

Figure 6.2: Configuration for the simulation of synthetic data.

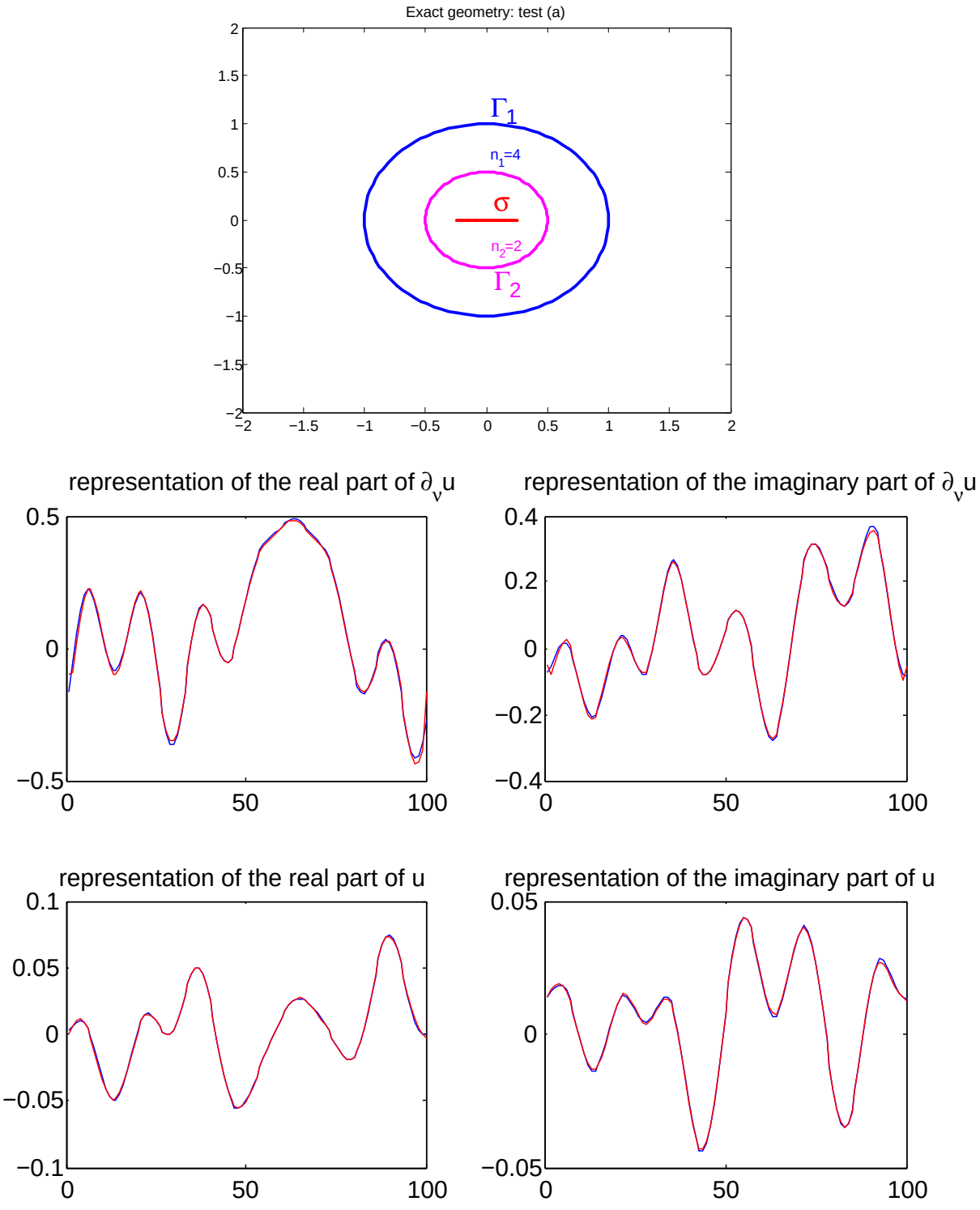

Figure 6.3: Reconstruction of the Cauchy data on Γ_2 in the case of test (a) using the data completion algorithm (red) the exact data (blue) without added noise.

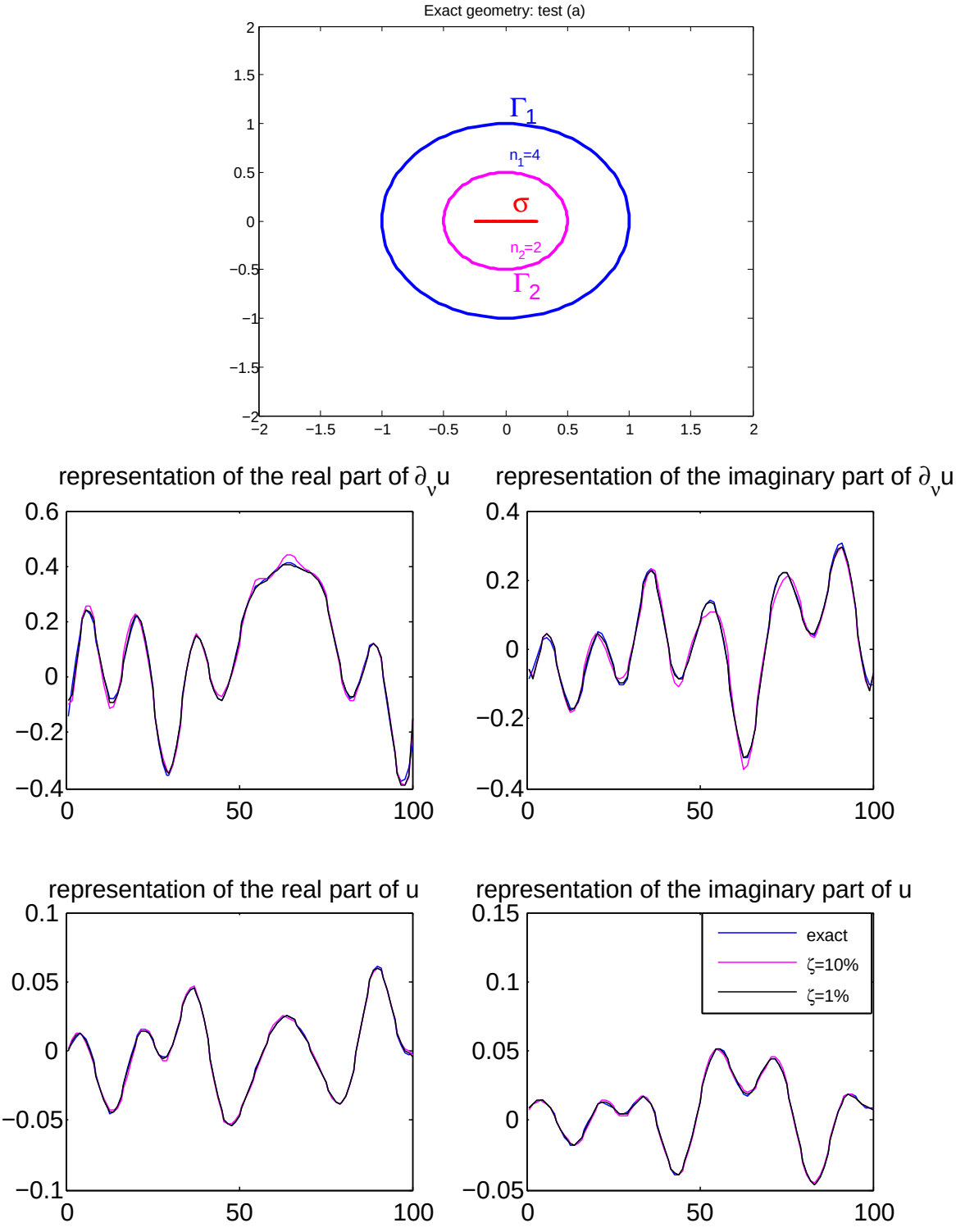

Figure 6.4: Reconstruction of the Cauchy data on Γ_2 in the case of test (a) using the data completion algorithm (red) the exact data (blue) with added noise ζ.

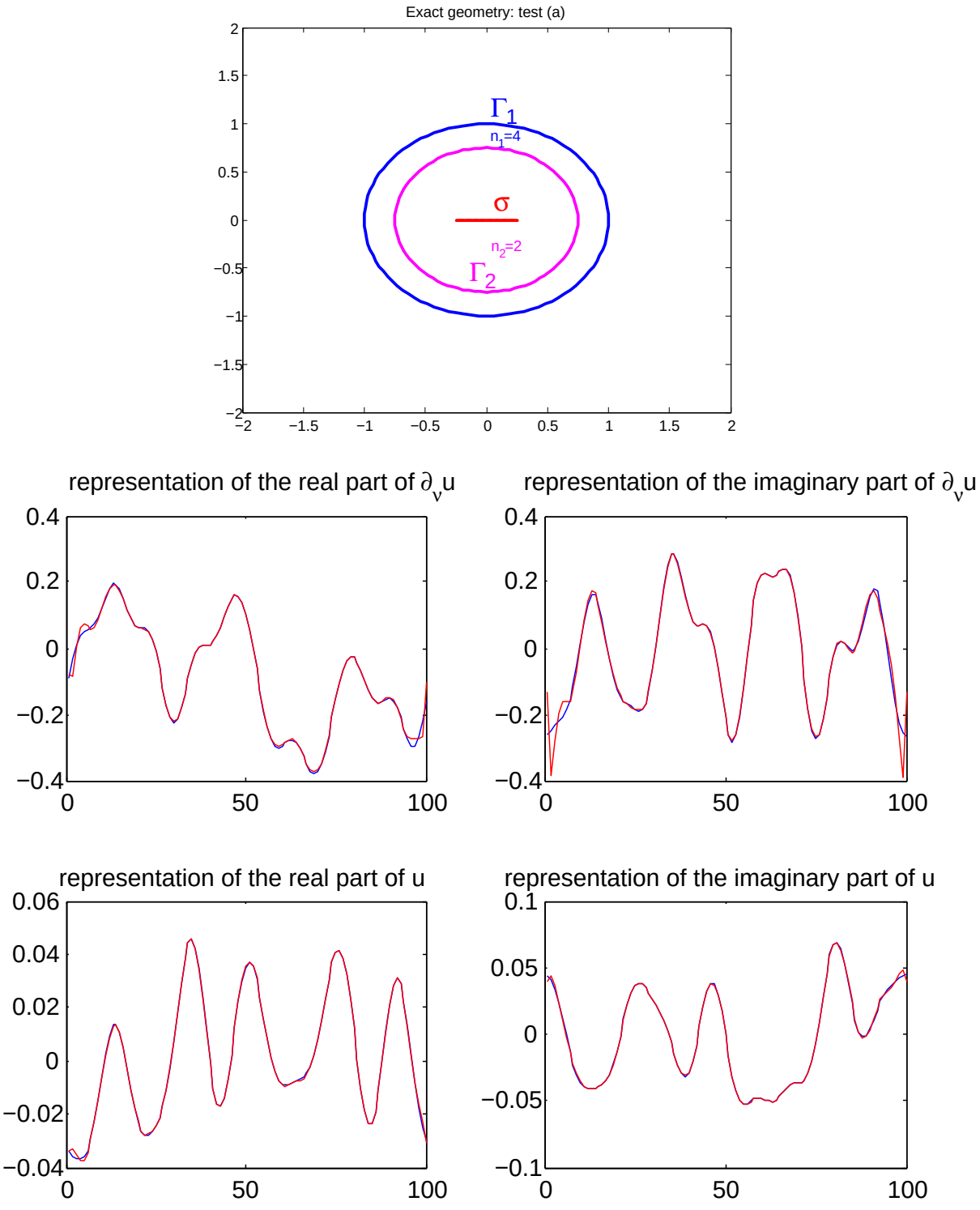

Figure 6.5: Reconstruction of the Cauchy data on Γ_2 in the case of test (a) using the data completion algorithm (red) the exact data (blue) without added noise.

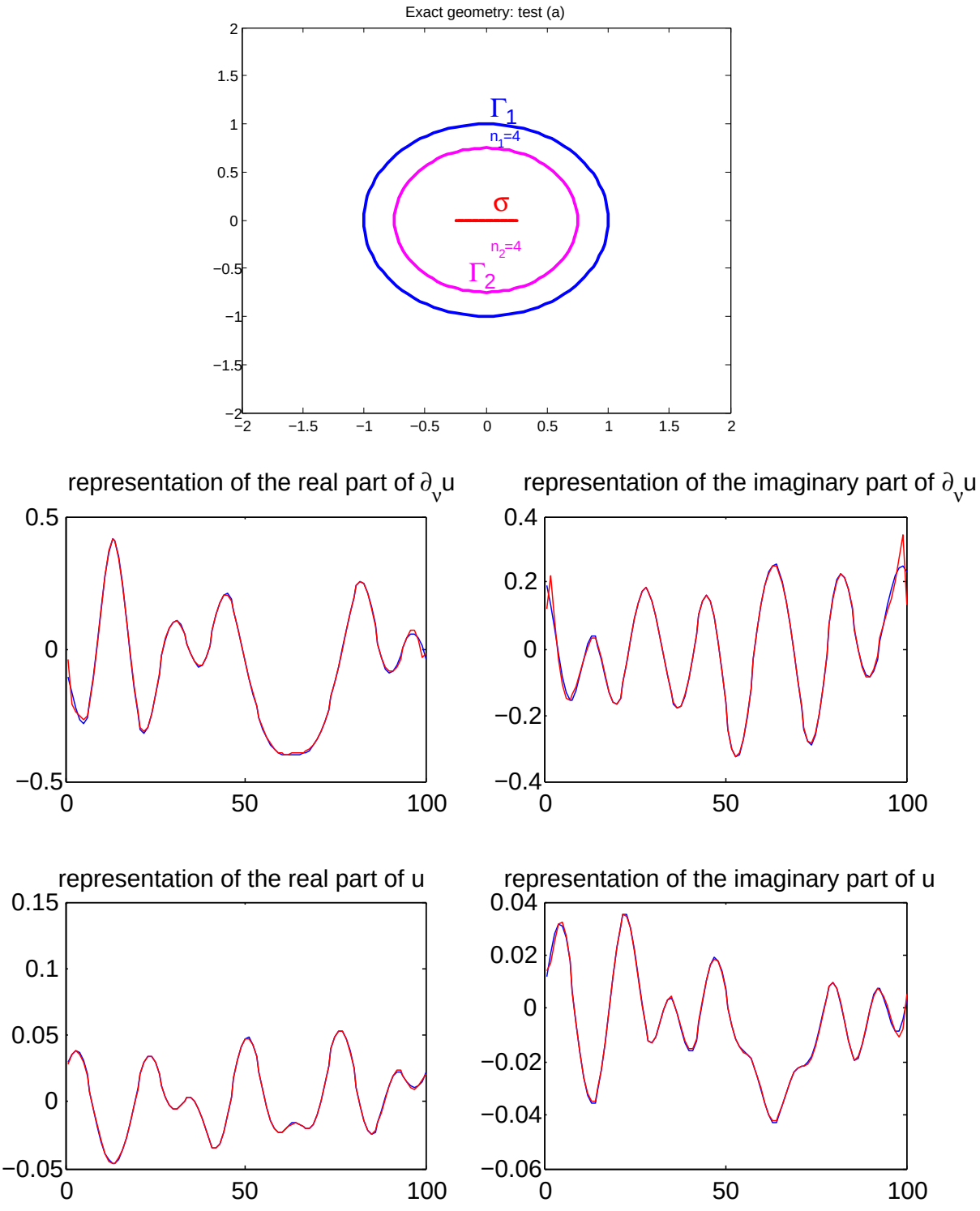

Figure 6.6: Reconstruction of the Cauchy data on Γ_2 in the case of test (a) using the data completion algorithm (red) the exact data (blue) without added noise.

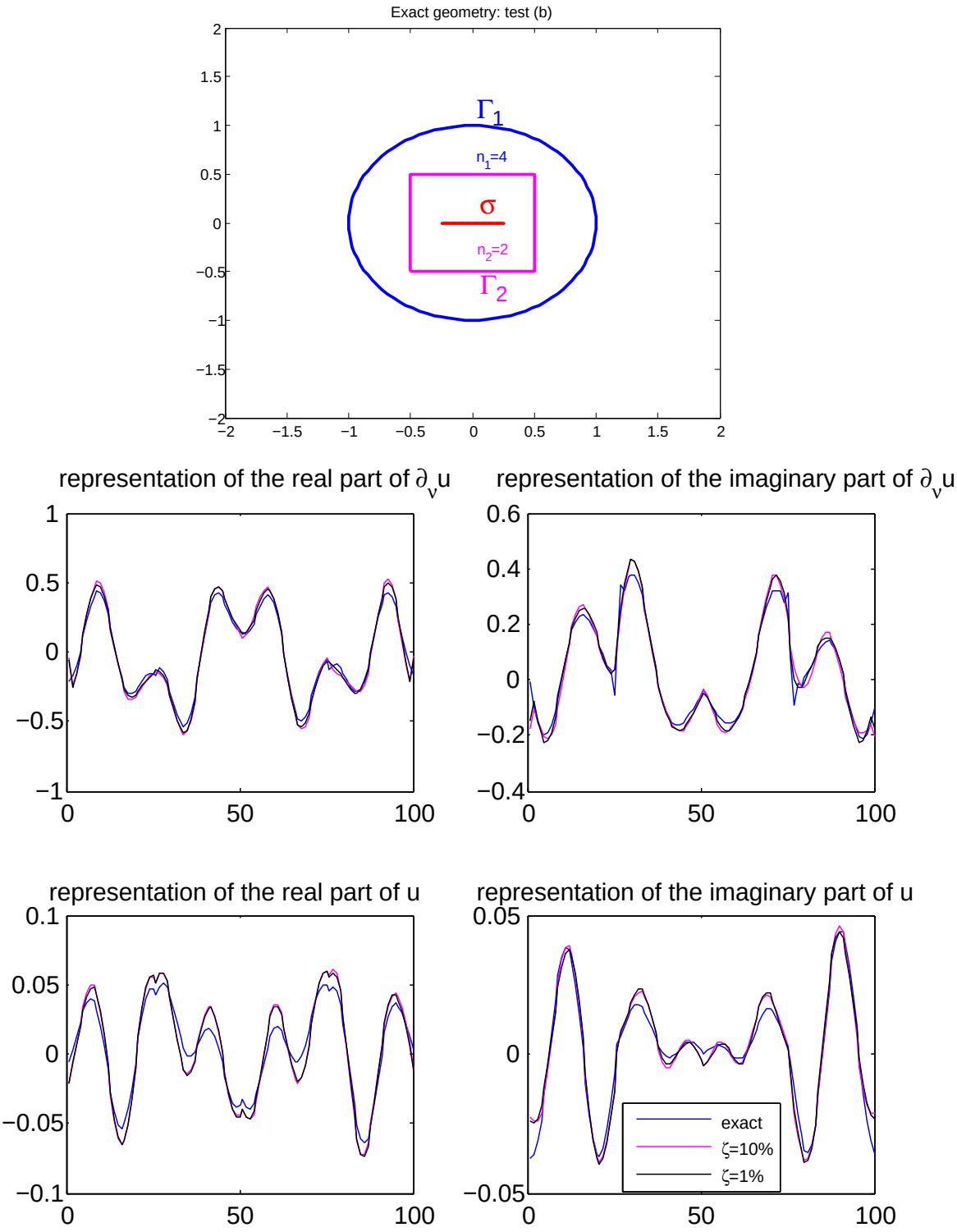

Figure 6.7: Reconstruction of the Cauchy data on Γ_2 in the case of test (b) using the data completion algorithm (red) the exact data (blue) with added noise ζ.

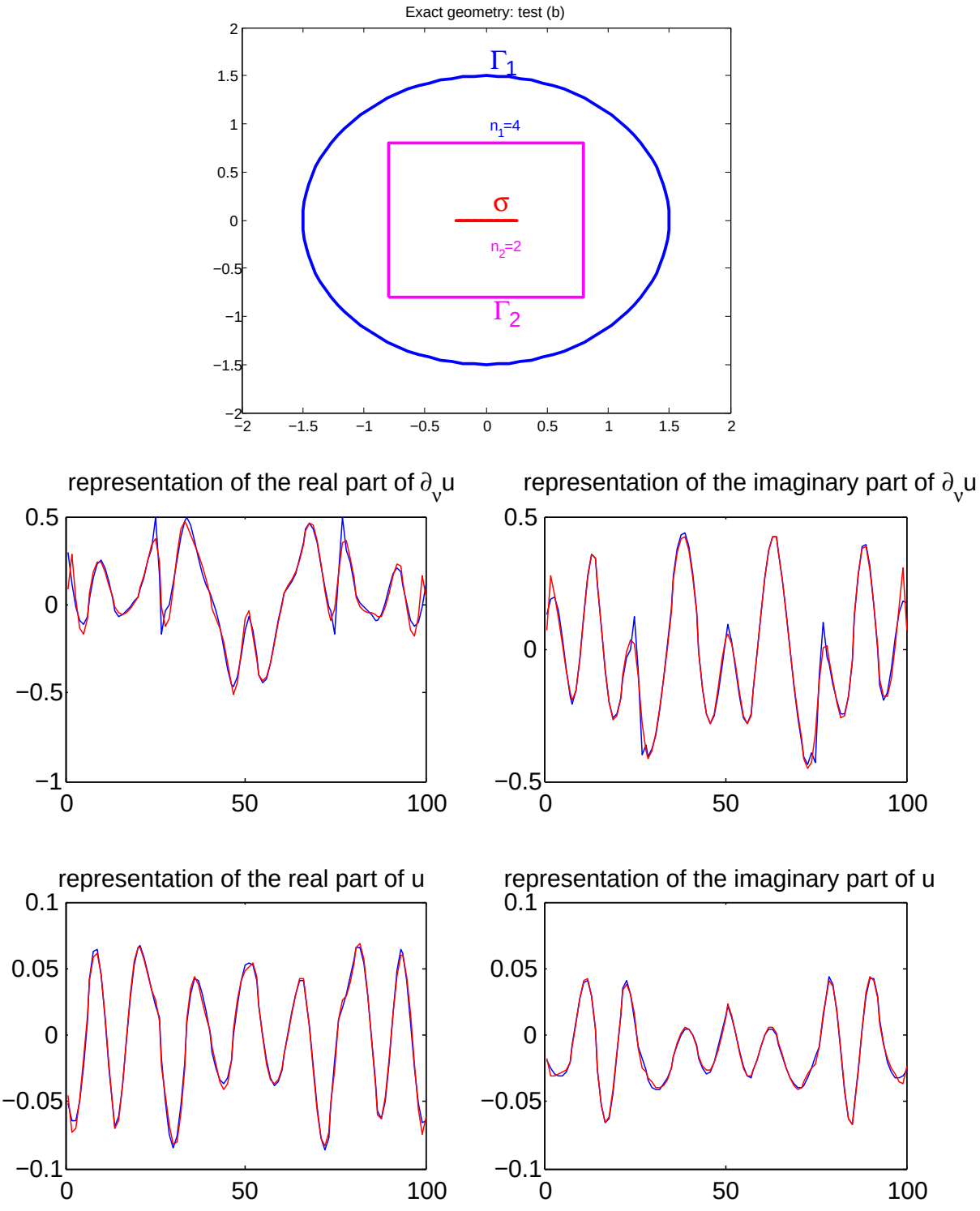

Figure 6.8: Reconstruction of the Cauchy data on Γ_2 in the case of test (b) using the data completion algorithm(red) the exact data (blue) without added noise.

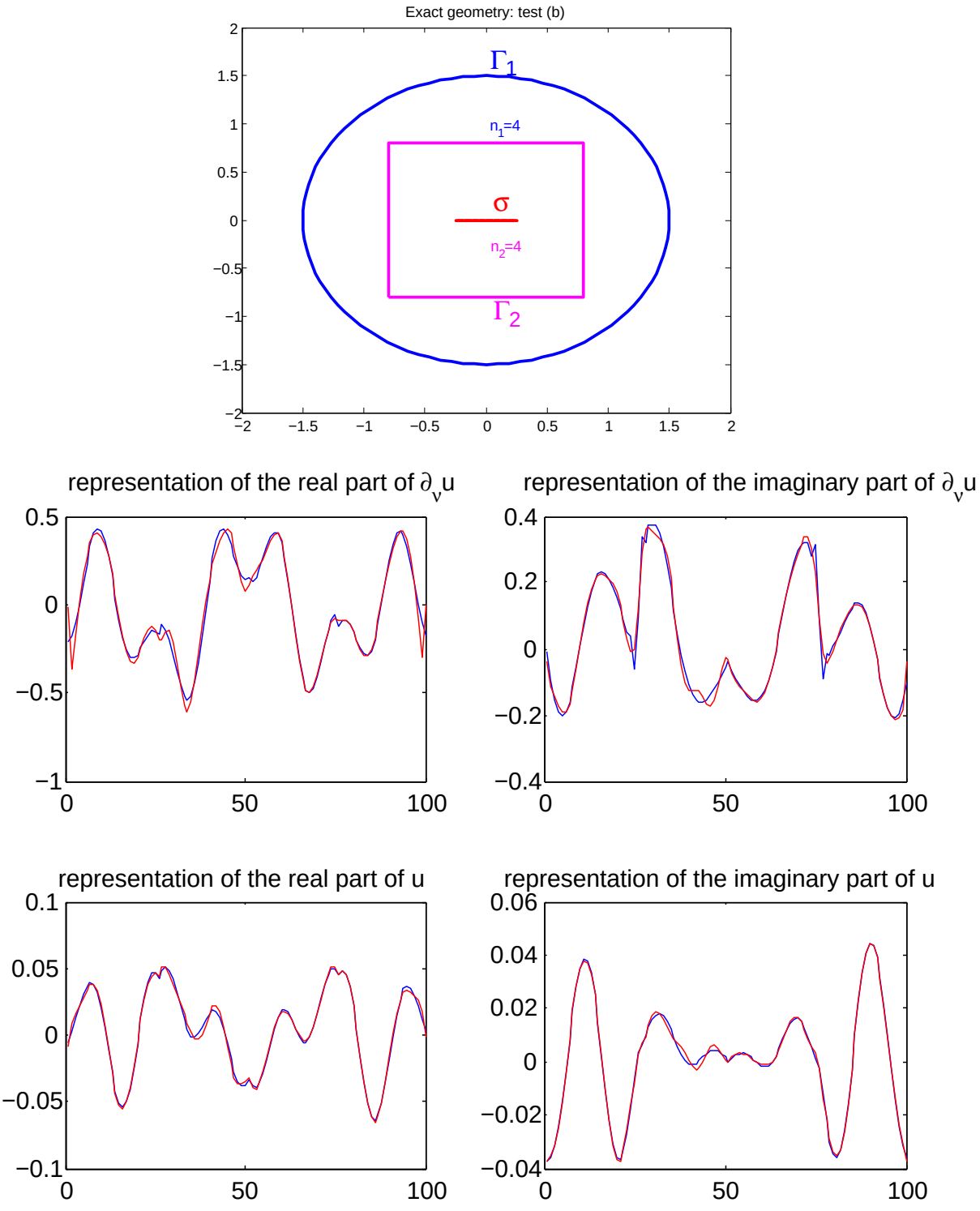

Figure 6.9: Reconstruction of the Cauchy data on Γ_2 in the case of test (b) using the data completion algorithm (red) the exact data(blue) without added noise.

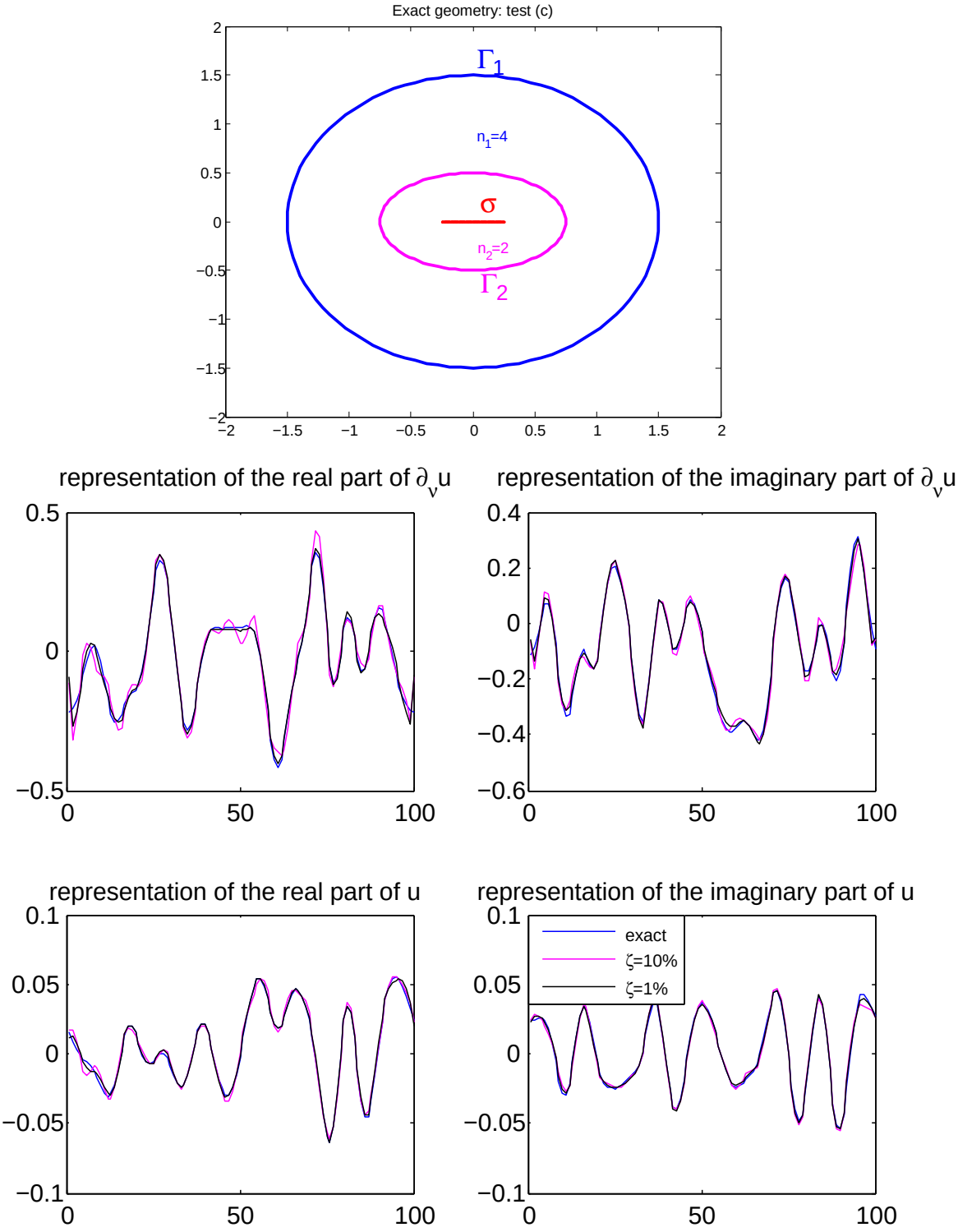

Figure 6.10: Reconstruction of the Cauchy data on Γ_2 in the case of test (c) using the data completion algorithm (red) the exact data (blue) with added noise ζ.

6.3 Application of the data completion algorithm to the RG-LSM

6.3.1 Configuration for the inverse scattering problem

We start this section by introducing the setting of our inverse problem that consists in reconstructing the crack in a stratified domain. We assume that we have an inhomogeneous medium with index of refraction n, which is piecewise-constant that can be a complex-valued function with non-negative imaginary part. Let $\Omega_2 \subset \mathbf{R}^m$ be a subdomain with a constant index n_2 containing the crack σ which is a smooth non-intersecting open arc. We also assume that Ω_2 is embedded in a subdomain Ω_1 with a constant index n_1.

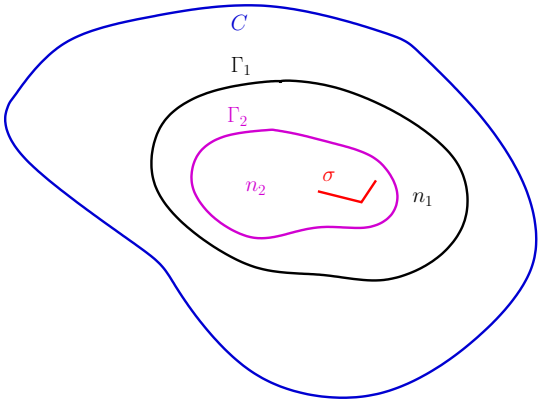

Figure 6.11: Representation of the domain

The forward problem that we consider consists in applying an incident wave $u^i = G(\cdot, x_0)$ for a point source $x_0 \in \mathbf{R}^m \setminus \bar{\Omega}_1$ and measuring the total field on Γ_1. We denote by G the Green function of the whole domain satisfying (6.29).

$$\Delta G(\cdot, x_0) + k^2 n G(\cdot, x_0) = -\delta_{x_0} \quad \text{in } \mathbf{R}^m, \tag{6.29}$$

and the Sommerfeld radiation condition

$$\lim_{r=|x|\to+\infty} r^{\frac{m-1}{2}} (\partial_r G(\cdot, x_0) - ikn G(\cdot, x_0)) = 0, \qquad \text{uniformly for all } \hat{x} = \frac{x}{|x|}.$$

Hence, the total field $u = u^s + u^i$ is solution of (6.30), where u^s is the scattered field

$$\begin{cases} \Delta u + k^2 n u = -\delta_{x_0} & \text{in } \mathbf{R}^m \setminus \overline{\sigma} \\ \partial_\nu u_\pm \pm \lambda^\pm u_\pm = 0 & \text{on } \sigma \end{cases} \tag{6.30}$$

and the Sommerfeld radiation condition

$$\lim_{r=|x|\to+\infty} r^{\frac{m-1}{2}} (\partial_r u^s(\hat{x}) - ikn u^s(\hat{x})) = 0, \qquad \text{uniformly for all } \hat{x} = \frac{x}{|x|}.$$

Our inverse problem consists in retrieving the crack σ knowing all the measurements of the Cauchy data $(f_{x_0}, g_{x_0}) = (u(., x_0), \partial_\nu u(., x_0))_{|\Gamma_1}$ on Γ_1 for all the points source $x_0 \in C$, where C is a regular boundary of an open domain that contains Ω_1. The issue is that the RG-LSM algorithm cannot be applied in this case since the domain is stratified. To tackle this issue, we propose to apply the data completion algorithm introduced in the previous sections to find all the measurements of the Cauchy data $(u(., x_0), \partial_\nu u(., x_0))_{|\Gamma_2}$ for all $x_0 \in C$, which consequently makes easy the use of the RG-LSM algorithm since Ω_2 has a constant index.

Algorithm

Assuming that we have generating the data $(u(., x_j), \partial_\nu u(., x_j))_{|\Gamma_1}$ on the boundary Γ_1 for $\tilde{n}$ point sources $(x_j)_{j=1:\tilde{n}}$. Then the algorithm is decomposed on two steps:

- **Step 1:** reconstruct the Cauchy data on Γ_2 by solving for each $x_j, j = 1 : \tilde{n}$ the equation (6.26)
- **Step 2:** We solve (5.29) which enables to retrieve the crack as explained in Chapter 5 with $n = n_2$ and the index of the exterior domain is n_1.

6.3.2 Numerical experiments

In this subsection we give the numerical results for the crack reconstruction using the data given in the three tested domains presented in Section 6.2.2. Note that both line shaped and arc shaped cracks are considered. We give for the three domains a comparison between the crack reconstruction using the exact synthetic data and the reconstructed data. The experiments are conducted for 100 point sources uniformly distributed in the square with vertex $(-2.5, -2.5), (2.5, -2.5), (2.5, 2.5), (-2.5, 2.5)$ and 100 discretization points on Γ_1 and Γ_2. The considered wave length is $\lambda = 1$.

We show that the results obtained by using the reconstructed Cauchy data and the exact data are close for the different crack shapes and impedance values considered in the experiments. This can be explained by the fact that, although the reconstructed data are slightly different from the exact ones, which can be considered as a kind of noisy data for the crack reconstruction problem, the stability of the RG-LSM algorithm reconstruction is generated by the use of Tikhonov regularization by solving (5.24) [see Section 5.4.1].

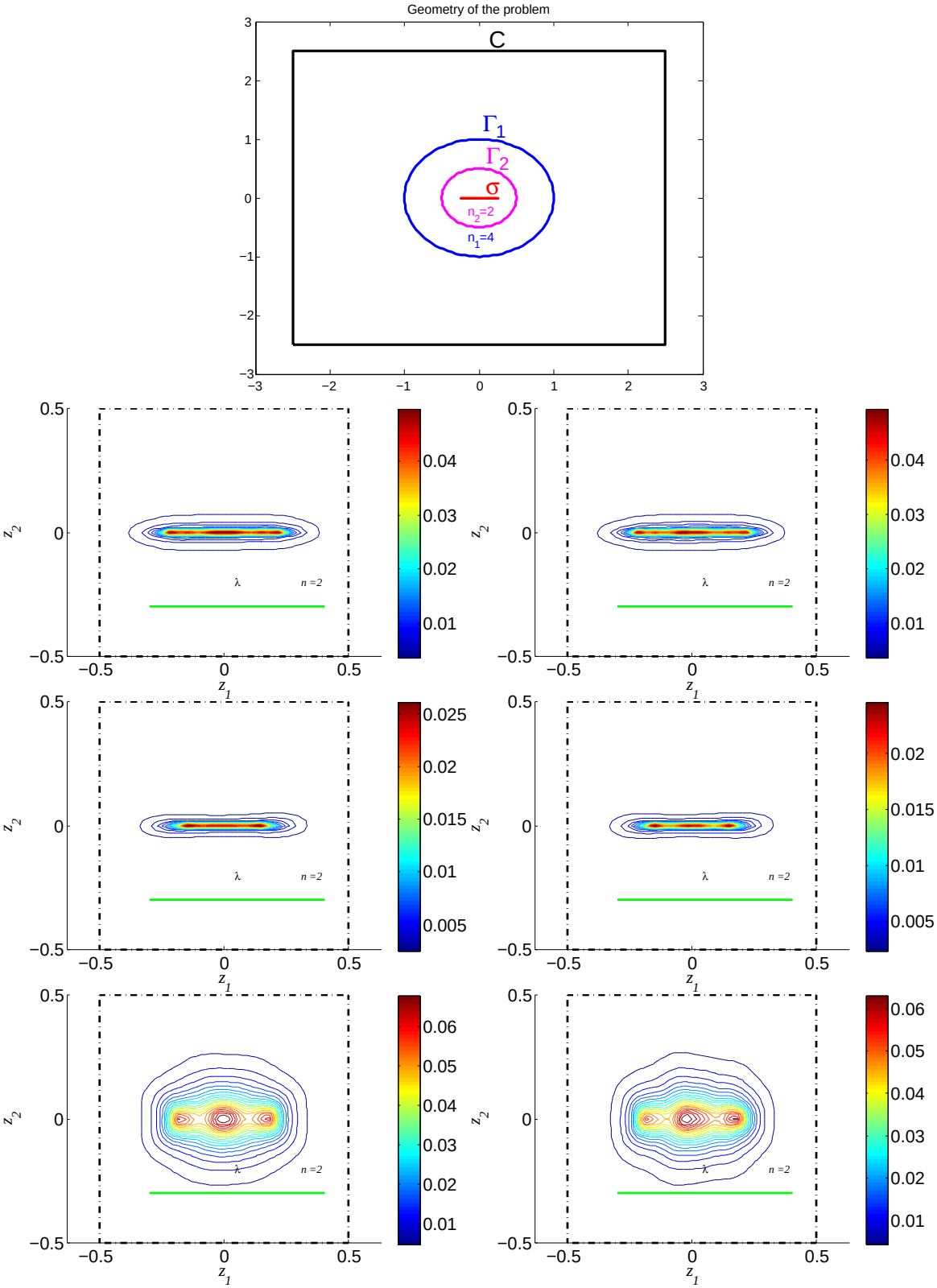

Figure 6.12: Reconstruction of a segment crack $\sigma = [-0.25, 0.25] \times \{0\}$ associated to test (a) using 100 discretization points on Γ_1, Γ_2 and σ, for $\lambda^{\pm} = 10^3$ (in the first line), $\lambda^{\pm} = 10^{-3}$ (in the second line) and $\lambda^{\pm} = 10$ (in the third line), using the exact data (left) and the reconstructed data (right).

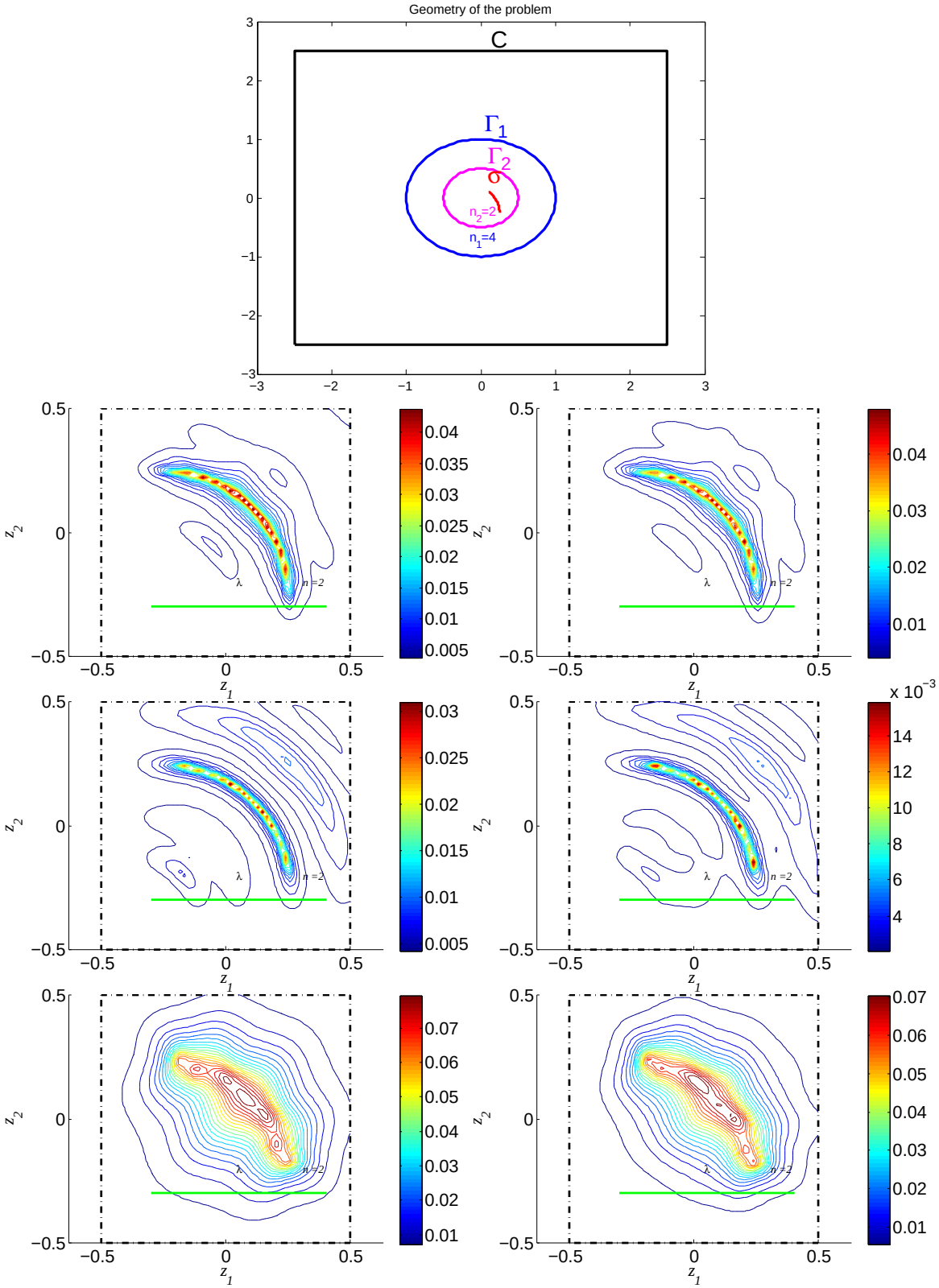

Figure 6.13: Reconstruction of an open arc crack centered on $(-0.25, -0.25)$ with radius $r = 0.5$ associated to test (a), using 100 discretization points on Γ_1, Γ_2 and σ, for $\lambda^{\pm} = 10^3$ (in the first line), $\lambda^{\pm} = 10^{-3}$ (in the second line) and $\lambda^{\pm} = 10$ (in the third line), using the exact data (left) and the reconstructed data (right).

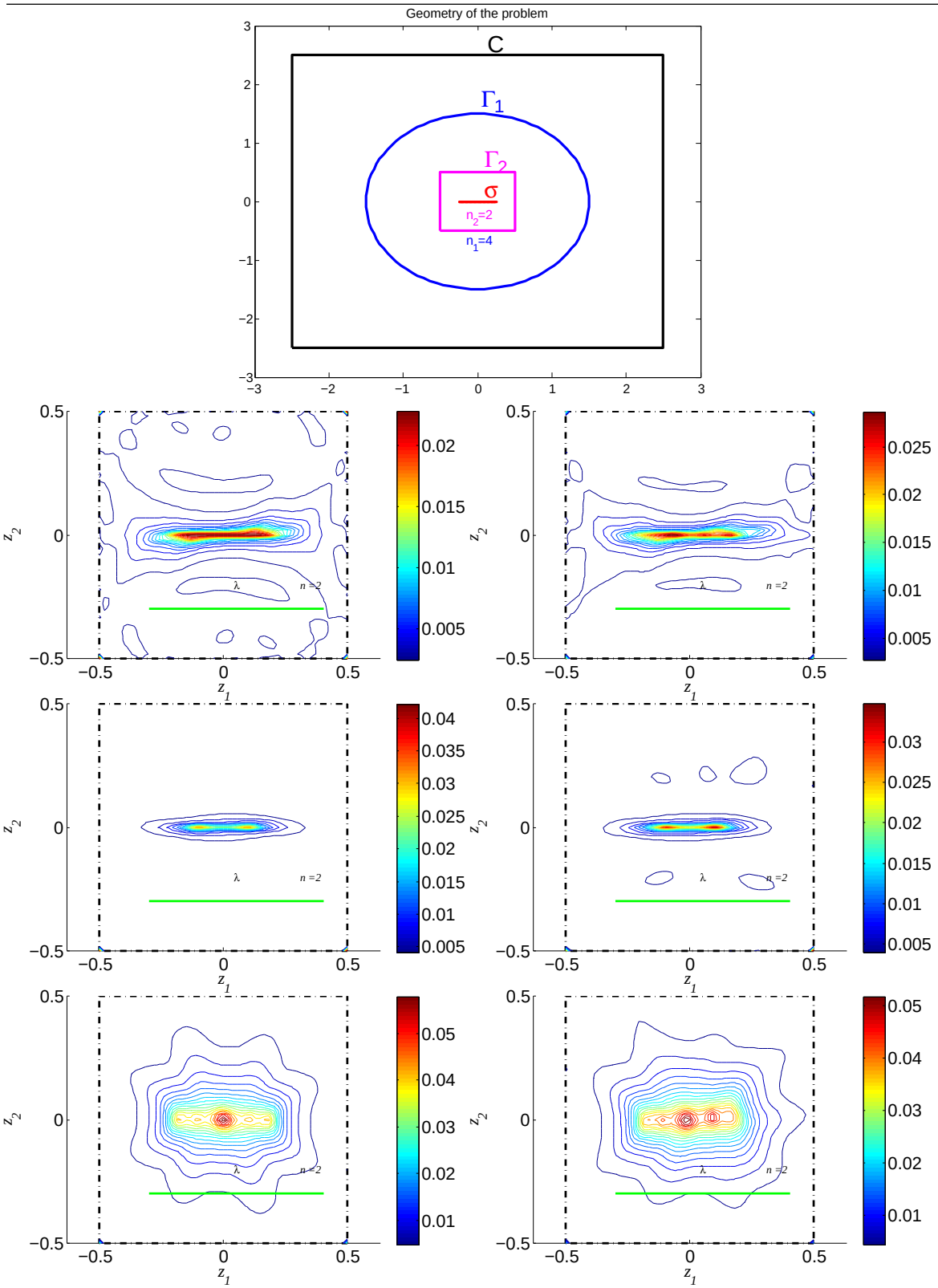

Figure 6.14: Reconstruction of a segment crack $\sigma = [-0.25, 0.25] \times \{0\}$ associated to test (b) using 100 discretization points on Γ_1, Γ_2 and σ, for $\lambda^{\pm} = 10^3$ (in the first line), $\lambda^{\pm} = 10^{-3}$ (in the second line) and $\lambda^{\pm} = 10$ (in the third line), using the exact data (left) and the reconstructed data (right).

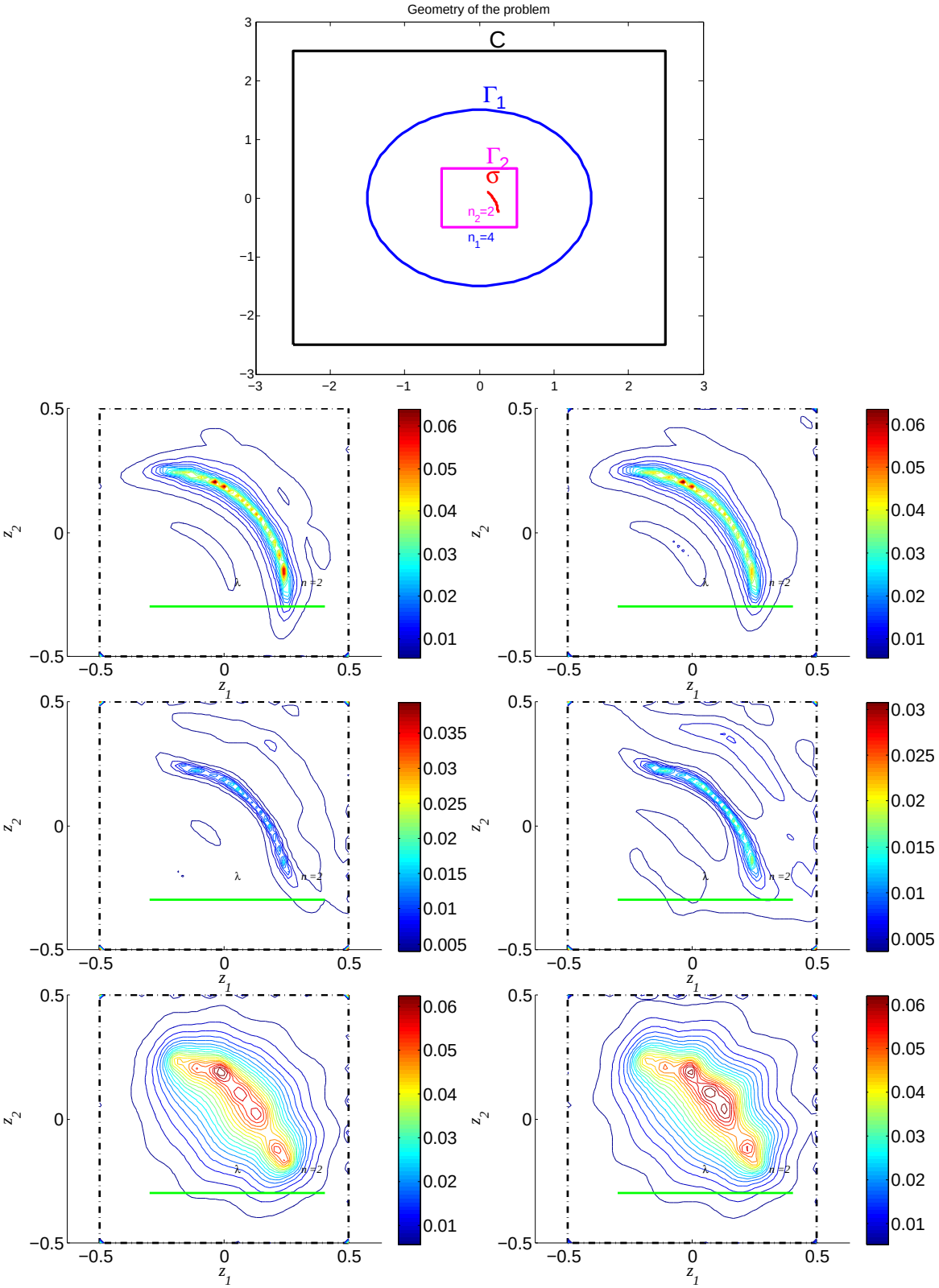

Figure 6.15: Reconstruction of an open arc crack σ centered on $(-0.25, -0.25)$ with radius $r = 0.5$ associated to test (b) using 100 discretization points on Γ_1, Γ_2 and σ, for $\lambda^{\pm} = 10^3$ (in the first line), $\lambda^{\pm} = 10^{-3}$ (in the second line) and $\lambda^{\pm} = 10$ (in the third line), using the exact data (left) and the reconstructed data (right).

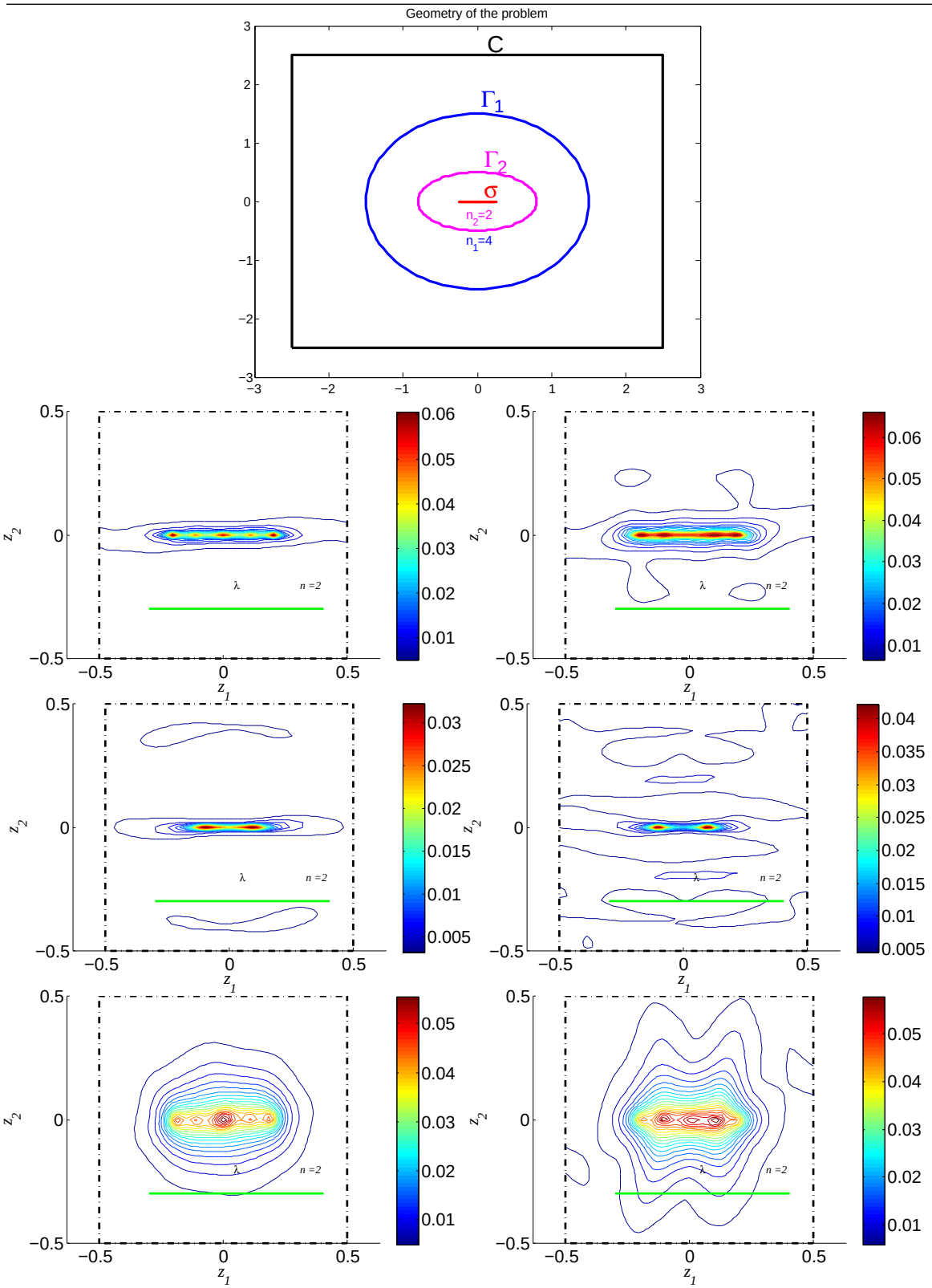

Figure 6.16: Reconstruction of a segment crack $\sigma = [-0.25, 0.25] \times \{0\}$ associate to test (c) using 100 discretization points on Γ_1, Γ_2 and σ, for $\lambda^{\pm} = 10^3$ (in the first line), $\lambda^{\pm} = 10^{-3}$ (in the second line) and $\lambda^{\pm} = 10$ (in the third line), using the exact data (left) and the reconstructed data (right).

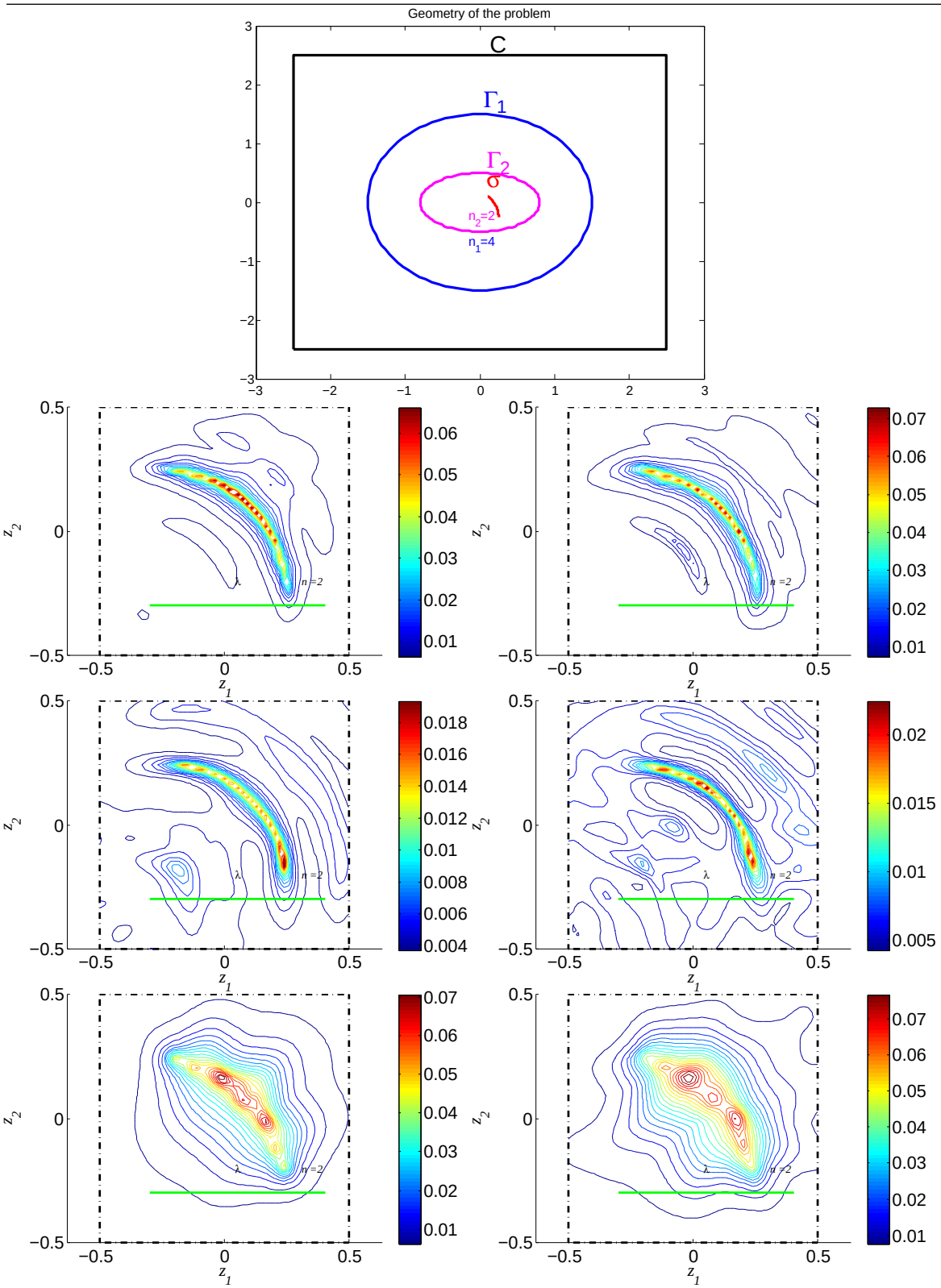

Figure 6.17: Reconstruction of an open arc crack σ centered on $(-0.25, -0.25)$ with radius $r = 0.5$ associated to test (c) using 100 discretization points on Γ_1, Γ_2 and σ, for $\lambda^{\pm} = 10^3$ (in the first line), $\lambda^{\pm} = 10^{-3}$ (in the second line) and $\lambda^{\pm} = 10$ (in the third line), using the exact data (left) and the reconstructed data (right).

Figures 6.12-6.13 show that in the case of a circular geometry of the inner and the exterior boundary as in test (a) we have a very good reconstruction since no difference between the reconstruction using the reconstructed data and the exact one can be noticed. In the case of a non circular geometry, Figures 6.14, 6.15, 6.16 and 6.17 also show that a good reconstruction is obtained but with a small difference between the two results. This small difference is due to the small difference between the two data, which is not noticed in the case of a circular geometry as shown in the previous Section.

6.4 Conclusion

In this study, a data completion method for the Helmholtz equation is developed. The main advantage of the proposed method is that it provides a simple and fast algorithm and it also gives stable results for a problem (i.e. Cauchy problem) that is known to be severely ill posed. Using the boundary conditions and the surface representation of the solution, we have derived a linear integral equation system that has to be verified by the missing Cauchy data. Using this formulation of the problem, the main difficulties consist in proving the injectivity and the densness of the range of the used operator, which has been tackled by characterizing its kernel and its range. The latter properties are used to prove that an approximate solution can be given using Tikhonov regularization and the Morozov discrepancy principle. Moreover in our formulation, the available Cauchy data are multiplied by an operator that has the same range as the operator to be inverted, even with an adding noise on the initial data, which induces the robustness of our method. In the second part of this chapter, we have presented an application of the data completion algorithm to the crack reconstruction using the RG-LSM algorithm. The crack reconstruction given with the reconstructed data is very close to the one obtained with the synthetic data which proves the efficiency of this method, and consequently enables us to generalize the use of the RG-LSM to more realistic and complicated cases such as the detection of a buried obstacle in a stratified domain (e.g. detection of mine buried in the sol, imaging of anomalous under the skin, etc.) knowing the index of refraction of each layer or sub-domain. This data completion step enables us to keep benefit from the main advantage of the RG-LSM which consists in avoiding the computation of the Green function of the stratified domain.

Conclusion

Conclusions

The focus of the research described in this dissertation is the inverse scattering problem in the context of acoustic and electromagnetic waves. The aim is the application of some sampling methods to reconstruct cracks in the case of impedance boundary conditions on both sides of the crack. Note that the sampling methods have been largely studied during the last decade due to their attractiveness in terms of their implementation simplicity, their numerical rapidity and their performance when only limited knowledge about the scatterer is available.
By building up on earlier studies on the LSM, we have theoretically justified the use of this method to reconstruct cracks with different shapes and for different ranges of the impedance values in the case of impedance boundary conditions on both sides of the crack. Overall, the results show high precise reconstructions, especially for small and high magnitudes of the impedance values. However, the quality of the results slightly deteriorates for intermediary impedance values. In this latter case, the quality of the reconstruction is sensitive to the reconstructed normals and also to the frequency. Our method of determination of the impedance values shows also that the reconstruction is accurate in most of the cases, with relatively less accuracy in the case of intermediary impedance values.

The application of the Factorization method was challenging due to the difficulties that arise on the theoretical level. The challenge was to find a good factorization of the far-field operator and to prove that this factorization respects the theoretical framework of the method. We analyzed both the $F_\sharp$ method and the so-called inf criterion. From, the numerical side, we only considered the $F_\sharp$ method. The case of impedance boundary conditions causes similar difficulties in designing the numerical algorithm as for the LSM, since it also requires a proper choice of the orientation of the probing "small" crack. The numerical results show a slightly better performance of the $F_\sharp$ method as compared to the LSM method even for intermediary impedance values.

Building on the work of F. Delbary and N. Zeev and F. Cakoni, the use of the RG-LSM has been extended to the case of impedance boundary conditions and the efficiency of the developed method has been numerically shown for different crack shapes. However, in order to make more realistic the use of our method, a new data completion algorithm has been developed and coupled to the RG-LSM to enable a reconstruction of cracks embedded in stratified domains. The numerical results show overall a good reconstruction quality obtained using this method. It should be noted that in some cases the reconstructed data are different from the exact one, which may impact the quality of the results. The stability of the crack shape reconstruction is ensured by the use of Tikhonov regularization.

Directions for future work

A natural avenue for further research would be to extend the investigations of the LSM and the Factorisation method to 3D settings on Maxwell's equations or elasticity. For the acoustic case (scalar) the theoretical justifications developed in this dissertation are valid for any space dimension, and particularly in 3D settings. Another interesting further work would be to apply the Factorization method in the case of inhomogeneous domains with near-fields. An idea to do so would consist in developing a method that associates the RG-LSM and the Factorization method.

Bibliography

[1] I. Akduman and R. Kress. Electrostatic imaging via conformal mapping. *Inverse Problems*, 18:1659–1672, 2002. [cited at p. 36]

[2] G. Alessandrini and L. Rondi. Determining a sound-soft polyhedral scatterer by a single far-field measurement. *Proc. Amer. Math. Soc*, 133:1685–1691, 2005. [cited at p. 31]

[3] C. J. S. Alves, J. Ben Abdallah, and M. Jaoua. Recovery of cracks using a point-source reciprocity gap function. *Inverse Problems in Science and Engineering*, 12:519–534, 2004. [cited at p. 104]

[4] S. Andrieux and A. Ben Abda. Identication of planar cracks by complete over-determined data: inversion formulae. *Inverse Problems*, 12:553–63, 1996. [cited at p. 3, 104]

[5] T. Arens. Why linear sampling works. *Inverse Problems*, 20:163–173, 2004. [cited at p. 37]

[6] T. Arens and L. Lechleiter. The linear sampling method revisited. *J. Integral Equations Appl.*, 21:179–202, 2009. [cited at p. 37]

[7] C. Bellis. *Qualitative methods for inverse scattering in solid mechanics*. PhD thesis, Ecole Polytechnique Palaiseau, 2010. [cited at p. 3, 35]

[8] C. Bellis and M. Bonnet. Crack identification by 3d time domain elastic or acoustic topological sensivity. *Comptes Rendus Mécanique*, 337:124–130, 2009. [cited at p. 35]

[9] A. Ben Abda, R. Ben Fatma, and D. Tromeur-Dervout. An Aitken-like acceleration method applied to missing boundary data reconstruction for the Cauchy–Helmholtz problem. *C. R. Acad. Sci. Paris, Ser. I*, 348:93–97, 2010. [cited at p. 125]

[10] A. Ben Abda, F. Delbary, and H. Haddar. On the use of the reciprocity–gap functional in inverse scattering from planar cracks. *Math. Models Methods Appl. Sci.*, 15:1553–1574, 2005. [cited at p. 3, 104]

[11] A. Ben Abda, M. Kallel, J. Leblond, and J.P. Marmorat. Line segment crack recovery from incomplete boundary data. *Inverse Problems*, 18:1057–1077, 2002. [cited at p. 3, 104]

[12] F. Ben Belgacem. Why is the Cauchy problem severely ill–posed? *Inverse Problems*, 23:823–836, 2007. [cited at p. 124]

[13] F. Ben Belgacem and H. El Fekih. On Cauchys problem: I. a variational steklov–poincaré theory. *Inverse Problems*, 21:1915–36, 2005. [cited at p. 124]

[14] F. Ben Hassen, Y. Boukari, and H. Haddar. Application of the linear sampling method to retrieve cracks with impedance boundary conditions. *INRIA Technical report*, RR-7478:http://hal.archives–ouvertes.fr/inria–00543901/PDF/RR–7478.pdf, 2010. [cited at p. 72, 95, 115]

[15] M. Bonnet. Fast identification of cracks using higher-order topological sensitivity for 2-D potential problems. *Eng. Anal. Bound. Elem.*, 35:223–235, 2011. [cited at p. 3]

[16] L. Bourgeois. A mixed formulation of quasi-reversibility to solve the Cauchy problem for Laplaces equation. *Inverse Problems*, 21:1087–1104, 2005. [cited at p. 124]

[17] L. Bourgeois. Convergence rates for the quasi-reversibility method to solve the Cauchy problem for the Laplace's equation. *Inverse Problems*, 22:413–430, 2006. [cited at p. 124]

[18] G. Bozza, M. Brignone, M. Pastorino, M. Piana, and A. Randazzo. Crack detection in dielectric structures by a linear sampling approach. *ijsise*, 3:73–80, 2010. [cited at p. 3]

[19] M. Brignone, G. Bozza, R. Aramini, M. Pastorino, and M. Piana. A fully no-sampling formulation of the linear sampling method for three-dimensional inverse electromagnetic scattering problems. *Inverse Problems*, 25:015014–20, 2009. [cited at p. 38]

[20] F. Cakoni and D. Colton. The determination of the surface impedance of a partially coated obstacle from far field data. *SIAM J. Appl. Math*, 2:709–723, 2003. [cited at p. 60]

[21] F. Cakoni and D. Colton. The linear sampling method for cracks. *Inverse Problems*, 19:279–295, 2003. [cited at p. 3, 7, 10, 11, 42, 43, 72]

[22] F. Cakoni and D. Colton. *Qualitative Methods in Inverse Scattering Theory*. Springer-Verlag, 2006. [cited at p. 37, 59]

[23] F. Cakoni, D. Colton, and P. Monk. *The linear sampling method in inverse electromagnetic scattering*. Society for Industrial and Applied Mathematics (SIAM), 2011. [cited at p. 37]

[24] F. Cakoni and H. Haddar. Identification of partially coated anisotropic buried objects using electromagnetic Cauchy data. *J. Integral Equations Appl.*, 19:359–389, 2007. [cited at p. 105]

[25] F. Cakoni, R. Kress, and C. Schuft. Simultaneous reconstruction of shape and impedance in corrosion detection. *Methods Appl. Anal.*, 17:357–377, 2010. [cited at p. 59]

[26] H. Cao, M. V. Klibanov, and S. V. Pereverzev. A carleman estimate and the balancing principle in the quasi-reversibility method for solving the Cauchy problem for the Laplace equation. *Inverse problems*, 25:035005–(21pp), 2009. [cited at p. 124]

[27] J. Cheng and M. Yamamoto. Uniqueness in an inverse scattering problem within non-trapping polygonal obstacles with at most two incoming waves. *Inverse Problems*, 19:1361–1384, 2003. [cited at p. 31]

[28] A. Cimetière, F. Delvare, M. Jaoua, and F. Pons. Solution of the Cauchy problem using iterated Tikhonov regularization. *Inverse Problems*, 17:553–570, 2001. [cited at p. 124]

[29] D. Colton. Inverse acoustic and electromagnetic scattering theory. *Inverse Problems*, 47:76–109, 2003. [cited at p. 32]

[30] D. Colton and H. Haddar. An application of the reciprocity gap functionnal to inverse scattering theory. *Inverse Problems*, 21:383–398, 2005. [cited at p. 104]

[31] D. Colton, H. Haddar, and P. Monk. The linear sampling method for solving the electromagnetic inverse scattering problem. *SIAM J. Sci. Comp*, 24:719–731, 2002. [cited at p. 37]

[32] D. Colton, H. Haddar, and M. Piana. The linear sampling method in inverse electromagnetic scattering theory. *Inverse Problems*, 19:S 105–S 137, 2003. [cited at p. 37]

[33] D. Colton and A. Kirsch. A simple method for solving inverse scattering problems in the resonance region. *Inverse Problems*, 12:383–393, 1996. [cited at p. 37]

[34] D. Colton and R Kress. *Inverse acoustic and electromagnetic scattering theory, second ed.* Springer-Verlag, 1998. [cited at p. 10, 21, 29, 30, 32]

[35] D. Colton and P. Monk. A novel method for solving the inverse scattering problem for time harmonic acoustic waves in the resonance region. *SIAM J. App. Math*, 26:506–523, 1986. [cited at p. 35]

[36] D. Colton, M. Piana, and R. Potthast. A simple method using Morozov's discrepancy principle for solving inverse scattering problems. *Inverse Problems*, 13:1477–1493, 1997. [cited at p. 37, 38]

[37] D. Colton and B. D. Sleeman. Uniqueness theorems for the inverse problem of acoustic scattering. *IMA J. Appl. Math*, 31:253–259, 1983. [cited at p. 31]

[38] F. Delbary. *Identifications de fissures par des ondes acoustiques.* PhD thesis, Université de Paris 6, 2006. [cited at p. 9, 10, 42, 59, 60, 104, 105]

[39] F. Delbary, M. Brignone, G. Bozza, R. Aramini, and M. Piana. A visualization method for breast cancer detection using microwaves. *SIAM J. Appl. Math.*, 70:2509–2533, 2010. [cited at p. 105]

[40] J. Elschner and M. Yamamoto. Uniqueness in determining polygonal sound-hard obstacles with a single incoming waves. *Inverse Problems*, 22:355–419, 2006. [cited at p. 31]

[41] H. W. Engl, M. Hanke, and A. Neubauer. *Regularization of inverse problems*. Kluwer Academic Publishers Group, 1996. [cited at p. 136]

[42] J. Hadamard. *Lectures on Cauchys problem in linear partial differential equa- tions*. Dover, New York, 1953. [cited at p. 124]

[43] M. A. Hamdi. *Formulation variationnelle par équations intégrales pour le calcul de champs acoustiques linéaire proches et lointains*. PhD thesis, Université de Technologie de Compiègne, 1982. [cited at p. 21]

[44] H. Han and H-J. Reinhardt. Some stability estimates for Cauchy problems for elliptic equations. *J. Inv. Ill-Posed Problems*, 5:43754, 1997. [cited at p. 124]

[45] F. Hecht. *FreeFem++,Third edition, version 3.10-2*. Laboratoire Jacques-Louis Lions, Université Pierre et Marie Curie, Paris, 2010. [cited at p. 7]

[46] I. Horchani. *Application du gradient topologique à l'identification de fissures*. PhD thesis, Université de Tunis el Manar, 2009. [cited at p. 35]

[47] T. Hrycak and V. Isakov. increased stability in the continuation of solutions to the Helmholtz equation. *Inverse Problems*, 20:697712, 2004. [cited at p. 124]

[48] M. Ikehata and H. Itou. An inverse problem for a linear crack in an anisotropic elastic body and the enclosure method. *Inverse Problems*, 24:025005, 21, 2008. [cited at p. 3]

[49] O. Ivanyshyn and R. Kress. Inverse scattering for surface impedance from phase–less far field data. *J. Comput. Phys.*, 230:3443–3452, 2011. [cited at p. 59]

[50] A. Kirsch. The factorization method for a class of inverse elliptic problems. *Math.Nachr*, 278:258–277, 2005. [cited at p. 38]

[51] A. Kirsch and N. Grinberg. The linear sampling method in inverse obsta- cle scattering for impedance boundary conditions. j. inv. ill-posed problems. *J. Inv. Ill-Posed Problems*, 10:171185, 2002. [cited at p. 38]

[52] A. Kirsch and N. Grinberg. The factorization method for obstacles with a- priori separated sound-soft and sound-hard parts. *Math. Comput. Simulation*, 66:267–279, 2004. [cited at p. 38]

[53] A. Kirsch and N. Grinberg. *The Factorization method for inverse problem*. Oxford lecture series in Mathematics and its applications, 2008. [cited at p. 30, 38, 39, 72, 74, 78, 98]

[54] A. Kirsch and R. Kress. *An optimization method in inverse acoustic scattering*. Boundary elements IX, Vol3. Fluid Flow and Potential Applications, Brebbia et al,Springer, 1987. [cited at p. 35]

[55] A. Kirsch and S. Ritter. A linear sampling method for inverse scattering from an open arc. *inverse Problems*, 16:89–105, 2000. [cited at p. 38, 39, 42, 72]

[56] A. Kirsch and S. Ritter. The music algorithm and the factorization method in inverse scattering theory for inhomogeneous media. *inverse Problems*, 18:1025–1040, 2002. [cited at p. 38]

[57] R. Kress. Inverse scattering for shape and impedance. *Inverse Problems in Engineering Mechanics (eds Bui el al.),(Balkema, Rotterdam)*, pages 425–432, 1994. [cited at p. 34]

[58] R. Kress. Integral equation methods in inverse obstacle scattering. *Engineering Anal, with Boundary Elements*, 15:171–197, 1995. [cited at p. 34]

[59] R. Kress. Inverse scattering from an open arc. *Math. Meth. in the Appl. Sci*, 18:267–293, 1995. [cited at p. 34]

[60] R. Kress. Inverse elastic scattering from a crack. *Inverse Problems*, 12:667–684, 1996. [cited at p. 34]

[61] R. Kress and K-M. Lee. Integral equation methods for scattering from an impedance crack. *J. Comput. Appl. Math.*, 161:161–177, 2003. [cited at p. 7, 9, 10]

[62] R. Kress and W. Rundell. Inverse scattering for shape and impedance. *Inverse Problems*, 17:1075–1085, 2001. [cited at p. 34, 59]

[63] R. Kress, N. Tezel, and F. Yaman. A second order newton method for sound soft inverse obstacle scattering. *Inverse and Ill-Posed Problems*, 17:173–185, 2009. [cited at p. 34]

[64] R. Lattes and J.L. Lions. *Methodes de quasi-reversibilité applications*. Dunod, 1967. [cited at p. 124]

[65] W.M.C. LEAN. *Strongly Elliptic Systems and Boundary Integral Equations*. Cambridge University Press, Cambridge, 2000. [cited at p. 9, 11, 127, 129]

[66] C. Liu. An inverse obstacle problem: a uniqueness theorem for balls. In *Inverse problems in wave propagation (Minneapolis, MN, 1995)*, pages 347–355. Springer, 1997. [cited at p. 31]

[67] H. Liu and J. Zou. Uniqueness in an inverse obstacle scattering problem for both sound-hard and sound-soft polyhedral scatterers. *Inverse Problems*, 22:515539, 2006. [cited at p. 31]

[68] J. Liu and Sini. M. Reconstruction of cracks of different types from far-field measurements. *Math. Meth. Appl. Sci*, 33:950–973, 2010. [cited at p. 3, 59, 72]

[69] L. Marina, L. Elliottb, P.J. Heggsc, D.B. Inghamb, D. Lesnicb, and X. Wena. Bem solution for the cauchy problem associated with helmholtz-type equations by the landweber method. *Engineering Analysis with Boundary Elements*, 28:10251034, 2004. [cited at p. 125]

[70] F. Mnif. *Identification de cavits par les ondes acoustiques et lastiques*. PhD thesis, Université de Tunis el Manar, 2006. [cited at p. 34]

[71] L. Monch. A newton method for solving the inverse scattering problem for a sound-hard obstacle. *Inverse Problems*, 12:309323, 1996. [cited at p. 34]

[72] L. Monch. On the inverse acoustic scattering problem by an open arc: the sound-hard case. *Inverse Problems*, 13:13791392, 1997. [cited at p. 34]

[73] P. Monk and J. Sun. Inverse scattering using finite elements and gap reciprocity. *Inverse Problems and Imaging*, 1:643–660, 2007. [cited at p. 105]

[74] A. Nachman. Reconstruction from boundary measurements. *Ann. Math.*, 128:53176, 1988. [cited at p. 32]

[75] J. C. Nédélec. *Acoustic and electromagnetic equations*, volume 144 of *Applied Mathematical Sciences*. Springer-Verlag, 2001. [cited at p. 15]

[76] R. G. Novikov. A multidimensional inverse spectral problem for the equation $-\Delta\psi+(v(x)-Eu(x))\psi=0$. *Funktsional. Anal. i Prilozhen.*, 22:11–22, 1988. [cited at p. 32]

[77] R. Potthast. A fast new method to solve inverse scattering problems. *Inverse Problems*, 12:731–742, 1996. [cited at p. 36]

[78] G. Ramm. Recovery of the potential from fixed energy scattering. *Inverse Problems*, 4:877–86, 1988. [cited at p. 32]

[79] T. Reginska and K. Reginski. Approximate solution of a cauchy problem for the helmholtz equation. *Inverse Problems*, 22:975–989, 2006. [cited at p. 125]

[80] L. Rondi. Uniqueness for the determination of sound-soft defects in an inhomogeneous planar medium by acoustic boundary measurements. *Trans. Amer. Math. Soc.*, 1:213–239, 2003. [cited at p. 32]

[81] W. Rundell. Recovering an obstacle and its impedance from Cauchy data. *Inverse Problems*, 24:045003, 22, 2008. [cited at p. 60]

[82] A. Schumacher. *Topologieoptimisierung von Bauteilstrukturen unter Verwendung von Lopchposition- ierungkrieterien*. PhD thesis, Universitat-Gesamthochschule-Siegen, 1995. [cited at p. 34]

[83] M. Shiffer. Variational methods in the theory of Riemann surfaces. In *Contributions to the theory of Riemann surfaces*, Annals of Mathematics Studies, no. 30, pages 15–30. Princeton University Press, 1953. [cited at p. 31]

[84] J. Sokolowski and A. Zochowski. On the topological derivative in shape optimization. siam j. control optim. *SIAM J. Control Optim*, 37:1241–1272, 1999. [cited at p. 34]

[85] N. Zeev and F. Cakoni. The identification of thin dielectric objects from far field or near field scattering data. *SIAM J. Appl. Math.*, 69:1024–1042, 2009. [cited at p. 3, 42, 72, 104, 105]